PALAEOECOLOGY OF AFRICA
International Yearbook of Landscape Evolution and Palaeoenvironments
32

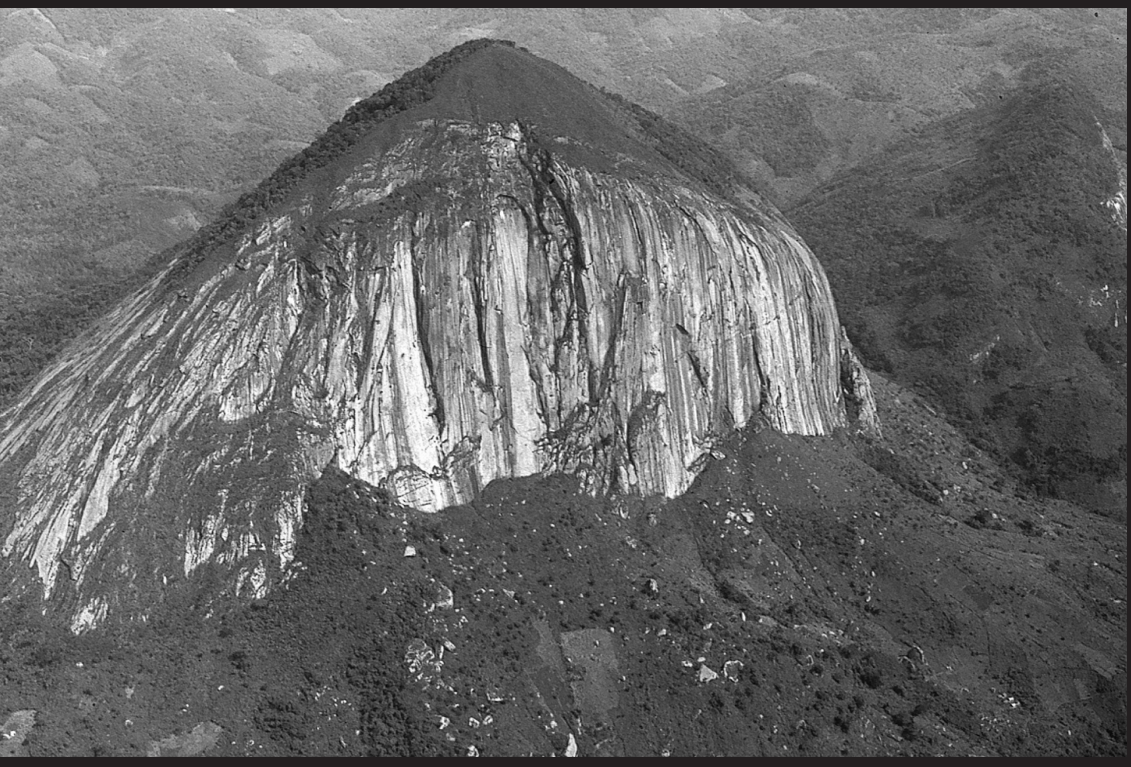

New Studies on Former and Recent Landscape Changes in Africa

Jürgen Runge

CRC Press
Taylor & Francis Group
A BALKEMA BOOK

NEW STUDIES ON FORMER AND RECENT LANDSCAPE CHANGES IN AFRICA

Palaeoecology of Africa

International Yearbook of Landscape Evolution
and Palaeoenvironments

ISSN 0168-6208

Volume 32

New Studies on Former and Recent Landscape Changes in Africa

Editor

Jürgen Runge

Centre for Interdisciplinary Research on Africa (ZIAF),
Johann Wolfgang Goethe University, Frankfurt am Main, Germany

CRC Press
Taylor & Francis Group
Boca Raton London New York Leiden

CRC Press is an imprint of the
Taylor & Francis Group, an **informa** business

A BALKEMA BOOK

Front cover: Granitic inselberg (Bornhardt) north of Lake Kivu located on the tectonically uplifted graben shoulder of the Western Rift Valley between Rwanda and the DR of Congo in about 2000 m asl. (Photo: J. Runge, March 1992).

This edition of Palaeoecology of Africa was generously supported by the "Georg und Franziska Speyersche Hochschulstiftung", Konrad-Adenauer-Straße 15, 60313 Frankfurt am Main, Germany.

CRC Press/Balkema is an imprint of the Taylor & Francis Group, an informa business

Typeset by V Publishing Solutions Pvt Ltd., Chennai, India
Printed and bound in Great Britain by CPI Group (UK) Ltd, Croydon, CR0 4YY

Published by: CRC Press/Balkema
P.O. Box 11320, 2301 EH Leiden, The Netherlands
e-mail: Pub.NL@taylorandfrancis.com
www.crcpress.com – www.taylorandfrancis.com

Library of Congress Cataloging-in-Publication Data

New studies on former and recent landscape changes in Africa / [edited by] Jürgen Runge.
p. cm.—(Palaeoecology of Africa ; volume 32)
Summary: "This book treats former and recent landscape evolution and past environments of the African continent (e.g. climate change, vegetation dynamics and growing impact of humans on ecosystems) and will be of interest to all concerned with low latitudes ecosystem changes and their respective interpretation in the framework of natural climate and vegetation change evidenced by a variety of methods that allow us to read and learn from 'proxy data' archives. Archaeologists, Palynologists, Palaeobotanists, Geographers, Geologists and Geomorphologists will find this edition equally useful for their work"—Provided by publisher.
Includes bibliographical references and indexes.
ISBN 978-1-138-00116-9 (hardback)—ISBN 978-1-315-81505-3 (eBook PDF)
1. Palaeoecology—Africa. 2. Geology—Africa. I. Runge, Jürgen, 1962-

QE720.2.A35N49 2013
561'.1096—dc23

2013035070

ISBN: 978-1-138-00116-9 (Hbk)
ISBN: 978-1-315-81505-3 (eBook PDF)

Contents

Foreword and Introduction

I take pleasure in presenting a further edition (volume 32) of the internationally recognized and acclaimed series 'Palaeoecology of Africa' (PoA). Already since 1966 the series has published a large number of interdisciplinary scientific papers on landscape evolution and on former environments of selected areas within the African continent. Since the re-edition and re-launch of 'Palaeoecology of Africa' in 2007/2008 it is the fifth volume of the yearbook series that follows the new concept and layout under the restructured editorial board and by support of the publishing houses Routledge and CRC Press. Therefore, the ambitious goal of the editorial board and its editor in chief to have one book a year was almost reached. Many thanks go to all the contributing authors, colleagues and friends who directly and indirectly contributed during the last years to make this re-edition of 'Palaeoecology of Africa' a reality and a success.

This year's edition presents nine interdisciplinary scientific papers and reviews on former and recent landscape evolution and on past environments (e.g., climate change, vegetation dynamics and growing impact of humans on ecosystems). These papers expand horizons and interconnections to various types and methodologies of research on environmental dynamics from the Pliocene up to the present. Regional case studies cover Nigeria, Cameroon, selected sites within the Congo basin, Kenya, Malawi, Namibia and South Africa. This volume also gives space to researchers originating from Africa presenting their new findings to a wider international audience.

Today, by growing awareness of the worldwide impact of Global Change, it has become obvious that aside of the northern and southern hemisphere Polar region also the environmental setting in Africa was subject to considerable changes over time. Natural shifts in climate have caused repeated and strong modification in the area dynamics of ecosystems located in lower latitudes. By a variety of 'proxy data'—researched and applied by the different authors from numerous disciplines—an attempt is made to reconstruct the evolution of landscapes over space and time, underlining that 'the past is the key to the future'. Besides such spatio-temporal oscillations in forested and savanna areas of Africa volume 32 of 'Palaeoecology of Africa' also focuses on possible relationships between environmental change and human impacts, also on the perception of the phenomenon of recent 'climate changes' by different stakeholders.

The nine chapters brought together are quite different in topics, methods, style and length. All manuscripts have been internationally reviewed by one or two experts and corrected several times. Within the University of Frankfurt Physical Geography working group, formatting of the papers for PoA layout and style was reliably done by Nadia Anoumou and Dr. Joachim Eisenberg. Apart from cartographic art work partly carried out by the principal authors themselves, Peter Blank (Bielefeld) and Joachim Eisenberg (Frankfurt) revised numerous maps, figures and graphs by doing additional professional cartographic work for the book. Especially the contributions submitted by the colleagues with an 'African background' sometimes evidenced severe problems in producing good quality maps and figures; they and their contributions gained profit from these time consuming and joint efforts on cartography.

Chapter 1 by O.A. Boboye and I.M. Akaegbobi from the historic Nigerian University of Ibadan looks at two basins (terrestrial Sokoto B. and offshore Niger Delta B.) studying the benthonic foraminiferal microfauna. Aside of the stratigraphic features discovered and interpreted within the sedimentary traps, they evidenced by identifying foraminiferal assemblages, species diversity and abundance that the palaeoenvironment in the Late Miocene (about 13 Ma) and Maastrichtian to Eocene (about 70–55 Ma) originally showed fluctuating salinities and limited circulation under anaerobic conditions. Furthermore, specific sedimentary features allowed the identification of multiple transgressions as well as regressions within the basin environments.

Chapter 2, presented by a joint South African–Dutch–Norwegian research team around G. Langejans looks by applying a very sophisticated and complex research approach (studies on shellfish and other faunal remains together with archaeological records) on Late Pleistocene (beach) environments (Marine Isotope Stages 4 and 5, around 70–130 ka) at Blombos Cave with the Still Bay Industry on the southern terrestrial edge of the South African subcontinent. Comparison with climate models and transferring such findings directly from marine sediments to the terrestrial environment seems to be complex and difficult. Therefore, the emergence of Still Bay Industry could have been less triggered by former climate changes, and it is considered unlikely as an adaptation to a harsh and resource depleted environment.

Palaeoenvironmental evidence for 'younger' (OIS 1–3, 2–50 ka) climate and vegetation changes in Sub-Saharan Africa (pre-LGM, LGM, Younger Dryas [YD] and Holocene) is illustrated by the editor's working group from Goethe University in Frankfurt. They introduce finds from different field sites in Cameroon, Central African Republic and in D.R. Congo (former Zaire). Using geomorphological, stratigraphical and pedological methods (alluvia and slope sediments as proxies) together with numerous radiocarbon data illustrate sensitive rainforest-savanna landscape dynamics before, during and after the LGM. A probable YD event in the eastern Congo basin at the onset of the Holocene is evidenced by impressive stone-line features in hillwash and re-deposited fluvial sediments. A conceptual model of the geomorphodynamic activity in Central Africa since OIS 3 is presented, connecting the field sites within the upper Congo Basin. Comparable to this previous study, chapter 4 focus on Quaternary sequences covering OIS 1–3 by the example of the already intensively studied Barombi Mbo crater lake in Cameroon. P. Giresse, J. Maley and A. Zogning highlight the influence of (neo-) tectonics on the crater lake level and the depositional environment by using lacustrine sediments. However, low lake levels during the LGM and YD are considered to be cased by a significantly drier climate in the region.

Another Cameroonian lake, Lake Assom, located farer north than Lake Barombi Mbo, is studied in chapter 5 by P. Giresse and S. Ngos III. They look on Late Holocene morphodynamics (erosion and sedimentation) in the lake's catchment that led to deposition of about 70 cm thick sediments on the lake bottom. Some radiocarbon data are presented on what is considered to have been a former debris flow. Comparisons with other lake level variations in the wider study area propose a growing seasonality and irregularity of rainfall during the Late Holocene.

Chapter 6 by T. Lüdecke and H. Thiemeyer from the Senckenberg Institute and the Goethe University, both located in Frankfurt, presents again older palaeoenvironmental data on the Plio-Peistocene transition (Chiwondo and Chitimwe beds) located on a tectonically active area on the northern edge of Lake Malawi. Their focus is mainly on relationships between sediment characteristics and the respective palaeoenviroment against the background of hominid evolution in this East African Rift zone. Fluvial deposits studied generally reveal a high pedogenic overprint by abundant carbonate nodules. Weathering processes (soil formation), geomorphological processes

and considerations of landscape dynamics under modified climate and vegetation cover are in this case 'proxies' used to explain the palaeoenvironmental setting.

In chapter 7 K. Heine, U. Rust (1940–2012) and A. Hilgers are touching an old scientific dispute if there is at all a Younger Dryas (YD) event on the southern hemisphere? By revisiting and discussing the Eksteenfontein pollen section in the winter-rain realm of the Northern Cape Province these authors conclude that sudden late-glacial cooling phases of the Southern Hemisphere were caused by the Antarctic Cold Reversal (ACR, c. 14,700–12,700 ka BP) and were confused with the YD event.

The chapters 8 and 9 are mainly looking on historical and present-day landscape dynamics in lower latitudes evidenced by field studies and statistical/empirical data acquisition. Severe landscape degradation in Nigeria (Anambra State) started as early as 1850 and is described and studied by E.I. Okoyeh, I.M. Akaegbobi and B.C. Egboka (chapter 8). Widespread gully erosion and mass wasting (landslides) over soft Tertiary rocks caused water scarcity and loss of economic trees and herbs. Reclamation measures, up so far, all failed. The authors suggest remedial measures and discuss problems of sustainable landscape management in Nigeria.

In chapter 9 C.-R. Nguimalet carried out detailed statistical and spatio-temporal examinations (1958–1995) on selected river catchments of Kenya and Central African Republic (CAR). The choosen examples (Malewa River in Kenya, and Tomi, Gribingui and Fafa Rivers in CAR) are quite different in size, shape and environmental setting. However, the author carefully worked out some trends and relationships between rainfall and discharge variability during the observation period and assess the findings against the background of ongoing climate change.

In conclusion one can state that palaeoecological information in Africa is still subjected to large methodological and geographical gaps. Most records are qualitative and even if time resolution of terrestrial records has become somewhat better in the last years there are still large spatial and dating uncertainties. Multi-proxy and multi-archive studies need to be developed further, and 'Palaeoecology of Africa' can serve as an innovative and modern forum for that. Furthermore, it has become clear that the linkage between models, marine and terrestrial records contains a lot of challenges to future interdisciplinary research.

Finally, I take this opportunity to place on record my gratitude to the publishing houses Routledge and CRC Press with Senior Publisher Janjaap Blom and his team for the continuous support of 'Palaeoecology of Africa'.

Jürgen Runge
Frankfurt
July 2013

This page intentionally left blank

Contributors

Izuchukwu M. Akaegbobi

Department of Geology, University of Ibadan, Ibadan, Nigeria. Email: izumike20022002@yahoo.com

Eva Becker

Institute of Physical Geography, Johann Wolfgang Goethe University, Frankfurt am Main, Altenhöferallee 1, D-60438 Frankfurt, Germany. Email: eva.becker@geosphaere.de

Olugbenga A. Boboye

Department of Geology, University of Ibadan, Ibadan, Nigeria. Email: boboyegbenga@yahoo.com

Gerrit L. Dusseldorp

Centre for Anthropological Research, University of Johannesburg, Johannesburg, South Africa. Email: g.dusseldorp@gmail.com

Boniface C. Egboka

Department of Geological Sciences, Nnamdi Azikiwe University, Awka, Nigeria.

Joachim Eisenberg

Institute of Physical Geography, Johann Wolfgang Goethe University, Frankfurt am Main, Altenhöferallee 1, D-60438 Frankfurt, Germany. Email: j.eisenberg@em.uni-frankfurt.de

Pierre Giresse

Centre de Formation et de Recherche sur les Environnements Méditerranéens, UMR 5110-CNRS, Université Perpignan Via-Domitia, France, Email: giresse@univ-perp.fr

Klaus Heine

Philosophische Fakultät I, Universität Regensburg, Regensburg, Germany, Email: klaus.heine@geographie.uni-regensburg.de

Christopher S. Henshilwood

Institute for Human Evolution, University of the Witwatersrand, Johannesburg, South Africa. Department of Archaeology, History, Cultural Studies and Religion, University of Bergen, Bergen, Norway. Email: Christopher.Henshilwoos@ahkr.uib.no

Alexandra Hilgers

Geographisches Institut, Universität zu Köln, Zülpicher Straße 49, D-50674 Köln, Germany, Email: a.hilgers@uni-koeln.de

Geeske H.J. Langejans

Faculty of Archaeology, Leiden University, Leiden, The Netherlands. Centre for Anthropological Research, University of Johannesburg, Johannesburg, South Africa. Email: geeske.langejans@gmail.com

Tina Lüdecke

Institute of Geoscience, Johann Wolfgang Goethe University, 60438 Frankfurt, Germany. Biodiversity and Climate Research Centre (BiK-F) & Senckenberg, Frankfurt, Germany, Email: Tina.Luedecke@senckenberg.de

Jean Maley

Département Paléoenvironnements et Paléoclimatologie, ISEM-CNRS, Université de Montpellier-2, Montpellier, France, Email: jean.maley@neuf.fr

Marion Neumer

RODECO Consulting GmbH, Hindenburgring 18, D-61348 Bad Homburg, Germany. Email: marion_neumer@yahoo.de

Simon Ngos III

Department of Earth Sciences, University of Yaoundé I, Yaoundé, Cameroon, Email: sngos@yahoo.com

Cyriaque-Rufin Nguimalet

Laboratoire de Climatologie, de Cartographie et d'Etudes Géographiques (LACCEG), Département de Géographie, Faculté des Lettres et Sciences Humaines, Université de Bangui, BP 1037, Bangui, RCA, Email: cyrunguimalet@googlemail.com

Karen L. van Niekerk

Department of Archaeology, History, Cultural Studies and Religion, University of Bergen, Bergen, Norway. Email: Karen.Niekerk@ahkr.uib.no

Elizabeth I. Okoyeh

Department of Geological Sciences, Nnamdi Azikiwe University, Awka, Nigeria, Email: reallizkay@yahoo.com

Jürgen Runge

Institute of Physical Geography, Johann Wolfgang Goethe University, Frankfurt am Main, Altenhöferallee 1, D-60438 Frankfurt, Germany. Email: j.runge@em.uni-frankfurt.de

Uwe Rust (1940–2012)

Geographisches Institut, Ludwig-Maximilian-Universität, München, Germany.

Mark Sangen

Institute of Physical Geography, Johann Wolfgang Goethe University, Frankfurt am Main, Altenhöferallee 1, D-60438 Frankfurt, Germany. Email: m.sangen@em.uni-frankfurt.de

Heinrich Thiemeyer

Institute of Physical Geography, Johann Wolfgang Goethe University, Frankfurt am Main, Altenhöferallee 1, D-60438 Frankfurt, Germany, Email: thiemeyer@em.uni-frankfurt.de

Appolinaire Zogning

National Institute of Cartography, Ministry of Scientific Research and Innovation, Yaoundé, Cameroon.

CHAPTER 1

Palaeoecological conditions in the Sokoto Basin and the deep offshore Niger Delta (Nigeria) evidenced by benthonic foraminiferal microfauna

Olugbenga A. Boboye & Izuchukwu M. Akaegbobi
Department of Geology, University of Ibadan, Ibadan, Nigeria

ABSTRACT: A qualitative and quantitative foraminifera study has been carried out on outcrops and bore hole cutting samples. The outcrop samples were obtained from Taloka, Dange, Kalambaina, Dukamaje and Wurno formations exposed within the Sokoto Basin while the cutting samples were from two exploratory wells (BX-1 and LAT-1) which are located within Oil Mining Lease (OML) 65, deep offshore of Niger Delta Basin. This work provides information on the palaeoecological inferences and age interpretation of the depositional environments. The foraminiferal assemblages recovered from the samples are composed of benthonic and few planktonic species. Benthonic species are represented by calcareous taxon with diverse test types (porcelaneous, hyaline) and arenaceous taxon of simple morphology. The fauna assemblages are of considerable ecological and stratigraphic importance in the studied areas. A biostratigraphic study was carried out on composite samples from sixty-five (BX-1 well) and fifty-six (LAT-1 well) cuttings sampled at 20 m intervals from Niger Delta Basin, while forty outcrop samples were from the Sokoto Basin. The microfossil analyses and identification was done under the Scanning Electron Microscope (SEM). The results show that bulk of the lithofacies is composed of shale, mudstone and sandy mudstone, sandstone, limestone and siltstone. The colour varied from light grey to dark grey with intercalated coarse to fine-grained sandstone beds. A total of seventy six foraminifers' species have been recovered. The microfossil assemblages recorded delineated the biostratigraphic sequence based on their evolutionary trend. The composition of the foraminiferal assemblage, species diversity and abundance suggest that the palaeoenvironment of Niger Delta and Sokoto Basin are deposited in the marginal marine through inner neritic to outer neritic regimes typifying hyposaline conditions. The dark coloured shale characterized the environment as fluctuating salinities and limited circulation which prevailed under anaerobic conditions in the late Miocene (13.82 to 5.332 Ma.) (Niger Delta), and Maastrichtian to Eocene (70.6 ± 0.6 to 55.8 ± 0.1 Ma.) (Sokoto). Cycles of transgression and/or regression were also identified based on the facies assemblages.

1.1 INTRODUCTION

This study presents the Cenozoic foraminiferal biostratigraphy in the deep offshore of the Niger Delta and the Nigerian sector of the Sokoto Basin. The study areas lie between 4°–5°02′N and 3°–9°E in the Oil Mining Lease (OML) 65 and 13°–13°50′N and 5°10′–5°50′E respectively (Figures 1a, b). The geology, structures, depositional environments, source rocks, and hydrocarbon potentials of these basins have been intensively studied and well documented. The earliest geological work on

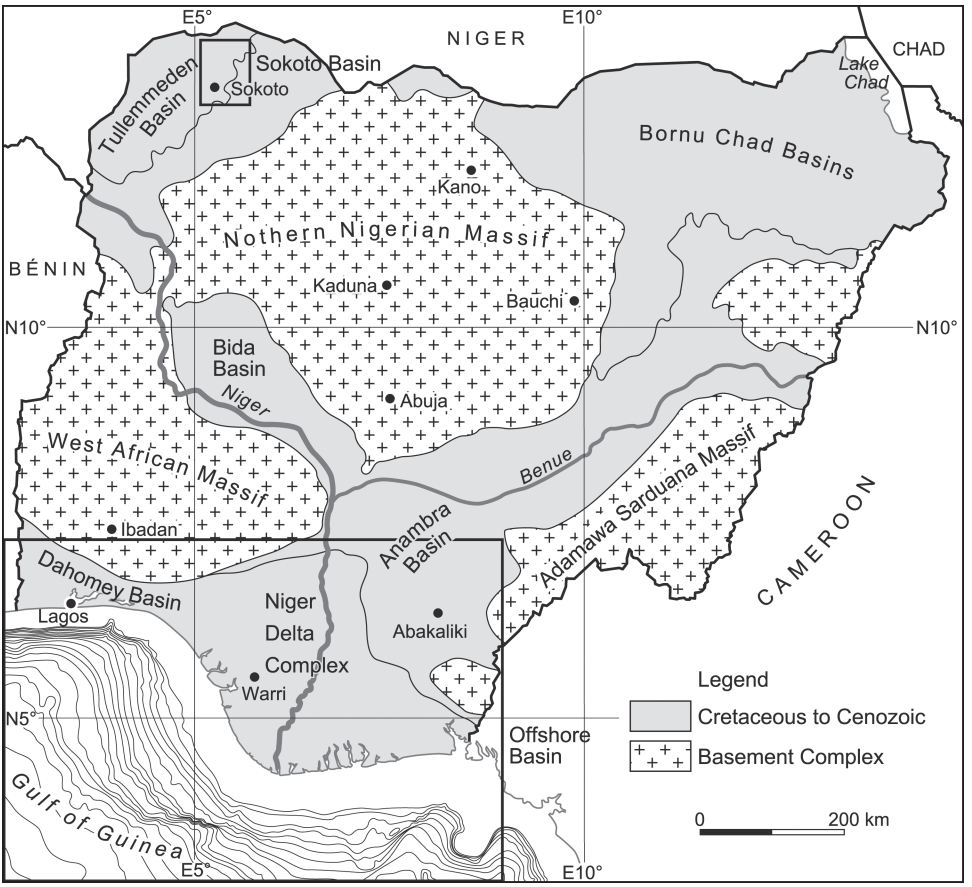

Figure 1a. Geological Map of Nigeria (modified after Whiteman, 1982).

these basins have been reported by the following authors (Addeh and Duze, 1988; Adegoke, 1969; Adegoke *et al.*, 1975, 1976; Reyment, 1959, 1960, 1963, 1965; Allen, 1964, 1965; Parkinson, 1967). They proposed an estuarine to freshwater palaeoenvironment of deposition for the sediments; microfauna and the geology of the Sokoto Basin have been studied. Other workers (Carter, 1960; Parker 1964; Kogbe 1976) studied the Cretaceous and Tertiary sediments of the Sokoto Basin. These workers have suggested several geological successions. The age of these deposits have been controversial. Gwandu Formation forms a part of the 'Continental Terminal'. Amongst the workers that have worked on foraminferal evaluation in the Niger Delta are Seglie *et al.* (1982) and Adeniran (1997) amongst others. Boboye and Adeleye (2009) identified four condensed sections for the foraminiferal assemblages and four zones for the calcareous nannofossil in the Niger Delta which was correlated to the NN13, NN11, NN10 and NN9 of Global Cycle Chart (Boboye and Adeleye, 2009). Other workers with diverse reports on biostratigraphy of this basin include Ogbe (1982), Ozumba (1995), Salard-Cheboldaeff and Dejax (1991), Salami (1984) amongst others. However, planktonic biostratigraphy of the Neogene in the basins is limited to few references. Detailed work on the subsurface stratigraphy,

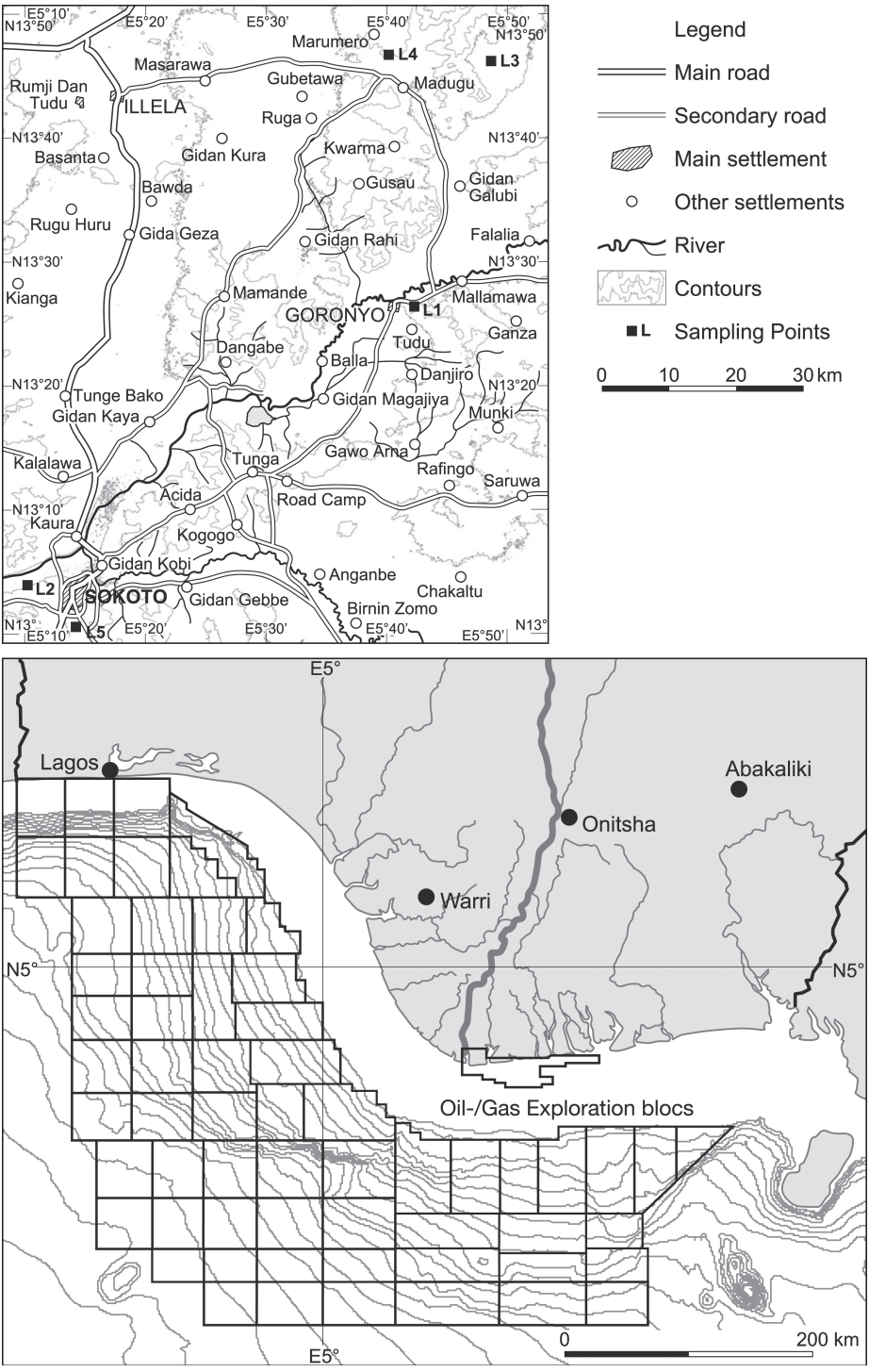

Figure 1b. Sokoto and deep offshore Niger Delta Basins study areas (modified after Obaje *et al.*, 2004).

sedimentation and structures of the Tertiary Niger Delta Basin has been done and reviewed by Short and Stauble (1967), Asseez (1976), Hospers (1971), Merki (1972) and Weber and Daukoru (1975). Okosun (1999) studied the taxonomy and biostratigraphy of Ostracods and foraminifera of two boreholes in Sokoto Basin and these were based on palaeoecological and interpretation of the depositional environments. Petters (1978) reported that the Dange Formation contains a rich diversity of agglutinated foraminifera.

1.2 GEOLOGIC SETTING AND STRATIGRAPHY OF THE STUDY AREAS

1.2.1 Niger Delta Basin

The study areas are part of the Tertiary Niger Delta Basin, which is defined in terms of lithology consists of both marine and non-marine sedimentary rocks. It is a petroliferous province in the southern part of Nigeria (Figure 2). Allen (1964, 1965) studied the recent surface sediments of the Niger Delta Basin and classified the sedimentary bodies recognized as younger suite elder and repositioned break (Regression) these he assigned of Pleistocene and Holocene age. He further observed that the Late Quaternary Niger Delta is based on essential concentric facies elements as in many other clastic deltas rather than on radial elements as in the Mississippi bird–foot delta. Three main subsurface lithostratigraphic units recognized and delineated are Akata, Agbada and Benin formations (Short and Stauble, 1967), which are in turn overlain by diverse

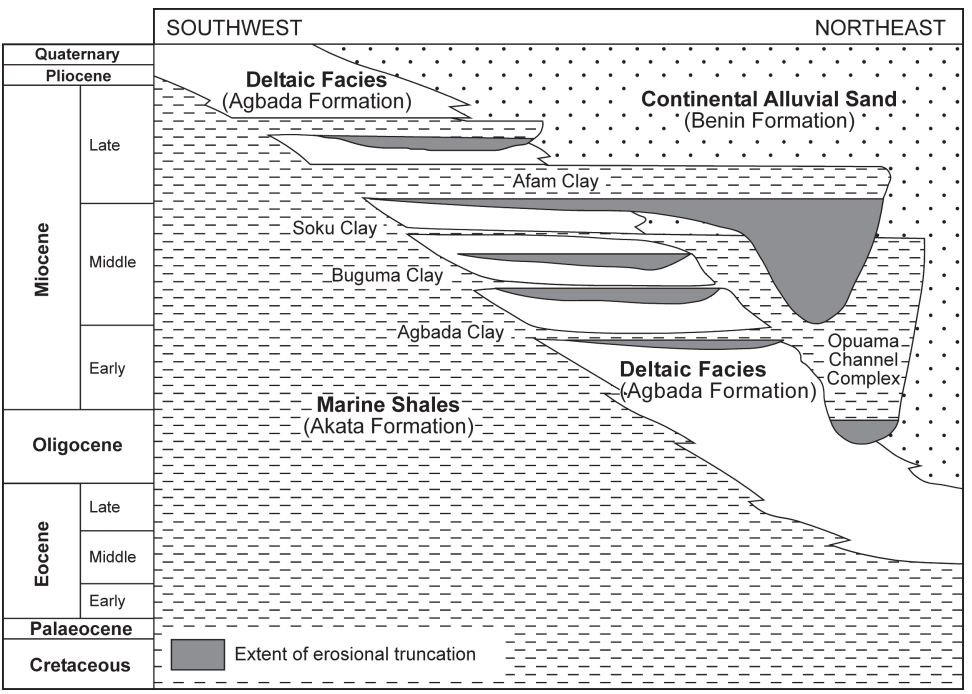

Figure 2. Stratigraphic column showing the three formations of the Niger Delta (modified from Shannon and Naylor, 1989 and Doust and Omatsola, 1990).

types of Quaternary deposits. The Akata Formation is dominantly shale of marine origin while the Agbada Formation is a paralic facies of shale and sand. The Benin Formation is a continental deposit made up of mainly sandstone. The Quaternary deposits consist of either a relatively uniform lithology of sand, silt, sand-silt-clay mixtures with clay and peat increasingly more predominant seaward. The three formations are stratigraphically superimposed in space and time and range from Eocene to recent in age.

In this study, the lithofacies that characterized the wells in the Niger Delta Basin include light to dark grey shale, silty mudstone and sandy mudstone with intercalations of sandstone beds. The sandstone range from coarse to fine grained, angular to rounded and poor to well sorted (Figures 4a, b). The accessory minerals present in profusion include ferruginous material, mica flakes and some shell fragments. The stereo binocular microscope was used to describe the samples. The studied intervals from the Niger Delta Basin ranged from 2210 m to 3508 m (BX-1 well) and 28050 m to 3960 m (LAT-1 well) depths (Figures 4a, b).

1.2.2 Sokoto Basin

The Sokoto Basin of West Africa covering an estimated area of 700,000 km^2 (Kogbe and Sowunmi, 1980) extends into northwestern Nigeria where it is referred to as the Sokoto Basin. The basin broadly covers an area underlain predominantly by crystalline rocks to the east and sedimentary terrain to the northwestern half. All of the samples used in this work emanated within the basin. In the southeastern sector of the basin, up to 2000m of clastic sequences overlies the basement. Moreover, in the Sokoto basin sequences of semi consolidated gravels, sands, clay, some limestone and ironstone are found. The sedimentary sequences are sub-divided from bottom to top into the late Jurassic to early Cretaceous Illo and Gundumi Formations (Continental

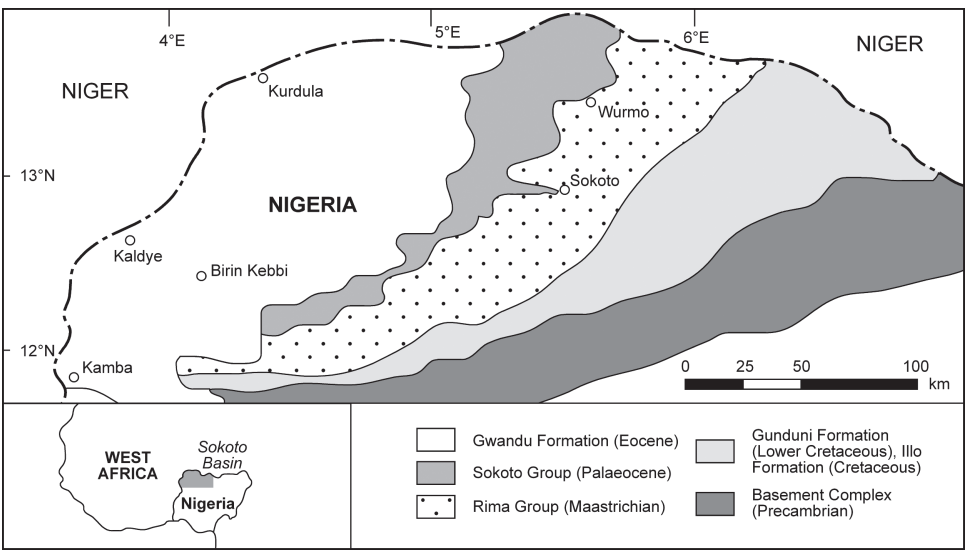

Figure 3. Stratigraphic units showing the formations of the Sokoto Basin (modified after Oteze, 1991).

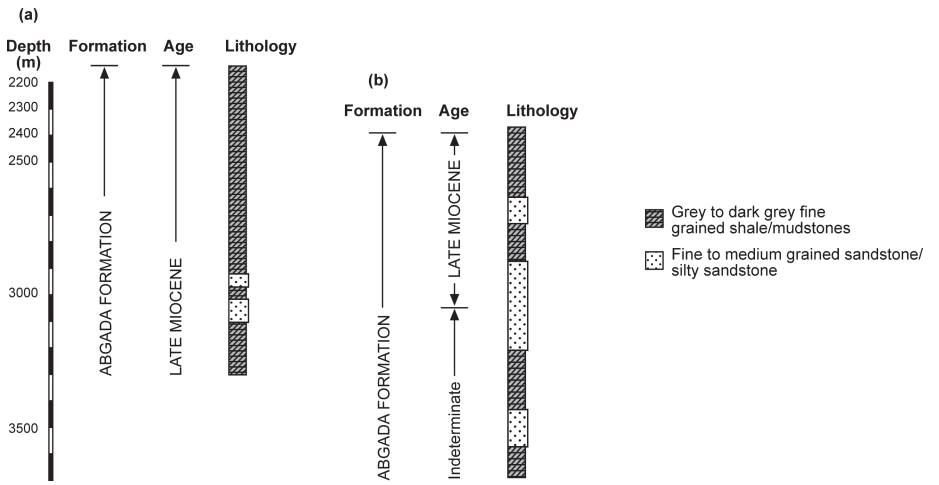

Figure 4. (**a**) Lithostratigraphy of BX-1 and (**b**) LAT-1 well (Niger Delta Basin).

Intercalaire), the Maastrichtian Rima Group (sub-divided into Taloka, Dukamaje and Wurno Formations), the late Palaeocene Sokoto Group (sub-divided into Dange, Kalambaina and Gamba Formations) and the Eocene-Miocene Gwandu Formation (Figure 3). Overlying all the formations is a laterite cap usually up to 12 m thick in some localities.

In this study, five exposed outcrops (Taloka, Dange, Kalambaina, Dukamaje and Wurno Sections) in Sokoto Basin were studied in which the basin formations are well represented (Figures 4c–f Figure 5). The Taloka Formation consists of interbedded grey to dark mudstones to the grained friable sand with some thin bands of carbonaceous shale and siltstone. It is fine to coarse grained heterogeneous sand and sandstone with interbedded shale, contains masses of gypsum and ferruginous materials.

South of Wurno, the Taloka formation and Wurno formation cannot be differentiated because of the thinning out Dukamaje Formation. Dukamaje Formation consists predominantly of shales with some limestones and mudstones. The formation is of dark fossiliferous shale with white spheroidal nodules and some thin limestone bands. The shales contain numerous fragments vertebrae and limbs bones bed highly fossiliferous lies near the base. Wurno Formation consists of thin friable, fine grained sandstones intercalated with soft mudstones. It is well exposed at Wurno. The sediments are dark coloured, loosely consolidated and susceptible to weathering, they consists of pale friable fine grained sandstones, siltstone and intercalated mudstones. Small scale load cast, bioturbation structures and flaser bedding noted in the Taloka Formation are also abundant in the Wurno Formation. The Kalambaina Formation consists of a marine white, clayey limestone and shale. The type section of the formation is at the quarry of the cement factory, near the Kalambaina village located about 6 km to the south west of Sokoto Township. Dange Formation consists of grey, yellowish brown, dark grey clay shales. The top is calcareous with thin laminations of limestone between the clay. The shale includes bands of fibrous gypsum with numerous irregular phosphatic nodules. The nodules are characteristically marked with irregular striations and have an off-white external colour, but bluish-grey internally.

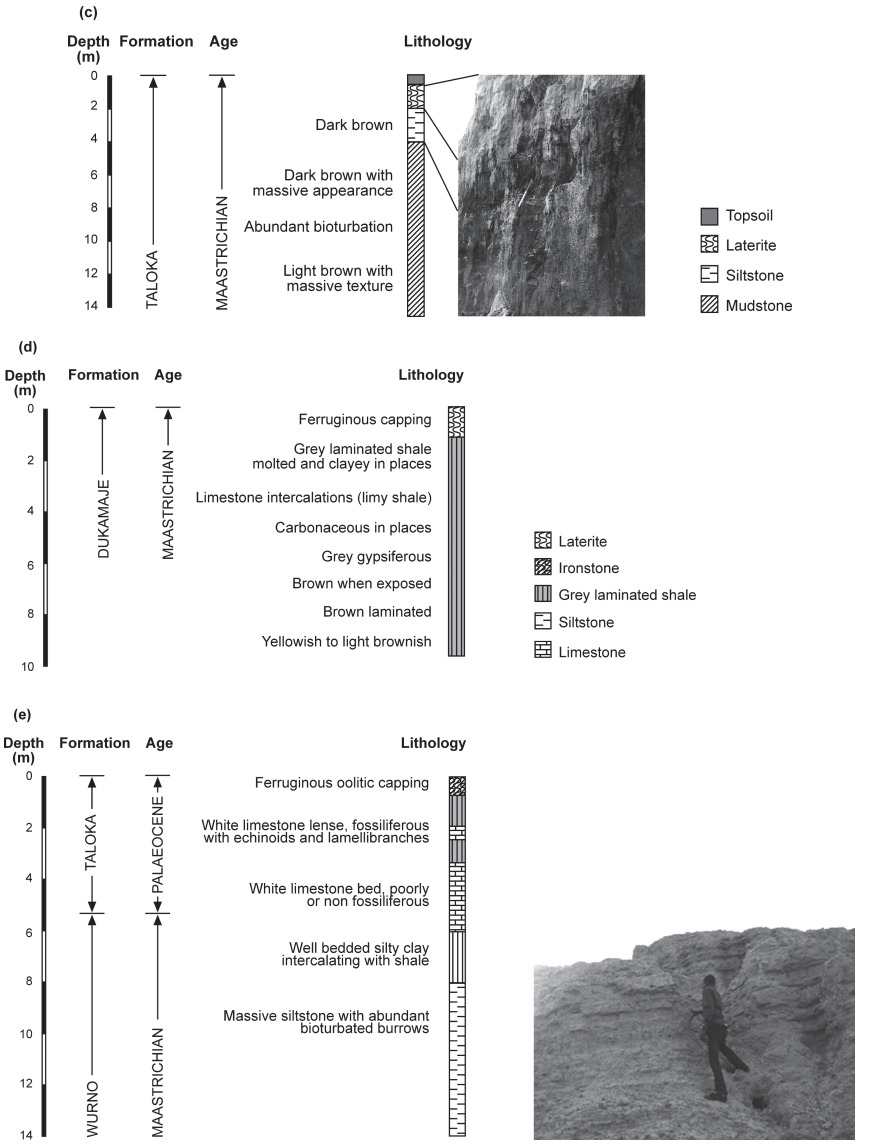

Figure 4. (**c**) Lithostratigraphy of locality One at Taloka exposing Taloka Formation, (**d**) locality Two at Dongodajji, showing Dukamaje Formation and of (**e**) locality Three at Gada, showing section of Wurno at the outskirt of exposure at Wurno village (Sokoto Basin).

1.3 RESULTS AND DISCUSSION

1.3.1 Materials and methodology

An integrative lithologic and biostratigraphic analyses have been carried out on outcrops and cutting samples (composite) from each of the formations in the basins. Twenty grammes of each composite sample are weighted using an electronic balance.

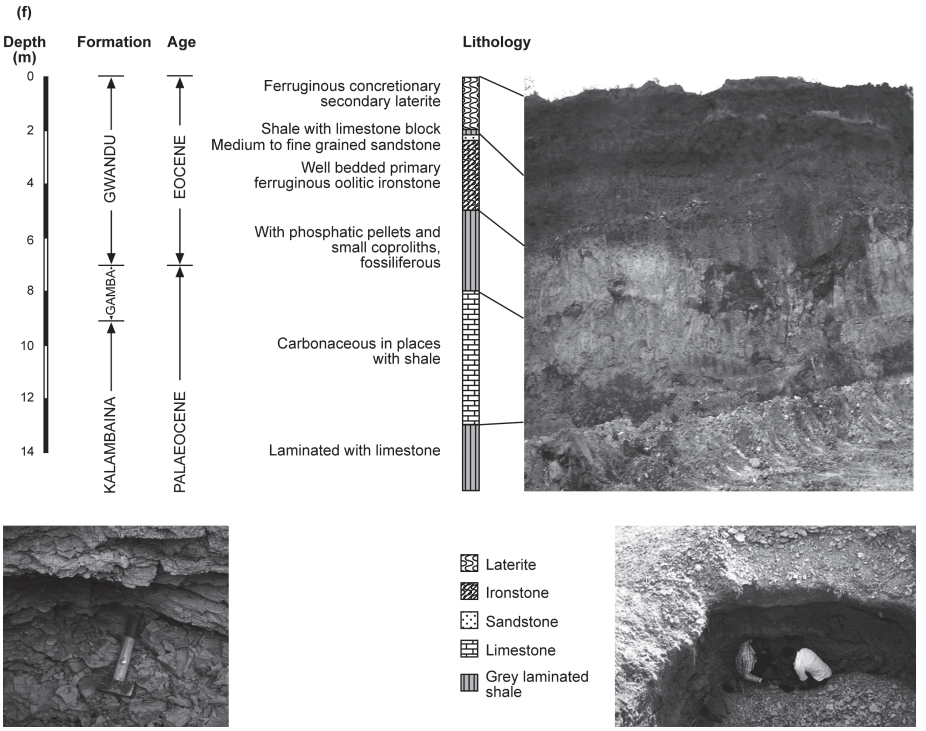

Figure 4. (**f**) Lithostratigraphy of locality four at Gada, showing Wurno and Dange Formations (Sokoto Basin).

They were disaggregated carefully into small aggregates so as not to destroy the microfossils and later heated to drain any moisture that may be present and also to enable the fossils separate from the samples. One to two teaspoonful of anhydrous sodium carbonate Na_2CO_3 and 10% concentrated hydrogen peroxide (H_2O_2) were added. The mixtures were then heated to boil until all the samples smeared completely. These were later soaked with distilled water for 24 hours.

The samples were later washed thoroughly under a gently running tap to let out the mud using a mesh sieve size of 63 microns (200 mesh) until the samples were clean. The residues were then transferred into a funnel to drain samples and were later dried at 80ºC. Each washed and dried samples was dry-sieved through a set of mesh size consisting of three grades sieve; 30 and 60 (apertures 500 and 251 microns respectively) to facilitate the picking process. The analysis was done under Leitz-Wetzler binocular microscope, and then covered with cover slides for identification which involved morphological examination of the picked foraminifera fauna and consultation of relevant monographs and local type's species. The frequency count was based on a minimum of 100 specimens. The percentage of each species was computed factoring in the number of specimens of the species relative to the total number of the specimen per sample.

1.3.2 Micropalaeontology

A total of sixty four (64) foraminifera species comprising of nineteen (19) planktonic, 33 calcareous and 12 agglutinating species have been recovered (Tables 1–4).

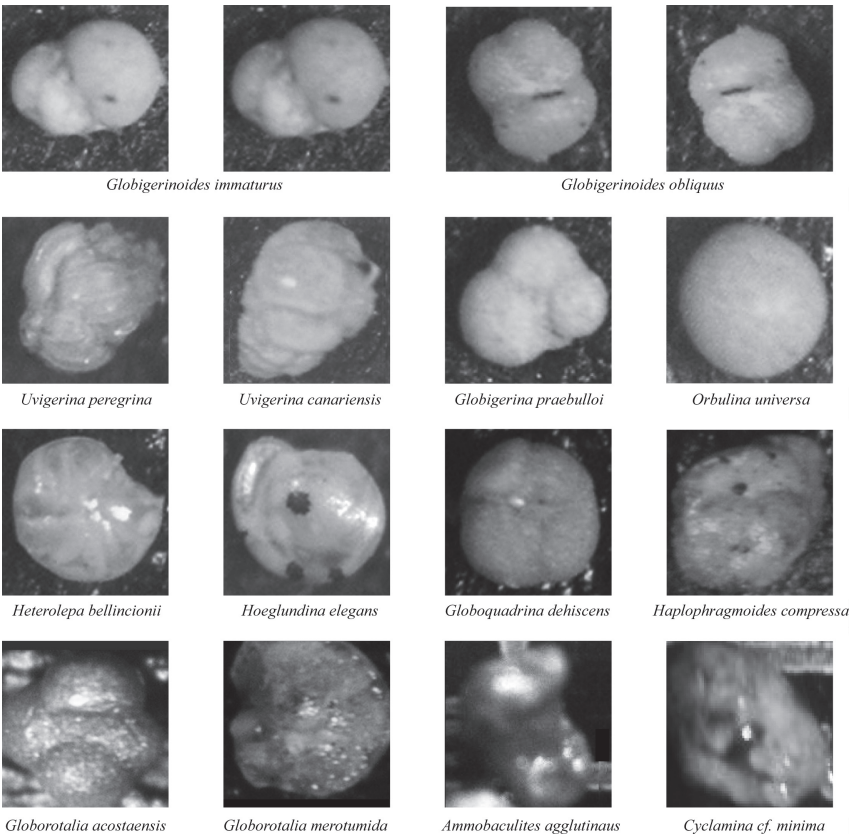

Figure 5. Some foraminifera assemblages recorded from the study areas.

Table 1. Results of foraminifera species from Niger Delta Basin (BX-1 well and LAT-1 well).

Depth (m)	Planktonic (P)	Calcareous (C)	P/C ratio
2833	30	10	3
2866	51	16	3
2900	56	3	19
2950	30	16	2
3000	4	2	2
3033	52	25	2
3050	2	3	0.7
3083	6	3	2
3100	4	5	0.8
3133	17	20	0.9
3166	1	6	0.2
3233	4	1	4
3266	3	1	3
3283	20	6	3
3316	6	6	1
3366	2	1	2

Table 2. Results of foraminifera species from Sokoto Basin (samples from Dange Formation).

Depth (m)	Species diversity	Agglutinated (%)	Arenaceous (%)	Calcareous (%)
7.21–8.27	5	100	–	–
15.54–16.2	6	100	–	–
16.61–16.92	4	100	–	–
17.61–18.10	3	100	–	–
19.20–20.21	11	73	27	–
20.21–21.43	4	100	–	–
22.82–22.97	5	80	20	–
22.97–23.66	3	–	–	–
23.66–23.91	2	–	–	–
23.91–24.63	0	–	–	–

Table 3. Results of foraminifera species from Sokoto Basin (samples from Dukamaje Formation).

Depth (m)	Species diversity	Agglutinated (%)	Arenaceous (%)	Calcareous (%)
7.10–8.20	3	–	100	–
15.00–15.90	2	–	100	–
16.00–16.92	2	–	100	–
17.00–18.10	5	–	80	–
19.00–20.21	–	–	–	–
20.00–21.43	4	–	80	–
22.00–22.97	3	–	100	–
22.97–23.66	3	–	100	–

Table 4. Results of foraminifera species from Sokoto Basin (samples from Gamba Formation).

Depth (m)	Species diversity	Agglutinated (%)	Arenaceous (%)	Calcareous (%)
6.00– 9.80	4	–	–	100
10.54–16.20	5	–	20	80
16.50–16.90	4	–	25	75
17.50–18.00	3	–	–	100
19.00–20.00	3	–	–	100
20.20–21.43	5	–	20	80
22.82–22.97	5	–	20	80
22.97–23.66	3	–	25	75
23.66–23.91	2	–	–	100
23.91–24.63	0	–	–	–

The preservation of foraminiferal microfossils within the study intervals are poor. This could be as a result of terrigenous influx which could be responsible for poor representation of some foraminifera most especially the planktonic species. They have been fragmented hence could not be presented with the complete forms. Some assemblages recovered include *Globorotalia acostaensis, Spaeroidinella bulloides, Globorotalia acostaensis, Orbulina universa*, and *Globoquadrina altispira, Globigerina praebulloides, Globigerinoides immaturus, Globigerinoides obliquus, Globigerinoides sacculiferus, Globaguadrina dehiscens, Globorotalia margaritae, Sphaeriodinellopsis seminulina* are the common planktonic species. The rare planktonic species are *Globorotalia menardii, Globorotalia pseudomioceniza, Globorotali humerosa* and *Neogloboquadrina dutertrei*. Calcareous foraminifera also has common and rare species. Most common species are *Gyroidina soldanic, Heterolepa floridana*. The calcareous foraminifer is mainly characterized by rare species of *Amphicoryna scalaris, Hanzawaia boueara*, *Heterolepa bellincionii*, *Nodosaria* spp, *Urigenna peregrine*, *Cibicides pruecurscrius* and *Stilostomella vemeulli*. The agglutinated foraminifera are characterized by rare species which occur at the lower section of the wells. These rare species include *Textularia* spp., *Eggerella bradii, Succammina complanata, Trochammina* spp., *Vermeuilina* spp. Other microfaunas occasionally encountered in the wells are shelly fragments which occur mainly in the upper section.

1.3.3 Biostratigraphy and palaeoecology

Diverse types of characteristic benthonic foraminifera have been used for deciphering palaeoenvironment of the Cenozoic sediments; however, this study has shown the different species of foraminifera identified in the basins.

In the Sokoto Basin, some intervals were barren of fossil fauna, while some formations are fairly fossiliferous, since microfauna thrived well in the limestone strata which characterized Dange Formation. It consists predominantly of benthonic with arenaceous and calcareous forms as evidenced by their distribution (Tables 1–4, Figures 6–8) (Allen, 1965; Adegoke *et al.*, 1976; Boboye and Adeleye, 2009; Okosun, 1999).

The stratigraphic abundant species recovered from the sections in Sokoto Basin include *Ammondicus cretaceous, Ammobaculities expanses, Epidella africana, Eponides pseudoelevatus, Eponides plummerae, Haplophragmoides bradyi* and *Lenticulina midwayensis*. Other foraminifera peculiar to Kalambaina Formation include *Bolivina midwayensis, Elpphideiela africana, Gavenilinela danica, Pararotalia perclara* and *Rotalia* sp. The planktonic foraminifera species recorded in the Niger Delta Basin include *Globigerina praebulloides, Globigerinoides immaturus, Globigerinoides obliquus, Globorotalia acostaensis, Globigerinoides sacculiferus, Globaguadrina dehiscens, Globorotalia margaritae, Orbulina universa, Sphaeriodinellopsis seminulina, Globorotalia menardii, Globorotalia pseudomioceniza, Globorotali humerosa, Neogloboquadrina dutertrei, Amphicoryna scalaris, Hanzawaia boueara, Heterolepa bellincionii, Nodosaria* spp., *Urigenna peregrine, Stilostomella vemeulli, Textularia* spp., *Eggerella bradii, Succammina complanata, Trochammina* spp., *Vermeuilina* spp., *Globorotalia merotumida* and *Globorotalia pleisiotumida*.

The palaeoenvironment is evident from the stratigraphic distribution of the foraminifera in these basins (microfauna diversity and abundance significant). From the foraminiferal assemblage in these formations, it is suggested that the formations were deposited in environments of fluctuating salinities such as lagoon and estuaries with restricted circulation. Anaerobic conditions suggested by the presence of

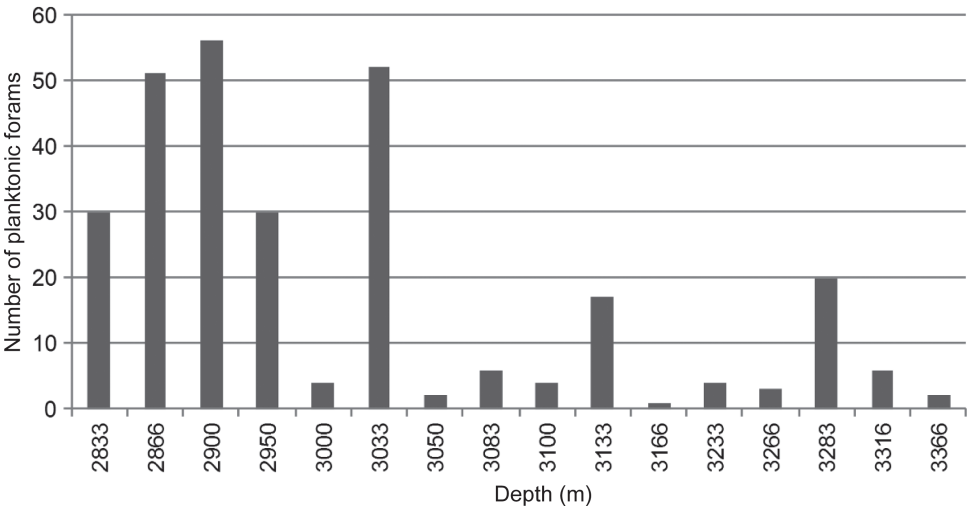

Figure 6. Variation of planktonic foraminifera with depth.

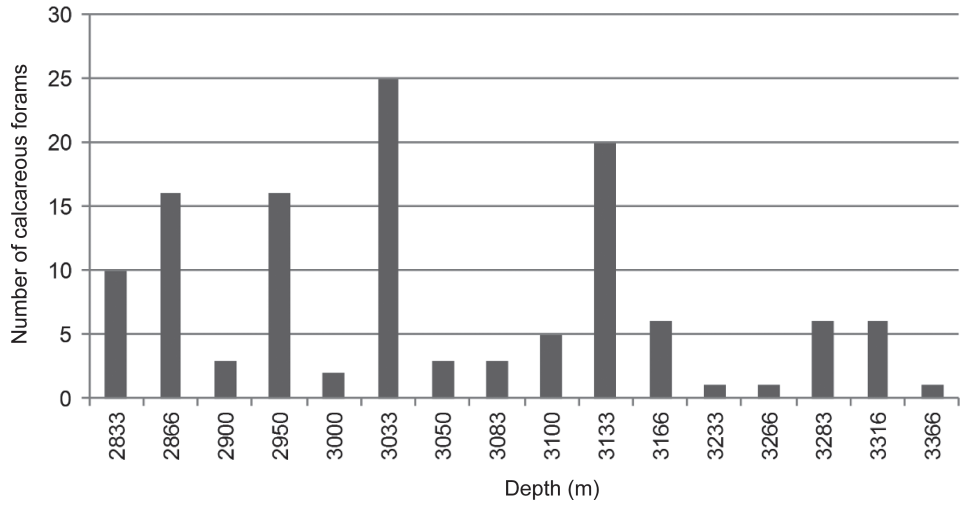

Figure 7. Variation of calcareous foraminifera with depth.

the dark shale occurred during the deposition of the Kalambaina Formation and that the transgression was at its weak band fully marine conditions were obtained (Okosun, 1999). The high productivity of some of the microfauna in addition to the absence of agglutinated foraminifera in Kalambaina formation corroborates this deduction. The presence of larger foraminifera such as *Operculiniodes bermudezi* (Kalambaina Formation) indicates a shallow depth of deposition. Nummulites are symbiont that associate with algae and flourish in clear warm water of normal salinity within the photic zone generally found at shallower level of less than 50 m. The abundance of benthonic foraminifera indicates shallow depositional environ-

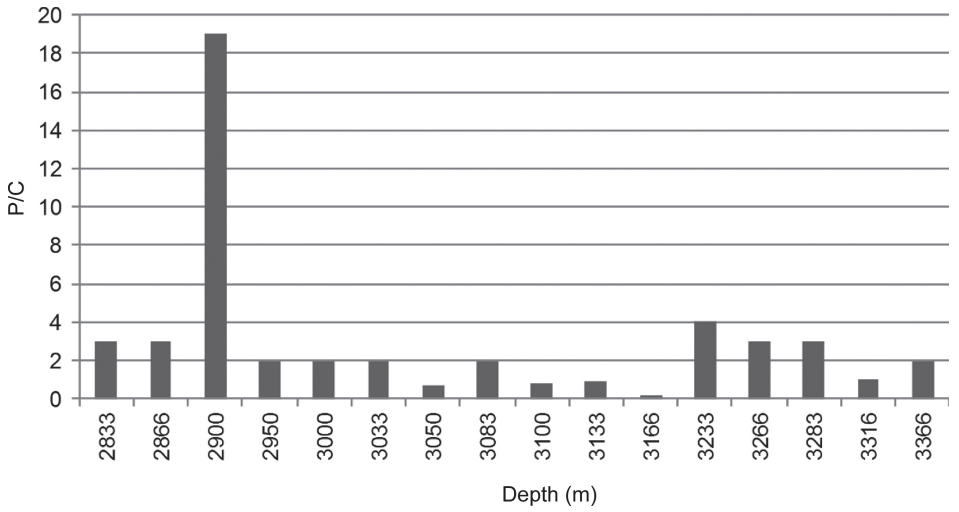

Figure 8. Variation of Planktonic/Calcareous (P/C) foraminifera with depth.

ment. Petters (1982, 1984) reported that the Dange Formation and Gamba shale Formation which consists of shale lithofacies contain rich but low diversity agglutinated foraminifera, while the marl bed interbeds contain both agglutinated and calcareous species but with preponderance of the calcareous forms. The Kalambaina Formation contains mainly calcareous forms with reduced or no agglutinated fauna. It was observed that the Kalambaina Formation contains only calcareous fauna (Tables 3, 4). It can also be concluded that the Palaeocene carbonates facies of the Sokoto Basin were deposited during periods of fluctuating salinities and at more shallow depths. The restriction of agglutinated foraminifera to the Dange Formation suggests a transitional or marginal marine palaeoenvironment for its deposition.

The agglutinated forms like *Haplophragmoides hausa* and *Ammobaculites expansus*, which have least demand for carbonate shell construction are most abundant in hypersaline conditions which typify marginal marine environment and the presence of hyaline forms such as *Midwayensis parallela* expansa suggest that hypersaline condition prevailed during the deposition of the sediment of Dange Formation. On the basis of the fauna characterizing Kalambaina Formation and Gamba shales, the environment of deposition is inferred to be inner neritic environment.

The black shale and its associated diagenetic pyrites crystals suggest deposition in anaerobic environment that resulted from restricted circulation at the early stage of the transgression during the deposition of Dange Formation. During the deposition of Kalambaina Formation, a freer circulation became dominant. The intercalation of gypsiferous horizons in the shale facies corroborates salinities and arid climate. The Wurno Formation marks the end of Late Maastrichtian depositional cycle and a renewed phase of coastal plain sedimentation. It is very similar to the Taloka Formation which exhibit horizontal beds, burrows, and composed of muddy siltstones, mudstones and fine-grained sandstones at the base of the Wurno Formation which are not well exposed at the type sections.

An arenaceous foraminifera assemblage occur at the lower and middle sections of the Wurno Formation at the type section, this include *Miliammina* sp., *Textularia*

sp., *Ammobaculites* sp., and *Trochammina* sp. These are evidences of marine influence; hence most of the Wurno formations could be placed within the Palaeocene marine cycle (Parker, 1964). The Wurno Formation is succeeded with thickness of about 10 m of gypsiferous shale.

The Dange Formation is rich in Palaeocene vertebrate remains, and also contains a sporadic arenaceous foraminiferal assemblage. However, there is a 1m thickness of marl in the lower section that is shelly in some locations and also contains abundant *Cibicides simplex*, in addition to arenaceous foraminifera. The Kalambaina Formation of over 10 m thickness in outcrop is highly fossiliferous marl embedded with limestone nodules, and some very argillaceous parts. It is rich but low diversity of molluscan and echinoid megafossil assemblages have been reported (Parker, 1964). The Kalambaina Formation was deposited during the maximum extent of the last Saharan Epeiric Sea. Its deposits overstep those of the Maastrichtian transgression, and contain a rich, warm, and shallow-water benthonic foraminiferal assemblages comprise mainly of *Rotaliids, Cibicidis, Nonionids, Pararotalia, Elphidiella* and the larger foraminifera *Operculinoides bermudezi.*

The foraminiferal assemblage of Dukamaje Formation includes *Ammobaculites* sp., *Ammodiscus siliceus, Haplophragmoides excavata, Textularia* sp., *Trochammina* sp., and traces of *Qrbignyna inflata*. The marl band has an admixture of predominantly calcareous taxa, together with a subsidiary content of arenaceous species. Calcareous forms include *Guembelitria cretacea, Gavelinella* sp., *Nonion* sp., and *Nonionella* sp. There is re-occurrence of an entire arenaceous assemblage in the upper shale unit of the Dukamaje Formation. The presence of *Guembelitria cretacea* supports Late Maastrichtian age for the formation. The youngest fossiliferous marine strata in southeastern Sokoto Basin are those of the Gamba Formation, which is greenish grey phosphatic shale with sharks' teeth and arenaceous foraminifera. The Gamba Formation is about 2 m thick in outcrop but is missing in some localities due to disconformity. The shale of Gamba Formation represents a regressive deposit which marks the final withdrawal of the sea from the region.

The samples retrieved from Sokoto Basin are generally fossilliferous and possess a low diversity of foraminifera assemblages dominated by arenaceous forms. The agglutinated forms are restricted to Dange Formation. The degree of compaction of the shale to some extent has affected the state of preservation of the microfossils, this is evident in the lower section of Dukamaje Formation. Forms identification was difficult since their diagnostic features were either obliterated or flushed.

The palaeoenvironment of deposition identified in the Niger Delta Basin as shown in the exploratory wells sections were based on fauna assemblages that characterized them. From the top of the well intervals, fauna such as *Sphaerodinella dehiscens, Haplophragmoides* sp., *Globigerinoides sacculiferus, Cyclammina cancellata* and *Trochamina proteus* were identified suggesting an inner neritic marine environment. From the basal to the upper sections, an outer neritic environment is suggested; this is evident with the occurrence of *Cyclammina minima, Bathysiphon* sp., *Valvulina flexilis*, *Trochamina proteus*, and *Lenticulina inornata*. At the interval of 3843 m to 3863 m, inner neritic foraminifera were again encountered, which was preceded by the arenaceous indeterminate forms of coastal deltaic environment as encountered from 3923 m to 3963 m. The transition from inner neritic to coastal–deltaic environment suggests a period of transgression which could be due to eustatic sea level rise. The change in the environment as evident in the encountered foraminifera forms transgress into the middle neritic environment. The inner neritic foraminifera were not part of this transition which continues into the outer neritic environment.

1.4 CONCLUSIONS

Analyses of the benthonic foraminiferal microfauna of southeastern Sokoto and Niger Delta Basins have been carried out. The study revealed not only the occurrence of age diagnostic species, but also the existence of palaeobiogeographically significant forms in the Palaeocene. There is a close similarity between the Palaeocene benthonic assemblages of the Sokoto Basin and those of the epicontinental Boreal and Meridional Provinces of Europe.

In the Sokoto Basin, similar faunal elements include large, thick-walled species of the *Rotaliids, Elphidiella* which indicate that there was an extensive fauna exchange within the contiguous Mediterranean region during the Palaeocene. The bulk of the lithofacies constitute silty mudstone, sandy mudstone and shale with intercalations of coarse to fine grained sandstone beds. It was observed that Kalambaina Formation contains only calcareous non agglutinated fauna forms, suggesting that the Palaeocene carbonates facies of the formation were deposited during period of fluctuating salinities and at more shallow depths. The restriction of agglutinating foraminifera to the Dange Formation indicates a transitional or marginal marine palaeoenvironment for its deposition. The agglutinated forms which have least demand for carbonate shell construction are most abundant in hypersaline conditions which typify marginal marine environment and the presence of hyaline forms indicate hypersaline condition prevailed during the deposition of the sediment of Dange Formation. The black shale and its associated diagenetic pyrites crystals suggest deposition in anaerobic environment that resulted from restricted circulation during the deposition of Dange Formation at the early stage of the transgression.

The presence of *Guembelitria cretacea* supports a Late Maastrichtian age for the Dukamaje Formation. Apart from the presence of the microfaunas, the presence of Mososaurin bones and fish teeth in Dukamaje and Taloka also confirmed a Maastrichtian age to these formations and the environments are brackish water. Thus, there was an extensive fauna exchange within the contiguous Mediterranean region during the Palaeocene. Benthonic foraminifera which were restricted to carbonate facies along the margins of the Tethys Sea, such as *Operculinoides bermudezi*, was observed in the outcropping part of the Kalambaina marl and limestone.

In the Palaeocene sequence of Sokoto Basin, *Operculinoides bermudezi* was observed in the outcropping part of the Kalambaina marl and limestone in the basin. The Palaeocene benthic foraminiferal microfaunas of the Sokoto Basin have much in common with mainland Europe and the Mediterranean, those of the Southern Nigerian Sedimentary basin (Niger Delta) show close affinity with the Gulf Coastal Region of the United States. The distinctiveness of the two major West African Palaeocene foraminiferal microfaunas supports the recognition of the two areas as separate palaeogeographic provinces, between which was no faunal interchange. From the foraminifera assemblages, in the Palaeocene of Nigeria it is evident that the Southern Nigerian Sedimentary Basin did not derive its fauna through the so-called Trans-Saharan Seaway as claimed by some workers. Foraminifera data do not suggest any direct faunal exchange between the Sokoto and the southern Niger Delta Basins. The foraminiferal species recovered from Sokoto Basin suggest Late Maastrichtian age for Dukamaje Formation base on the occurrence of *Guembelitria cretacea*, Danian to Selandian for Wurno Formation with the occurrence of *Miliammina* sp., *Textularia* sp., *Ammobaculites* sp., and Trochammina and Thanetian age for Dange, Kalambaina and Gamba formations based on the co-occurrence of *Haplophragmoides excavata* and *Ammodiscus siliceus* respectively, this corroborate the earlier workers.

REFERENCES

Addeh, J.E. and Duze, T.M., 1988, Statistical Study of Organic Matter in the Niger Delta. *Nigerian Association of Petroleum Explorationists Bulletin, Nigeria*. Vol. **3. (1),** pp. 104–127.

Adegoke, O.S., 1969, Eocene Stratigraphy of Southern Nigeria: Extract de Memoires du B.R.G.M. No. **69**, pp. 23–49.

Adegoke, O.S., Abibo, T., Mochu, L., Odebode, M.O. and Nwachukwu, J.L., 1975, *Sedimentology of Lagos Lagoon and Harbour*, Proceedings 6th African Micopalaentology Coll. Tunis 1974.

Adegoke, O.S., Omatsola, M.E. and Salami, M.B., 1976, Benthonic foraminifera Biofacies of the Niger Delta. Inst. Int. Symp. On Benthonic Foraminifera on Cont. Margin. Past A. *Ecology and Biology Maritime–Sedt Spcecial Publication* **1**, pp. 276–292.

Adeniran, B.V., 1997, Quantitative Neogene planktic foraminiferal biostratigraphy of western Niger Delta, Nigeria. *Nigeria Association of Petroleum Explorationistes Bulletin,* **12(1),** pp. 54–69.

Allen, J.R.L., 1964. Sedimentation in the modern delta of the River Niger, West Sedimentology, *Bulletin American Association of Petroleum Geologists, U.S.A*., **1**, pp. 26–34.

Allen, J.R.L., 1965, Late Quaternary Niger Delta and adjacent areas: sedimentary environments and lithofacies. *Bulletin American Association of Petroleum Geologists, U.S.A*., **49**, pp. 547–600.

Asseez, L.O., 1976, Review of stratigraphic sedimentation and structure of the Niger Delta. In Geology of Nigeria, edited by Kogbe, C.A. (University of Ife, Center for Advanced Studies), pp. 259–272.

Boboye, O.A. and Adeleye, A.M., 2009, High resolution biostratigraphy of Early Pliocene to Late Miocene Calcareous nannoplankton and foraminiferal, Deep Offshore Niger Delta, Nigeria. *European Journal of Science Research*, **34(3)**, pp. 308–325.

Carter, J.D. 1960, *Sokoto Sheet 2, 1:250,000 Series.*—Geological Survey of Nigeria.

Doust, H. and Omatsola, E., 1990, *Niger Delta*. In Divergent/passive Margin Basins, edited by Edwards, J.D., and Santogrossi, P.A., Memoir **48**: Tulsa, Bulletin American Association of Petroleum Geologists, pp. 239–248.

Hospers, J., 1971, The Geology of the Niger Delta area. In The Geology of eastern Atlantic continental margin, edited by Delany, F.M., Great Britain Institute of Geological Science report, **70(16)**, pp. 121–142.

Kogbe, C.A., 1976, *The cretaceous and Paleocene sediments of southern Nigeria in Geology of Nigeria*, edited by Kogbe, C.A., (Elizabethan Pub. Co.), p. 273.

Kogbe, C.A. and Sowunmi, M.A., 1980, The Age of the Gwandu Formation (Continental Terminal) in the North Western Nigeria. VIC Coll. African Micropal. Tunis (1974). *Annales des Mines et de la Geologie,* **III(28)**, pp. 43–53.

Merki, P.J., 1972, Structural Geology of the Cenozoic Niger Delta. In African Geology, edited by Dessauvagie, T.F.J. and Whiteman, A.J. (University of Ibadan press), pp. 635–646.

Obaje, N.G., Wehner, H., Scheeder, G., Abubakar, M.B. and Jauro, A., 2004, Hydrocarbon prospectivity of Nigeria's Inland basins: From the viewpoint of Organic geochemistry and organic petrology. *American Association of Petroleum Geologists,* Bulletin, **87**, pp. 325–353.

Ogbe, F.G.A., 1982, The biostratigraphy of the Niger Delta, Nigeria. *Journal of Mining and Geology,* **18(2)**, pp. 19–71.

Okosun E.A., 1999, Late Paleocene biostratigraphy and palaoecology of Sokoto Basin. Northwestern. *Nigeria Journal of Mining and Geology*, **35(2),** p. 153.

Oteze, 1991 Portability of Groundwater from the Rima Group Aquifers in the Sokoto Basin, Nigeria. *Journal of Mining and Geology* **27(1)**, pp. 17–23.

Ozumba, M.B., 1995, Late Miocene-Pliocene biostratigraphy, Offshore Niger Delta. *Bulletin, Nigerian Association of Petroleum Explorationist.* **10(1)**, pp. 40–48.

Parker, D.H., 1964, Paleocene fossils from Sokoto Province, Northwestern Nigeria.—Rec. Geological Survey.

Parkinson, B., 1967, The Post-Cretaceous stratigraphy of southern Nigeria. *Quarterly Journal of Geology Society*, London, **63**, pp. 311–320.

Petters, S.W., 1978, Formaminfera palaeoecology of the southeastern part of the Maastrichtian-Palaeocene Saharan Epeiric Sea. *Journal of Foraminiferal*, **8(4)**, pp. 303–313.

Petters, S.W., 1982, Central West African Cretaceous Tertiary benthic foraminifera and stratigraphy. *Palaeontographica Abt. A.*, **179**, pp. 1–104.

Petters, S.W., 1984, Some late Tertiary foraminifera from Parabe-1, western Niger Delta. *Revista Espanola de Micropaleontologia*, **11**, pp. 119–133.

Reyment, R.A., 1959, The foraminifera genera Afrobolivina and Bolivina in the upper Cretaceous and lower Tertiary of West Africa. *Stockholm Contributions to Geology*, **3**, pp. 1–57.

Reyment, R.A., 1960, The Cretaceous/Tertiary boundary of Nigeria. *Reports of Geology Survey, Nigeria*, **1957**, pp. 68–86.

Reyment, R.A., 1963, Studies on the Nigeria upper Cretaceous and lower Tertiary ostracoda part 2, Danian, Palaeocene and Eocene ostracoda. *Stockholm contributions to Geology*, **10**, pp. 1–286.

Reyment, R.A., 1965, Aspects of Geology of Nigeria. (Ibadan, Nigeria: University of Ibadan Press), p. 145.

Salami, M.B., 1984, Late Cretaceous and early Tertiary palynofacies of Southwestern Nigeria. *Revista Espanol, Micropaleontology*, **16(1/3)**, pp. 415–423.

Salard-Cheboldaeff, M. and Dejax, J., 1991, Palynostratigraphy of Deltaic Environment. *Journal of African Earth Science*, **12(1 & 2)**, pp. 353–361.

Seglie, G.A., Baker, M.B and Schneidermann, N., 1982, *Biostratigraphy and paleoenvironments of the Northern Niger Delta and their significance to Petroleum Geology*, unpublished report Gulf Oil Company, Nigeria.

Shannon, P.M. and Naylor, D. 1989 Petroleum Basin Studies: London, Graham and Trotman, p. 206.

Short, A.J. and Stauble, K.L., 1967, Outline of the Geology of the Niger Delta. *Bulletin American Association of Petroleum Geologists*, U.S.A. Memoir, **51**, pp. 761–779.

Stolk, J., 1965, *Contribution a l'étude des corrélations microfauniques des Tertiare Inferieur de la Nigeria Méridionale.* (France: Colloquium of Micropaleontologia Memoir), **32**, pp. 247–275.

Weber, K.J. and Daukoru, E.M., 1975, Petroleum Geology of the Niger Delta. *9th World Petroleum Congress Proceedings*, **2**, pp. 209–221.

This page intentionally left blank

CHAPTER 2

A hazy shade of winter: Late Pleistocene environments and behavioural adaptations at Blombos Cave, South Africa

Geeske H.J. Langejans
Faculty of Archaeology, Leiden University, Leiden, The Netherlands
Centre for Anthropological Research, University of Johannesburg, Johannesburg, South Africa

Gerrit L. Dusseldorp
Centre for Anthropological Research, University of Johannesburg, Johannesburg, South Africa

Karen L. van Niekerk
Department of Archaeology, History, Cultural Studies and Religion, University of Bergen, Bergen, Norway

Christopher S. Henshilwood
Institute for Human Evolution, University of the Witwatersrand, Johannesburg, South Africa
Department of Archaeology, History, Cultural Studies and Religion, University of Bergen, Bergen, Norway

ABSTRACT: Major behavioural changes during the Late Pleistocene in Africa are often linked to climate change; specifically so the beginning of Marine Isotope Stage 4 and the appearance of the Still Bay Industry. However, little is known about the local environmental settings of Middle Stone Age sites and recent research shows that global climatic trends, recorded in ice and deep sea cores, cannot simply be juxtaposed on local situations. Here we explore the influence of local climate change on human subsistence strategies during Marine Isotope Stages 5 and 4 at Blombos Cave (South Africa). We examine the changes in small shellfish and large mammal prey to determine respectively a) the local climatic situation and b) how the changing climate may have influenced subsistence. In terms of climatic indicators, the shellfish spectra suggest that phases M3 (Marine Isotope Stage 5c) and M1 (approximate onset of Marine Isotope Stage 4) fall within the present day species and Sea Surface Temperature range of the Agulhas marine province; Blombos is currently located in this warmer province. The M3 phase is somewhat cooler than the M2 Upper/M1; the latter are associated with the Still Bay Industry. In terms of heterogeneity and evenness, the mammal assemblages reflect no major changes in hunting strategies. Other local climate proxies indicate relatively warm and wet conditions for the M2 Upper/M1; when appraised against climate models this suggest that the beginning of the Still

Bay was not as dramatic as has been supposed. In this light it is unlikely that the Still Bay Industry was an adaptation to a harsh and resource depleted environment.

2.1 INTRODUCTION

Southern Africa during the Pleistocene is characterised by a variable climate, and rain regimes were periodically subjected to drastic changes (Blome *et al*., 2012; Dansgaard *et al*., 1993; Jouzel *et al*., 2007; Petit *et al*., 1999; Scholz *et al*., 2007; Shackleton, 1982; Thackeray, 2007; Waelbroeck *et al*., 2002; Ziegler *et al*., 2013). It is often reasoned that climatic and environmental developments influenced human behaviour during the African Late Pleistocene (e.g., Compton, 2011; Henshilwood, 2008a; Marean, 2010; Bar-Matthews *et al*., 2010; McCall, 2007; McCall and Thomas, 2012; Ziegler *et al*., 2013). Especially, the appearance and disappearance of the Still Bay and Howiesons Poort technocomplexes, characterised by 'precocious archaeological records' have been linked to climate change. However, these complexes are distributed over large parts of southern Africa (e.g., Jacobs *et al*., 2008a; Henshilwood, 2012; Lombard, 2012). In addition, we know little of the local environmental settings of many Middle Stone Age (MSA) sites. Reconstructing local (Sea Surface) temperatures and precipitation regimes is difficult as it is unclear how the cold Benguela and warm Agulhas currents (Figure 1), the subtropical convergence and northern and southern hemisphere forcing behaved and what effect this had on temperatures and precipitation (compare for example Bar-Matthews *et al*., 2010; Chase, 2010; Jacobs *et al*., 2008b; Stuut *et al*.,

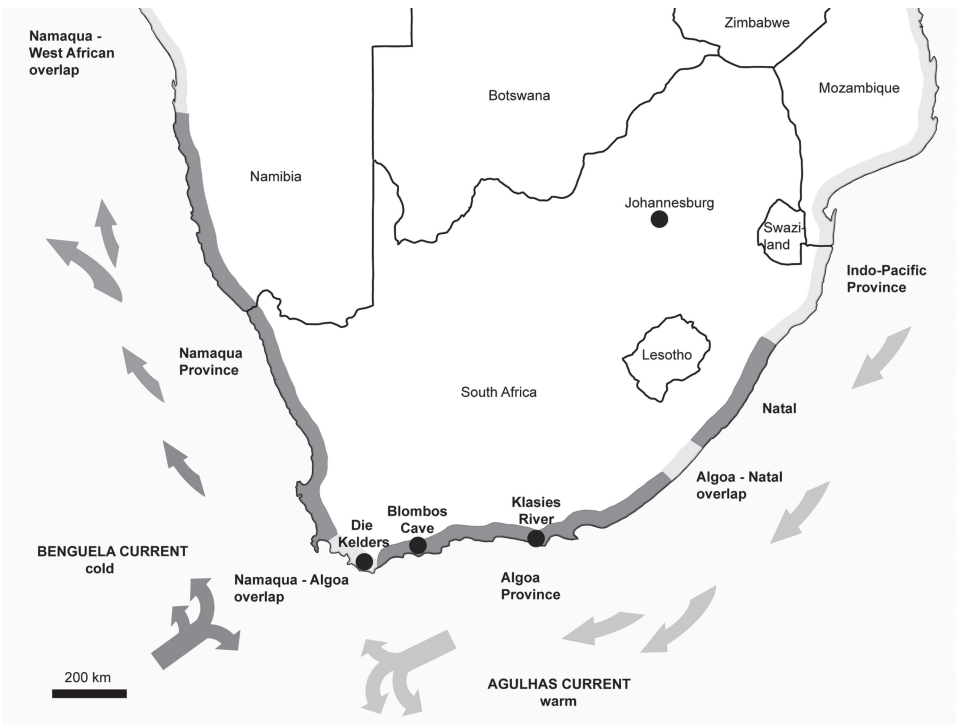

Figure 1. Map of southern Africa with the archaeological sites, marine provinces and oceanic currents.

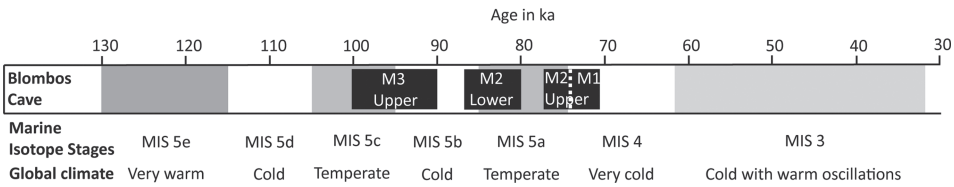

Figure 2. Overview of the stratigraphic sequence, dating, and correlation to Marine Isotope Stages (MIS) and global climate at Blombos Cave.

2004). In addition, recent research shows that we cannot simply juxtapose global climatic trends recorded in ice and deep sea cores on the local South African situation (Blome *et al*., 2012; Chase, 2010; Chase and Meadows, 2007).

Within the MSA, dated between 250–30 ka years ago, several stone tool industries are distinguished. One early technocomplex, associated with archaeological evidence for "modern" behaviour is the Still Bay Industry (~74 ka) (Jacobs and Roberts, 2008; Jacobs *et al*., 2013). This industry is characterised by finely made bifacial points. In addition, from the Still Bay levels at Blombos Cave, located on the southern coast of South Africa (Figure 1), bone tools, shell beads and engraved pieces of ochre were also recovered (e.g., d'Errico *et al*., 2005; Henshilwood, 2012; Henshilwood *et al*., 2009). Blombos Cave plays an important part in the discussion concerning the origins of modern human behaviour. The archaeological record of the occupations preceding the Still Bay at Blombos appears less refined, for example, they lack bone tools and beads.

It has been suggested that environmental changes, associated with the beginning of Marine Isotope Stage (MIS) 4 (~73 ka, Henshilwood, 2008a, Table 2; Martinson *et al*., 1987) influenced human behaviour, leading to the Still Bay technocomplex (e.g., Ambrose and Lorenz, 1990; Jacobs and Roberts, 2008; McCall and Thomas, 2012) (Figure 2). The focus of this paper is the local climate at Blombos Cave and the aim is to characterise local environmental setting, understand how environmental changes may have influenced human subsistence strategies and how this may be recognised. We used the shellfish assemblages from Blombos Cave to characterise the local coastal environment; molluscs are habitat-specific and therefore a valuable local data source. They provide information on the type of environment they lived in (e.g., rocky shored *versus* sandy beaches) and local Sea Surface Temperatures; in many climate models Sea Surface Temperatures are linked to terrestrial climate (e.g., Chase, 2010). We combined the climatic data with faunal information from Blombos Cave to see how climatic changes may have influenced human subsistence strategies.

2.2 MATERIALS AND METHODS

Blombos Cave is situated directly on the coastline, overlooking the Indian Ocean (Figure 1). The cave was formed in a cliff in calcified sediments of the Bredasdorp Group. The site contains a Later Stone Age (LSA) sequence (<2000 b.p.) and a sequence of MSA deposits (Henshilwood *et al*., 2001). The MSA deposits are grouped in three phases: M1, M2 and M3. These phases represent a long occupation sequence. The M3 accumulated between ~105 and 90 ka, during MIS 5c–b (Henshilwood *et al*., 2011). In this paper we examine the sequence from the upper M3, starting around ~100 ka, onwards. A hiatus separates the M3 and M2 Lower occupations in time. The M2 Lower was deposited between ~84 and ~80 ka (Henshilwood *et al*., 2011; Jacobs *et al*., 2013). The dates from the M2 Upper show a high degree of variation (with values between

77 and 69 ka) (Jacobs *et al*., 2013). The occupation levels of the M2 Lower contain no Still Bay artefacts and represent low-intensity occupations, while the M2 Upper levels do contain few Still Bay artefacts and represent more intensive occupations (Jacobs *et al*., 2013; Thompson and Henshilwood, 2011). Jacobs *et al*. (2013) suggest that the earliest possible date for the start of the Upper M2 occupations and thus the Still Bay is 75.5 ka, which implies a hiatus between the lower and upper M2 deposits. Overlying the M2, the M1 phase has yielded the most abundant Still Bay record. M1 is capped by a layer of undisturbed aeolian sediments and the M1 occupation is thus thought to end around 71 ka (Jacobs *et al*., 2013). OSL dates place the M1 between 75 and 71 ka (Henshilwood, 2012); using a statistical model Jacobs *et al*., (2013) constrain this further to 72.2 and 71.3 ka. TL dates on burnt lithics from the M1 yielded slightly older dates, suggesting that the M1 falls between ~78–74 ka (Tribolo *et al*., 2006).

The occupations at Blombos thus took place against the background of fluctuating global climate, with the M3 phase spanning the transition from MIS 5c to 5b, i.e., from a relatively warm to a cooler phase. The M2 Lower occupations occurred during the early part of the relatively warm MIS 5a interstadial. Depending on the dating of the Still Bay, the Still Bay occupations fall within MIS 4, or span the transition between MIS 5a and 4 (Henshilwood, 2008b; Henshilwood *et al*., 2011; Jacobs *et al*., 2013; Waelbroeck *et al*., 2002).

At Blombos Cave, marine shellfish remains are found throughout the sequence, but some units are richer than others. In this study we add to previously published data of the larger/foraged species (Henshilwood *et al*., 2001; Langejans *et al*., 2012). It includes not only remains from squares E5 (quadrants a, b), F4 (all quadrants) and F5 (all quadrants), but also E4 (all quadrants), F6 (quadrants a and b) and H6 (quadrant a). In addition, we report on the identification and analysis of incidental (non-food) species from square E5. Stratigraphically, the sample spans MSA layers BZ in the M1 down to CJ in the M3 Upper. This is, for MSA standards, a large and representative sample from ongoing work (for a detailed discussion of the site and its finds see Henshilwood *et al*., 2001). The review of the faunal data is based on the taxonomic composition of the fauna from the 1992–1999 excavations at the site (Henshilwood *et al*., 2001), combined with the taphonomic studies on the fauna from the 2000, 2002 and 2004 excavations (Thompson and Henshilwood, 2011).

2.2.1 Shellfish

Archaeological sites are one potential data source on past climatic circumstances; however, most materials at archaeological sites were brought in by humans. This precludes using them to document environmental change and as subsequent correlates for changes in human behaviour since the information sources are not independent. That, for example, excludes most shellfish and mammal fauna. However, not all marine shellfish remains at archaeological sites represent the remains of exploited species. Incidentals are small shellfish (≤3 cm) that were not food items (Bigalke, 1973; Buchanan, 1988; Kyle *et al*., 1997), but were brought in with other shellfish, for example in the *byssus* (threads or beards) of mussels or in the stomachs of fish and birds (Erlandson and Moss, 2001; Jerardino, 1997). Therefore, we consider the small shellfish species from Blombos Cave good proxies to characterise local Sea Surface Temperatures.

All shellfish, incidentals and food items, from Blombos Cave were characterised in terms of their preferred temperature range. The environment and Sea Surface Temperatures around South Africa's coasts are influenced by two major Oceanic currents (Figure 1). The Benguela Current flows northwards, transporting cold water from the polar zones along the West coast. The Agulhas Current originates in the Indian

Ocean and brings warm waters along the eastern shores. For the study area, the relative strength and temperature of the Agulhas Current and the location of the of the Subtropical Convergence zone, the boundary between subtropical/temperate and arctic waters are considered more influential than the global climatic developments. For example, a comparison of local terrestrial climatic proxies with Antarctic ice-core data shows that the temperature developments in South Africa do not mimic those from the ice core (Chase, 2010). Hence, the information from the marine molluscs is considered most informative about actual local developments.

The current coast around Blombos Cave is characterised as a rocky shore and it is likely that during the M3, M2 and M1 phases this type of coast also dominated. The large shellfish are typical for this type of coast and only in the M1 is there a small percentage of sandy beach species (*Donax serra*, 1.25%) (Langejans *et al*., 2012). In addition, a large part of the archaeological fish species require tidal/rock pools, rocky substrate or kelp forests and all species also occur around Blombos Cave today; thus the ancient setting was probably similar to present day (Van Niekerk, 2011). In the absence of high-resolution seismic data for the offshore we can only suggest that the palaeo-shore was most likely a rocky one due to the continental shelf and the sediment wedge that extends West from the Gouritz River. The rocky inner shelf probably consists of offshore outcrops of the extremely resilient Table Mountain Sandstone (Birch, 1980, 1978). This wedge, about 10 km wide, would have provided the rocky substrate for the sea fauna to thrive.

During the occupation phases the distance from the cave to the sea shore differed, changing with rising and falling sea levels. Using the dates provided by Henshilwood *et al*., 2011 and Jacobs *et al*., 2013 and the palaeo-scape model by Fisher *et al*. (2010), we come to the following average distances: M3, 3.32 km; M2 Lower, 2.67 km; M2 Upper, 4.99 km; M1, 15.80 km (Figure 3). Note that different interpretations of the

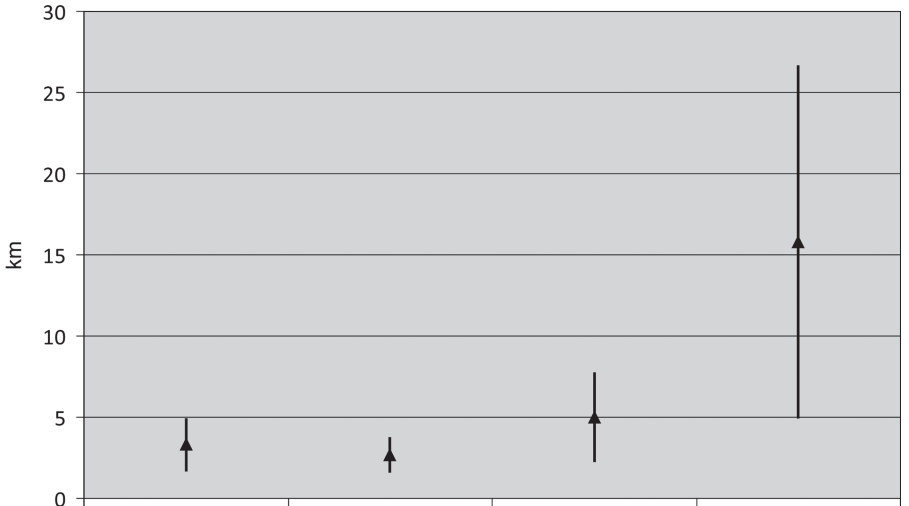

	M3	M2 Lower	M2 Upper	M1
Min	1.74	1.67	2.33	4.99
Max	4.89	3.66	7.65	26.6
▲ Average	3.32	2.67	4.99	15.80

Figure 3. Reconstruction of the average distance from Blombos Cave to the sea shore (using Fisher *et al.*, 2010; Henshilwood *et al.*, 2011; Jacobs *et al.*, 2013).

dating will lead to different reconstructed distances. Although the increase in distance over time is a persistent trend, the high value for the M1 hinges on a date of 72.5 ka. If the M1 were to be dated earlier (cf. Tribolo *et al*., 2006), the sea would have been closer to the cave; if the M1 is younger than assumed here (cf. Guérin *et al*., 2013), the sea would be further away.

South Africa has semi-diurnal tides and the cycle of low and high tide occurs about twice per day. The two low tides are of equal magnitude, but the high tides generally do not have the same magnitude (SADCO, 2008). The timing and extent of the tidal peaks depend on the lunar and solar cycles. The South African coast has a general tidal range of about 1 m and at Mossel Bay the maximum annual tidal range is about 2.4 m (Hydrographic Office, 2011; SADCO, 2008).

The different Sea Surface Temperatures on the eastern and western coasts result in a taxonomic differentiation of shellfish communities. The shellfish communities can be divided into so-called marine provinces (Figure 1); currently, Blombos Cave is located in the Algoa province (Kilburn and Rippey, 1982). The marine provinces are characterised by the percentages of three categories: warm to cold species (species that occur along the entire coast), warm water endemics and cold water endemics. We fitted the Pleistocene assemblages of incidental and large shellfish from Blombos in these categories and compared them to present-day composition of the marine provinces (Kilburn and Rippey, 1982). In an attempt to further untangle the environmental data, we used the geographical occurrence of species, as described in the literature, to characterised them as West Coast, Cape, or East Coast typicals (Appeltans *et al*., 2012; Natal Museum—Mollusc Collection, 2007; Dempster and Branch, 1999; Hammond and Griffiths, 2006; Kensley, 1973; Kilburn pers. comm. 2011; Kilburn and Rippey, 1982; Turton, 1932). Where possible we made the distinction between the more tropical northern and the more temperate southern East coast.

For this analysis we used the Minimum Number of Individuals (MNI) and grams of shell and we calculated the percentage MNI per member; unfortunately, all representations have disadvantages (Claasen, 1998). When using MNI, small and intensively collected larger species will appear to dominate the assemblage. In addition, when calculating shellfish MNI only one to two parts are diagnostic per specimen. Considering that it is unlikely that all shells survived in an archaeological assemblage, rare species are underrepresented when using MNI data. When using shell weight, species with heavy shells appear dominant. Note that for *Turbo sarmaticus* we used the operculum (closing part attached to foot of the mollusc) to calculate the MNI; the shells and opercula weights were combined for the weight calculations.

2.2.2 Fauna

It has been suggested that the Still Bay and the later Howiesons Poort technocomplexes are adaptations to situations characterised by a low resource density, and in the case of the Still Bay combined with a low resource predictability (e.g., Ambrose and Lorenz, 1990; McCall, 2007). To evaluate this, we correlated the environmental data to the Blombos faunal assemblages. From a behavioural ecological point of view, a decrease in the availability of highly ranked resources should result in a broadening of the exploited resource base (Dusseldorp, 2012a; Nagaoka, 2002). This in turn would lead to more diverse archaeological faunal assemblages, and a more even representation of the taxa in the assemblages (e.g., Clark, 2011; Jones, 2004; Lupo and Schmitt, 2005; Lyman, 2008; Stiner and Munro, 2002). Moreover, the representation of animal size classes is expected to change in situations of resource stress. Foragers

generally prefer large-sized prey (Dusseldorp, 2012a, 2010; Winterhalder, 1987, 2001). Unless intervening factors, such as technological innovations that make the exploitation of small species more efficient (e.g., Wadley, 2010), an increase in the representation of animals of smaller body size is expected to be associated with resource depletion.

If the resource base broadened, the number of represented species (NTAXA) in the Still Bay faunal assemblages is expected to increase. However, simply comparing NTAXA for the different levels does not provide a good test of the diversity of faunal assemblages, since it is related to sample size (Lyman, 2008). The Shannon–Wiener index (H) allows an evaluation of the diversity of faunal assemblages, taking sample size into account. H is therefore often used when trying to determine the level of specialisation of faunal exploitation strategies in archaeological assemblages (Cruz-Uribe, 1988; Neeley and Clark, 1993). The index is calculated as follows (Equation (1)).

$$H = -\sum P_i(\ln P_i) \tag{1}$$

In Equation (1), P_i is the proportion of taxon i in the assemblage. H generally is a number between 1.5 and 3.5. The higher the number, the higher the degree of assemblage heterogeneity (Cruz-Uribe, 1988; Lyman, 2008).

From H, the Shannon index of evenness (e) can be calculated (Equation (2)).

$$e = H/\ln S \tag{2}$$

In Equation (2), H is the index of heterogeneity and S is the NTAXA represented in the assemblage. The Shannon evenness index e falls between 0 and 1. Higher values indicate even assemblages, a value of one signifies an assemblage in which all taxa are equally abundant, and lower values indicate more uneven assemblages, i.e., dominated by one or a few of the represented taxa (Lyman, 2008).

We calculated H and e based on the published taxonomic analysis of the 1992–1999 excavations at Blombos Cave (Henshilwood *et al.*, 2001). We based our calculations on the Number of Identified Specimens (NISP) per taxon, instead of using MNI. MNI is a derived measure, and its use is controversial (e.g., Plug and Plug, 1990). MNI provides a minimum estimate; the actual number of represented individuals may have been substantially higher. Moreover, the use of MNI tends to inflate the importance of rare species (Lyman, 2008; Plug and Plug, 1990). To calculate the proportion a specific taxon has in the assemblage, we considered only the NISP. Specimens designated by Henshilwood *et al.* (2001) to bovid size class only were omitted from these calculations. Some exceptions were made, if bones or individuals were classified to family level (e.g. Hyaenidae) and no bones were assigned to a specific species, the family was counted as one represented taxon.

Additionally, since there is a relation between animal body size and population density (Silva *et al.*, 2001, 1997), it is expected that the abundance of large mammals will decrease more rapidly than that of small mammals if resource abundance decreases. Hence, we evaluated the representation of the different animal size classes per archaeological level. We calculated the representation of animal body size classes based on the published taxonomic identifications (Henshilwood *et al.*, 2001) and also reviewed the results of the taphonomic analysis (Thompson and Henshilwood, 2011). With regard to the taxonomic analysis, we classified all represented species according to animal size classes as used by Marean *et al.* (2000)

and grouped them with the appropriate category of bovid bones identified to bovid size class only.

Finally, to understand whether the faunal assemblages reflect changes in the predominant environments that were exploited by the site's occupants, we looked at the importance of grazers relative to browsers and mixed feeders for the ungulates represented at the site. We classified the ungulates represented at the site as either grazer, browser or mixed feeder following Rector and Verrelli (2010). We then calculated a ratio of grazers to mixed feeders and browsers per level by dividing the ∑NISP of grazers by the ∑NISP of browsers and mixed feeders.

2.3 RESULTS

2.3.1 Shellfish

In Table 1 the taxonomic composition of the marine mollusc assemblages in terms of MNI and weight for the Blombos MSA members are presented. For all species we characterised their distribution over the marine provinces and their preferred coastal geography. Table 2 provides the 'endemic characterisation' of several marine provinces, some localities along the coast and the Blombos MSA members. This characterisation is illustrated in Figure 4. It is important to note that beside the tropical Natal province, the species characterisation in most provinces is dominated by molluscs that thrive in both warm and cold waters. The current provinces and localities with low Sea Surface Temperatures have a high percentage of cold water endemics. Moving East along the coast the number of cold water endemics and catholic species decrease in importance; warm water endemics increase (Kilburn and Rippey, 1982). To create similar bar graphs for the MSA at Blombos we used West coast species to represent cold water endemics, warm water endemics are represented by combining the numbers of all East coast species; and the warm–cold group consists of all catholic and Cape species. The incidental Blombos M3 and M2 Upper samples contain a small cold water signal. The composition of the M3 assemblage is most similar to the present situation at Cape Agulhas. In the M2 Lower, warm water endemics make up almost half of the assemblage, there is a very faint cold water signal, and the remainder of the assemblage is catholic. The M2 Upper and M1 are comparable to the Algoa province (Figure 4). Cape Agulhas is the most western point of the Algoa province and its coolest part.

Another way to study the data in terms of environment is by examining the geographical range of the represented species as typified in the province and coast ID in Table 1. In this representation the Cape forms a separate group and we deem this more accurate than grouping Cape species with catholic ones. Overall, there are at least five incidental species represented in the assemblage, which is dominated by *Chiton* sp.; 59 individuals remain unidentified. Unfortunately, there is no information on how many of the large shellfish were unidentified.

The small species in M3 are dominated by types that appear along the entire South African coast (>85%). About 9% of the assemblage consists of East coast species and the West coast and Cape species make-up under 4%. Compared to the M3, there are less catholic species in the M2 Lower, there are no West coast species, the Cape specific species account for slightly less than 5% of this assemblage, and the East coast species for almost 52%. The warm–cold species in the M2 Upper are more abundant compared to the M2 Lower; in the M2 Upper the West coast and Cape

Table 1. Overview of the mollusc assemblages from Blombos Cave. Species in bold are the large food items; species in normal font are the incidentals. Endemic ID indicates which species are cold and warm water endemics. Note that most species occur in both cold and warm water. The province ID specifies in which marine province a species occurs; the provinces are codes as follows: 1 = West Africa–Namaqua overlap; 2 = Namaqua; 3 = Namaqua–Algoa overlap; 4 = Algoa; 5 = Algoa–Natal overlap; 6 = Natal; 7 = Indo–Pacific. The coast ID are compiled as follows: West coast = 1–3 and 2; Cape = 1–4, 2–4, 3, 3–4; complete East coast = 3–6, 3–7, 4–6, 4–7; southern East coast = 3–5; northern East coast = 5–7, 6–7, 7; entire coast = 1–5, 1–6, 1–7, 2–5, 2–6, 2–7. MNI: Minimum Number of Individuals; weight in grams (using Appeltans *et al.*, 2012; Natal Museum—Mollusc Collection, 2007; Dempster and Branch, 1999; Hammond and Griffiths, 2006; Kensley, 1973; Kilburn, pers. comm., 2011, Kilburn and Rippey, 1982.

Species	Endemic ID	Province ID	Coast ID	M3		M2 (Lower)		M2 (Upper)		M1	
				MNI	Mass	MNI	Mass	MNI	Mass	MNI	Mass
Haliotis midae	Cold–warm	2–4	Cape	43.00	8593.00	2.00	402.10	4.00	990.00	4.00	198.20
Haliotis midae juvenile	Cold–warm	2–4	Cape	0.00	0.00	0.00	0.00	1.00	5.23	0.00	0.00
Haliotis spadicea	Cold–warm	2–6	Entire coast	14.00	132.00	4.00	57.00	30.00	344.80	26.00	339.30
Diodora sp.	Cold–warm	2–7	Entire coast	0.00	0.00	0.00	0.00	0.00	0.00	1.00	0.07
Amblychilepas scutellum hiantula	Warm	3–7	East coast	0.00	0.00	0.00	0.00	0.00	0.00	1.00	0.30
Fissurella mutabilis	Cold–warm	1–7	Entire coast	3.00	0.03	0.00	0.00	1.00	0.04	2.00	0.10
Fissurellidae	?	?	?	2.00	0.00	0.00	0.00	0.00	0.00	2.00	0.17
Helcion pruinosus	Cold–warm	2–5	Entire coast	10.00	0.16	0.00	0.00	0.00	0.00	2.00	0.14
Helcion pectunculus	Cold–warm	1–5	Entire coast	1.00	0.03	0.00	0.00	1.00	0.01	1.00	0.03
Cymbula compressa	Cold	1–3	West coast	0.00	0.00	0.00	0.40	0.00	0.00	2.00	30.50

(*Continued*)

Table 1. *Continued*

Species	Endemic ID	Province ID	Coast ID	M3		M2 (Lower)		M2 (Upper)		M1	
				MNI	Mass	MNI	Mass	MNI	Mass	MNI	Mass
Cymbula compressa juvenile	Cold	1–3	West coast	0.00	0.00	0.00	0.00	1.00	0.11	0.00	0.00
Cymbula granatina	Cold	1–3	West coast	236.00	4352.00	404.00	159.00	1.00	35.00	1.00	27.00
Cymbula miniata juvenile	Cold–warm	1–6	Entire coast	7.00	0.24	0.00	0.00	1.00	0.05	3.00	0.08
Cymbula oculus	Cold–warm	2–4	Cape	606.00	14360.30	14.00	479.00	52.00	1027.00	84.00	1931.30
Cymbula oculus juvenile	Cold–warm	2–4	Entire coast	3.00	0.08	0.00	0.00	0.00	0.00	0.00	0.00
Scutellastra argenvillei	Cold–warm	1–4	Cape	369.00	14336.00	16.00	503.30	24.00	789.00	27.00	1097.70
Scutellastra argenvillei juv.	Cold–warm	1–4	Cape	4.00	0.48	2.00	0.11	8.00	1.67	11.00	2.97
Scutellastra barbara	Cold–warm	1–6	Entire coast	0.00	0.00	0.00	0.00	0.00	0.00	1.00	5.00
Scutellastra barbara juvenile	Cold–warm	1–6	Entire coast	32.00	4.51	2.00	0.21	1.00	0.06	2.00	0.39
Scutellastra cochlear	Cold–warm	2–5	Entire coast	3.00	13.00	0.00	0.00	0.00	0.00	0.00	0.00
Scutellastra cochlear juvenile	Cold–warm	2–5	Entire coast	215.00	90.79	8.00	3.62	12.00	5.63	19.00	4.54

Scutellastra granularis juvenile	Cold–warm	1–6	Entire coast	2.00	0.21	0.00	0.00	0.00	0.00	0.00	0.00
Scutellastra longicosta	Cold–warm	2–6	Entire coast	2.00	28.00	1.00	7.00	0.00	1.00	1.00	4.00
Scutellastra longicosta juvenile	Cold–warm	2–6	Entire coast	267.00	94.48	4.00	0.86	28.00	7.42	35.00	7.05
Scutellastra tabularis	Warm	3–5	Southern East coast	0.00	37.00	0.00	0.00	0.00	0.00	0.00	0.00
Patelloid profunda	Warm	4–7	East coast	0.00	0.00	0.00	0.00	0.00	0.00	1.00	0.27
Gibbula cicer	Cold–warm	1–4	Cape	2.00	0.08	0.00	0.00	0.00	0.00	0.00	0.00
Gibbula multicolor	Cold–warm	2–4	Cape	1.00	0.01	0.00	0.00	0.00	0.00	0.00	0.00
Oxystele sp. *(tigrina* or *sinensis)*	Cold–warm	2–4	Cape	181.00	3086.00	31.00	594.00	62.00	981.00	58.00	436.30
Oxystele variegate	Cold–warm	1–5	Entire coast	7.00	0.83	0.00	0.00	12.00	1.09	4.00	0.52
Tricolia capensis	Cold–warm	1–7	Entire coast	0.00	0.00	1.00	0.01	1.00	0.01	4.00	0.01
Tricolia formosa	Warm	3–5	Southern East coast	0.00	0.00	0.00	0.00	1.00	0.01	0.00	0.00
Tricolia kochii	Warm	3–5	Southern East coast	0.00	0.00	0.00	0.00	0.00	0.00	1.00	0.14
Turbo sarmaticus shell	Cold–warm	2–4	Cape	3688.00	64,894.00	119.00	3238.00	648.00	3907.00	372.00	4119.00

(*Continued*)

Table 1. *Continued*

Species	Endemic ID	Province ID	Coast ID	M3		M2 (Lower)		M2 (Upper)		M1	
				MNI	Mass	MNI	Mass	MNI	Mass	MNI	Mass
Turbo sarmaticus operculum	Cold–warm	2–4	Cape	1158.00	16,976.00	272.00	3592.00	698.00	8421.00	970.00	12502.00
Turbo sarmaticus juvenile	Cold–warm	2–4	Cape	2.00	0.30	0.00	0.00	2.00	0.47	7.00	0.08
Turbo cidaris operculum	Cold–warm	1–6	Entire coast	5.00	0.17	1.00	0.04	3.00	0.15	9.00	0.41
Nodilitorina knysnaensis	Warm	3–7	East coast	59.00	1.51	31.00	0.95	39.00	1.15	49.00	2.16
Dendropoma corallinaceum	Cold	1–3	West coast	1.00	0.03	0.00	0.00	0.00	0.00	0.00	0.00
Turritella carinifera	Cold–warm	2–7	Entire coast	4.00	0.45	2.001	0.04	10.00	0.32	21.00	1.23
Bostrycapulus aculeatus	Cold–warm	2–6	Entire coast	0.00	0.00	0.00	0.001	1.00	0.08	6.00	0.96
Crepidula porcellana	Cold–warm	1–6	Entire coast	0.00	0.00	0.00	0.00	1.00	0.01	1.00	0.12
Vaughtia scrobianlata	Cold–warm	2–5	Entire coast	0.00	0.00	0.00	0.00	2.00	0.01	4.00	0.17
Nucella dubia	Cold–warm	1–5	Entire coast	1.00	0.09	0.00	0.00	1.00	0.15	0.00	0.00
Burnupena sp.	?	?	?	3.00	0.51	1.00	0.03	7.00	0.20	5.00	0.30
Burnupena denseliriata	Cold–warm	3	Cape	0.00	0.00	0.00	0.00	2.00	0.32	0.00	0.00
Anachis kraussii	Cold–warm	2–6	Entire coast	0.00	0.00	0.00	0.00	0.00	0.00	1.00	0.01
Bulia diluta	Warm	4–7	East coast	0.00	0.00	0.00	0.00	0.00	0.00	1.00	0.07
Bullia sp.	?	?	?	0.00	0.00	0.00	0.00	0.00	0.00	1.00	0.05
Nassarius kraussianus	Cold–warm	2–7	Entire coast	1.00	0.01	0.00	0.00	0.00	0.00	0.00	0.00

Nassarius pyramidalis	Warm	4–6	East coast	1.00	0.01	0.00	0.00	0.00	0.00	0.00	0.00
Nassarius sp.	?	?	?	0.00	0.00	1.00	0.00	1.00	0.02	0.00	0.00
Nassarius plebejus	Cold–warm	3–4	Cape	0.00	0.00	0.00	0.00	0.00	0.00	3.00	0.08
Austromitra capensis	Cold–warm	2–5	Entire coast	0.00	0.00	1.00	0.01	0.00	0.00	0.00	0.00
Gibberula burnupi	Warm	7	Northern East	1.00	0.01	0.00	0.00	0.00	0.00	0.00	0.00
Clionella sinuata	Cold–warm	1–4	Cape	1.00	0.18	0.00	0.00	0.00	0.00	0.00	0.00
Clionella striolata juvenile?	Cold	2	West coast	2.00	0.02	0.00	0.00	0.00	0.00	0.00	0.00
Clionella sp.	?	?	?	1.00	0.01	0.00	0.00	0.00	0.00	0.00	0.00
Turbonilla sp.	?	?	?	1.00	0.00	0.00	0.00	0.00	0.00	0.00	0.00
Siphonaria concinna	Cold–warm	2–6	Entire coast	81.00	5.64	8.00	0.30	5.00	0.33	8.00	0.66
Trimusculus costatus	Cold–warm	2–6	Entire coast	0.00	0.00	0.00	0.00	0.00	0.00	1.00	0.04
Acanthochitona garnoti	Cold–warm	2–4	Cape	2.00	0.04	0.00	0.00	0.00	0.00	0.00	0.00
Dinoplax gigas juvenile	Cold–warm	3–4	Cape	4.00	4.04	1.00	0.01	0.00	0.00	1.00	0.04
Dinoplax gigas	Cold–warm	3–4	Cape	441.00	19,333.00	55.00	1293.00	118.00	2687.00	168.00	3172.00
Chiton nigrovirescens	Cold–warm	1–5	Entire coast	3.00	0.53	0.00	0.00	2.00	0.11	1.00	0.02
Chiton indet.	?	?	?	18.00	4.58	2.00	0.11	3.00	2.93	10.00	5.20
Neocardia angulata	Cold–warm	1–6	Entire coast	1.00	0.00	0.00	0.00	0.00	0.00	0.00	0.00
Neocardia limoides	Cold–warm	3–4	Cape	2.00	0.01	0.00	0.00	0.00	0.00	3.00	0.01

(*Continued*)

Table 1. *Continued*

Species	Endemic ID	Province ID	Coast ID	M3		M2 (Lower)		M2 (Upper)		M1	
				MNI	Mass	MNI	Mass	MNI	Mass	MNI	Mass
Barbatia foliata	Warm	5–7	Northern East coast	0.00	0.00	0.00	0.00	0.00	0.00	1.00	0.01
Barbatia sculpturata	Cold–warm	2–4	Cape	1.00	0.02	0.00	0.00	0.00	0.00	1.00	0.02
Aulacomya ater	Cold–warm	1–4	Cape	6.00	7.82	0.00	0.00	0.00	0.00	0.00	0.00
Choromytilus meridionalis	Cold–warm	1–4	Cape	3.00	1.31	0.00	0.36	3.00	3.70	0.00	0.00
Perna perna	Warm	3–7	East coast	502.00	1804.30	969.00	3117.00	2205.00	7202.00	3625.00	14731.00
Loripes clausus	Warm	4–7	East coast	1.00	0.20	0.00	0.00	1.00	0.14	0.00	0.00
Melliteryx fortidentata	Warm	3–5	Southern East coast	0.00	0.00	0.00	0.00	0.00	0.00	1.00	0. 01
Thecalia concamerata	Cold–warm	2–4	Northern East coast	0.00	0.00	0.00	0.00	4.00	0.11	1.00	0.02
Trachycardium sp.	Warm	6–7	Northern East coast	0.00	0.00	0.00	0.00	0.00	0.00	1.00	0.48
Mactra glabrata	Cold–warm	1–7	Entire coast	0.00	0.00	0.00	0.00	0.00	0.00	1.00	0.38
Donax serra	Cold–warm	1–4	Cape	2.00	2.00	0.00	4.00	0.00	2.00	68.00	570.00
Donax sordidus	Cold–warm	3–4	Cape	0.00	0.00	0.00	0.00	0.00	0.00	1.00	0.18
Tivela sp. juvenile	?	?	?	0.00	0.00	0.00	0.00	0.00	0.00	1.00	0.03
Venus verrucosa	Cold–warm	1–7	Entire coast	1.00	0.00	0.00	0.00	0.00	0.00	0.00	0.00
Hiatella arctica	Cold–warm	2–4	Cape	1.00	0.00	0.00	0.00	0.00	0.00	0.00	0.00

Table 2. Overview of the mollusc characterisation of several southern African marine provinces, locations along the coast (West to East) (Kilburn and Rippey, 1982) and theMembers from Blombos Cave. For the average monthly Sea Surface Temperatures (SST) for both False Bay and Cape Agulhas, Hermanus data was used. For the first the temperatures should be somewhat lower and for the latter somewhat higher (NOAA, 2013; Seatemperature.org, 2013). Note that some values are not absolute, but larger or smaller than values.

Species ID	Namaqua province Port Nolloth–Sunset Beach	False Bay Hermanus	Cape Agulhas Hermanus	Algoa province Mossel Bay–East London	Natal province Port St. John's–Durban	M3 incidentals (%)	M3 foraged (%)	M2 Lower incidentals (%)	M2 Lower foraged (%)	M2 Upper incidentals (%)	M2 Upper foraged (%)	M1 incidentals (%)	M1 foraged (%)
SST January	17.7°C–18.5°C	19.9°C	19.9°C	20.7°C–24.5°C	25.9°C–25.9°C	x	x	x	x	x	x	x	x
SST July	13.4°C–15.2°C	15.6°C	15.6°C	16°C–21.3°C	21.8°C–21.9°C	x	x	x	x	x	x	x	x
Warm water endemics	0.0%	2.4%	5.0%	>26.0%	80.0%	9.0	14.1	57.4	54.8	42.0	68.9	29.1	71.9
Cold water endemics	25.0%	12.0%	5.0%	≤1.0%	0.0%	0.4	6.6	0.0	22.8	0.7	0.0	0.0	0.1
Warm–cold	>70.0%	>80.0%	>80.0%	>70.0%	<20. 0%	90.6	79.3	42.6	22.4	57.3	31.1	70.9	28.1

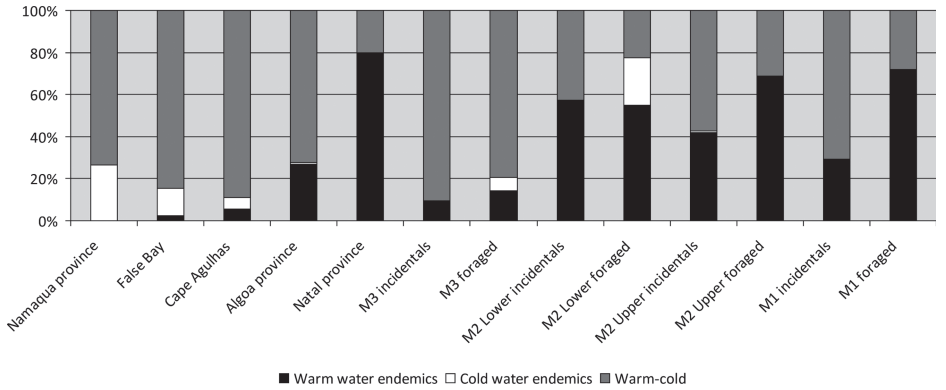

Figure 4. Graph illustrating the characterisation of several southern African marine provinces, places along the coast (West to East) and the Blombos Cave members; the incidentals refer to the assemblage of small non-food species and the foraged group to the exploited large species. Note that certain values are not absolute, but rather the minimum or maximum values.

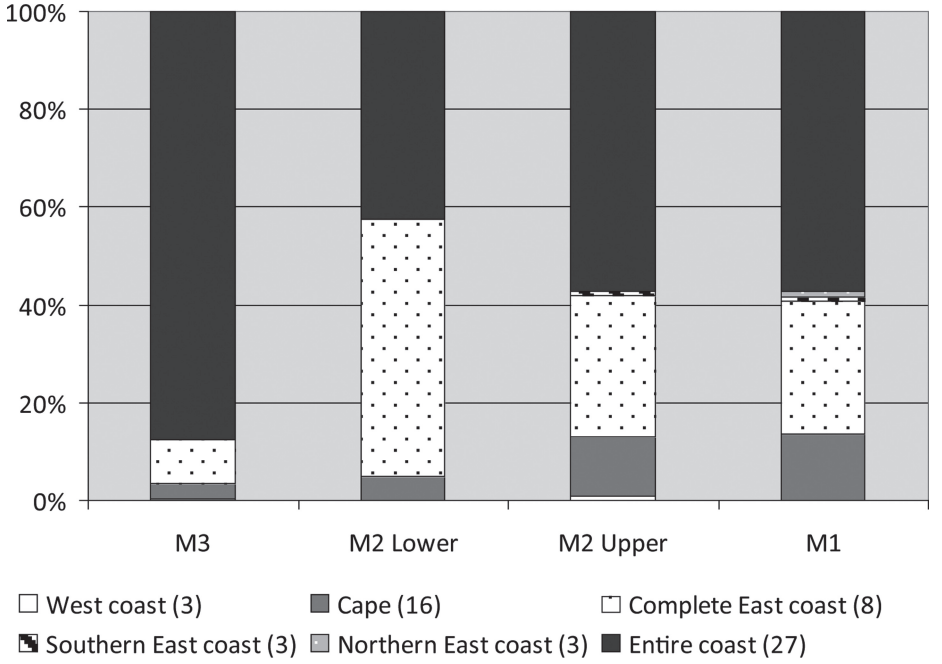

Figure 5. Graph with percentages Minimum Number of Individuals (MNI) of small shellfish across the Blombos members. The shellfish are organised by geographical occurrence; the number in brackets is the number of species represented.

species account for about 13%, the East coast species form 29% of the assemblage and less than 1% are species that occur specifically along the southern East coast. The M1 characterisation is similar to the M2 Upper, but there are no West coast species and the Cape species are represented by over 13%. About 1% of the M1 assemblage consists of (tropical) northern East coast species.

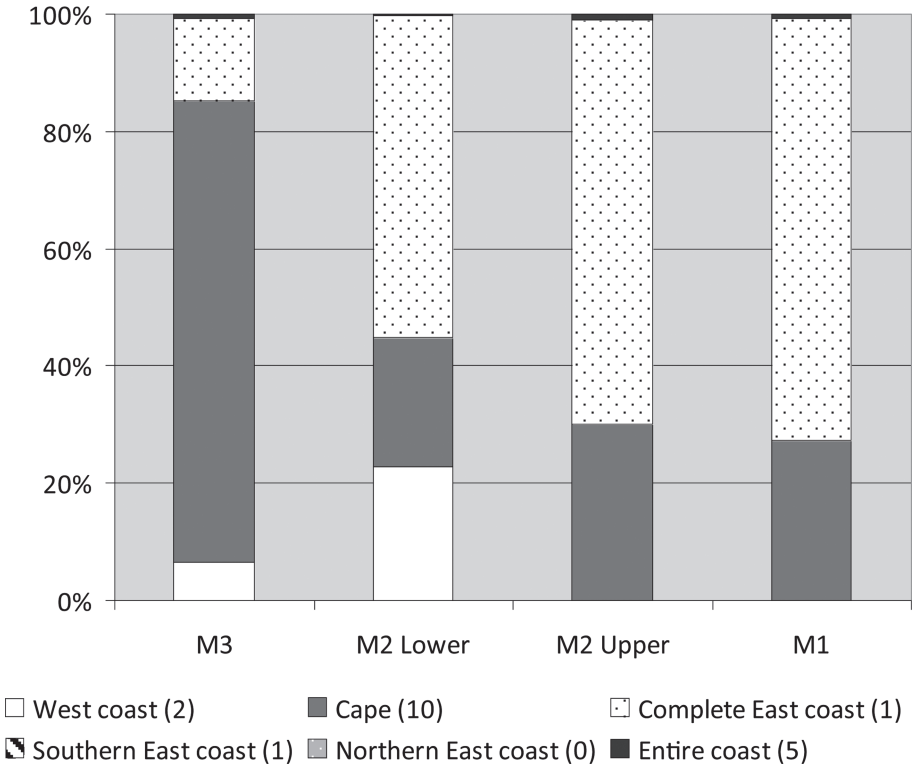

Figure 6. Graph with percentages Minimum Number of Individuals (MNI) of large shellfish in the Blombos members. The shellfish are organised by geographical occurrence; the number in brackets represents the number of species that partake per area.

The composition of the large marine mollusc assemblages, exploited for food by the cave's inhabitants, is also illustrated in Figures 4 and 6 The 'endemic characterisation' characterisation in Figure 4 is as follows: the M3 is similar to the current situation at Cape Agulhas; the M2 Lower is unlike any present day situation, as high numbers of both cold and warm water endemic are present. Note that in the M2 Lower only one cold water endemic species, the granite limpet (*Cymbula granatina*), is present. The M2 Upper and the M1 are most comparable to the present-day Natal characterisation. In the geographical characterisation (Figure 6), Cape specific species dominate the M3 assemblage (~78%), followed by East coast (~14%) and West coast species (~6%). In the M2 Lower, East coast species form about 55% of the assemblage, West coast species are present in almost 23%, and Cape species in 22%. The M2 Upper on the other hand contains less than 1% West coast species, Cape species form about 30% of the assemblage and East coast species dominate at almost 69%. The M1 is similar to the M2 Upper: there are slightly less Cape species (~27%) and more East coast species (~72%). For the foraged assemblage, the East coast group consists of only one species, namely brown mussel (*Perna perna*). The characterisation of the foraged shellfish is considered less reliable than the incidentals as humans preferentially selected these food items (Langejans *et al*., 2012).

2.3.2.1 Fauna

The heterogeneity (*H*) and evenness (*e*) values for the faunal assemblages are listed in Table 3. Both the heterogeneity and evenness of the M1 are greater than for the M3. This suggests that diets during the M1 were broader than during the M3. The values of the M2 mimic those of the M3, however, because they represent both pre-Still Bay and Still Bay occupations, divided by an occupation hiatus, it is difficult to interpret these values. If we assume that the exploitation of rock hyrax (*Procavia capensis*) and Cape dune molerat (*Bathyergus suillus*) was not part of the domain of large mammal exploitation, but represent an extension of gathering activities and leave them out of the calculations, the pattern reverses (cf. Dusseldorp, 2012b). Thus, for large mammal exploitation, diet breadth and evenness appear to decrease in the M1 compared to the M3.

Based on the taxonomically identified assemblage, the contribution of small animals is lower during the M1 than in the other members, while the representation of size classes III and IV is higher (Figure 7). Based on the taphonomic analysis by Thompson and Henshilwood (2011), this pattern is even more dramatic (Figure 8). Their study also distinguishes between the M2 Lower and M2 Upper, showing that in the M2 Upper the contribution of small-bodied species is largest of all occupation phases at the site (Thompson and Henshilwood, 2011).

The larger size classes are probably underrepresented at the site since carcasses of larger animals are more likely to be processed in the field, with only selected body parts transported to the site (Lupo, 2006; Metcalfe and Barlow, 1992). Recently it was attempted to link the cortical thickness of unidentified bone fragments to animal size classes and this approach works well on contemporary experimental samples. When applied to the Blombos materials from the M2 Upper and M1, bones of larger animal size classes are better represented in the unidentified than in the identified sample (Reynard, 2011). Thompson and Henshilwood's (2011) analysis shows that the degree of fragmentation in the M2 and M1 appears to be significantly higher than in the earlier M3. Reynard (2011) has shown that fragment length in the M1 and M2 Upper is small compared to southern African LSA and Iron Age sites as well as modern brown hyena (*Parahyaena brunnea*) and spotted hyena (*Crocuta crocuta*) dens, suggesting fragmentation was intense. Moreover, the ratio of identified elements to unidentified elements appears to be higher for the smaller size classes.

Finally, the ratio of grazers to mixed feeders and browsers is listed in Table 4. Grazers increase in importance throughout the sequence, but not dramatically. However, the diet of animals traditionally classified as mixed feeders, or even browsers may have incorporated a significant amount of grasses (Faith, 2011). This suggests that the ratio of grazing ungulates to browsers and mixed feeders underestimates the increase in grasses in the environments at Blombos Cave.

Table 3. Overview of the fauna assemblages at Blombos Cave and the heterogeneity and evenness factors (using Henshilwood *et al.*, 2001; Lyman, 2008).

Level	∑NISP	NTAXA	*H*	*e*	∑NISP excluding molerat and hyrax	*H* excluding molerat and hyrax	*e* excluding molerat and hyrax
M3	724	28	1.464	0.439	148	2.337	0.726
M2	601	23	1.459	0.465	108	2.456	0.807
M1	898	25	1.785	0.555	310	2.167	0.691

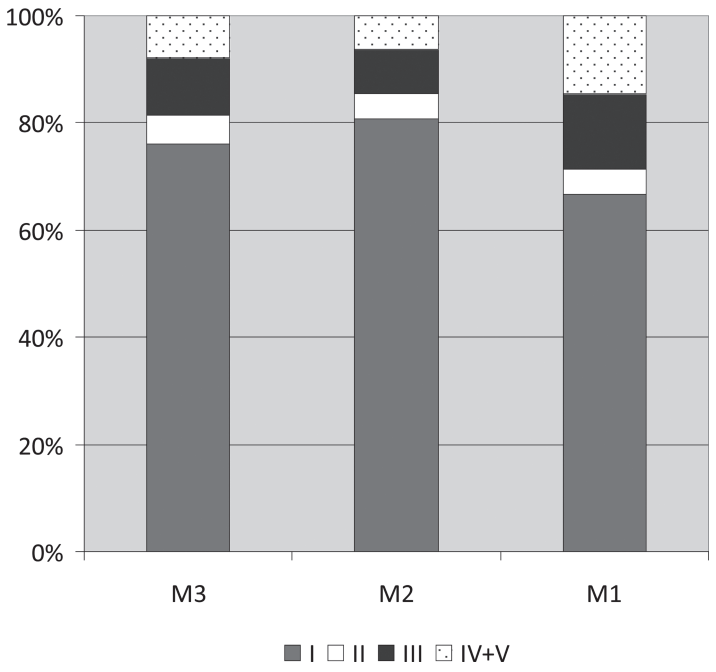

Figure 7. The representation of animal size classes for the three members based on the taxonomic study. Size class I: <23 kg; II: 23–87 kg; III: 85–295 kg; IV–V: >295 kg (for size classes Brain, 1981; data from Henshilwood *et al.*, 2001).

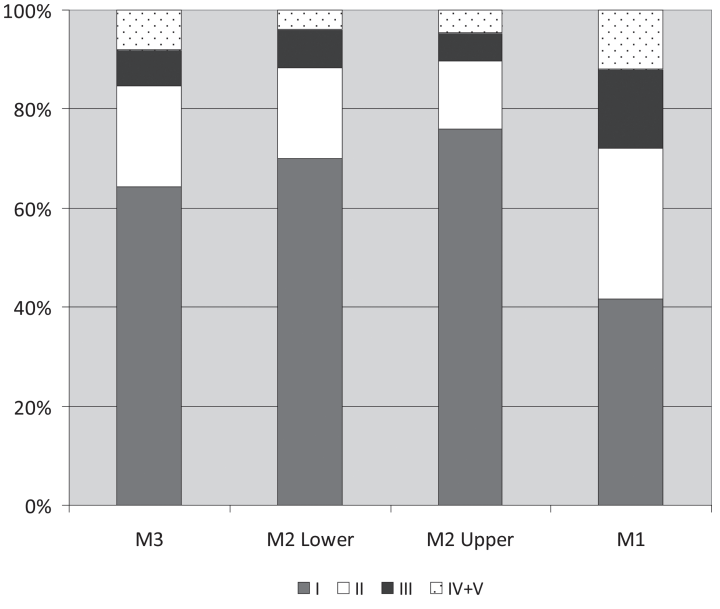

Figure 8. The representation of animal size classes based on the taphonomic study by Thompson and Henshilwood (2011). Note that in this analysis a distinction between M2 Lower and Upper was made. Size class I: <23 kg; II: 23–87 kg; III: 85–295 kg; IV–V: >295 kg (for size classes Brain, 1981; data from Henshilwood *et al.,* 2001).

Table 4. Ratio of grazers to browsers and mixed feeders for the bovid assemblages at Blombos Cave (based on Henshilwood *et al.*, 2001); a high value implies more grazers than browsers/mixed feeders.

Level	Grazers/(browsers + mixed feeders)
M3	0.13
M2	0.16
M1	0.17

2.4 DISCUSSION

2.4.1 Shellfish

The ∑MNI of the shellfish differs greatly between the members and this has repercussions for the quality of the results. For the small and large species respectively the numbers are as follows: M3: 726 and 3571, M2 Lower: 61 and 1769, M2 Upper: 138 and 3200, M1: 206 and 5044. The M2 Lower sample is very small and therefore less reliable than the other members. The characterisation of incidental shellfish species in Figures 4 and 5 demonstrates that during the M3 at Blombos, Sea Surface Temperatures were somewhat lower than the present day. Of all the locations of which the current situation is represented in Figure 4, the classification of the M3 is most similar to Cape Agulhas, the coolest part of the Algoa province. Due to its small sample size we will not attempt to interpret the M2 Lower assemblage. The M2 Upper characterisation is similar to the M1 and both members fall in the modern Algoa range. The M2 Upper may have been cooler as there is a small cold water signal and the M1 contains a faint tropical signal. Interestingly, the Cape specific species are much better represented in the M2 Upper and M1 compared to the M3 (and M2 Lower). It appears that the Sea Surface Temperature during the M3 was lowest; however, all phases fall within present Algoa values.

The characterisations of the large exploited marine molluscs present a partly different story (Figures 4 and 6), but for the M3 there are similarities with the small incidental species. The exploited Cape species dominate the M3 and in combination with the West coast/cold signal this indicates relatively cool Sea Surface Temperatures. The M2 Lower provides a complex signal, and due to the sample size we exclude it from further interpretation. The large and small species characterisations of the M2 Upper and M1 are also comparable, but in Figure 4 these phases are most similar to the warm Natal situation. In Figure 6 the warm East coast species dominate both assemblages and for both phases there is a relatively high percentage of cooler Cape specific species; this leads us to conclude that Sea Surface Temperatures were not tropical and both members fall within the current Algoa range. Also, the warm East coast signal of the exploited species is inflated because it consists of one species only. The enormous increase of the East coast brown mussel during the M2 s and M1 is the result of a change in foraging and transport behaviour (Langejans *et al.*, 2012). During the M1, the shoreline was further away from the cave (Figure 3), leading people at Blombos to select and preferentially transport brown mussel over other species because they are easy to transport and because they preserve well (Langejans *et al.*, 2012). Due to changes in foraging behaviour the interpretation of the large species is more complex than for the small species. However, the assemblage composition of the larger molluscs does support our contention that Sea Surface Temperatures during the M3 were lower than during the M2 Upper and the M1.

The dataset of the small species is limited and hopefully it will be increased in the future. However, using different ways to characterise the assemblage confirms trends. The M3 was comparable to the present situation at Cape Agulhas and thus perhaps somewhat cooler than the current situation at Blombos Cave. The M2 Upper is comparable to current Blombos Sea Surface Temperatures; the M1 might have featured slightly higher temperatures.

2.4.2 Integrating the shellfish with climate models and other proxies

Climate reconstructions for the Late Pleistocene are complex and at times contradictory. Also, traits, such as 'cold', 'warm', 'wet', 'dry', cannot explain changes in the bio-productivity of the landscape on their own.

Correlating the beginning of the Still Bay to global temperature curves based on oxygen isotope ratios in polar ice cores is complex as the dating of the Still Bay remains debated (compare Guérin *et al*., 2013; Jacobs *et al*., 2013, 2008b; Tribolo *et al*., 2006). Some models, relying on oxygen isotope data, propose that the Still Bay appeared during a cold and arid phase, when the landscape was open (Ambrose and Lorenz, 1990; Deacon, 1989; McCall, 2007). During these conditions humans were required to innovate, resulting in the Still Bay Industry (Ambrose and Lorenz, 1990; McCall, 2007). More recently, models relying on the interaction of the Circumpolar Current and Westerlies (winds) suggest that MIS 4 was a cool and humid phase (Blome *et al*., 2012; Chase, 2010). With higher precipitation, vegetation bioproductivity would increase and edible biomass would be more abundant compared to the situation envisaged by previous models. It appears that the cold/wet model fits with, although sparse, local data, such as (micro) fauna analysis. However, after 75 ka, local data no longer support this model (which indicate warm/wet instead of modelled warm/dry); due to less insolation variability and intensity, changes in the Intertropical Convergence Zone (Ziegler *et al*., 2013), and local Sea Surface Temperatures, ocean evaporation and water vapour transport to land (Blome *et al*., 2012) become more important climatic drivers than the Westerlies. Punctuated northern hemisphere cold Heinrich events may have pushed the Intertropical Convergence Zone southwards, leading to increased rainfall in southern Africa (Figure 9). Recently the appearance of the Still Bay has been linked such a wet event (Ziegler *et al*., 2013). Of course, adjustments to the dating of the Still Bay Industry may greatly affect proposed correlations between global climate and the appearance of the Still Bay Industry.

While Blome *et al*. (2012), Ziegler *et al*. (2013) and Chase (2010) argue for higher humidity associated with MIS 4 and the onset of the Still Bay, Bar-Matthews *et al*. colleagues (2010) use speleothem isotope data to argue that the period need not have been characterised by an increase in overall humidity, but by changing seasonality of the rainfall pattern. They propose that the cooling associated with MIS 4 resulted in increased summer rainfall, instead of all-year or predominantly winter rainfall. This would lead to an increased importance of C4 grasses and a concomitant increase in grazing animals. It may be that, if terrestrial temperatures cooled, in addition to changing seasonality of rainfall, a decrease in the amount of evaporation resulted in increased humidity.

Our observations imply that during the M2 Upper and M1 occupations the Sea Surface Temperatures were comparable to present day Algoa province values. During the M3 Sea Surface Temperatures at Blombos Cave were somewhat lower than at present, but fit within the general Algoa range. High Sea Surface Temperatures mean that the Circumpolar Current was positioned more towards Antarctica compared to times of lower Sea Surface Temperatures. Because its position was more southerly, there was more space for Agulhas leakage; this is warm water that 'leaks' from the Algulhas Current to the cold Benguela Current. In other words, leakage occurs when the warm

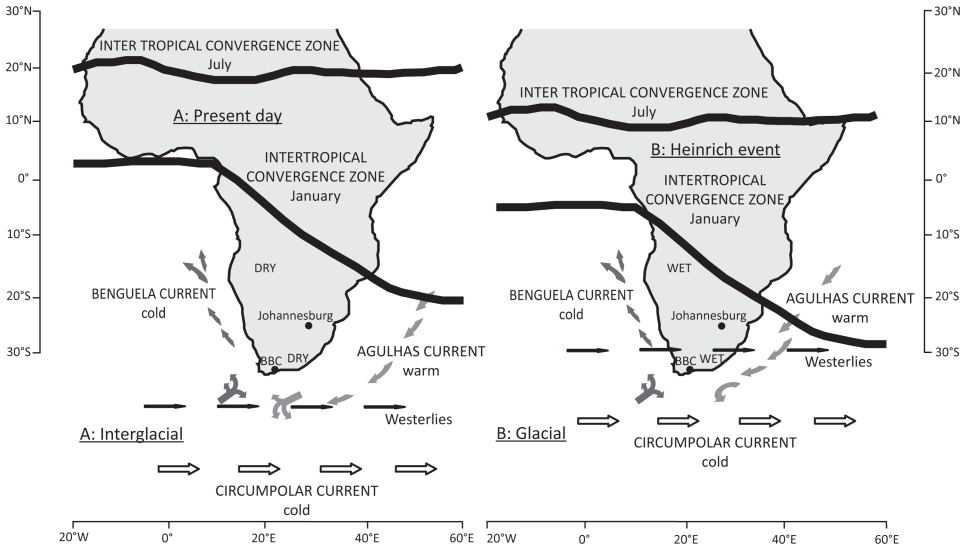

Figure 9. A. Illustration of an idealised Interglacial situation where the Intertropical Convergence Zone is located northwards; the Circumpolar Current is relatively far north, restricting Agulhas leakage and thus the warming of the Benguela Current, and pushing the Westerlies north. B. Illustration of a possible northern hemisphere cold Heinrich event that pushes the Intertropical Convergence Zone southwards. Also in this image an idealised Glacial situation where the Circumpolar Current is located further south, allowing Agulhas leakage and warming of the Benguela Current, and pulling the Westerlies pole-ward (Blome *et al.*, 2012; Chase, 2010, Ziegler *et al.*, 2013).

Agulhas Current is less constrained by a weaker cold Circumpolar Current. As the Circumpolar Current moves south, the Westerlies move with it (Figure 9). As a result there is often less precipitation on land in the East coast region of South Africa.

MIS 5c was a temperate phase, somewhat cooler than the present for which the Westerlies model predicts wetter terrestrial conditions. The cold MIS 4 is also a wet phase because after 75 ka years ago other factors, including Heinrich events, have a greater influence on terrestrial climate than the Westerlies/Circumpolar Current. Our results propose that Sea Surface Temperatures were not depressed during the M1 occupation at Blombos Cave; this appears an atypical MIS 4 signal. As also discussed by others (Blome *et al.*, 2012; Chase, 2010), local proxies, namely (micro) mammal dimensions and species composition, tortoise dimensions, find densities and (micro) mammal data, also from nearby Klasies River, suggest increased rainfall during the M1 occupation (Table 5). Interestingly, the suggested increased seasonal rainfall for MIS 4 (Bar-Matthews *et al.*, 2010) appears not endorsed by the local data.

The SAS or MSA II member at Klasies River is dated between ~100 to ~80 ka years ago (Wurz, 2002) and therefore overlapped in time with the Blombos M3 and M2 Lower occupations. Micro-mammal and mammal studies indicate that the vegetation during the MSA II was denser than pro- and preceding phases (Avery, 1987; Klein, 1976; Wurz, 2002). The MSA II witnessed less seasonal fluctuations than previous periods and the average annual rainfall is estimated at 500–800 mm (Avery, 1987), and the mean average temperature at 15.5°C (Thackeray, 1987). A subsequent study of micro-mammals confirmed these findings and elaborated that there is a trend in increased rainfall and closed vegetation throughout the MSA II period. Rainfall became less seasonal, particularly in

Table 5. Overview of local climate and environmental and behavioural proxies from Blombos Cave from Henshilwood *et al*. (2001), Nel (2013, 2007, 2006), Langejans *et al*. (2012), Reynard (2011), Thompson and Henshilwood (2011). SST: Sea Surface Temperatures. X: no data/interpretation available.

	M3 Upper	M2 Lower	M2 Upper	M1
SST incidental shellfish	Low end of current range	Current range	Current range	Current range, possibly slightly warmer
Micro-mammal environment	Grassland dominates. Stable fynbos component. More open compared to lower layers	Grassland dominates. Decrease in fynbos compared to M3. Shrubs replaced by trees/bushes	Grassland dominates. Most bushy of all phases.	Grassland dominates. Dunes covered with vegetation. Decline in fynbos compared to M2 Upper, increase grass component.
Micro-mammal rainfall	Increased summer rainfall and annually drier compared to lower layers	Increasing moisture. Lower layers more non-seasonal rainfall.	x	Increased general rainfall particularly in lower layers. Less seasonal rainfall, particularly in uppermost units.
Tortoise rainfall	Dry (but less so than the M2)	Dry	Dry	Most moist of all phases
Micro-mammal climate	No evidence for cold conditions	Generally warm	x	Generally cooler and possibly colder in uppermost units.
Tortoise climate	Warm (but less so than the M2)	Warm	Warm	Coolest of all phases
Bone fragments/m^3	x	314.00	1541.00	4750
Shellfish kg/m^3	68.40	31.80		17.5
Detached lithic pieces/m^3	29,284.00	2935.00		21,825.50
Occupation intensity humans (micro-mammals)	Punctuated intense occupations	Low	Intense	Intense
Average distance to shore km	3.32	2.67	4.99	15.80

later stages of the MSA II; this would have been contemporaneous with the M2 Lower (Nel, 2013). It is, however, unclear if the vegetation consisted of afromontane forest or fynbos as both do well in non-seasonal rainfall regimes (Nel, 2013).

Our analysis suggests that Sea Surface Temperatures fell within current values and imply that the differences between phases were not vast. The Blombos micro-mammal signal is also consistent over time and changes in climate and environment were subtle; grassland dominates the vegetation throughout the sequence, followed by trees/bushes (Nel, 2013). Only during the deposition of the M3 were Sea Surface Temperatures on the low end of the current range. The environment during the M3 contained a stable fynbos component and was open. There was less rainfall compared to the preceding M3 Lower layers (>100 ka), but summer rainfall increased. The temperature was relatively high and there are no indications for a cold environment. The site was intensely, but intermittently occupied.

Although the signal is complex, the Sea Surface Temperatures during the M2 appear to fall within the current range. There is less fynbos compared to the M3 and shrubs are replaced by trees and bushes. Annual temperatures were relatively high and the M2 Lower appears to have been a wet phase with less seasonal rainfall than the M3. The tortoise data indicate dry circumstances for the M2, but considering the other proxies also from Klasies River it is unclear how this should be interpreted. During the M2 Lower the occupation density of the site was low. Sea Surface Temperatures during the M2 Upper were again comparable to present day values. There was open bushy grassland with relatively high annual temperatures and rainfall. The site occupation was medium to intense.

It is possible that the M1 Sea Surface Temperatures were slightly higher than today, but they at least ranged within current values. It is likely that further from the cave the landscape was more open, with an increasing grass component. There was a decline in fynbos, and around the cave the vegetation became dense on nearby sand dunes. Dunes generally stabilise when there is enough precipitation to grow vegetation; however, they also stabilise when there is little sediment available when the dunes are close to the shore (Bateman *et al*., 2011; Carr *et al*., 2007, 2006). The latter does not concur with the distances to the sea shore as presented in Figure 3, but the first appears plausible. This phase received the highest annual rainfall of all phases. The micro-mammals indicate more non-seasonal rainfall, contradicting other interpretations (Bar-Matthews *et al*., 2010). Although still warm, the Still Bay M1 was also the coolest of all members and its very last stages were cooler than the earliest ones (Nell, 2013). The site was occupied intensely during this time.

It is complex to interpret the entirety of local data and place them in global and regional climatic models. The local data suggests that Sea Surface Temperatures, the annual terrestrial temperatures and precipitation were never extremely low or high during the occupation phases; moreover, they may well fall within current ranges. Like the terrestrial signal and quite unpredicted, the reconstructed Sea Surface Temperatures for the M1 do not follow global MIS 4 climate trends.

The obvious question arises what exactly is meant by "cool/warm" and "wet/dry". Presently, at nearby Still Bay the mean annual precipitation is 419 mm and the mean annual temperature range is 15–21°C, and Blombos Cave lies in the all-year rainfall zone (Department of Environmental Affairs and Tourism, 2000; WeatherReports.com). The current precipitation is less than the reconstructed 500–800 mm for the MSA II at Klasies River (Avery, 1987); the current temperature range may be higher than the reconstructed mean average of 15.5°C for the MSA II (Thackeray, 1987). In addition today's vegetation is characterised as De Hoop limestone fynbos, here the grass-component is largely absent. Although, currently the driest of the limestone fynbos types, this area may have held other limestone fynbos or renosteveld communities (Rebelo *et al*.,

2011). On the whole, it appears that, from a hunter-gatherer perspective, the Pleistocene environment was more productive than during the Holocene (Faith, 2011).

The MSA II at Klasies River and therefore M3 and M2 Lower were probably wetter and cooler than today and for precipitation this was increasingly so. Meaning that the M2 Lower was wetter than the M3; Table 5 confirms this. With higher non-seasonal rainfall it is likely that the resource depleted fynbos component was not dominant; the micro-mammals and mammals confirm a major grass-component for all Blombos phases. As most proxy values are compared to their preceding reading, this implies that *final* M1 was probably much cooler and wetter than the present day.

2.4.3 Mammal Fauna

The heterogeneity and evenness indices of the faunal assemblages suggest that animal exploitation during the M1 was less focussed than during the preceding M3 phase. However, if we exclude Cape dune molerat and rock hyrax from the calculations, it appears that large mammal exploitation was more focussed compared to the M3 (Dusseldorp, 2012b). The importance of large-bodied animals is highest in the M1. This is interesting in view of the relationship between body size and population density. During the M1, exploitation of large-bodied animals, living in lower population densities than smaller-bodied animals, not only increases, but becomes more focused. This suggests that the encounter rates with high-ranked prey increased; i.e., large herbivore population sizes were probably higher than in previous phases.

Moreover, grazers appear to be slightly more important in the M1 than the M3. The increased presence of grazers has been used to suggest that the environment during the occupation of the M1 was characterised by wetter conditions than the preceding phases and than currently (Henshilwood *et al.*, 2001); this increase supports inferences from the other local proxies.

The relative importance of molerat and rock hyrax in the faunal assemblage decreased in the M1 (Henshilwood *et al.*, 2001). The amount of shellfish per volume of excavated sediment also decreased. The decrease in the importance of shellfish is related to lower sea levels and hence an increased transport distance from the seashore to the site (Henshilwood *et al.*, 2001; Langejans *et al.*, 2012). This suggests that the role of the site in the subsistence and mobility strategies of its occupants changed. Thus, the increased importance of large animal exploitation may reflect a changing function of the site, or changing seasonality of the site's occupation. A change in function to a site more specifically geared to large mammal hunting activities may also have led to a decrease in the representation of molerat and rock hyrax. The importance of Still Bay point manufacture in the M1 compared to the M2 Upper (Villa *et al.*, 2009) probably supports a change in function.

The connection between exploited fauna and environment is not straightforward, as the faunal representation not only tracks changes in availability due to environmental changes, but is also influenced by human preference and changing technology. However, even if changes in the representation of resources may be partly explained by changing site function, we argue that some general conclusions can be drawn from the faunal data. The increased importance of large-bodied animals in the M1 is a notable change and combined with the decreased heterogeneity and evenness for the assemblages (excluding molerat and rock hyrax) this suggests that prey availability and/or hunting success rate increased substantially.

During the M1 resources were neither scarce nor unpredictable as proposed by some (Ambrose and Lorenz, 1990; McCall, 2007). A recent explanation for the appearance of the Still Bay Industry is that the period was characterised by decreased plant

productivity, to which groups responded by adopting a larger focus on large mammal hunting with frequent residential moves (McCall and Thomas, 2012). The bifacial toolkit, with Still Bay points functioning as reliable weapons, is consistent with this hypothesis. However, the M1 level represents the remains of high-intensity occupations by larger groups, and shows that resources, such as shellfish, were transported to the site over considerable distances. This contradicts the proposed frequent residential moves. Instead the site may have functioned as a central place occupied in a system geared to logistical mobility, with expeditions bringing resources (e.g., shellfish) from disparate locations to the site.

Unfortunately, the data from the M2 phase are difficult to evaluate. During the pre-Still Bay M2 Lower, large-bodied animals were less important than during the preceding M3. Their importance was lowest in the earliest M2 Upper Still Bay occupation (Thompson and Henshilwood, 2011). However, both M2 phases are characterised by small sample sizes. Since taxonomically identified specimens were published for the complete M2 and not the M2 Lower and Upper separately, we cannot evaluate how the heterogeneity and evenness developed for these phases. Including rock hyrax and molerat, the indices from the M2 show an evenness and heterogeneity similar to that of the M3. Excluding these small mammals, the evenness and heterogeneity are higher than both the M1 and M3. This suggests that large mammal exploitation may have been less successful during the M2 than during both preceding and subsequent phases.

Thus, the Still Bay appeared during a phase with the lowest representation of large-bodied animals. It may be that environmental circumstances precipitated a decrease in herbivore biomass during M2 Upper times. The decreasing prey availability may then have given rise to specialised hunting weapons (Still Bay points), in order to maximise hunting success. This explanation foregrounds environmental change in the origin of the Still Bay. However, the shellfish and micro-mammal data do not support it and other explanations for the changes in the composition of faunal assemblages cannot be excluded. The importance of Still Bay points is lower during the M2 (N = 6) than during the M1 (N = 269) (Henshilwood, 2008a). The relative importance of bone points to the bifacial Still Bay points shows that bone points are more important in the M2 (21 vs. 6 repectively) than in the M1 (32 vs. 269 repectively) (Henshilwood 2008a, 2008b). This suggests that the relative importance of different hunting weapons used by the site's occupants shifted to the use of Still Bay points in the M1, while bone points appear to have been the weapon of choice in the M2. Similarly, other hallmarks of the Still Bay archaeological record, such as beads, are present in much lower quantities in the M2 (N = 10) compared to the M1 (N = 107) (d'Errico *et al.*, 2005; Henshilwood, 2008a). This suggests that increased emphasis on social networks to buffer risks of resource scarcity (cf. McCall and Thomas, 2012) does not fully explain their role in the Still Bay archaeological record.

2.5 CONCLUSION

The data on Blombos Cave reviewed here highlight that many environmental and behavioural proxies do not yield corresponding results. What is more, the local proxies do not match with all current climate models. We suggest that, on the basis of the available evidence, it is not possible to correlate the advent of behavioural changes to uniform climate and environmental changes. Moreover, some of the differences between the results from local proxies suggest that the relationship between global environmental change and local changes in Sea Surface Temperatures, terrestrial temperature and precipitation may not be as straightforward as often assumed.

The composition of the incidental shellfish assemblages suggests that Sea Surface Temperatures during the M3 were lower than during the M2 Upper and M1. Since no definitive consensus has been reached on the dating of the Still Bay Industry, we cannot correlate the M1 with certainty to either MIS 5a or MIS 4. The most recently published dates suggest the Still Bay must be dated to early MIS 4 (Jacobs *et al*., 2013). Nevertheless, the higher Sea Surface Temperature as indicated by the shellfish might suggest a MIS 5a date. An earlier date for the M1 would fit the reconstruction proposed by Blome *et al*. (2012, Figure 14) or Ziegler *et al*. (2013), where temperate MIS 5a Sea Surface Temperatures co-occur with wetter terrestrial conditions. In addition, the increased dune vegetation in the M1 may be the result of increased precipitation, but if the M1 is older, the sea may also have been closer. The decrease in sediment availability in combination with increased non-seasonal rainfall would consolidate dunes, restrict movement and allow vegetation growth (cf. Carr *et al*., 2006). Since changes in the local sea currents need not be exactly correlated to the dating of global climatic changes in polar ice cores a date in early MIS 4 remains a possibility. However, a later date (associated with a clear cool MIS 4 signal) as suggested by Guérin *et al*. (2013) seems unlikely at this stage.

The mammal assemblages suggest that the terrestrial environment during the M1 was more productive than during the pre-Still Bay M3. It certainly was not less productive. On the whole the Blombos phases are relatively similar and considering that rainfall may have been higher than today, the associated environments was probably more productive than today. Based on the micro-mammals, only the very end of the M1 presents a different environmental scenario (Nel, 2013). The increased importance of small bodied prey during the M2 Upper suggests that encounter rates with large prey were depressed. However, it is unlikely that this is the result of decreasing herbivore biomass, as the climate proxies do not indicate decreased environmental productivity. Rather, a change in hunting strategy may have been the result of changing occupation seasons or a change in site function. The possible hiatus between the M2 Lower and Upper complicate the exact circumstances triggering the origins of the Still Bay technocomplex. Although we cannot conclusively prove that the Still Bay Industry was not a response to low resource abundance, its greatest flowering during the period of highest apparent resource abundance at Blombos suggests that alternative hypotheses may be more probable.

ACKNOWLEDGEMENTS

This research was sponsored by the National Research Foundation (South Africa), and by The Netherlands Organisation for Scientific Research with a Veni grant (The Netherlands). We want to thank Richard Kilburn (Kwa-Zulu-Natal Museum, South Africa), Adam Yates (Museum and Art Gallery of the Northern Territory, Australia) and Dai Herbert (Kwa-Zulu-Natal Museum, South Africa) for their help with the shellfish identification. We also thank the Iziko Museum Cape Town (South Africa) for access to the material and our reviewers for their useful comments.

REFERENCES

Ambrose, S.H. and Lorenz, K.G., 1990, Social and ecological models for the Middle Stone Age in southern Africa. In *The Emergence of Modern Humans: An Archaeological Perspective*, edited by Mellars, P. (Edinburgh: Edinburgh University Press), pp. 3–33.

Appeltans, W., Bouchet, P., Boxshall, G.A., De Broyer, C., De Voogd, N.J., Gordon, D.P., Hoeksema, B.W., Horton, T., Kennedy, M., Mees, J., Poore, G.C.B., Read, G., Stöhr, S., Walter, T.C. and Costello, M.J., 2012, *World Register of Marine Species*, http://www.marinespecies.org, access date: 4-7-2011.

Avery, D.M., 1987, Late Pleistocene coastal environment of the Southern Cape Province of South Africa: Micromammals from klasies river mouth. *Journal of Archaeological Science*, **14**, pp. 405–421.

Bar-Matthews, M., Marean, C.W., Jacobs, Z., Karkanas, P., Fisher, E.C., Herries, A.I.R., Brown, K., Williams, H.M., Bernatchez, J., Ayalon, A. and Nilssen, P.J., 2010, A high resolution and continuous isotopic speleothem record of paleoclimate and paleoenvironment from 90 to 53 ka from Pinnacle Point on the South coast of South Africa. *Quaternary Science Reviews*, **29**, pp. 2131–2145.

Bateman, M.D., Carr, A.S., Dunajko, A.C., Holmes, P.J., Roberts, D.L., McLaren, S.J., Bryant, R.G., Marker, M.E. and Murray-Wallace, C.V., 2011, The evolution of coastal barrier systems: A case study of the Middle-Late Pleistocene Wilderness barriers, South Africa. *Quaternary Science Reviews*, **30**, pp. 63–81.

Bigalke, E.H., 1973, The exploitation of shellfish by coastal tribesmen of the Transkei. *Annals of the Cape Provincial Museums (Natural History)*, **9**, pp. 159–175.

Birch, G.F., 1980, Nearshore Quaternary sedimentation of the South coast of South Africa (Cape Town to Port Elizabeth). *Bulletin of the Geological Survey of South Africa*, **67**, p. 20.

Birch, G., 1978, The bathymetry and geomorphology of the inner shelf between Cape Seal and Cape Recife. *Joint Geological Survey/University of Cape Town Technical Report*, **11**, pp. 118–121.

Blome, M.W., Cohen, A.S., Tryon, C.A., Brooks, A.S. and Russell, J., 2012, The environmental context for the origins of modern human diversity: A synthesis of regional variability in African climate 150,000–30,000 years ago. *Journal of Human Evolution*, **62**, pp. 563–592.

Brain, C.K., 1981, *The Hunters or the Hunted? An Introduction to African Cave Taphonomy*, (Chicago: University of Chicago Press).

Buchanan, W.F., 1988, *Shellfish in Prehistoric Diet*, (Oxford: Archeopress).

Carr, A.S., Bateman, M.D. and Holmes, P.J., 2007, Developing a 150 ka luminescence chronology for the barrier dunes of the southern Cape, South Africa. *Quaternary Geochronology*, **2**, pp. 110–116.

Carr, A.S., Thomas, D.S.G. and Bateman, M.D., 2006, Climatic and sea level controls on Late Quaternary eolian activity on the Agulhas Plain, South Africa. *Quaternary Research*, **65**, pp. 252–263.

Chase, B.M., 2010, South African palaeoenvironments during marine Oxygen Isotope Stage 4: A context for the Howiesons Poort and Still Bay industries. *Journal of Archaeological Science*, **37**, pp. 1359–1366.

Chase, B.M., Meadows and M.E., 2007, Late Quaternary dynamics of southern Africa's winter rainfall zone. *Earth-Science Reviews*, **84**, pp. 103–138.

Claasen, C., 1998, *Shells*, (Cambridge: Cambridge University Press).

Clark, J.L., 2011, The evolution of human culture during the later Pleistocene: Using fauna to test models on the emergence and nature of "modern" human behavior. *Journal of Anthropological Archaeology*, **30**, pp. 273–291.

Compton, J.S., 2011, Pleistocene sea-level fluctuations and human evolution on the southern coastal plain of South Africa. *Quaternary Science Reviews*, **30**, pp. 506–527.

Cruz-Uribe, K., 1988, The use and meaning of species diversity and richness in archaeological faunas. *Journal of Archaeological Science*, **15**, pp. 179–196.

d'Errico, F., Henshilwood, C., Vanhaeren, M. and van Niekerk, K., 2005, *Nassarius kraussianus* shell beads from Blombos Cave: Evidence for symbolic behaviour in the Middle Stone Age. *Journal of Human Evolution*, **48**, pp. 3–24.

Dansgaard, W., Johnsen, S.J., Clausen, H.B., Dahl-Jensen, D., Gundestrup, N.S., Hammer, C.U., Hvidberg, C.S., Steffensen, J.P., Sveinbjornsdottir, A.E., Jouzel, J. and Bond, G., 1993, Evidence for general instability of past climate from a 250–kyr ice-core record. *Nature*, **364**, pp. 218–220.

Deacon, H.J., 1989, Late Pleistocene palaeoecology and archaeology in the southern Cape, South Africa. In *The Human Revolution. Behavioural and Biological Perspectives on the Origins of Modern Humans*, edited by Mellars, P. and Stringer, C. (Edinburgh: Edinburgh University Press), pp. 547–564.

Dempster, Y. and Branch, G.M., 1999, A review of the genus *Burnupena* Iredale, 1918 (Gastropoda: Buccinidae), with descriptions of two new species. *Annals of the Natal Museum*, **40**, pp. 173–204.

Department of Environmental Affairs and Tourism, University of Pretoria and GIS Business Solutions, 2000, Mean annual precipitation, *Environmental Potential Atlas for the Western Cape*.

Dusseldorp, G.L., 2012a, Studying prehistoric hunting proficiency: Applying optimal foraging theory to the Middle Palaeolithic and Middle Stone Age. *Quaternary International*, **252**, pp. 3–15.

Dusseldorp, G.L., 2012b, Tracking the influence of technological change on Middle Stone Age hunting strategies in South Africa. *Quaternary International*, **270**, pp. 70–79.

Dusseldorp, G., 2010, Prey choice during the South African Middle Stone Age: Avoiding dangerous prey or maximising returns? *African Archaeological Review*, **27**, pp. 107–133.

Erlandson, J.M. and Moss, M.L., 2001, Shellfish feeders, carrion eaters, and the archaeology of aquatic adaptations. *American Antiquity*, **66**, pp. 413–432.

Faith, J.T., 2011, Ungulate community richness, grazer extinctions, and human subsistence behavior in southern Africa's Cape Floral Region. *Palaeogeography, Palaeoclimatology, Palaeoecology*, **306**, pp. 219–227.

Fisher, E.C., Bar-Matthews, M., Jerardino, A. and Marean, C.W., 2010, Middle and Late Pleistocene paleoscape modeling along the southern coast of South Africa. *Quaternary Science Reviews*, **29**, pp. 1382–1398.

Guérin, G., Murray, A.S., Jain, M., Thomsen, K.J. and Mercier, N., 2013, How confident are we in the chronology of the transition between Howieson's Poort and Still Bay? *Journal of Human Evolution*.

Hammond, W. and Griffiths, C., 2006, Biogeographical patterns in the fauna associated with southern African mussel beds. *African Zoology*, **41**, pp. 123–130.

Henshilwood, C.S., 2008a, Winds of change: Palaeoenvironments, material culture and human behaviour in the Late Pleistocene (~77 ka–48 ka ago) in the Western Cape Province, South Africa. *Goodwin Series*, **10**, pp. 35–51.

Henshilwood, C.S., 2008b, Holocene prehistory of the southern Cape, South Africa. Excavations at Blombos Cave and the Blombosfontein Nature Reserve, (Oxford: Archaepress).

Henshilwood, C.S., 2012, Late Pleistocene techno-traditions in Southern Africa: A review of the Still Bay and Howiesons Poort, c. 75–59 ka. *Journal of World Prehistory* **25**, pp. 205–237.

Henshilwood, C.S., d'Errico, F. and Watts, I., 2009, Engraved ochres from the Middle Stone Age levels at Blombos Cave, South Africa. *Journal of Human Evolution*, **57**, pp. 27–47.

Henshilwood, C.S., d'Errico, F., van Niekerk, K.L., Coquinot, Y., Jacobs, Z., Lauritzen, S.-E., Menu, M. and García-Moreno, R., 2011, A 100,000-year-old ochre-processing workshop at Blombos Cave, South Africa. *Science*, **334**, pp. 219–222.

Henshilwood, C.S., Sealy, J.C., Yates, R., Cruz-Uribe, K., Goldberg, P., Grine, F.E., Klein, R.G., Poggenpoel, C., van Niekerk, K. and Watts, I., 2001, Blombos Cave, southern Cape, South Africa: Preliminary report on the 1992–1999 excavations of the Middle Stone Age levels. *Journal of Archaeological Science*, **28**, pp. 421–448.

Hydrographic Office and South African Navy, 2011, *Tide Information*, (http://www.sanho.co.za/tides/tide_index.htm, access date: 23-8-2011.

Jacobs, Z. and Roberts, R.G., 2008, Testing times: Old and new chronologies for the Howieson's Poort and Still Bay industries in environmental context. *Goodwin Series*, **10**, pp. 9–34.

Jacobs, Z., Hayes, E.H., Roberts, R.G., Galbraith, R.F. and Henshilwood, C.S., 2013, An improved OSL chronology for the Still Bay layers at Blombos Cave, South Africa: further tests of single-grain dating procedures and a re-evaluation of the timing of the Still Bay Industry across southern Africa. *Journal of Archaeological Science*, **40**, pp. 579–594.

Jacobs, Z., Roberts, R.G., Galbraith, R.F., Deacon, H.J., Grun, R., Mackay, A., Mitchell, P., Vogelsang, R. and Wadley, L., 2008a, Ages for the Middle Stone Age of southern Africa: Implications for human behavior and dispersal. *Science*, **322**, pp. 733–735.

Jacobs, Z., Wintle, A.G., Duller, G.A.T., Roberts, R.G. and Wadley, L., 2008b, New ages for the post-Howiesons Poort, late and final Middle Stone Age at Sibudu, South Africa. *Journal of Archaeological Science*, **35**, pp. 1790–1807.

Jerardino, A., 1997, Changes in shellfish species composition and mean shell size from a Late-Holocene record of the West coast of southern Africa. *Journal of Archaeological Science*, **24**, pp. 1031–1044.

Jones, E.L., 2004, Dietary evenness, prey choice, and human–environment interactions. *Journal of Archaeological Science*, **31**, pp. 307–317.

Jouzel, J., Masson-Delmotte, V., Cattani, O., Dreyfus, G., Falourd, S., Hoffmann, G., Minster, B., Nouet, J., Barnola, J.M., Chappellaz, J., Fischer, H., Gallet, J.C., Johnsen, S., Leuenberger, M., Loulergue, L., Luethi, D., Oerter, H., Parrenin, F., Raisbeck, G., Raynaud, D., Schilt, A., Schwander, J., Selmo, E., Souchez, R., Spahni, R., Stauffer, B., Steffensen, J.P., Stenni, B., Stocker, T.F., Tison, J.L., Werner, M. and Wolff, E.W., 2007, Orbital and millennial Antarctic climate variability over the past 800,000 years. *Science*, **317**, pp. 793–796.

Kensley, B., 1973, *Sea Shells of Southern Africa. Gastropods*, (Cape Town: Maskew Miller).

Kilburn, R. and Rippey, E., 1982, *Sea Shells of Southern Africa*, (Johannesburg: Macmillan South Africa).

Klein, R.G., 1976, The mammalian fauna of the Klasies River Mouth sites, southern Cape Province, South Africa. *The South African Archaeological Bulletin*, **31**, pp. 75–98.

Kyle, R., Pearson, B., Fielding, P.J., Robertson, W.D. and Birnie, S.L., 1997, Subsistence shellfish harvesting in the Maputaland Marine Reserve in northern KwaZulu-Natal, South Africa: Rocky shore organisms. *Biological Conservation*, **82**, pp. 183–192.

Langejans, G.H.J., van Niekerk, K.L., Dusseldorp, G.L. and Thackeray, J.F., 2012, Middle Stone Age shellfish exploitation: Potential indications for mass collecting and resource intensification at Blombos Cave and Klasies River, South Africa. *Quaternary International*, **270**, pp. 80–94.

Lombard, M., 2012, Thinking through the Middle Stone Age of sub-Saharan Africa. *Quaternary International*, **270**, pp. 140–155.

Lupo, K., 2006, What explains the carcass field processing and transport decisions of contemporary hunter-gatherers? Measures of economic anatomy and zooarchaeological skeletal part representation. *Journal of Archaeological Method and Theory*, **13**, pp. 19–66.

Lupo, K.D. and Schmitt, D.N., 2005, Small prey hunting technology and zooarchaeological measures of taxonomic diversity and abundance: Ethnoarchaeological evidence from Central African forest foragers. *Journal of Anthropological Archaeology*, **24**, pp. 335–353.

Lyman, R.L., 2008, *Quantitative Paleozoology*, (Cambridge: Cambridge University Press).

Marean, C.W., 2010, Pinnacle Point Cave 13B (Western Cape Province, South Africa) in context: The Cape Floral kingdom, shellfish, and modern human origins. *Journal of Human Evolution*, **59**, pp. 425–443.

Marean, C.W., Abe, Y., Frey, C.J. and Randall, R.C., 2000, Zooarchaeological and taphonomic analysis of the Die Kelders Cave 1 Layers 10 and 11 Middle Stone Age larger mammal fauna. *Journal of Human Evolution*, **38**, pp. 197–233.

Martinson, D.G., Pisias, N.G., Hays, J.D., Imbrie, J., Moore Jr, T.C. and Shackleton, N.J., 1987, Age dating and the orbital theory of the ice ages: Development of a high-resolution 0 to 300,000-year chronostratigraphy. *Quaternary Research*, **27**, pp. 1–29.

McCall, G.S., 2007, Behavioral ecological models of lithic technological change during the later Middle Stone Age of South Africa. *Journal of Archaeological Science*, **34**, pp. 1738–1751.

McCall, G. and Thomas, J., 2012, Still Bay and Howiesons Poort foraging strategies: Recent research and models of culture change. *African Archaeological Review*, **29**, pp. 7–50.

Metcalfe, D. and Barlow, K.R., 1992, A model for exploring the optimal trade-off between field processing and transport. *American Anthropologist*, **94**, pp. 340–356.

Nagaoka, L., 2002, The effects of resource depression on foraging efficiency, diet breadth, and patch use in southern New Zealand. *Journal of Anthropological Archaeology*, **21**, pp. 419–442.

Natal Museum—Mollusc Collection, 2007, *Biodiversity Occurrence Data (AfrOBIS)*, accessed through GBIF data portal, http://data.gbif.org/datasets/resource/401, access date: 5-7-2011.

Neeley, M.P. and Clark, G.A., 1993, The human food niche in the Levant over the past 150,000 Years. *Archeological Papers of the American Anthropological Association*, **4**, pp. 221–240.

Nel, T.H., 2006, *Palaeoenvironmental reconstruction based on faunal analysis: A case study of the Middle Stone Age levels at Blombos Cave, South Africa*, MA Thesis, (Bergen: University of Bergen).

Nel, T.H., 2007, Middle Stone Age palaeoenvironments: A study of faunal material from Blombos Cave, southern Cape, South Africa. *Nyame Akuma*, **68**, pp. 52–61.

Nel, T.H., 2013, *Micromammals, climate change and human behaviour in the Middle Stone Age, southern Cape, South Africa. Examining the possible links between palaeoenvironments and the cognitive evolution of Homo sapiens*, PhD Thesis, (Bergen: University of Bergen).

NOAA, 2013, *Monthly Mean SST Charts (1984–1998)*, (http://www.ospo.noaa.gov/Products/ocean/sst/monthly_mean.html, access date: 12-3-2013.

Petit, J.R., Jouzel, J., Raynaud, D., Barkov, N.I., Barnola, J.M., Basile, I., Benders, M., Chappellaz, J., Davis, M., Delaygue, G., Delmotte, M., Kotlyakov, V.M., Legrand, M., Lipenkov, V.Y., Lorius, C., Pepin, L., Ritz, C., Saltzman, E. and Stievenard, M., 1999, Climate and atmospheric history of the past 420,000 years from the Vostok ice core, Antarctica. *Nature*, **399**, pp. 429–436.

Plug, C. and Plug, I., 1990, MNI counts as estimates of species abundance. *The South African Archaeological Bulletin*, **45**, pp. 53–57.

Rebelo, A.G., Boucher, C., Helme, N., Mucina, L. and Rutherford, M.C., 2011. Fynbos Biome. In *The Vegetation of South Africa, Lesotho and Swaziland*, edited by Mucina, L. and Rutherford, M.C. (Stralitzia 19, South African National Biodiversity Institute), pp. 53–219.

Rector, A.L. and Verrelli, B.C., 2010, Glacial cycling, large mammal community composition, and trophic adaptations in the Western Cape, South Africa. *Journal of Human Evolution*, **58**, pp. 90–102.

Reynard, J.P., 2011, *The Unidentified Long Bone Fragments from the Middle Stone Age Still Bay Layers at Blombos Cave, Southern Cape, South Africa*, MSc Thesis, (Johannesburg: University of the Witwatersrand).

SADCO, 2008, *Tidal information*, (Council for Scientific and Industrial Research South Africa), http://sadco.csir.co.za/, access date: 28-6-2011.

Scholz, C.A., Johnson, T.C., Cohen, A.S., King, J.W., Peck, J.A., Overpeck, J.T., Talbot, M.R., Brown, E.T., Kalindekafe, L., Amoako, P.Y.O., Lyons, R.P., Shanahan, T.M., Castaneda, I.S., Heil, C.W., Forman, S.L., McHargue, L.R., Beuning, K.R., Gomez, J. and Pierson, J., 2007, East African mega droughts between 135 and 75 thousand years ago and bearing on early-modern human origins. *Proceedings of the National Academy of Sciences*, **104**, pp. 16416–16421.

Seatemperature.org, 2013, *South African Sea Temperatures*, (http://www.seatemperature.org/africa/south-africa/, access date: 12-3-2012.

Shackleton, N.J., 1982, Stratigraphy and chronology of the Klasies River Mouth deposits: Oxygen isotope evidence. In *The Middle Stone Age at Klasies River Mouth in South Africa*, edited by Singer, R. and Wymer, J. (Chicago: Chicago University Press), pp. 194–199.

Silva, M., Brimacombe, M. and Downing, J.A., 2001, Effects of body mass, climate, geography, and census area on population density of terrestrial mammals. *Global Ecology and Biogeography*, **10**, pp. 469–485.

Silva, M., Brown, J.H. and Downing, J.A., 1997, Differences in population density and energy use between birds and mammals: A macroecological perspective. *Journal of Animal Ecology*, **66**, pp. 327–340.

Stiner, M.C. and Munro, N.D., 2002, Approaches to prehistoric diet breadth, demography, and prey ranking systems in time and space. *Journal of Archaeological Method and Theory*, **9**, pp. 181–214.

Stuut, J.-B.W., Crosta, X., van der Borg, K. and Schneider, R., 2004, Relationship between Antarctic sea ice and southwest African climate during the late Quaternary. *Geology*, **32**, pp. 909–912.

Thackeray, J.F., 2007, Sea levels and chronology of Late Pleistocene coastal cave deposits at Klasies River in South Africa. *Annals of the Transvaal Museum*, **44**, pp. 219–220.

Thackeray, J.F., 1987, Late Quaternary environmental changes inferred from small mammalian fauna, southern Africa. *Climatic Change*, **10**, pp. 285–305.

Thompson, J.C. and Henshilwood, C.S., 2011, Taphonomic analysis of the Middle Stone Age larger mammal faunal assemblage from Blombos Cave, southern Cape, South Africa. *Journal of Human Evolution*, **60**, pp. 746–767.

Tribolo, C., Mercier, N., Selo, M., Valladas, H., Joron, J.L., Reyss, J.L., Henshilwood, C., Sealy, J. and Yates, R., 2006, TL dating of burnt flint lithics from Blombos Cave (South Africa): Further evidence for the antiquity of modern human behaviour. *Archaeometry*, **48**, pp. 341–357.

Turton, W., 1932, *The Marine Shells of Port Alfred, S. Africa*. (London: Oxford Univesity Press).

Van Niekerk, K.L., 2011, *Marine Fish Exploitation during the Middle and Later Stone Age of South Africa*, PhD Thesis, (Cape Town: University of Cape Town).

Villa, P., Soressi, M., Henshilwood, C.S. and Mourre, V., 2009, The Still Bay points of Blombos Cave (South Africa). *Journal of Archaeological Science*, **36**, pp. 441–460.

Wadley, L., 2010, Were snares and traps used in the Middle Stone Age and does it matter? A review and a case study from Sibudu, South Africa. *Journal of Human Evolution*, **58**, pp. 179–192.

Waelbroeck, C., Labeyrie, L., Michel, E., Duplessy, J.C., McManus, J.F., Lambeck, K., Balbon, E. and Labracherie, M., 2002, Sea-level and deep water temperature changes derived from benthic foraminifera isotopic records. *Quaternary Science Reviews*, **21**, pp. 295–305.

WeatherReports.com, *Weather report for Still Bay, South Africa*, (http://www.weatherreports.com/South_Africa/Stilbaai, access date: 18-8-2011.

Winterhalder, B., 2001, The behavioural ecology of hunter-gatherers. In *Hunter-Gatherers, An Interdisciplinary Perspective*, edited by Panter-Brick, C., Layton, R.H. and Rowley-Conwy, P., (Cambridge: Cambridge University Press), pp. 12–38.

Winterhalder, B., 1987, The analysis of hunter-gatherer diets: Stalking an optimal foraging model. In *Food and Evolution, Toward a Theory of Human Food Habits*, edited by Harris, M. and Ross, E.B. (Philadelphia: Temple University Press), pp. 311–341.

Wurz, S., 2002, Variability in the Middle Stone Age lithic sequence, 115,000–60,000 years ago at Klasies River, South Africa. *Journal of Archaeological Science*, **29**, pp. 1001–1015.

Ziegler, M., Simon, M.H., Hall, I.R., Barker, S., Stringer, C. and Zahn, R. 2013, Development of Middle Stone Age innovation linked to rapid climate change. *Nature Communications* **4**: Article 1905.

This page intentionally left blank

CHAPTER 3

Late Quaternary valley and slope deposits and their palaeoenvironmental significance in the Upper Congo Basin, Central Africa

Jürgen Runge & Mark Sangen
Centre for Interdisciplinary Research on Africa (ZIAF) and Institute of Physical Geography, Johann Wolfgang Goethe University, Frankfurt am Main, Germany

Marion Neumer
RODECO Consulting GmbH, Bad Homburg, Germany

Joachim Eisenberg & Eva Becker
Centre for Interdisciplinary Research on Africa (ZIAF) and Institute of Physical Geography, Johann Wolfgang Goethe University, Frankfurt am Main, Germany

ABSTRACT: A great deal of palaeoenvironmental research on tropical alluvia and slope sediments was based on the erroneous assumption of the long term persistence of a relatively stable climate and associated vegetation in low latitudes during the Quaternary. Recent geomorphological and ecosystem history research in Cameroon, the Central African Republic and in the eastern Congo basin (Democratic Republic of Congo) has provided evidence of the frequent occurrence of multi-layered alluvia and fans in river valleys as well as stratified slope deposits (hillwash, stone-lines, pedisediments) that reflect former modifications of the environment. Numerous radiocarbon data indicate that tropical ecosystems are highly sensitive to climate change through modification of surfaces and run-off dynamics. A well documented stratigraphic record characterised by variable sediment layers of 2.0–5.5 metres thick spans the Holocene and the Pleistocene back to 50 kyrs BP. Buried stone-lines indicate once drier, more open landscapes under alternating wet and dry climates in currently humid and semi-humid regions. A conceptual morphodynamic model is presented to summarize process response to former environmental modifications. Nevertheless as river catchments and slopes are 'open' fluvial systems in landscapes the problem of possible stratigraphical hiati in the sediment strata and subsequent pedogenesis has to be taken into consideration when interpreting these complex structures.

3.1 INTRODUCTION

The African lower latitudes covered by dense evergreen and semi-deciduous rain forests, high woody biomass mosaics and savanna woodlands have long been recognized as evolutionary ancient ecosystems and were assumed to be climatically stable over a

long time. Species richness in places and deeply weathered soils and saprolites on ancient Gondwana rocks supported generalized hypothesises that, at least throughout the Cretaceous and Tertiary period the vegetational features remained relatively unchanged. This perception of tropical geomorphological stability within the zone of predominantly peneplanated surfaces, and the possible variations of morphodynamic processes within river catchments and on slopes, have been neglected for a long time (compare Runge, 2001, 2008). This is surprising because in neighbouring (partly former) desert regions, like on the margins of the Sahara and the 'Mega-Kalahari' on the southern hemisphere, considerable changes in the environmental settings have been early detected in the form of palaeodunes, lake sediments, palaeontological evidence, artefacts, rock art, and others, that had been correctly interpreted as representing major climate and associated environmental change (a Neolithic "green" Sahara) (e.g., Monod, 1938; Williams and Faure, 1980; Woodward *et al.*, 2007; Baumhauer and Runge, 2009).

Meanwhile, it has become evident that these previous assumptions about the stability of low latitudes ecosystems in West and Central Africa over time cannot generally be validated. Natural shifts in climate over the last 50,000 yrs, during the Pleistocene and Holocene, have caused repeated, strong modification in the spatial dynamics of these ecosystems that are, due to equally modified morphodynamics, well reflected in the structure and in the composition of surface sediments such as hillwash and stone-lines (Runge, 2001). Because changes in vegetation cover influence the surface sediment flux, infiltration capacity, erodability and run-off in fluvial systems, alluvia of tropical rivers can be useful as proxy-data for palaeoenvironmental interpretation at landscape scale.

This paper summarizes and reviews physiogeographical studies on multilayered, stratified surface and river sediments along the rain forest-savanna transition of West and Central Africa with priority given to Cameroon, Central African Republic and the Democratic Republic of Congo (D.R. Congo) (formerly Zaire) (Figure 1). It will be elaborated how these forest and savanna boundaries, often highly sensitive to former and recent natural and human triggered environmental changes (Thomas, 2004), are reflected within the geomorphological and stratigraphical context. For some regions (e.g., Cameroon) the first alluvial stratigraphies are presented here, but in a wider context the accumulated findings are summarised from ~15 years of geomorphological research in equatorial Central Africa.

3.2 RESEARCH TO DATE

3.2.1 General features of valley and slope deposits in Sub-Saharan Africa

Similar evidence of changing fluvial-morphological and sedimentary processes in tropical rivers and on catchment slopes due to climatic and ecological instability since the Quaternary were reported from Australia (Thomas *et al.*, 2001), Asia (Thorp and Thomas, 1992; Latrubesse *et al.*, 2005) and South America (Latrubesse, 2003; Latrubesse and Rancy, 1998, 2000; Latrubesse and Franzinelli, 2002, 2005; Steveaux, 2000; Steveaux and Souza, 2004). There are also some publications for West (Pastouret *et al.*, 1978; Thomas and Thorp, 1980, 1995, 2003; Hall *et al.*, 1985; Zabel *et al.*, 2001) and Central Africa (Giresse *et al.*, 1982, 2005; Preuss, 1986a, 1986b, 1990; Runge, 1992, 1996; Kadomura, 1995; Marret *et al.*, 2001, 2006; Thomas, 2000).

There is no general interpretation or universal concept to explain fluvial deposits on slopes and in valleys of the humid tropics impacted by climate and landscape

change. Alluvial deposits in the tropics are apparently more interlocked with colluvia of the interfluves and slopes than it is the case in the temperate regions (Fölster, 1983; Thorp and Thomas, 1992; Runge, 2001). The more intensive rearrangement of coarse and fine material in the glacial periods on slopes and in valleys has led to a less prominent morphological development of fluvial terraces and this complicates the spatio-temporal correlation of different terrace levels and alluvial deposits. Alexandre *et al.* (1994) differentiate river deposits according to humid and arid climatic periods in the Shaba province (Biano Plateau and Lupembashi Valley, Alexandre-Pyre, 1971; Mbenza, 1983; Mbenza *et al.*, 1984). The observed alluvial accumulations in the spacious, flat valley systems with bottom rock outcrops are often topped by compact gravel layers partially consolidated by iron induration (french 'gravier sous berge'). They are covered by interbedded sands and sandy clays which contain single stonelines (strata of coarser material). Alexandre *et al.* (1994) interpreted these lines as residual debris that exposed and redeposited in conjunction with incision of the river under more humid conditions. Van Zinderen Bakker and Clark (1962) assign similar detrital accumulations at the Luembe River in northeastern Angola primarily to a period of arid climate. More recent fluvial erosion under humid conditions has not yet led to dissection of these detrital layers. Radiocarbon datings of the hanging layer following the 'gravier sous berge' strata resulted in Holocene ages of 6.8–6.3 kyrs (van Zinderen Bakker and Clark, 1962; De Ploey, 1966–68, 1968; Alexandre *et al.*, 1994). Runge and Tchamié (2000) describe related phenomena from the Niantin River valley in northern Togo, West Africa, and assume an Ogolian age around 18 kyrs for the accumulation of vast pebbles accumulations and of other coarse material over solid bedrock. Here, ^{14}C (AMS) data of overlying alluvia published by Runge and Tchamié, 2000) gave ages of only several hundred years. This suggests very effective morphodynamic activity of fluvial tropical systems by lateral erosion and redeposition of the complete alluvial body in the course of singular excessive events of discharge.

3.2.2 Unique findings from tropical Central Africa

In the Mbari valley in the Central African Republic undisturbed alluvial sediments with a thickness of several metres were dated to 8 kyrs BP (Runge, 2002). This corroborates the thesis of a more or less continuous accumulation of sands and clays in the early Holocene under more humid climatic conditions. In Nigeria, at the northwestern limit of the volcanic Jos Plateau, Zeese (1991) defines two humid cool climatic periods with strong valley erosion between 20–18 kyrs BP and around 11 kyrs BP (Younger Dryas?). Zeese (1991, 1996) postulates the filling up of valleys by alluvia with sandy accumulation up to 15 metres thick, with poorly graded fluvial and/or colluvial sediments deposited during late glacial times. Preuss (1986a, 1986b) introduced a longer sedimentary sequence in the region of the Ruki River in the central Congo basin (D.R. Congo), which is believed to have taken place under semi-arid to arid climatic conditions, e.g., with a Last Glacial Maximum (LGM) to post-LGM age of 19–17.7 kyrs. Early on De Ploey (1964, 1965, 1968) proposed on the western limit of the Congo basin in the Malebo-(Stanley) Pool near Kinshasa/Brazzaville a Late Quaternary sediment stratigraphy: from 42 kyrs onwards there was strong erosion ('Maluékien'), subsequently abundant accumulation of sand until around 37 kyrs. During the 'Njilien' (~40–30 kyrs) there was podzolization of this sands under alternating humid warm to cool climatic conditions and in the high glacial 'Léopoldvillien' (~15–12 kyrs BP) it was again cooler and dryer with the alluvium showing alternation between humid to semi-arid(?) conditions, and strong fluvial activity with incision of interfluves. Before the

onset of the Holocene a strong mobility of the sediments with erosion and deposition of surface layers starts again around 16 kyrs and ends just before 11 kyrs BP in the western Congo. De Ploey (1964, 1965) augurs a temporary, climatic controlled thinning out of the vegetation cover with an increased morphodynamic activity on slopes and within river valleys. From ~12–3 kyrs BP, during the 'Kibangien', a predominant tendency to a renewed propagation of rain forest persists in Central Africa.

Close to the surface, layers with predominant coarse material ('stone-lines') occur widely spread as stratigraphical markers of discontinuities in the development of landscapes in the Central Congo basin and also in the surrounding swell regions (Waegemans, 1953; Stoops, 1967; Alexandre and Soyer, 1987; Runge, 1992, 1997). For the formation of surface layers and stone-lines, termites, particularly the giant termites *Macrotermes subhyalinus* RAMBUR (ex *Bellicositermes bellicosus rex*), whose mounds reach up to 3 to 5 metres in height and 10 to 60 metres in diameter, play a decisive role. Because of large partially-fossilized termite mounds within the present rain forest, it can be assumed that they have been formed under savanna-like, sparsely wooded environments and to have been overgrown in the Holocene by the expanding rain forest. The flux and rate of sedimentation in the submarine Congo estuary decreased between 11.2–10.3 kyrs and 10.3–8.4 kyrs from 160 cm to 35 cm per 1000 yrs. This could be an indication of a significant shift in climate, one that led to an expansion of forests, a reduction in termite activity and an associated reduction in bioturbation in Central Africa (Runge and Lammers, 2001).

Alluvium and slope sediments sometimes contain archaeological material. Little is known as to how prehistoric people lived as hunter-gatherers in the transitional regions between dense rain forests and open savanna woodlands in Central Africa. The last 70,000 yrs correspond with the northern hemisphere Würm/Weichsel glaciation (oxygen isotope stages, OIS 5e to 2), were often characterized by repeated shifts in climate and therefore changes in vegetation cover.

Lanfranchi and Schwartz (1990) provide an overview of the Middle Stone Age (MSA) to the Late Stone Age (LSA) and finally to the Neolithic and Iron Age. In the Congo-Brazzaville the Maluékien (70–40 kyrs BP) was relatively dry and cold with MSA artefacts frequently discovered in layers of coarse material (stone-lines) within multilayered soil-sediments. The Maluékien was followed by the Njilien (40–30 kyrs BP) which established again humid conditions with the return of closed forests to the region (see above). The last point corresponds to the fact that no evidence for palaeolithic industries for this time was found.

On the Batéké plateau north of Kinshasa and Brazzaville tropical podzols were developed in the former Mega-Kalahari Sands, clear evidence for striking modifications of the environment (Schwartz, 1988). Shortly before, during and after the maximum of the Earth's last glaciation (30–12 kyrs BP) the climate reverted once again to very dry (up to 50% less precipitation) and 'cold' (mean annual temperatures 4–6°C less, see Runge, 2001) conditions with an open, morphodynamically highly sensitive landscape (i.e., strong erosion and deposition). Larger streams and also smaller rivers showed high riverbed mobility and because of a probable strong seasonality of climate, slope sediments (hillwash) and alluvia were deposited extensively and they also frequently redeposited inside channels as cut and fill structures. Within this open environment isolated forest relicts around and along rivers were a common feature (Runge, 2001) and LSA industries of the Lupembien from approximately 30–12 kyrs BP have been frequently discovered within such sediments (Clist, 1987).

From 12 kyrs BP onwards the climate shifted back again to humid warm conditions ('Kibangien A') which caused a rapid recolonisation of the low latitudes with dense rain forest. Stone cultures with microlithes are known for the 'Tshitolien'

(~12–2,35 yrs BP) within forested or at least woody biomass dominated landscapes with reduced surface morphodynamics. Open savanna environments showed comparable features of LSA industries summarized under the 'Wiltonien'. The 'First Millenium (BC) Crisis' around 3000 yrs BP ('Kibangien B') with an extraordinary strong aridification triggered the shrinkage of forests while savannas started again to expand (Maley, 2002).

3.3 OUTLINE OF THE CENTRAL AFRICAN STUDY AREA

Climatically Central Africa is dominated by the western African monsoon, which supplies seasonal rainfall with the migration of the ITCZ (Figure 2a). Rainfall ranges from 3000 to 1200 mm^{-yr} and occurs during one or two rainy seasons, depending on distance from the equator. This accounts for the evolution of bimodal hydro-climatic regimes across the equatorial regions. Climatic changes during the Late Quaternary in Central Africa were mainly triggered by extraterrestrial forcing (precession cycle; e.g., Gasse *et al.*, 2008) and glacial as well as interglacial boundary conditions (atmosphere-biosphere-cryosphere dynamics) on both hemispheres, which induced global feedbacks and modified the atmospheric (Hadley/Walker-circulation) and oceanic (bipolar see-saw) cycles (Vidal and Arz, 2004). As a consequence, tropical Africa experienced ITCZ and African monsoon belt displacements with rainfall variations and far-reaching impacts across landscapes, rivers, ecosystems and geomorphodynamic processes (Kadomura, 1995; Schneider *et al.*, 1997; Gasse, 2000; Thomas, 2000, 2008; Zabel *et al.*, 2001; Lézine and Cazet, 2005; Weldeab *et al.*, 2007).

Geologically the Congo basin structure results from subsequent tectonic deformation that occurred during terrestrial sedimentation since the Palaeozoic (Figure 2b). It contains layers of clastic sediments that reach between 2000 and 4000 m in thickness (Evrard, 1957; REGIDESO, 1985). The central part of the basin, with seasonally flooded river plains and extended alluvia, is characterized by flat, plateau-like to rolling surfaces ~300–400 m above sea level (m asl). The main fluvial system, the Congo-Lualaba River is 4374 km long and has a catchment area of 3,747,320 km^2. It describes an initially south to north, from Kisangani, with a westerly oriented, bow to curve-like river pattern that crosses the equator twice (Runge, 2007). To the North and partly to the West (Cameroon, Central African Republic—CAR) and to the South (Angola, Shaba) the basin is limited by gentle but extended rises with peneplains (500–1400 m asl). These surfaces are widely covered by deeply weathered lateritic soils over Precambrian basement.

In Cameroon the north-western rise of the Congo basin represents the catchment areas of the Sanaga, Nyong and Ntem Rivers, draining across a peneplain step to the Atlantic Ocean, and those of the Boumba, Dja and Ngoko, tributaries of the Sangha, which drains into the Congo River (Olivry, 1986; Runge, 2007). The Sanaga River is the major river in Cameroon with a catchment area of about 133 000 km^2 and a length of 976 km. From its source on the 'Surface de Meiganga' (Cretaceous, Post-Gondwana) at 1050 m asl it flows southwards. On the 'Inner Plateau' (Eocene, African I) it changes its flow direction to the west along the Sanaga fault which is part of the pan-African Central Cameroon Shear Zone (Segalen, 1967; Toteu *et al.*, 2004). Most of the drainage network in Southern Cameroon is characterized by the pan-African structures of the heterogeneous, generally crystalline basement rocks (Kuete, 1990).

In the East, the basin is abruptly terminated by marked Tertiary graben and rift structures (3000 m asl); and finally, the Western limit in transition to the Atlantic Ocean is formed by an uplifted and again eroded Precambrian orogen (Cahen and Lepersonne, 1948; Cahen *et al.*, 1984; Boulvert, 1996; Runge, 2001).

Figure 1. Location map of Central Africa with study areas mentioned in the text.

The shape of the approximately 1000 km wide central Congo basin is round to oval which earlier gave rise to the hypothesis of a former, enormous, so-called 'Congo Lake' (Cornet, 1894). Subsequent more detailed studies on the sediments within the basin indicated deposition under nonlacustrine, temporarily semi-arid environmental conditions (De Ploey *et al.*, 1968; République du Zaire, 1974). Sediments overlying the Congo Craton and building up this basin are mainly of Carboniferous to Permian or Mesozoic age (Figure 2b). The basin was originally a nearly horizontal surface. Later, it was deepened by epirogenic crustal movements and subsequent deformation while progressively more sediment was deposited over it (Lepersonne, 1978; Petters, 1991). The widespread sandy to clayey 'Lualaba-Lubilash' strata correspond to the Mesozoic South African 'Karoo Sequence' (Veatch, 1935), more recently known as the 'Karoo Supergroup'. In the eastern Congo basin, close to Walikale, glacial deposits such as tillites and dropstones derived from drifting icebergs of the Permo-Carboniferous 'dwyka' glaciation outcrop at the surface (Série de Lukuga, Série de Walikale, Boutakoff, 1948; Runge, 2001).

Deep drillings on the southern limit of the basin, at Samba (2039 m) (République du Zaire, 1974), and the unsuccessful oil exploration site Mbandaka-I (4350 m), provide an indication of the morphology and total sediment thickness of the Congo basin. At Mbandaka, Permian to Carboniferous sediments (Série de Lukuga) are found at 2100 m depth, whereas east of Kisangani these formations crop out. Precambrian schists and quarzitic sandstones occur below 2887 m. The granitic basement of the Congo Craton lies below 4350 m (REGIDESO, 1985).

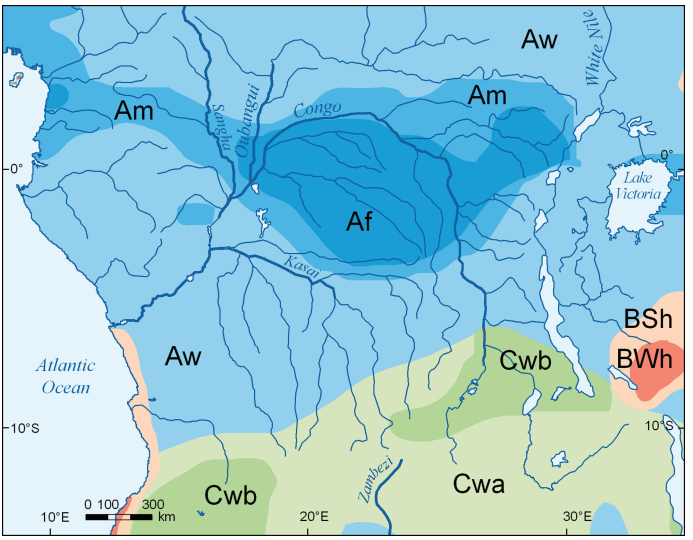

Figure 2a. Central African climate after the Köppen-Geiger climate classification updated by Peel *et al.* (2007).

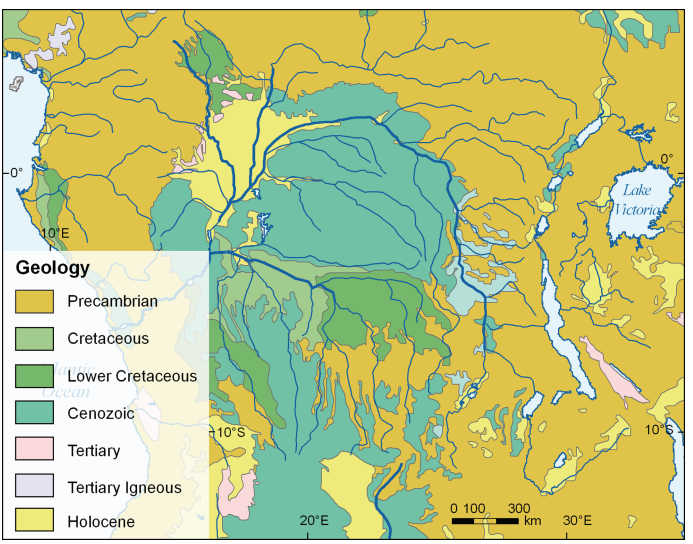

Figure 2b. Major geological units of Central Africa (U.S. Geological Survey, 2002).

The flat to undulating part of the basin in the centre has been covered by rain forest since a period of severe aridification during the LGM when the forest was replaced by savanna vegetation (Runge, 2001). At the surface, Tertiary and Quaternary sediments, clayey and sandy alluvium of fluvial origin predominate and reach a thickness of 90–200 m (Evrard, 1957; REGIDESO, 1985).

The vegetation cover of the wider catchment (Figure 2c), including the large Congo's right bank river Oubangui on the northern edge (Runge and Nguimalet, 2005),

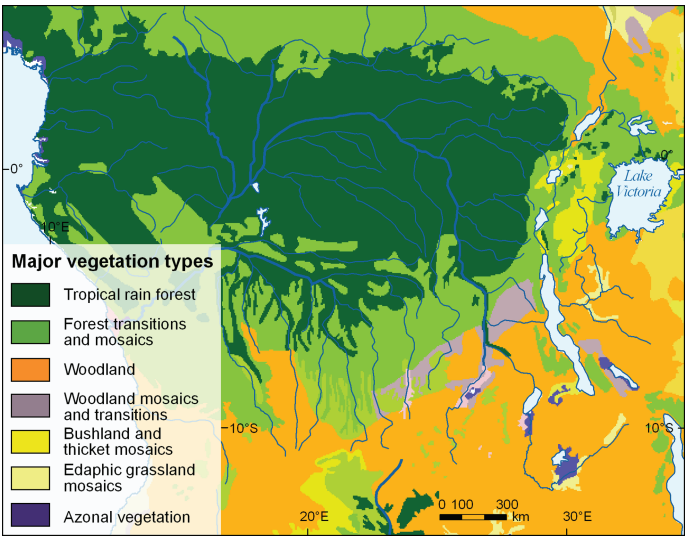

Figure 2c. Central African vegetation map after White (1983).

is dominated in the northern part by an open savanna-woodland mosaic that changes southward to subhumid to humid rain forest with an annual precipitation of 1600–1800 mm in the centre (Figures 2a and 2c), and up to 2400 mm in the eastern Kivu (Sillans, 1958; Bultot, 1971–1977). In the savanna areas bush fires are frequent, however, because of the economic decline in former Zaire, negative migration over the last 30 years has enabled the return of high woody vegetation in the areas that are humid enough (Runge and Neumer, 2000).

3.4 STRATIGRAPHY AND PALAEOENVIRONMENTAL EVIDENCE OF TROPICAL ALLUVIA IN CENTRAL AFRICA

Floodplains with thick alluvia evolve over time and there is growing evidence for that it is most likely that also tropical rivers store sediments for periods of at least 10^4 years (Thomas, 1998; Thomas and Thorp, 2003) or more (Runge *et al.*, 2006), long enough to record major changes in climate before, around and after the LGM, including Holocene environmental shifts. However, for the LGM there are numerous areas with no interpretable records (cf. Ledru *et al.*, 1998; Thomas, 2008). Many parts of the humid tropics in West and Central Africa were significantly drier for several millennia during this period, but became rapidly wetter during the warming at the end of the Pleistocene (Giresse *et al.*, 1994; Maley and Brenac, 1998; Runge, 2001; Gasse, 2005). It is still not known if a Younger Dryas (YD) event again with probably drier and cooler conditions was also recognizable in lower latitudes (Taylor *et al.*, 1993; Lezine and Cazet, 2005). For both of the LGM and the YD, which must have significantly modified the entire geoecosystem of an area, it is not clear to what extent they climatically influenced the cultural complexity of the palaeolithic people. The picture becomes slightly clearer looking at the coincidence in timing between further aridification that reduced the rain forest's extension (Maley, 2002) starting in Central Africa around 3000 yrs ago ('First Millenium Crisis'), and perhaps triggering settlement expansion of farming and ceramic manufacturing populations (Schwartz, 1992).

3.4.1 Cameroon

Investigations on alluvial sedimentary basins of equatorial tropical fluvial systems have been undertaken in southern Cameroon during 2004–2008 (Figure 1). Along selected meandering and anabranching to anastomosing reaches of major southwestern, into the Gulf of Guinea (Ntem, Nyong and Sanaga) and southeastern, into the Congo basin (Boumba, Dja and Ngoko) draining rivers, suitable alluvial sediment-archives for palaeoenvironmental research could be recovered. Among geomorphological investigations and topographic cross sections, 160 corings reaching maximum depths of 550 cm were sampled on river benches, levees, cut-off and periodical branches, islands and terraces as well as in seasonal inundated floodplains and backswamps. Corresponding sedimentary profiles and transects recovered multilayered, sandy to clayey alluvia having sedimentary form-units and palaeosols. Numerous radiocarbon (AMS) dated samples (Table 1) from buried organic layers and macro-remains embedded in these units yielded Middle-Pleniglacial to recent ages (^{14}C-ages around 48 to 0.2 kyrs BP) including LGM and Holocene records.

Alternating form-units (sandy, silty and clayey layers, palaeosurfaces and palaeosols) display fluctuations in the morphological response of the fluvial systems to climatic variability and other extrinsic and intrinsic triggers. Although the sedimentary record varies among the studied river reaches, buried organic sediment layers were found in almost all alluvial basins of examined southern Cameroonian rivers.

Field work was done across anabranching river reaches and inside an anastomosing section of the Ntem River near Ma'an in SW Cameroon (Runge *et al.*, 2006; Sangen, 2007, 2008, 2009, 2011). Here a multi-channelled fluvial system composed of several seasonal river branches, stillwater locations, rapids, islands and seasonally inundated swamps has been generated by neotectonic (Eisenberg, 2007, 2008, 2009) and fluvial-morphological activity. At some sites two terrace levels (dry and rainy season) were identified. Most profiles show very similar stratigraphic features. Using these sedimentary records and studies from additional anabranching reaches on the Nyong and Sanaga Rivers, a classification of five sedimentary units was made.

Unit 1: Middle Pleniglacial—Oxygen-Isotope-Stage 3—(OIS 3 ~58–27 kyrs BP)

Predominately Precambrian granitic or gneissic basement rock is covered by saprolite of alternating thickness (10–200 cm). At sites L08 and L14 of the anastomosing Ntem fluvial system (cf. Sangen, 2012: Fig. 24), in some distance of the recent river channels, basement is covered by coarse-grained sandy deposits interspersed with thin buried organic layers (10–20 cm) including high debris and macro-remain content. These currently oldest-known sedimentary units, found in around 400 cm depth, yielded Late Pleistocene (Middle Pleniglacial) ^{14}C-ages of 48 and 45 kyrs BP and were allocated to palaeochannels of a former aggradational braiding Ntem river system, which prevailed during a cool but moist semi-arid to sub-humid phase in a generally less forested environment (Maley, 1993, 1996, 2001). Sediments of similar characteristics and age (43 kyrs BP in core C28) were found in the upper catchment of the Nyong River near Akonolinga (Figure 3). These Late Pleistocene sediments evidence landscape destabilisation and stronger erosion by fluvial systems. The rivers delivered occasional flushes of sandy deposits and were associated with frequent channel migrations and floodplain reorganisations.

Unit 2: Late Middle to Upper Pleniglacial (OIS 2 ~30–12 kyrs BP)

Additional fine-grained sandy layers (~80% sand) locally intermixed with sandy buried organic layers (20–100 cm) and macro-remains (wood, leaves, etc.) occur at various

Table 1. Selected radiocarbon ^{14}C data and $\delta^{13}C$ values of alluvia from Cameroon, 2005–2007.

Core no.	Location	Depth (cm)	Organic material	^{14}C (AMS) BP	Calendric age (cal BP), (2σ 68%)	$\delta^{13}C$ (‰)	Lab. no.
Sanaga							
C01 (3°N, 10°E)	Dizangué/Lac Ossa	200–218	Organic sediment	128.52 ± 0.90 pMC	Recent	–19.6	LTL2104A
C06	Dizangué/Lac Ossa	360–365	Organic sediment	9321 ± 90	10,515 ± 132	–27.2	LTL2106A
C13 (5°N, 13°E)	Bélabo	390–400	Organic sediment	16,117 ± 200	19,294 ± 325	–28.2	LTL2107A
C14	Bélabo	335–340	Organic sediment	1766 ± 50	1693 ± 72	–29.7	LTL2108A
C15	Bélabo	381	Macro-rest	1196 ± 45	1130 ± 58	–28.7	LTL2109A
C19 (5°N, 13°E)	Ngoktélé	240–260	Macro-rest	14 ± 100	108 ± 125	–24.2	LTL2110A
C19 (5°N, 13°E)	Sakoudi	213	Organic sediment	3894 ± 50	4327 ± 72	–29.2	LTL2111A
Nyong							
B01 (3°N, 11°E)	Njock	200–225	Organic sediment	2134 ± 41	2161 ± 100	–27.3	Erl-8941
B03	Makak	160–180	Macro-rest	–2105 ± 34	Recent	–29.8	Erl-8944
		235–245	Macro-rest	–4116 ± 31	Recent	–29.4	Erl-8946
B05	Lipombe II	100–120	Macro-rest	707 ± 38	637 ± 48	–28.2	Erl-8943
B06 (3°N, 10°E)	Donenda	180–200	Macro-rest	4093 ± 47	4656 ± 117	–29.7	Erl-8945
B07	Dehane	280–300	Macro-rest	400 ± 40	428 ± 72	–28.7	Erl-8942
C22 (4°N, 13°E)	Benana	255–265	Macro-rest	1946 ± 50	1902 ± 56	–27.7	LTL2112A
C23 (3°N, 12°E)	Akonolinga	150–160	Organic sediment	28,358 ± 300	32,788 ± 411	–20.1	LTL2113A
C28	Akonolinga	420	Organic sediment	42,940 ± 1500	46,680 ± 1817	–19.6	LTL2114A
Exposure	Akonolinga	230	Organic sediment	902 ± 45	832 ± 61	–24.2	LTL2117A
C30 (3°N, 12°E)	Ayos	280	Macro-rest	724 ± 45	679 ± 28	–25.8	LTL2115A
Exposure	Ayos	180	Organic sediment	1508 ± 50	1419 ± 65	–18.0	LTL2116A
C31 (3°N, 11°E)	Mengba	260–280	Organic sediment	13,357 ± 60	16,295 ± 418	–	LTL2118A

Ntem interior delta							
L02	Meyo Ntem	100–120	Macro-rest	1066 ± 53	995 ± 51	–27.0	Erl-8249
		160–180	Macro-rest	1104 ± 52	1024 ± 53	–29.2	Erl-8250
C02	Nyabibak	380–400	Macro-rest	5379 ± 51	6162 ± 95	–29.0	Erl-9573
L05	Meyo Ntem	220–240	Macro-rest	908 ± 50	835 ± 61	–29.4	Erl-8251
L08	Meyo Ntem	300–320	Macro-rest	45,596 ± 4899	50,851 ± 5663	–31.4	Erl-8252
Test	Aloum II	78–88	Organic sediment	8402 ± 67	9408 ± 75	–30.6	Erl-9574
C11	Aloum II	120–140	Macro-rest	6979 ± 58	7822 ± 76	–30.1	Erl-9575
C13	Meyos	120–140	Macro-rest	14,020 ± 106	17,271 ± 229	–28.1	Erl-9567
		140–160	Macro-rest	17,570 ± 141	20,981 ± 336	–26.5	Erl-9568
		160–180	Macro-rest	18,719 ± 161	22,389 ± 377	–26.5	Erl-9569
		180–200	Organic sediment	17,197 ± 132	20,647 ± 322	–28.8	Erl-9570
		250–263	Organic sediment	18,372 ± 164	22,011 ± 341	–27.6	Erl-9571
L14	Abong	340–360	Macro-rest	48,230 ± 6411	53,096 ± 6876	–29.6	Erl-8254
L17	Meyos	280–300	Macro-rest	14,263 ± 126	17,467 ± 265	–27.3	Erl-8253
		280–300	Macro-rest	13,690 ± 100	16,781 ± 251	–24.2	LTL2103A
L18	Nyabessan	140–160	Macro-rest	587 ± 64	596 ± 46	–29.1	Erl-8270
		200–220	Macro-rest	2337 ± 55	2389 ± 73	–31.9	Erl-8271
L19	Nyabessan	320–340	Macro-rest	2189 ± 52	2216 ± 78	–29.5	Erl-8272
C20	Nyabessan	430–440	Organic sediment	2479 ± 43	2571 ± 106	–28.8	Erl-9576
L22	Nyabessan	140–160	Macro-rest	3894 ± 57	4324 ± 79	–28.1	Erl-8273
L24	Nnémeyong	80–100	Macro-rest	441 ± 46	482 ± 39	–30.6	Erl-8266
		120–140	Macro-rest	671 ± 52	623 ± 46	–28.7	Erl-8267
L25	Nnémeyong	160–180	Macro-rest	21,908 ± 302	26,239 ± 583	–27.0	Erl-8268
		220–240	Macro-rest	22,398 ± 316	26,978 ± 631	–29.1	Erl-8269
L27	Akom	100–120	Macro-rest	443 ± 57	453 ± 72	–26.4	Erl-8261
		160–180	Macro-rest	427 ± 52	440 ± 74	–27.6	Erl-8262

(*Continued*)

Table 1. *Continued.*

Core no.	Location	Depth (cm)	Organic material	^{14}C (AMS) BP	Calendric age (cal BP), (2σ 68%)	δ^{13}C (‰)	Lab. no.
C27	Nyabessan	270–280	Organic sediment	3829 ± 46	4257 ± 87	–28.5	Erl-9577
L30	Tom	140–160	Macro-rest	1381 ± 49	1309 ± 30	–28.2	Erl-8260
L32	Nkongmeyos	60–80	Charcoal	217 ± 46	196 ± 103	–28.0	Erl-8255
C32	Nkongmeyos	145–150	Organic sediment	954 ± 39	865 ± 50	–28.9	Erl-9572
L34	Nkongmeyos	100–120	Macro-rest	435 ± 51	448 ± 70	–27.4	Erl-8256
L36	Aya Amang	140–160	Macro-rest	4341 ± 60	4945 ± 75	–27.2	Erl-8263
L37	Aya Amang	320–340	Macro-rest	30,675 ± 770	34,962 ± 702	–30.8	Erl-8264
L38	Aya Amang	220–240	Macro-rest	5306 ± 64	6096 ± 85	–31.4	Erl-8265
L40	Anguiridjang	360–380	Macro-rest	2339 ± 52	2393 ± 65	–27.9	Erl-8259
L46	Nkongmeyos	80–100	Macro-rest	8291 ± 89	9277 ± 127	–27.5	Erl-8599
		120–140	Macro-rest	10,871 ± 99	12,846 ± 101	–28.3	Erl-8258
L49	Nkongmeyos	180–200	Organic sediment	10,775 ± 144	12,744 ± 155	–30.1	Erl-8257
					CalPal (online)		

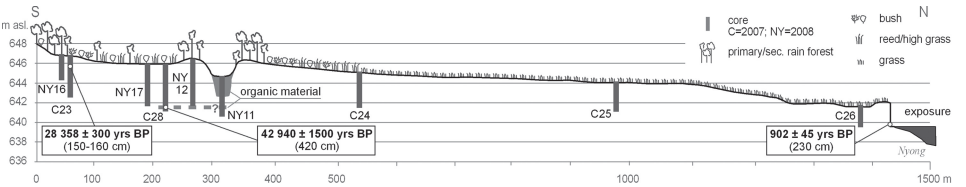

Figure 3. Catena along a Nyong valley section close to Akonolinga.

depths (1–3 m, e.g., samples C13, L17, L25, L37, Table 1) over basement and saprolite. The latter are well preserved when under the water table (dry season) and like the oldest buried organic sedimentary units characterized by low acidic pH (2–4) and high C/N-ratios at their most concentrated points (centre). They are interpreted as swampy palaeosurfaces and palaeosols (gyttia) which were formed during the Middle (30 kyrs BP) and Upper Pleniglacial (22–14 kyrs BP).

After more humid conditions at c. 27 kyrs BP, first cool and sub-humid (Léopoldvillien) and afterwards cool and arid (~2–5°C temperature decrease and ~50% less rainfall) conditions of the LGM prevailed. Subsequent to a period of enhanced run-off with frequent floods, floodplain overbank deposition and swamp formation as well as cut and fill episodes during the Njilien, the fluvial system responded to the LGM environmental conditions with modified fluvial-morphological processes, marked by major decline in run-off (erratic and inhibited) and minimal sedimentation (sandy sediments with minor organic matter and macro-remains). Under hypothermal ('displuvial', Giresse *et al.*, 1982) hydro-climatic conditions probably severe river-bed erosion and avulsion emerged, also intensified by major rain forest fragmentation (Maley, 1991, 2001). Summing up, sedimentary unit 2 hints to a new transformation across the southern Cameroonian fluvial systems, which were associated with a channel shift towards the NE and swamp formation in the SW.

Unit 3: Early to Middle Holocene (OIS 1, 12–4 kyrs BP)

An overlying unit consists of sandy to silty clay (>50% clay) generally fining upward and derived from obviously progradational fluvial systems (e.g., lower Nyong, Ntem interior delta). Reduction processes in the lower and oxidation processes in the upper part of this unit indicate seasonal groundwater fluctuation. Often reduction and oxidation zones are separated by a thin concentrated iron layer.

Maxima in iron content mark a stratigraphical boundary between this and lower sedimentary units. Several ^{14}C-dates between 8 and 4 kyrs BP probably allocate it to the Holocene (Kibangien A), especially the African Humid Period (AHP, maximum ~9–6 kyrs BP; De Menocal *et al.*, 2000) and Middle Holocene (5–4 kyrs BP). The AHP was warm and humid with short arid interruptions and marked by a major increase in rainfall and tropical rain forest expansion to its maximum (Maley, 2001; Leal, 2004). Especially the onset of the AHP, prevailing in concert with the northern hemispheric Bølling-Allerød, was associated with abundant sedimentation, lateral and vertical accretion, cut and fill sequences and incision of smaller channels into former/older floodplains (Thomas, 2000; Lézine and Cazet, 2005; Weldeab *et al.*, 2005). From ~5 kyrs BP seasonal climatic conditions (pronounced rainy and dry seasons) returned with stabilization of river banks and terraces, seasonal floods in combination with overbank deposition, avulsion and crevasse splay processes. The Early and Middle Holocene sedimentary units can be found widespread in the alluvial record of Cameroonian rivers.

Across the Nyong (Akonolinga, Donenda, Mengba) and Sanaga (Bélabo, Mbargué, Sakoudi) Rivers they locally display profound thicknesses (2–4 m) and high clay fraction (80–90%) at sites in certain distance from the active channels. In the Ntem anastomosing section they are less profound and restricted to still water locations inside the alluvial plain. While oldest unit 3 sediments thus manifest enhanced fluvial activity and widespread floodplain reworking in concert with Pleistocene-Holocene transition climate reversal, younger Holocene alluvia either indicate the consolidation of fluvial environments.

Unit 4: Late Holocene (4–2.5 kyrs BP)

In western equatorial Africa the Holocene Optimum was followed by another arid phase around 4–2.5 kyrs BP which modified seasonality, caused flood peaks and mean discharges to decline and led to the deposition of sandier sediments; it was repeatedly associated with rain forest fragmentation (Maley, 1992, 2002; Jolly *et al.*, 1998; Vincens *et al.*, 1998; Marchant and Hooghiemstra, 2004; Nguetsop *et al.*, 2004; Giresse *et al.*, 2005; Marret *et al.*, 2006; Runge *et al.*, 2006). Related sedimentary profiles documenting these Late Holocene modifications in the sedimentary record are common (e.g., Boumba, Ntem, Nyong and Sanaga alluvia; Sangen, 2009, 2011; Sangen *et al.*, 2010). Sedimentary profiles show a marked increase in sandy sediments (80–90%) for this period and at some level (around 1 m depth) an abrupt switch-back to fining-upward sequences reflecting a return to progradational processes. One location in the interior delta of the Ntem River (Nyabessan, Figure 4) clearly substantiates major impacts on palaeoenvironmental conditions during this period.

Here clayey (palustrine) sediments, yielding maximum ages of 4 kyrs BP, are in the upper 2 m interfused with sandy layers, indicating alternating turbulent and still water conditions (Figures 5 and 6). This is circumstantiated by archaeobotanical and palynological studies, which document that after 2820 ± 70 yrs BP drier conditions (longer seasonality) prevailed connected with a loss of primary and swampy species in the vegetation composition (Eggert *et al.*, 2006; Höhn *et al.*, 2008; Ngomanda *et al.*, 2009). This period has been referred to as 'First Millennium BC Crisis'.

Unit 5: Late Holocene to recent (since 2.5 kyrs BP)

Along the presently active channels of the Ntem, Nyong and Sanaga Rivers, the most recent sedimentary unit has been deposited (see Table 2). Profound (2–4 m) layers of coarse, medium and fine-grained sandy deposits have accumulated and yielded Late Holocene to recent ^{14}C ages (~2.5–0.2 kyrs BP). Today the rivers form aggradational sandy bed-load systems with enhanced overbank fine-grained sediment deposited

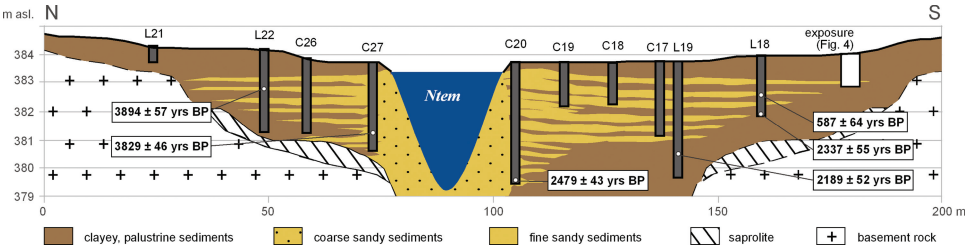

Figure 4. Transect across the Ntem valley southwest of Nyabessan in the Ntem interior delta.

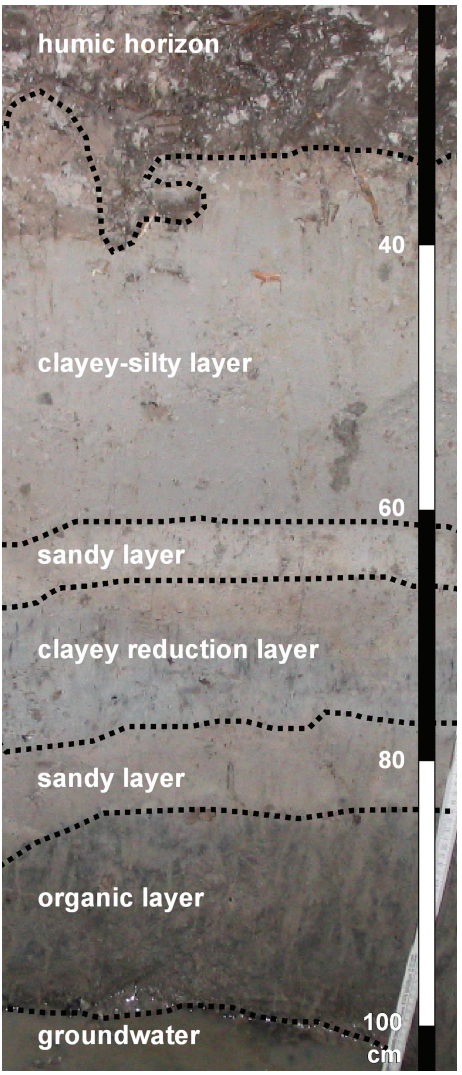

Figure 5. Exposure site at the southern end of the Nyabessan transect (Figure 3) showing a dark organic layer at the bottom of the profile (Photo: M. Sangen, 2006).

during flooding in the rainy season. Sandy river-bed sediments have been extensively deposited across the middle and lower reaches. Increasing human impact in the younger history (shifting cultivation, commercial logging, slash and burning) and rain forest clearing have increased erosion processes and sandy sediment supply so that across many river sections braid bars and sand banks have formed. Similar conditions have been observed on the Boumba, Dja and Ngoko Rivers in SE Cameroon where rivers are characterized by high (2–3 m) and stable riverbanks with adjacent seasonally flooded riparian zones.

Another alluvial palaeoenvironmental archive has been discovered in the Ngoko valley near Moloundou (~2°N, 15°E) at the border to the D.R. Congo. A cut-off channel

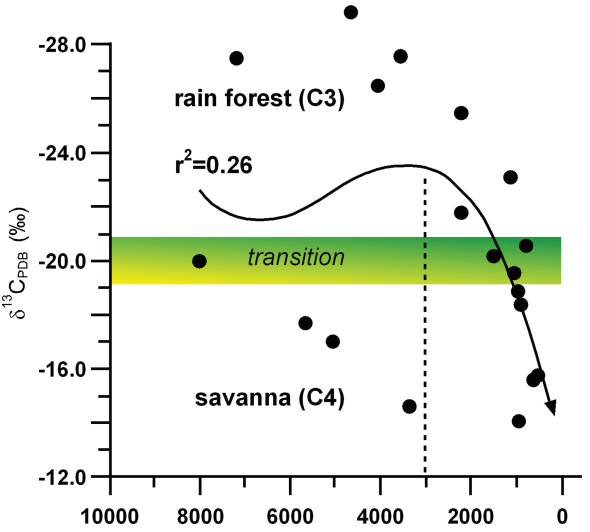

Figure 6. Polynomial regression (cubic fit) indicating a trend of aridification and savannization in eastern CAR since 3 kyrs BP (see Runge, 2002).

of the Ngoko (neck cut-off) has been transformed into a lake (Lac Mokounounou). At the inflow and outflow of this abandoned channel suitable alluvial sediments have been accumulated. At the outflow profound stratified sandy to clayey fossil organic alluvia were sampled up to 550 cm depth containing buried macro-remains (i.e., *Raphia* tree at the base of one coring). ^{14}C data from artribute this sedimentary archive to maximum ages around 1300 yrs. BP (Sangen *et al.*, 2010).

$\delta^{13}C$-values corresponding to the dated samples of the Ntem interior delta (–31.4 to –26.4‰) are evidence that at the particular drilling sites gallery rain forest ecosystems have prevailed during the corresponding time period (rain forest refuge theory, e.g., Hamilton, 1976, 1982; Littmann, 1987, 1988; Maley, 1989; Liedtke, 1990; Colyn *et al.*, 1991; Leziné and Cazet, 2005). The sampled macrorests, but also organic sediments all indicate (at least) gallery forests across the Ntem's multi-channelled fluvial system, which were able to persist in this fluvial habitat ('fluvial refuge'), even during arid periods. At Meyos (C13, L17) a swampy environment emerged during the LGM and at Anguiridjang (L37) similar conditions prevailed during the Njilien. From both sites suitable sediments for palaeobotanical studies were sampled in collaboration with botanists from Frankfurt University (K. Neumann) in 2005.

For the landscape history of the upper catchment area of the Nyong (Akonolinga and Ayos) a more or less transitional rain forest-savanna environment with $\delta^{13}C$-values around –20‰ is attested. Oldest ^{14}C ages (~43, 32 and 28 kyrs BP) found at this site correspond to $\delta^{13}C$-values of –19.6, –18.1 and –20.1‰, respectively. The $\delta^{13}C$ transition between forest and savanna can be explained on the one hand, as a mixing of pure C4 and C3 vegetation, resulting from frequent savanna-rain forest vegetation changes or, on the other hand, it could display relatively open savanna-woodland ecosystems. However, these interpretations depend on the analyzed macro-remains (buried fossil organic remains) and so misleading conclusions on actual former vegetation composition cannot be excluded.

Table 2. Radiocarbon ^{14}C data and $\delta^{13}C$ values of the Mbomou plateau samples (Runge, 1998, 2002).

Core/ sample no.	Depth (cm)	Material	^{14}C (AMS) BP	Calendric age (cal BP), (2σ, 95%)	$\delta^{13}C$ (‰)	Lab. no.
R026–01	0–20				–17	Beta-103533
R027–02a	0–10				–16.3	Beta-103534
R027–02b	10–20				–17.9	Beta-103535
R027–02c	20–30				–21.3	Beta-103536
R029–03a	0–25				–17.4	Beta-103537
R029–03c	50–75				–25.5	Beta-103538
R029–03e	100–125	Organic sediment	2220 ± 50 BP	BC 390 –150	–25.5	Beta-103539
R029–03g	150–175				–26.9	Beta-103540
R029–03i	200–225	Organic sediment	3570 ± 50 BP	BC 2025–1755	–27.6	Beta-103541
R029–03k	250–275				–29.9	Beta-103542
R029–03l	275–300				–30.3	Beta-103543
R029–03p	375–400	Organic sediment	7150 ± 50 BP	BC 6035–5935	–27.5	Beta-103544
R040–09a	0–25				–16.4	Beta-103545
R040–09d	75–100	Organic sediment	890 ± 40 BP	AD 1035–1245	–18.4	Beta-103546
R040–09f	125–150				–22.3	Beta-103547
R040–09h	175–200	Organic sediment	2210 ± 50 BP	BC 385–115	–21.8	Beta-103548
R045–11a	0–10				–15.7	Beta-103549
R045–11e	60–75				–21	Beta-103550
R045–11g	100–125	Organic sediment	950 ± 40 BP	AD 1010–1195	–14.1	Beta-103551
R045–11k	175–200	Organic sediment	1490 ± 50 BP	AD 450–655	–20.2	Beta-103552
R047–13a	0–20				–19.4	Beta-103553
R047–13b	180–200	Organic sediment	940 ± 50 BP	AD 1005–1220	–18.9	Beta-103554
R058–17a	0–20				–15.8	Beta-106884
R058–17g	110–125	Organic sediment	6200 ± 30 BP	AD 1220–1285	–15.6	Beta-106885
R058–17j	175–200	Organic sediment	1030 ± 30 BP	AD 885–1000	–19.6	Beta-106886
R064–21a	0–20				–18.7	Beta-104441
R064–21d	40–70				–21.1	Beta-104442
R064–21f	90–100	Organic sediment	3360 ± 70 BP	BC 1860–1845	–14.6	Beta-104458
R065–23a	0–20				–16	Beta-104443
R065–23c	30–40				–18.4	Beta-104444
R065–23f	200–235	Organic sediment	540 ± 40 BP	AD 1315–1345	–15.7	Beta-104459

(*Continued*)

Table 2. *Continued.*

Core/ sample no.	Depth (cm)	Material	^{14}C (AMS) BP	Calendric age (cal BP), (2σ, 95%)	δ^{13}C (‰)	Lab. no.
R067–24a	0–25				–18.2	Beta-104445
R067–24d	75–80				–15.5	Beta-104446
R067–24f	140–165				–15	Beta-104447
R067–24h	190–215	Organic sediment	1130 ± 50 BP	AD 790–1010	–13.1	Beta-104460
R068–26a	0–10				–18.6	Beta-104448
R068–26c	50–75				–17	Beta-104449
R068–26f	90				–16.8	Beta-104450
R068–26h	110–125	Organic sediment	780 ± 80 BP	AD 1045–1105	–20.6	Beta-104461
R072–28a	0–10				–16.3	Beta-104451
R072–28f	100–125				–24.7	Beta-104452
R072–28i	175–200	Organic sediment	5660 ± 70 BP	BC 4690–4350	–17.7	Beta-104462
R074–30a	0–25				–16.6	Beta-104453
R074–30c	50–75				–16.2	Beta-104454
R074–30f	100–125				–21.7	Beta-104455
R074–30h	175–200	Organic sediment	4050 ± 80 BP	BC 2875–2350	–26.5	Beta-104463
R077–32a	0–25				–15.5	Beta-104456
R077–32f	100–125				–19.5	Beta-104457
R077–32i	175–200	Organic sediment	8010 ± 100 BP	BC 7245–6585	–20	Beta-104464
R111–35a	0–20				–13.7	Beta-106887
R111–35e	75–90				–14.1	Beta-106888
R111–35 j	175–200	Organic sediment	4580 ± 40 BP	BC 3375–3300	–29.2	Beta-106889

3.4.2 Central African Republic (CAR)

3.4.2.1 Mbari valley and Mbomou plateau

The Mbomou plateau with its main NE–SW leading drainage axis, the Mbari River—that is approx. 450 km long and draining a catchment of 23,600 km^2 by a 2–3 km wide alluvial plain—forms a vast amphibolitic planation surface complex, almost 75,000 km^2 in size, close to the town of Bangassou on the border to the D.R. Congo (Figure 1). The slightly southerly inclined plateau with an elevation between 500 and 700 m asl forms a part of the north-equator swell (Asande rise) between the Congo basin in the south and the Lake Chad depression in the northwest.

Stratigraphic survey on Mbari's alluvial layers was carried out between 1995–1996 by applying stable carbon isotope ratio analysis (δ^{13}C) on palaeosols for detecting Holocene and recent shifts of the environment causing modified river morphodynamics expressed by a varying composition of river bank vegetation (C3/C4 plants, see

Mariotti, 1991). Drillings and cores of up to 4 metres in the alluvial zone of this river and ^{14}C (AMS) radiocarbon data proved the existence of early Holocene sediments reaching ages of up to 8 kyrs BP. This underlines that even geologically old planation surfaces possess sedimentological archives containing information about the Holocene landscape history (or even older, compare section on Cameroon).

Many of the surveyed profiles and cores showed a shift of the $\delta^{13}C$ towards smaller (< –20‰) forest indicating values with increasing depth. A few drills evidenced a shift towards a C3 dominated forest at first (between 2–3 kyrs BP) that is reversed again with increasing depth towards a C4 environment (~5 kyrs) which is characterized by grass species (see Table 2).

At the surface, the grass-grown alluvial soils show a brownish black to grayish yellow and at a greater depth also a dull orange to reddish brown colour, indicating the influence of alternating high and low groundwater level. In the majority of profiles, texture composition is dominated by clay (>60%). Separated sandy layers at greater soil depth indicate episodically occurring fluvial accumulations of the Mbari River. Silt, with an amount of 10–20% on average, is of minor importance within the alluvial sediment sequences. Values of pH, measured in H_2O(dest.) and KCl, range from 4.0 to 5.5. The content of soil organic carbon is comparably high inside this floodplain and reaches values of about 10–20%. Profile sections with a higher content of carbon indicate periods of soil formation when the input of fluvial sediments on the sites close to the active Mbari riverbed was reduced. Afterwards, these horizons have been buried by renewed sedimentation of the Mbari River, initiated by a more seasonal run-off regime (e.g., alternating dry and rainy season).

In profile R111 (Runge, 2002) the regular decrease of organic carbon with increasing depth indicated a 'normal' autochtonous soil development. $\delta^{13}C$ values indicate that a savanna grassland expanded into forest at least up to 4580 yrs BP. In profile R058 there is evidence for a buried organic horizon (i.e., palaeosol) by 12% of organic carbon, over 65% of clay and a Munsell colour of 5YR 6/2 (Runge, 2002). A savanna grassland environment existed at least since 620 yrs BP. $\delta^{13}C$ decreases with increasing depth, reaching a radiocarbon age of 1030 yrs BP at 200 cm. The $\delta^{13}C$ value may correspond to a mixed value of C3 and C4 plants, supporting the assumption of a forest regression before and since 1 kyr. An up to 4 m deep profile (R029, Runge, 2002) indicated a striking dominance of forest during the Holocene at least since 7150 yrs BP. In the upper part of the profile, a trend for forest regression since 2250 yrs BP was recognizable when the occurrence of savannas started to be more dominant than before. Also, the profile R067 shows by striking variations in texture (isolated and repeated layers of sand and silt) and in organic matter that obviously environmental conditions changed significantly in the Mbari valley. A savanna-forest mosaic bordered the banks of the Mbari around 780 yrs BP; then the environment shifted to a savanna environment, whereas in more recent times an increasing number of C3 dicotyledones (e.g., shrubs and trees) seems to have grown in the alluvial plain again. A more dynamic shift from savanna to forest and vice versa is evidenced by profile R072 (Runge, 2002) where an open savanna grassland existed probably between 6 and 5 kyrs; it was consequently around 3 kyrs replaced by a forest that changed again in more recent times into a more open grass and savanna woodland environment. One of the oldest profiles (R077, Runge, 2002) covers the Holocene by a radiocarbon age of up to at least 8010 yrs BP found at a soil depth of 200 cm. A savanna woodland or open forest vegetation was replaced by a savanna grassland at mid-Holocene times (5045 yrs BP). Since then, a slight trend to a further increase in savanna vegetation is recognizable by the examination of $\delta^{13}C$ data of the sediments.

It is quite clear that for all the studied soils and sediments, it has to be questioned carefully if these former alluvial deposits are completely uncontaminated,

as bioturbation, especially by termites, could have played a role (Runge, 2000). Summarizing the stratigraphic and carbon isotope features of the coring sites within the Mbari alluvial plain, it can be stated that several shorter climatic and hydrologic modifications during the Holocene, especially since 3 kyrs, have initiated a change in the vegetation cover on the Mbomou plateau and equally of the Mbari's discharge. It seems that the changing river geometry of the Mbari has obviously never resulted in a lasting, uniform dominance of forest or savanna. A more or less steady alternation of savanna-like and forest-like $\delta^{13}C$ environments around a transitional limit of –20‰ is recognizable (Figure 6). Again the $\delta^{13}C$ transition between forest and savanna can be explained on the one hand, as a mixing of pure C4 and C3 vegetation, resulting from frequent savanna-forest vegetation changes, or, on the other hand, it could be an indication for a 'static', relatively open savanna-woodland record. In conclusion, this could be interpreted in a way that the present 'rain forest island' at Bangassou surrounded by savanna grasslands and savanna woodlands already existed in a comparable way during the Holocene. An 'oscillating' vegetation mosaic of forest and savanna over time is most likely. This was caused by climatic variations resulting in a reduction or an increase of available moisture. Especially for the more recent time since 3 kyrs, there is an increasing human influence recognizable on the vegetation mosaic from bushfires and land use (Runge, 2002).

The comparison of ^{14}C (AMS) radiocarbon-dated samples with the corresponding $\delta^{13}C$ values shows a distribution pattern that marks the climatically and anthropogenically induced changes between forest and savanna environments on the northern fringe of the Congo basin. Figure 5 summarizes by a statistical approach an interpretation of the available 19 AMS data (Table 2) of organic alluvial sediments in relation to the changing $\delta^{13}C$ ratios (standard deviation of $\delta^{13}C$ samples = 4.683; standard error = 1.074). Applying a cubic fit (polynomial regression of degree 3 [$r^2 = 0.26$]) on the data, it can be stated that the aridification and savannization trends clearly developed since 3 kyrs, whereas somewhat earlier, there had been also slightly drier environmental conditions (Figure 6).

The derived indirect signal of climate and vegetation dynamics from alluvial sediments was compared with the palaeoclimatic proxy signal of Lake Chad (Maley, 1981; Servant, 1983; Pouyaud and Colombani, 1989; Boulvert, 1996). Correlations can be found between the high lake level of Lake Chad around 3.5 kyrs and the maximum of forest extent on the Mbomou plateau at around 3 kyrs, related to more humid climatic conditions. Another indication is the high lake level of Lake Chad during a wet period in the Sahel at around 8.5 kyrs. It may correspond with an increased forest extension on the Mbomou plateau that was shifted temporarily and spatially at around 7.5–7 kyrs. At 6.5 kyrs, the water level of Lake Chad reached another maximum. There was no evidence for such a phase within the alluvial record. Instead an increased period of aridification with an extension of savanna ecosystems took place on the Mbomou plateau at around 5 kyrs. This corresponds with a gentle lower lake level of Lake Chad indicating a drier climate at the same time. From ~1 kyr to more recent times, savanna vegetation on the Mbomou plateau has been increasing, maybe conditioned by the growing influence of humans. Lake Chad, besides short interruptions, is at the same time slowly drying out.

3.4.2.2 Mbaéré valley and Gadzi-Carnot plateau

The Mbaéré River drains the sandstone plateau of Gadzi-Carnot, which slopes SSE with an average incline of just 1.6‰ for 272 km towards the Congo basin (Figure 1). The Mbaéré covers a floodplain of up to 5 km wide in this sector which is covered by a dense flood forest. Similar to the Mbari valley in the eastern part of CAR, drilling

holes to just 2.2 m across the vast alluvial Mbaéré valley yielded several ^{14}C (AMS) radiocarbon dates of Early Holocene age.

The radiocarbon samples from the Mbaéré valley at depths less than 100 cm show recent to sub-recent ages (e.g., 236 ± 49 yrs BP, Table 3). This obviously refers from different sampling locations in the middle course section of the Mbaéré between 425 m and 450 m asl as well as the varying spatial arrangement in the transverse valley profile. A comparison of the data reveals that older ages do not arise from sediments at greater depths. Samples dated to ^{14}C-ages between 1450 ± 40 yrs BP and 6921 ± 71 yrs BP exist at depths of 100 to 120 cm. The sites located closest to the river bank with recent lateral morphodynamic processes to being the highest within the valley cannot be excluded as potential landscape archives of older material. At a terrace with Holocene sediments evidenced by charcoal resulting in radiocarbon ages ranging from

Table 3. Radiocarbon ^{14}C data and $\delta^{13}C$ values of the Mbaéré samples, 2004–2005 and 2006.

Core/ sample no.	Depth (cm)	Material	^{14}C (AMS) BP	Calendric age (cal BP), (2σ, 95%)	$\delta^{13}C$ (‰)	Lab. no.
Mbaéré samples 2004–2005						
M1	100–120	Organic sediment	1733 ± 56	BC 5924–5673	–29.6	Erl-8221
M2	60–80	Organic sediment	Recent	–	–29.6	Erl-8222
	180–200	Organic sediment	3323 ± 64	BC 1748–1489	–30.1	Erl-8223
B2	60–80	Organic sediment	Recent	–	–29.0	Erl-8220
K4	18–43	Macro-rest	236 ± 49	AD 1615–1694	–28.5	Erl-8214
	144	Charcoal	6921 ± 71	BC 5924–5673	–30.4	Erl-8213
Q1	100–120	Organic sediment	4011 ± 59	BC 2698–2399	–27.1	Erl-8219
N2	100–120	Organic sediment	1450 ± 40	AD 540–660	–24.9	Beta-201296
Mbaéré samples 2006						
Ba9	60–80	Charcoal	302 ± 35	AD 1483–1604	–26.3	Erl-10353
	160–180	Macro-rest	1176 ± 39	AD 770–906	–30	Erl-10354
Kp1	120–140	Macro-rest	197 ± 37	AD 1726–1813	–26.7	Erl-10357
	160–180	Macro-rest	176 ± 39	AD 1719–1818	–27.5	Erl-10358
	200–220	Charcoal	172 ± 36	AD 1719–1818	–28.6	Erl-10359
Kp5	100–120	Macro-rest	86 ± 36	AD 1804–1935	–29.7	Erl-10355
	180–200	Macro-rest	2396 ± 40	BC 556–392	–26.3	Erl-10356
Ké2	140–160	Macro-rest	2265 ± 40	BC 321–206	–27	Erl-10362
	180–200	Charcoal	1927 ± 40	BC 3–AD 140	–28.4	Erl-10363
Ké6	100–120	Macro-rest	2129 ± 40	BC 214–46	–32.5	Erl-10360
	180–200	Macro-rest	2739 ± 42	BC 978–809	–27.7	Erl-10361
Mo4	100–120	Charcoal	172 ± 32	AD 1721–1816	–30.9	Erl-10364
	180–200	Macro-rest	1304 ± 48	AD 645–782	–29.9	Erl-10365

6921 ± 71 to 1733 ± 56 yrs BP are found at 144 cm to 120 cm depth. At sites distal to the river and thus in the marginal areas of the valley, older archives buried by slope material were expected.

The recent organic sediments of the Mbaéré alluvia reveal $\delta^{13}C$ values of –29.0‰ and –29.6‰. These values point to conditions indicating dicotyledon forest (C3) vegetation forming the humus layer. The $\delta^{13}C$ values of the older samples range from –24.9‰ to –30.1‰, thus also suggesting forest dominated habitats at the time of humus formation.

The small variations in grain-size within the profiles, which mainly consist of sand (>85%) (Neumer *et al.*, 2008), indicate that on the sandstone plateau coarser weathering products found in the headwater's tributaries of the Mbaéré (up to ~40 mm size fragments of sandstone and lateritic gravel as well as quartz particles from eroded quartz veins) rapidly decrease in size by fluvial transport and weathering after deposition. In contrast to the slight textural variations, the continuity of the colour shading within the profiles (e.g., from 10 YR 3/2 to 2,5 YR 4/3), as well as the radiocarbon ages (Table 3), refer to more or less undisturbed and continuous sedimentation conditions. Some soil genesis obviously occurred during drier (i.e., non flooded conditions) climatic conditions when fluvial sedimentation was reduced (Neumer *et al.*, 2008). From the samples dated from middle to young Holocene ages the conclusion can be drawn that the pre-existing bio-geographic conditions, in particular the vegetation conditions repressing the sediment discharge, enhance the preservation of palaeoenvironmental archives in the form of small terrace patches in this region. The $\delta^{13}C$ values point to a permanent afforestation of the valley during the Holocene. Neither grass-dominated savanna vegetation nor flood grasslands, characteristic for valleys under comparable climatic conditions, have developed in this case. This is probably a result of the water storage function of the enormous alluvial fills with gradual runoff, supporting the development of a better adapted flood forest with tree species like *Uapaca heudelotii*, *Cathormion altissimum*, *Myragyna* sp. and *Raphia* sp. (Boulvert, 1986). The recent small-scale changes in vegetation composition, noticeable in this area, are linked to the recent hygric conditions. These changes indicate that the amount of water in the aquifer varies spatially and exerts a direct influence on the tree populations. It is hence to be assumed that arid phases caused a lower water table compared to today's conditions, which led to a decrease of the flood forest in favour of the rain forest. In ensuing more humid phases, the recolonisation of the valley plain with flood forest must have emanated from regional (gallery forest-like?) moister flood forest cells in proximity of the river.

3.5 SLOPE SEDIMENTS AND ALLUVIAL FANS IN RECENT RAIN FOREST ENVIRONMENTS IN CENTRAL AFRICA

3.5.1 D.R. Congo: Walikale-Osokari, Kivu (hillwash and stone-lines)

From 1992–1994 palaeoenvironmental field research along a road construction project was carried out in the environs of Osokari-Walikale (1°20′S/28°E, 600–700 m asl) situated in the Kivu province of the D.R. Congo (Figure 1). The area is drained mainly in a westerly direction by the rivers Lowa and Oso, which flow into the Lualaba and subsequently the Congo River (Runge, 2007). Geologically it is characterized by Precambrian rocks of the Burundien (1800–2100 Ma) which are frequently interspersed by post-tectonic intrusions of granite (950–1000 and 1300–1350 Ma). Overlying sedimentary rocks of silt- and sandstones (Serie de Lukuga) date back to the Permian and Carboniferous (République du Zaire, 1974). The Osokari-Walikale region occupies a

zone of landscape transition situated between the elevated areas of the Western Rift Valley (Mitumba Mountains > 3000 m asl) and the inner Congo basin (300–400 m asl). The relief is generally undulating with stronger and gorge-like fluvial incisions in places contrasting with tectonically controlled smaller alluvial basins. Hilly areas are related to weathered granitic domes and to resistant scarps of mica-slate and quarzite. Several uplifted planation levels of a probably Tertiary to Quaternary age can also be recognized.

Obviously most of the soils, pedisediments and alluvial deposits studied in the Osokari-Walikale area show undulating brown to yellow (10YR 5/4–10YR 4/6) hillwash layers, several centimetres to several metres in depth, which are underlain by similarly undulating stone-lines (Figure 7). These consist in part of in-situ weathered rounded quartz originating from quartz veins. But there are also stone-lines which seem to be of an allochthonous origin. These contain, apart from rounded quartz, pebble-like (fluvial?) detritus mixed up with iron-rich concretions, which seem to be the product of a former morphodynamic process (Runge, 1992, 1997). Subsequently these stony accumulations were buried by fine-grained sandy to silty sediments. Radiocarbon dating of charcoal which was occasionally found in these finer pedisediments yielded average dates up to 1000–2200 yrs BP (Runge, 2001). Also some recent radiocarbon ages were measured for charcoal found at depths of 1–2 m and bioturbation should be kept in mind for such sites. Regarding the texture of termite mounds and the corresponding hillwash there was no evidence that these hillwash sediments were derived from former termite mounds (Runge and Runge, 1995).

Figure 7. Road construction works under recent rain forest cover at the Osokari field site in the eastern Congo basin with fossil tree trunks (arrows) within the mottled- and pallid zone below a thick undulating stone-line that possibly marks the Pleistocene–Holocene transition (Photo: J. Runge, 1992).

In contradiction to the Cameroonian field sites described in this chapter, no artefacts were found inside stone-lines and the covering pedisediments of the eastern Congo basin. Below these hillwash-like sediments and stone-lines at average depths of 2–3 metres soil colours are changing to orange and strong brown (contrasting of hematite/goethite weathering). The content of kaolinitic clay increases up to 30%, whereas the sandy fractions decrease significantly. Iron-rich, nodular pisolites are frequently found. pH values range between 3.9 and 5.0. Deeper developed profiles show mottled and pallid soil horizons with a high content of kaolinitic clay and silt which make up 95% of the soil's texture.

There are also soil profiles in the Walikale-Osokari area in which saprolite or even unweathered rock is already reached at a depth of only two or three metres, or sometimes even less (cf. Runge, 1992). Concerning the regional distribution of stone-lines in the eastern D.R. Congo it can be stated that the commonness of layers of coarse and stony horizons in soils decreases from East to West near to Kisangani, whereas it increases closer to the Walikale area and the Western Rift Mountains. This could indicate a regional topographic gradient of increasing morphodynamics within an environment that probably must have been more open concerning vegetation cover than today (Runge, 1992).

Two extended road cuts, 36 km West of Walikale (Figure 1), allowed a deeper insight into the 'Late Quaternary landscape history' (Figure 7). At these locations the allochthonous character of the weathering profiles and of the accumulated sediments respectively becomes evident. Numerous fossil tree trunks were found at depths of 4.5 m to almost 8 m within the mottled and the pallid zone of the profile. Some trunks were also found in direct contact with the parent rock, which is a less weathered dark bluish-gray to bluish-black coloured silty clay- to sandstone (Permian). ^{14}C (AMS) samples of more than 10 fossil trunks and organic sediment at different locations of the road cut at the Osokari site yielded dates from large, up to 1 m diameter tree trunks of 12,960 ± 330, 13,190 ± 390, 17,650 ± 1020, 18,310 ± 860 to 31,920 ± 250 and 36,680 ± 440 yrs BP which corresponds from a pre-LGM to a high to late glacial age (Runge 1996, 2001). The $\delta^{13}C$ values up to –20 to –26‰ support the assumption of a tropical environment (C3 plants). Wood cell-structures of the tree trunks at Osokari were too degraded to determine species or even genera. In conclusion, the Osokari field site with its high to pre-LGM fossilized tree-trunks inside the mottled and pallid soil zone below the stone-line (see Figure 7) supports the assumption that these stone-lines could be considered as stratigraphic markers of the Pleistocene/Holocene transition formed after 13 kyrs BP in the western forelands of the Central Rift Valley (Runge, 1996, 2001; J. Maley, personal note). On account of obviously strong and spacious alluvial and colluvial sediment movements in river beds and on slopes between 13–2 kyrs BP, it is suggested that especially at the Pleistocene/Holocene transition (i.e., post 13–10 kyrs BP) enormous fluxes of coarser sediments coming from the elevated parts of the Western Rift Valley (>3000 m asl, Mitumba Mountains) were eroded, transported and deposited by fluvial processes in a then necessarily more open, less forested environment in the lower and marginal parts (500–1000 m asl) of the eastern Congo basin (Walikale, cf. Figure 1). Because of these widespread observed stratigraphic features in eastern Congolese soils or more appropriate 'pedisediments', emphasizing their allochthonous origin, it can be suggested that before, during and after the LGM a strong forest regression also took place in this area, like in other parts of the Congo basin. This generally contradicts the 'core-area' conceptions proposed by many biologists (cf. introduction of this chapter) which proposed the eastern Congo basin to be a major area of climate and environmental stability leading to the persistence of tropical rain forest during OIS 2. Whether this Late Pleistocene high energy erosion and accumulation event can

be free of doubt correlated and named a possible 'Younger Dryas' event at the onset of the Holocene in the Congo basin is still unproven. However, the formation of the large stone-line (Figure 6) during the Holocene is very unlikely as already denser and closed vegetation (rain forest) was reinstalled during the African Humid Period (AHP, ~9–6 kyrs BP, De Menocal *et al.*, 2000). The latter humid climate during the AHP might have significantly reduced the efficiency of geomorphic processes.

3.5.2 Central African Republic: Sadika, Gadzi-Carnot plateau (alluvial fan)

The Sadika is a small and quite short (<10 km) left tributary of the Mbaéré River draining a small catchment (~40 km^2) within the Gadzi-Carnot sandstone plateau. Field work and sampling was carried out 2004–2006 (Figure 1). The alluvial fan of the small river course, located under recent rain forest vegetation, seems to be no longer active. Therefore it is regarded as a 'fossil' geomorphological feature, extending into the Mbaéré floodplain close to its confluence with the Bodingué River (Figure 8). Such cone shaped deposits of sediments are mainly formed under drier climates (i.e., semi-humid to semi-arid) with thinned out vegetation and higher sediment mobility.

Despite difficulties in drilling and sampling due to high watertables, radiocarbon dating of the alluvial fan's samples shows that different samples at depths of approx. 100 cm often represent recent ages, whereas other samples at lower depths contain older material. ^{14}C age data ranges between 4162 ± 78 yrs BP (at 70 to 93 cm) and 951 ± 69 yrs BP (at 37 to 69 cm). Organic sediment at a depth of 37–69 cm of an exposure reveals an age between 951 ± 69 yrs BP (Table 4) and is definitely older than a sample of recent age from more than 99 cm. This is evidence for substantial reworking of the fan material, even when the environmental conditions of the surroundings might

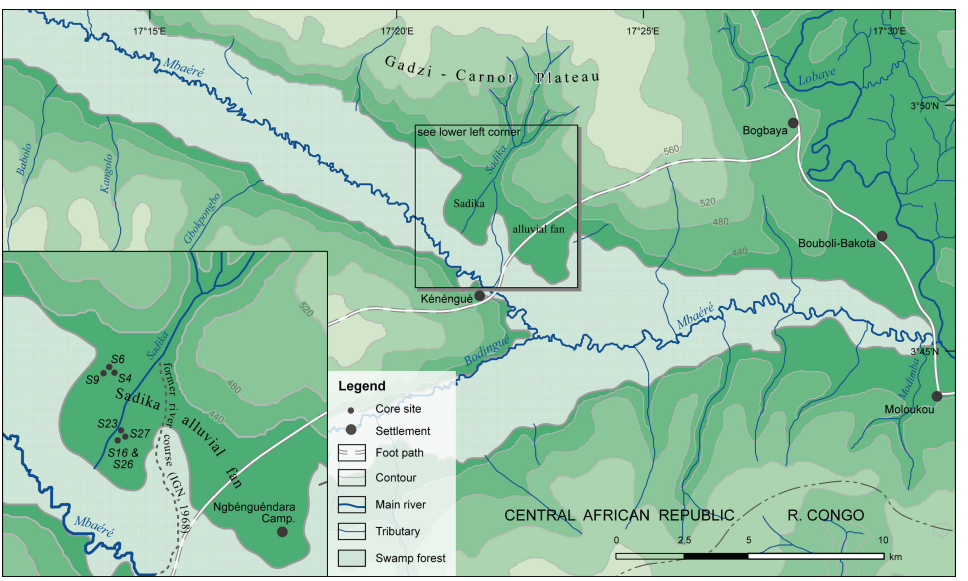

Figure 8. Location map showing the confluence of the Bodingué and the Mbaéré Rivers in the SW of the Central African Republic with a detailed map of the Sadika's alluvial fan (source: Carte de l'Afrique Centrale au 1:200,000—Mbaïki, 1968).

Table 4. Radiocarbon data and $\delta^{13}C$ values of soil samples from the Sadika alluvial fan, 2005.

Core/ sample no.	Depth (cm)	Material	^{14}C (AMS) BP	Calendric age (cal BP) (2σ 95%)	$\delta^{13}C$ (‰)	Lab. no.
S4	60–80	Organic sediment	1269 ± 63	AD 653–889	–22.7	Erl-8209
S6	37–69	Organic sediment	951 ± 69	AD 971–1223	–24.9	Erl-8210
S6	>99	Organic sediment	Recent	–	–29.8	Erl-8211
S9	79–95	Macro-rest	Recent	–	–15.9	Erl-8212
S16	80–100	Organic sediment	Recent	–	–26.8	Erl-8215
S23	101–112	Organic sediment	3191 ± 69	BC 1624–1312	–26.2	Erl-8216
S26	70–93	Organic sediment	4162 ± 78	BC 2906–2568	–28.8	Erl-8217
S27	111–135	Macro-rest	348 ± 48	AD 1453–1641	–27.5	Erl-8218

have remained at least during the Holocene relatively unchanged. Morphodynamics of these alluvial sediments could therefore have been driven by episodic events, which suggests that also under the recent closed rain forest cover, strong superficial run-off and erosion can occasionally take place. In addition to lateral surface morphodynamics, bioturbation could have also played a role for the composition of the fan deposit. However, because of the recent high water level ecological conditions for ants and termites are not very favourable.

The geomorphological situation on the alluvial fan implies that the material dated to recent age, and its associated $\delta^{13}C$ values, correlates to the present grass vegetation (C4). In contrast, the fossil organic carbon indicating older horizons of organic matter (palaeosols) provides $\delta^{13}C$ values ranging between –22.7‰ and –29.8‰. These values consequently suggest mainly dicot forest trees (C3) as the former vegetation type.

The sample analyses, particularly the radiocarbon data and the colour description of the samples, indicate an intensive reallocation of material and processes of soil genesis that have been repeatedly interrupted since the Mid-Holocene (Neumer *et al.*, 2008) and they attest to small-scale diversifications within the fan. These results, the Sadika's incision in the alluvial fan's sediments and localities where diffuse discharge occurs within the floodplain, suggest that processes of erosion and deposition dominate the current dynamics in this terrain (Neumer *et al.*, 2008). Given the steep incline and the sparse vegetation today it can be assumed that the discharge is carried out across the entire alluvial fan, particularly in high precipitation years or during single intense storm events. Accordingly, the deposited and remobilised sediments do not contain applicable information on landscape history at depths of one to two metres. Their accumulation is not climate but rather position and event induced, as shown by inverse radiocarbon ages within one profile. While the recent vegetation is dominated by savanna, $\delta^{13}C$ values referring to forest vegetation are an obvious indication that since 4162 ± 78 yrs BP changes of vegetation have been taken place. As no direct climatic impulse can be linked to it, an expansion of the forest within this time frame has to be explained by a shifting of the Sadika's course. Singular intense rain events could

therefore have played an important role. The anthropogenic influence, documented by regular slash-and-burn activities of the BaAka pygmies in historical times up to the present, may also have been conducive to such a vegetation alteration (Evrard, 1968; Nguimalet *et al.*, 2008).

3.6 BIOGEOMORPHIC RESPONSE TO QUATERNARY ENVIRONMENTAL CHANGES IN CENTRAL AFRICA

The described geomorphic features like larger and smaller floodplains with variable alluvia, shallow and steeper slopes with multilayered sediments, variable colluvia and alluvial fans within recent rain forest and rain forest-savanna transitional landscapes all underlined the obvious sensitivity of tropical relief in the low latitudes during the portion of Late Quaternary studied here (OIS 1–3). However, understanding their response to biogeomorphic and climatic modifications is quite complex and differs in scale, space and time. Considering the vast area of the Congo basin and the larger region of west-central Africa (with swells and mountain regions causing a huge diversity of tropical environments) an attempt is made to summarize these observations by a conceptual model (Figure 9). That they are representative for the whole Central African region remains to be demonstrated.

Conventional concepts of 'geomorphic stability' with soil formation and dense vegetation cover versus 'geomorphic instability' with less vegetation triggering morphodynamics on slopes and in river valleys can help to develop spatio-temporal models (e.g., Fölster, 1983 for Nigeria, and Thomas, 2008 with a review of different concepts). However, often the adjustment of common temperate landscape models into tropical systems can cause misinterpretations of ecosystems response. For example, a trans-regional comparison of lake level variations can be misleading because of significant differences in depth and shape of the water body, local rainfall variability, evaporation and also remote, internal and external influences on the system.

Figure 8 sketches out by a west to east oriented, continent wide perspective the morphodynamic interrelationships between environmentally induced modifications in different landscapes and geomorphic systems in the environs of the upper Congo basin. A generalized assessment and interpretation of the morphodynamic activity ("low" or "high") is made for each study region. The oldest alluvial records were found within river basins in southern Cameroon. There is evidence for slight variations in river geometry and flow regime during the OIS 3 and the Njilien with hardening of lateritic crusts during drier sections. The transition from the geomorphologically more or less stable LGM period to the African Humid Period (AHP), probably interrupted by several 'relapses' during a climatic deterioration supported the accumulation of hillwash locally interspersed by some stone-lines. Denser rain forest was gaining more space again during the Late Holocene until the already closed vegetation cover was quickly interrupted by strong aridification processes and the growing impact of humans leading to higher surface morphodynamics and partly to alluviation inside river beds. A hardening of iron rich soils into locally 'younger' lateritic crusts may have occurred also locally.

The radiocarbon data records from rivers and one alluvial fan from the Gadzi-Carnot plateau in CAR spans mainly the Holocene. Here, the LGM is supposed to have been a relatively stable period as based on evidence of the persistence of a 'fluvial' rain forest refuge dominated with swampy hydrologic conditions, although climatically interrupted by drier periods. In western CAR there is no evidence for a Younger Dryas event. During the First Millenium Crisis (FMC) around 3 ka a tendency to a reactivation of smaller alluvial fans under rain forest vegetation appears. Repeated pulses of sediment have possibly been due to individual extreme rainfall events.

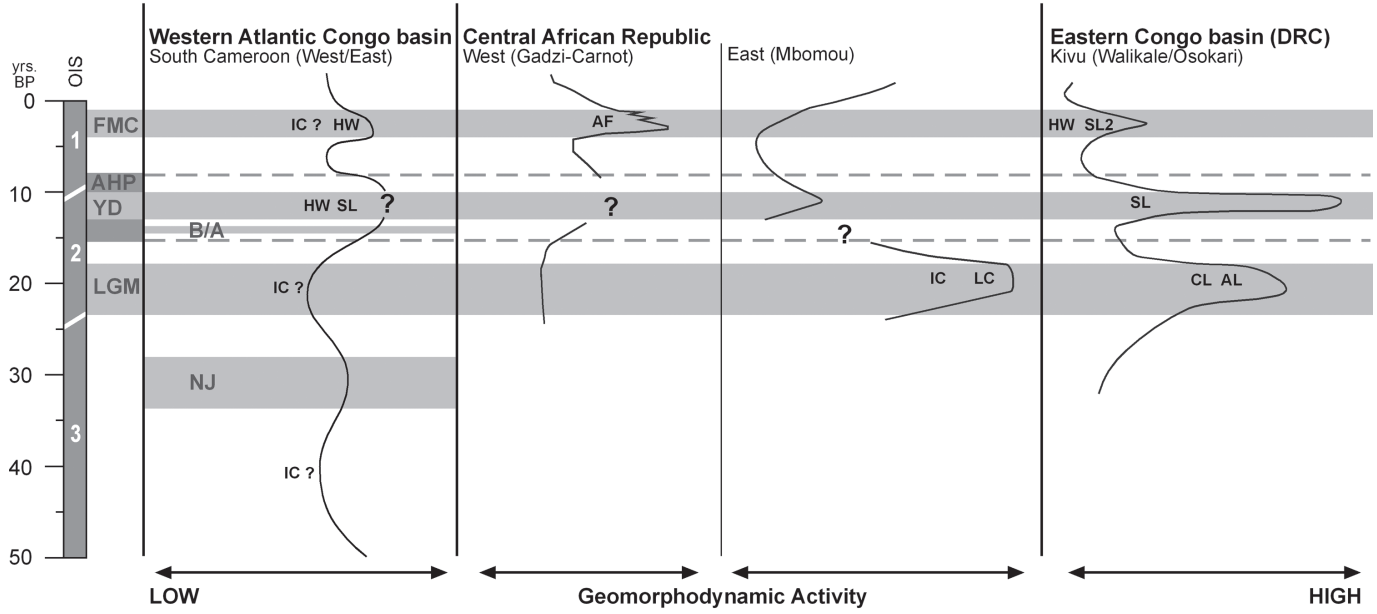

FMC	First Millenium Crisis	**AF**	Alluvial fan (episodic)	**SL**	major stone-line formation
YD	Younger Dryas (?)	**AL**	Alluviation in flood plains	**SL2**	second, smaller stone-line formation
B/A	Bølling Allerød	**CL**	Colluviation on slopes		
AHP	African Humid Period	**HW**	Hill wash/pedisediment formation		
LGM	Last Glacial Maximum	**IC**	Iron crust formation		
NJ	Njilien	**LC**	Lake Chad (low lake level)		

Figure 9. Conceptual model of geomorphodynamic activity in Central Africa since OIS 3 according to selected field sites.

For the eastern Mbomou plateau in eastern CAR a LGM period with hardening of iron rich, lateritic soils into solid crusts (local name: 'lakéré') was concluded by the hyperarid climate at that time corresponding with an extreme low lake level of Lake Chad (almost completely dried out). Between 5–3 ka, rain forest cover in the eastern Central African Republic was still stable and firmly established but changes were introduced with sudden periods of drying, and the growing influence of humans induced bush fires and forest clearing that favoured the establishment of savannas with riparian vegetation. Regular alluviation occurred along the river banks during alternating wet and dry seasons.

Because of its geomorphic setting in the forelands of the Central African Rift system, the eastern Congo (Kivu) area showed regular and strong pulses of sedimentation on slopes and in river beds (alluviation) before, during and after the LGM, at a probably Younger Dryas (YD) event ('stone line' formation) and also during the First Millenium Crisis (FMC, 'hillwash' formation) that could have caused a severe reduction in rain forest coverage.

3.7 SUMMARY AND OUTLOOK

Geomorphological, pedological and stratigraphical examinations on soils and sediments from six different field study areas—surveyed between 1992–2007—in northern Central Africa and the environs of the Congo basin (rain forest-savanna transition), revealed that many of these soils/sediments on slopes and interfluves have to be interpreted as allochthonous pedisediments and not in the more or less 'classical' perception of an in-situ, autochthonous weathering process with subsequent soil formation. Secondly, the studies on alluvia of smaller and larger tropical rivers underline that quite often, but certainly not always, the alluvial record of tropical floodplains contains a lot of stratigraphic features, markers and datable organic material that make them valuable as additional proxy-data archives for understanding the Late Quaternary climate and landscape evolution in lower latitudes.

However, the interpretation of the fluvial performance of erosion and sedimentation of tropical rivers and their deposits entails some problems, as the remobilisation and relocation of material, which can redound to give incorrect ^{14}C data for sediment archives. Furthermore, conditions across the studied catchments are not uniform and can complicate interpretations, especially in relation to anthropogenic impacts or the implications of (neo)tectonic events on the river discharges. Dating gaps emerge frequently, which can be attributed to the fact that at some sites, no sediment strata have been deposited or they have been disturbed by bioturbation due to occasional local inactivity.

Increasing humid conditions during the Pleistocene–Holocene transition (14–12 kyrs BP) and especially the Bølling-Allerød and the onset of the Holocene Pluvial/AHP (around 9 kyrs BP) caused modifications in the sedimentary style of the Ntem River; larger floods and increasing run-off as well as fluvial-morphological activity. These modifications are also well documented in the sedimentary records of the Congo and Niger Rivers (Marret *et al.*, 2001, 2006; Pastouret *et al.*, 1978; Schneider *et al.*, 1997; Zabel *et al.*, 2001). As a result, widespread scour and slope erosion and channel as well as floodplain incision occurred, generating sedimentation hiatuses in the alluvial records of most rivers. Accompanied by remobilization of older sediments and partial reformation of the floodplain, formerly existing swampy surfaces and channel systems of the Ntem alluvial plain were buried and infilled during these intense fluvial processes. Evidence for this hypothesis were also found in the sedimentary record of the Nyong (Mengba) and Sanaga (Belabo) Rivers yielding ^{14}C-dates around 16 and 14 kyrs BP, respectively. With returning seasonal conditions (~5 kyrs BP) comparable to nowadays, during the Holocene locally thick clayey-silty alluvial sequences were

deposited in dense vegetated catchments. Fluvial styles changed to anabranching and anastomosing (Ntem interior delta) patterns, often accompanied by the incision of smaller channels into former floodplains and the infilling of former incised valleys. Major fluvial sedimentary processes were characterized by avulsion, crevasse splaying and abundant overbank deposition during seasonal flooding and river banks became more stable. The upper Nyong and the Boumba, Dja as well as Ngoko fluvial systems displayed a less turbulent river system evolution. Alluvial archives are very limited and largely restricted to cut-off channels, which were investigated at Mengba and Nkolmvondo (Nyong), Mokounounou (Ngoko) and Moloundou (Dja). During the last millennia increasing human impact has altered the natural fluvial system processes by enhancing erosion and thereby increasing bed load and aggradation. This was indicated by sand bank formation in many channel reaches.

In the case of the mostly permanently flooded alluvial plain of the Mbaéré River it was evidenced that under the constant influence of water in combination with the coarse-pored sands, deriving from the plateau region, only a few interpretable traces regarding landscape history have been preserved in the valley fill permanently affected by water. At sites with lower terraces cut by the river, sampling was possible and evidenced Mid-Holocene to recent radiocarbon data. For successful site selection the geo-factors relief, vegetation and soil (moisture), varying partially abruptly in small-scale, have to be taken into consideration.

The study area of the Gadzi-Carnot plateau seems to have been relatively stable during the Holocene. Obviously it did not show marked vegetation dynamics (e.g., shifts of the savanna rain forest transition) as it was evidenced for the Mbomou Plateau in eastern CAR (Runge, 2002). However, based on the assumption of a high glacial forest regression between 20 and 15 kyrs (LGM), as described in several studies on the African tropics (cf. section on 'research to date'), the equatorial lowland rain forest in the plateau region was very likely replaced by savannas. If the flood forest had already established within the Mbaéré floodplain, it would possibly have been repressed by aridification to limited insular locations near the river with suitable moisture levels. The rain forest, on the other hand, must have colonised large parts of the valley, starting from the valley sides. With a change to more humid climate conditions which is assumed to have occured at ~12 kyrs in the Mbari valley (Runge, 2002), an advance of the rain forest on the plateau towards the savanna and a resettlement of the entire valley plain by flood forest is likely. This illustrates how the regionally varying climatic oscillations determined for Central Africa in the course of the Holocene (Gasse, 2000) are related to widely varying initial conditions in each area investigated. Furthermore, climatic oscillations between more humid and more arid conditions at other times in the Quaternary suggest that the vegetation succession, as described above, must have recurred numerous times in response to altered hydrologic conditions.

Considering 'core area' conceptions discussed since the 1970's (cf. Meggers *et al.* 1973) which flora and fauna of the tropical rain forest outlasted glacial climatic (arid) breaks, and expanded from there again after an initially isolated progression of the species, a special importance is attached to the Mbaéré valley as a temporary refugia during drier environment in the Holocene (around ~3 kyrs BP). Taking similar vegetation dynamics as basis regarding high glacial climatic changes, the valleys within the sandstone plateau could be considered as a fluvial refugia in terms of Colyn *et al.* (1991) and Maley (1995).

The eastern Congo example (Osokari-Walikale) is located in one of the formerly postulated LGM refugia of the rain forest. However, contradicting that interpretation, this region yields evidence hillwash and stone-line features that rather, than indicating environmental stability and the persistence of the rain forest, suggest it must have been significantly drier during the LGM and probably also during the YD (?) event. Rain

forest must have been temporarily replaced by an open, savanna-like vegetation that rendered possible strengthened slope and fluvial morphodynamics resulted in thick alluvia in valleys and in colluvia on foot slopes.

Because of the huge area the Congo basin and the limited and selective character of the palaeoenvironmental findings, it is difficult to draw a fully complete and accurate picture of the spatio-temporal landscape dynamics during the Late Quaternary in Central Africa. Nevertheless, the data summarized here suggests a region of far more environmental change and complexity during the Late Quaternary than it has often been proposed. According to the individual response of different larger and smaller rivers and their catchments, their regional climate position, geomorphic setting and proximity to the erosion base-levels of fluvial terrestrial systems, direct correlations within Central Africa, and to other parts of Africa, still contain many uncertainties.

ACKNOWLEDGEMENTS

We are most grateful that since 1994 the German Research Foundation (Deutsche Forschungsgemeinschaft, DFG) has been generously supporting extended field works in Central Africa by several grants (Ref.: RU 555/2-1/2-2/2-3, *Paläoklima Afrika*, RU 555/17-1 *Ngotto*, RU 555/14-1/14-2/14-3, *Forschergruppe 510*). Two reviewers (Peter Kershaw, Gerald Nanson) helped by useful comments and suggestions to improve this paper.

REFERENCES

Alexandre, J., K. Aloni, de Dapper, M., 1994, Géomorphologie et variations climatiques au Quaternaire en Afrique Centrale. *Géo-Eco-Trop*, **16**, pp. 167–205.

Alexandre, J. and Soyer, J., 1987, Les Stones-lines, conclusions de la journée d'étude. *Géo-Eco-Trop*, **11**, pp. 229–239.

Alexandre-Pyre, S., 1971, Le Plateau de Biano (Katanga). Géologie et Géomorphologie. *Académie Royale des Sciences Outre-Mer, Classe des Sciences Naturelles et Médicales, N.S.*, **18(3)**, pp. 1–151.

Baumhauer, R. and Runge, J., 2009, Holocene Palaeoenvironmental History of the Central Sahara.—*Palaeoecology of Africa*, **29**, pp. 1–252.

Boulvert, Y. 1986, *Carte phytogéographique de la République Centrafricaine à 1.1.000.000*. (ORSTOM), notice explicative 104, pp. 1–131.

Boulvert, Y., 1996, *Étude géomorphologique de la République Centrafricaine. Carte à 1:1.000.000 en deux feuilles ouest et est*. (ORSTOM), notice explicative, 110, pp. 1–258.

Boutakoff, N., 1948, Les formations glaciaires et postglaciaires fossilifères, d'âge permo-carbonifère (Karroo inférieur) de la région de Walikale (Kivu, Congo belge). *Mémoires de l'Institut Géologique de l'Université de Louvain*, **9(2)**, pp. 1–122.

Bultot, F., 1971–77, *Atlas climatique du bassin congolais*. (République Démocratique du Congo: Institut National pour l'étude agronomique du Congo I.N.E.A.C.). pp. 1–4.

Cahen, L. and Lepersonne, J., 1948, Notes sur la géomorphologie du Congo Occidental. *Annales du Musée du Congo Belge*, **1**, pp. 1–90.

Cahen, L., Snelling, N.J., Delhal, J. and Vail, J.R., 1984, *The geochronology and evolution of Africa*. (Oxford: Clarendon Press).

Carte de l'Afrique Centrale au 1:200.000—Mbaïki, NA-33-XXIV (1968). (Paris: IGN).

Clist, B., 1987, Early bantu settlements in west central Africa: A review of recent research. Current Anthropology, **28**, pp. 380–382.

Colyn, M., Gautier-Hion, A. and Verheyen, W., 1991, A re-appraisal of palaeoenvironmental history in central Africa: Evidence for a major fluvial refuge in the Zaire basin. *Journal of Biogeography*, **18**, pp. 403–407.

Cornet, J., 1894, Les formations post-primaires du basin du Congo. *Soc. Geol. Belge, Mém.*, **21**, pp. 251–258.

DeMenocal, P., Ortiz, J., Guilderson, T., Adkins, J., Sarntheim, M., Baker, L. and Yarusinsky, M., 2000. Abrupt onset and termination of the African Humid Period: Rapid climate responses to gradual insolation forcing. *Quaternary Science Reviews*, **19**, pp. 347–361.

De Ploey, J., 1964, Cartographie geomorphologique et morphogenese aux environs du Stanley-Pool (Congo). *Acta Geographica Lovaniensia*, **3**, pp. 431–441.

De Ploey, J., 1965, Position géomorphologique, génèse et chronologie de certains dépôts superficiels au Congo occidental. *Quarternaria*, **7**, pp. 131–154.

De Ploey, J., 1966–1968, Report on the Quaternary of the Western Congo. *Palaeoecology of Africa*, **4**, pp. 65–70.

De Ploey, J., 1968, Quaternary phenomena in the Western Congo. Proceedings of VII INQUA Congress. In *Means of correlation of Quaternary Successions*, edited by Morrison, B. and Wright, H.E., (Salt Lake City: University of Utah Press), pp. 501–515.

De Ploey, J., Lepersonne, J. and Stoops, G., 1968, Sédimentologie et origine des sables de la série des sables ocre et de la série des « grès polymorphes » (système du Kalahari) au Congo. *Geologische Wetenschappen*, **61**, pp. 1–72.

Eggert, M.K.H., Höhn, A., Kahlheber, S., Meister, C., Neumann, K. and Schweizer, A., 2006, Pits, graves and grains: Archaeological and archaeobotanical research in Southern Cameroon. *Journal of African Archaeology*, **4(2)**, pp. 273–298.

Eisenberg, J., 2007, Neotektonische Prozesse und geomorphologische Entwicklung des Ntem-Binnendeltas, SW-Kamerun. *Zentralblatt für Geologie und Paläontologie*, Teil I, **1/4**, pp. 37–45.

Eisenberg, J., 2008, A palaeoecological approach to neotectonics: The geomorphic evolution of the Ntem River in and below its interior delta, SW Cameroon. *Palaeoecology of Africa*, **28**, pp. 259–271.

Eisenberg, J., 2009, Morphogenese der Flusseinzugsgebiete von Nyong und Ntem in Süd-Kamerun unter Berücksichtigung neotektonischer Vorgänge. PhD-thesis, J.W. Goethe-University Frankfurt, pp. 1–219.

Evrard, P., 1968, *Recherches écologiques sur le peuplement forestier des sols hydromorphes de la cuvette congolaise*, (République Démocratique du Congo: Institut National pour l'étude agronomique du Congo I.N.E.A.C.), sér. scient. **110**.

Evrard, P., 1957, Les recherches géophysiques et géologiques et les traveaux de sondage dans la Cuvette congolaise. *Académie royale des Sciences coloniales. Mémoires in 8. Nouvelles série.* Tome VII, fasc., **1**, pp. 3–62.

Fölster, H., 1983, Bodenkunde—Westafrika (Nigeria, Kamerun) 4°–8° N, 3°15′–9°30′ E) Bodengesellschaften. *Afrika-Kartenwerk,* **W4**, pp. 1–101.

Gasse, F., 2000, Hydrological changes in the African tropics since the Last Glacial Maximum. *Quaternary Science Reviews*, **19**, pp. 189–211.

Gasse, F., 2005, Continental palaeohydrology and palaeoclimate during the Holocene. *Comptes Rendus Geoscience*, **337**, pp. 79–86.

Gasse, F., Chalié, F., Vincens, A., Williams, M.A.J. and Williamson, D., 2008, Climatic patterns in equatorial and southern Africa from 30,000 to 10,000 years ago reconstructed from terrestrial and near-shore proxy data. *Quaternary Science Reviews* **27**, pp. 2316–2340.

Giresse, P., Bongo-Passi, G., Delibrias, G., and Du Plessy, J.C., 1982, La lithostratigraphie des sediments hemiplagiques du delta profond du fleuve Congo et ses indications sur les paléoclimats de la fin du Quaternaire. *Bulletin Société Géologie française*, **24**, pp. 803–815.

Giresse, P., Maley, J. and Brenac, P., 1994, Late Quaternary palaeoenvironments in the Lake Barombi Mbo (West Cameroon) deduced from pollen and carbon isotopes of organic matter. *Palaeogeography, Palaeoclimatology, Palaeoecology*, **107**, pp. 65–78.

Giresse, P., Maley, J. and Kossoni, A., 2005, Sedimentary environmental changes and millennial climatic variability in a tropical shallow lake (Lake Ossa, Cameroon) during the Holocene. *Palaeogeography, Palaeoclimatology, Palaeoecology*, **218**, pp. 257–285.

Hall, A.M., Thomas, M.F. and Thorp, M.B., 1985, Late Quaternary alluvial placer development in the humid tropics: The case of the Birim Diamond Placer, Ghana. *Journal geological Society London*, **142**, pp. 777–787.

Hamilton, A.C., 1976, The significance of patterns of distribution shown by the forest plants and animals in tropical Africa for the reconstruction of Upper Pleistocene palaeoenvironments: A review. *Palaeoecology of Africa and the Surrounding Islands*, **9**, pp. 63–97.

Hamilton, A.C., 1982, *Environmental History of East Africa—A Study of the Quaternary*, (London, New York: Academic Press).

Höhn, A., Kahlheber, S., Neumann, K. and Schweizer, A., 2008, Settling the rain forest: The environment of farming communities in Southern Cameroon during the First Millennium BC. *Palaeoecology of Africa*, **28**, pp. 29–41.

Jolly, D., Harrison, S.P., Damnati, B. and Bonnefille, R., 1998. Simulated climate and biomes of Africa during the Late Quaternary: Comparison with pollen and lake status data. *Quaternary Science Reviews*, **17**, pp. 629–657.

Kadomura, H., 1995, Palaeoecological and palaeohydrological changes in the humid tropics during the last 20 000 years, with reference to equatorial Africa. In *Global Continental Palaeohydrology*, edited by Gregory, K.J., Starkel, L. and Baker, V.R., (New York: Wiley), pp. 177–202.

Kuete, M., 1990, Géomorphologie du plateau sud-Camerounais à l'ouest du 13°E. Thèse de Doctorat d'Etat, Université de Yaoundé 1.

Lanfranchi, R. and Schwartz, D. (Eds.), 1990, *Paysages Quaternaires de l'Afrique Centrale atlantique*, Collection Didactiques, (Paris: ORSTOM).

Latrubesse, E.M., 2003, The Late-Quaternary Palaeohydrology of Large South American Fluvial Systems. In *Palaeohydrology: Understanding Global Change*, edited by Gregory, K.J. and Benito, G., (Wiley & Sons), pp. 193–212.

Latrubesse, E.M., Rancy, A., 1998, The late quaternary of the Upper Juruá River, Southwestern Amazonia Brazil: Geology and vertebrate paleontology. In *Quaternary of South America and Antarctic Peninsula*, edited by J. Rabassa and M. Salemme, **11**, pp. 27–46.

Latrubesse, E.M. and Rancy, A., 2000, Neotectonic influence on tropical rivers of southwestern Amazon during the Late Quaternary: The Moa and Ipixuna river basins, Brazil. *Quaternary International*, **72**, pp. 67–72.

Latrubesse, E.M. and Franzinelli, E., 2002, The Holocene alluvial plain of the middle Amazon River, Brazil. *Geomorphology*, **44**, pp. 241–257.

Latrubesse, E.M. and Franzinelli, E., 2005, The late Quaternary evolution of the Negro River, Amazon, Brazil: Implications for island and floodplain formation in large anabranching tropical systems. *Geomorphology*, **70**, pp. 372–397.

Latrubesse, E.M., Steveaux, J.C. and Sinha, R., 2005, Tropical Rivers. *Geomorphology*, **70**, pp. 187–206.

Leal, M.E., 2004, The African rain forest during the Last Glacial Maximum, an archipelago of forests in a sea of grass. PhD thesis, Wageningen University, pp. 1–96.

Ledru, M.-P., Bertaux, J., Sifeddine, A. and Suguio, K., 1998, Absence of last glacial maximum records in lowland tropical forests. *Quaternary Research*, **49**, pp. 233–237.

Lepersonne, J., 1978, Structure géologique du bassin intérieur du Zaire. *Académie Royale des Sciences Outre-Mer, Classe des Sciences Naturelles et Médicales, N.S.*, **20**, 2, pp. 1–17.

Lézine, A.-M. and Cazet, J.P., 2005, High-resolution pollen record from core KW31, Gulf of Guinea, documents the history of the lowland forests of West Equatorial Africa since 40.000 yr ago. *Quaternary Research*, **64**, pp. 432–443.

Liedtke, H., 1990, Stand und Aufgabe der Eiszeitforschung. In *Eiszeitforschung*, edited by Liedtke, pp. 40–54.

Littmann, T., 1987, Klimaänderungen in Afrika während der Würm-Eiszeit. *Geoökodynamik*, **8**, pp. 245–257.

Littmann, T., 1988, Jungquartäre Ökosystemveränderungen und Klimaschwankungen in den Trockengebieten Amerikas und Afrikas. *Bochumer Geographische Arbeiten*, **49**, pp. 1–210.

Maley, J., 1981, Etudes palynologiques dans le bassin du Tchad et paléoclimatologie de l'Afrique Nord Tropicale, de 30 000 ans à l'époque actuelle. Coll. Trav. et Doc., **129**, (Paris: ORSTOM), pp. 1–586.

Maley, J., 1989, Late Quaternary climatic changes in the African rain forest: Forest refugia and the major role of sea surface temperatures variations. In *Paleoclimatology and Paleometeorology: Modern and Past Patterns of Global Atmospheric Transport*, edited by Leinen, M. and Sartnheim, M., NATO ASI Series, **282**, (Dordrecht, Boston, London) pp. 585–616.

Maley, J., 1991, The african rain forest vegetation and palaeoenvironments during late Quaternary. *Climatic Change*, **19**, pp. 79–98.

Maley, J., 1992, Mise en évidence d'une péjoration climatique entre ca. 2500 et 2000 ans B.P. en Afrique tropicale humide. Commentaires sur la note de D. Schwartz. *Bulletin de la Société Géologique de France,* **163**, pp. 363–365.

Maley, J., 1993, The climatic and vegetational history of the equatorial regions of Africa during the upper Quaternary. In *The Archaeology of Africa—Food, Metals and Towns,* edited by Shaw, T., Sinclair, P., Andah, B. and Okpoko, A., London and New York: Routledge), pp. 43–52.

Maley, J., 1995, Les fluctuations majeurs de la forêt dense humide Africaine au cours des vingt dernières millénaires. In *L'alimentation en Forêt Tropicale: Interactions Bioculturelles et Applications au Dévelopement*, edited by Hladik, C.M., (Paris: UNESCO Parthenon), pp. 1–14.

Maley, J., 1996, The African rain forest—main characteristics of changes in vegetation and climate from the Upper Cretaceous to the Quaternary. In *Essays on the Ecology of the Guinea-Congo Rain Forest*, edited by Alexander, I.J., Swaine, M.D. and Watling, W., Proceedings of the Royal Society of Edinburgh, **104B**, pp. 31–73.

Maley, J., 2001, The impact of arid phases on the African rain forest through geological history. In *African Rain Forest Ecology and Conservation—An Interdisciplinary Perspective*, edited by Weber, W., White, L., Vedder, A. and Naughton-Treves, L., (New Haven: Yale University Press), pp. 68–87.

Maley, J., 2002, A Catastrophic Destruction of African Forests about 2,500 Years Ago Still Exerts a Major Influence on Present Vegetation Formations. *IDS Bulletin*, **33/I**, pp. 13–30.

Maley, J. and Brenac, P., 1998, Vegetation dynamics, Palaeoenvironments and Climatic changes in the Forests of West Cameroon during the last 28,000 years BP. *Review of Palaeobotany and Palynology*, **99**, pp. 157–187.

Marchant, R. and Hooghiemstra, H., 2004, Rapid environmental change in African and South American tropics around 4000 years before present: A review. *Earth-Science Reviews*, **66**, pp. 217–260.

Mariotti, A., 1991, Le carbone 13 en abondance naturelle, tracer de la dynamique de la matiére organique des sols et de l'évolution des paléoenvironnements continentaux. *Cah. ORSTOM, Ser. Pedol.*, **26**, pp. 299–313.

Marret, F., Scourse, J.D., Versteegh, G., Fred Jansen, J.H. and Schneider, R., 2001, Integrated marine and terrestrial evidence for abrupt Congo River palaeodischarge fluctuations during the last deglaciation. *Journal of Quaternary Science*, **16(8)**, pp. 761–766.

Marret, F., Maley, J. and Scourse, J., 2006, Climatic instability in west equatorial Africa during the Mid- and Late Holocene. Quaternary International, **150**, pp. 71–81.

Mbenza, M., 1983, Evolution de l'environment géomorphologique de fonds de vallée au cours du quaternaire dans une région tropicale humide. Thèse Doc., Univ. Liège, Belgique.

Mbenza, M., Roche, E. and Doutrelepont, H., 1984, Note sur les apports de la palynologie et de l'etude des bois fossiles aux recherches géomorphologiques sur la vallée de la Lupembashi (Shaba-Zaire). *Revue de Paléobiologie*, Volume Spécial, pp. 149–154.

Meggers, B.J., Ayensu, E.S. and Duckworth, W.D., (eds.) 1973, Tropical forest ecosystems in Africa and South America: A comparative Review. (Washington: Smithonian Institution Press).

Monod, T., 1938, Gravures, peintures et inscriptions rupestres. Contributions à l'étude du Sahara occidental, 1, *Publications du Comité d'Ètudes Historiques et Scientifiques de l'Afrique Occidentale Française*, Sér. A, **7**, Larose, Paris.

Neumer, M., Becker, E. and Runge, J., 2008, Palaeoenvironmental studies in the Ngotto forest: Alluvial sediments as indicators of recent and holocene landscape evolution in the Central African Republic. *Palaeoecology of Africa*, **28**, pp. 121–137.

Ngomanda, A., Neumann, K., Schweizer, A. and Maley, J., 2009, Seasonality change and the third millennium BP rain forest crisis in Central Africa: A high resolution pollen profile from Nyabessan, southern Cameroon. *Quaternary Research*, **71**, pp. 307–318.

Nguetsop, V.F., Servant-Vildary, S. and Servant, M., 2004, Late Holocene climatic changes in West Africa, a high resolution diatom record from equatorial Cameroon. *Quaternary Science Reviews*, **23**, pp. 591–609.

Nguimalet, C.-R., Koko, M., Ngana, F. and Kondayen, A.I., 2008, Non Woody Forest Products (NWFPs) and food safety: Sustainable management in the Lobaye region (central African Republic). *Palaeoecology of Africa*, **28**, pp. 289–300.

Olivry, J.-C., 1986, *Fleuves et rivières de Cameroun*. (Paris: ORSTOM).

Pastouret, L., Chamley, H., Delibrias, G., Duplessy, J.C. and Theide, J., 1978, Late Quaternary climatic changes in Western Tropical Africa deduced from deep-sea sedimentation off the Niger Delta. *Oceanologica Acta*, **1**, pp. 217–232.

Peel, M.C., Finlayson, B.L. and McMahon, T.A., 2007, Updated world map of the Köppen-Geiger climate classification. *Hydrol. Earth Syst. Sci.,* **11**, pp. 1633–1644.

Petters, S.W., 1991, Regional Geology of Africa. *Lecture Notes in Earth Sciences,* **40**, pp. 1–722.

Pouyaud, B. and Colombani, J., 1989, Les variations extrêmes du lac Tchad: l'assèchement est-il possible? *Annales de Géographie*, **545**, pp. 1–23.

Preuss, J., 1986a, Jungpleistozäne Klimaänderungen im Kongo-Zaire-Becken. *Geowissenschaften in unserer Zeit*, **4(6)**, pp. 177–187.

Preuss, J., 1986b, Die Klimaentwicklung in den äquatorialen Breiten Afrikas im Jungpleistozän. Versuch eines Überblicks im Zusammenhang mit Geländearbeiten in Zaïre. *Marburger Geographische Schriften*, **100**, pp. 132–148.

Preuss, J., 1990, L'évolution des paysages du bassin intérieur du Zaire pendant les quarante derniers millénaires. In: Lanfranchi, R., Schwartz, D. (Eds.), Paysages quaternaires de l'Afrique centrale atlantique. ORSTOM, Paris, pp. 260–270.

REGIDESO, 1985, Etude sur les domaines hydrogéologiques du Zaire, Travaux de forage, Regie de distribution d'eau. Unpublished survey report, Kinshasa.

République du Zaire, 1974, *Notice explicative de la carte géologique du Zaire au 1/2 000 000*, (Tervuren: Département des Mines, Direction de la Géologie).

Runge, J., 1992, Geomorphological observations concerning palaeoenvironmental conditions in eastern Zaire. *Zeitschrift für Geomorphologie N.F.*, Suppl. Bd. **91**, pp. 109–122.

Runge, J., 1996, Palaeoenvironmental interpretation of geomorphological and pedological studies in the rain forest "core areas" of eastern Zaire (Central Africa). *South African Geographical Journal*, **78**, pp. 91–97.

Runge, J., 1997, Altersstellung und paläoklimatische Interpretation von Decksedimenten, Steinlagen (stone lines) und Verwitterungsbildungen in Ostzaire (Zentralafrika). *Geoökodynamik*, **18**, pp. 91–108.

Runge, J., 1998, Rezente und holozäne Vegetations- und Klimadynamik an der Regenwald/Savannengrenze in Nord-Kongo (Zaire) und der Zentralafrikanischen Republik (4°-5°20'N, 23°-25°E). *Zentralblatt für Geologie und Paläontologie*, Teil I, **1/2**, pp. 91–113.

Runge, J., 2000, Environmental and climatic history of the eastern Kivu area (D.R. Congo, ex Zaire) from 40 ka to the present. In *Southern Hemisphere Paleo- and Neoclimates (IGCP 341)*, edited by Smolka, P.P. and Volkheimer, W., (Berlin, Heidelberg, New York: Springer), pp. 249–262.

Runge, J., 2001, Landschaftsgenese und Paläoklima in Zentralafrika. Physiogeographische Untersuchungen zur Landschaftsentwicklung und klimagesteuerten quartären Vegetations- und Geomorphodynamik in Kongo/Zaire (Kivu, Kasai, Oberkongo) und der Zentralafrikanischen Republik (Mbomou), *Relief Boden Paläoklima*, **17**, (Berlin: Gebrüder Bornträger), pp. 1–294.

Runge, J., 2002, Holocene landscape history and palaeohydrology evidenced by stable carbon isotope ($\delta^{13}C$) analysis of alluvial sediments in the Mbari valley (5°N/23°E), Central African Republic. *Catena*, **48**, pp. 67–87.

Runge, J., 2007, Congo River. In *Large Rivers: Geomorphology and Management*, edited by Gupta, A., (Chicester, Singapore: Wiley and Sons), pp. 293–310.

Runge, J., 2008, Dynamics of Forest Ecosystems in Central Africa during the Holocene. Past-Present-Future. *Palaeoecology of Africa*, **28**, pp. 1–306.

Runge, J. and Lammers, K., 2001, Bioturbation by termites and Late Quaternary Landscape evolution on the Mbomou plateau of the Central African Republic (CAR). *Palaeoecology of Africa*, **27**, pp. 153–169.

Runge, J. and Neumer, M., 2000, Dynamique du paysage entre 1955 et 1990 à la limite forêt-savane dans le nord du Zaïre, par l'étude de photographies aériennes et de données LANDSAT-TM. In: *Dynamique à long terme des écosystèmes forestiers intertropicaux (ECOFIT)*, edited by Servant, M. and Servant-Vildary, S., (Paris: UNESCO, IRD), pp. 311–317.

Runge, J. and Nguimalet, C.R., 2005, Physiogeographic features of the Oubangui catchment and environmental trends reflected in discharge and floods at Bangui 1911–1999, Central African Republic. *Geomorphology*, **70**, pp. 311–327.

Runge, J., Eisenberg, J. and Sangen, M. 2006, Geomorphic evolution of the Ntem alluvial basin and physiogeographic evidence for Holocene environmental changes in the rain forest of SW Cameroon (Central Africa)—preliminary results. *Zeitschrift für Geomorph. N.F.,* Suppl., **145**, pp. 63–79.

Runge, J. and Runge, F., 1995, Late Quaternary palaeoenvironmental conditions in eastern Zaire (Kivu) deduced from remote sensing, morpho-pedological and sedimentological studies (Phytoliths, Pollen ^{14}C-data). *2e Symposium de Palynologie Africaine*, **31**, (Tervuren, Belgique: Publ. Ocass. CIFEG), pp. 109–122.

Runge, J. and Tchamié, T., 2000, Inselberge, Rumpfflächen und Sedimente kleiner Einzugsgebiete in Nord-Togo: Altersstellung und morphodynamische Landschaftsgeschichte. *Zbl. Geol. Paläont.*, Teil 1, **5/6**, pp. 497–508.

Sangen, M., 2007, Physiogeographische Untersuchungen zur holozänen Umweltgeschichte an Alluvionen des Ntem-Binnendeltas im tropischen Regenwald SW-Kameruns. *Zentralblatt für Geologie und Paläontologie*, Teil I, **1/4**, pp. 113–128.

Sangen, M., 2008, New evidence on palaeoenvironmental conditions in SW Cameroon since the Late Pleistocene derived from alluvial sediments of the Ntem River. *Palaeoecology of Africa*, **28**, pp. 79–101.

Sangen, M., 2009, Physiogeographische Untersuchungen zur pleistozänen und holozänen Umweltgeschichte an Alluvionen des Ntem-Binnendeltas und alluvialer Sedimente der Flüsse Boumba, Ngoko, Nyong und Sanaga in Süd-Kamerun. PhD thesis, J.W. Goethe-University, Frankfurt am Main, p. 343.

Sangen, M., 2011, New results on palaeoenvironmental conditions in equatorial Africa derived from alluvial sediments of Cameroonian rivers. *Proceedings of the Geologists' Association*, **122**, pp. 212–223.

Sangen, M, Eisenberg, J., Kankeu, B., Runge, J. and Tchindjang, M., 2010, New findings from geological, geomorphological and sedimentological studies on the palaeoenvironmental conditions in southern Cameroon. *Palaeoecology of Africa*, **30**, pp. 165–188.

Schneider, R.R., Price, B., Müller, P.J., Kroon, D. and Alexander, I., 1997, Monsoon-related variations in Zaire (Congo) sediment load and influence of fluvial silicate supply on marine productivity in the east equatorial Atlantic during the last 200,000 years. *Paleoceanography*, **12**, pp. 463–481.

Schwartz, D., 1988, *Histoire d'un paysage: Le Lousséké. Paléoenvironnements Quaternaires et podzolisation sur sables Batéké*. Etudes et Thèses, (Paris: ORSTOM).

Schwartz, D., 1992, Assèchement climatique vers 3 000 B.P. et expansion Bantu en Afrique centrale atlantique: Quelques réflexions. *Bulletin de la Société Géologique de France*, **3**, pp. 353–361.

Segalen, P., 1967, Les sols et la géomorphologie du Cameroun. *Cahier ORSTOM, Sér. Pédologie*, **V(2)**, pp. 137–188.

Servant, M., 1983, *Séquences continentales et variations climatiques: Évolution du bassin du Tchad au Cénozoique supérieur*, (Paris: ORSTOM).

Sillans, R., 1958, *Les savanes de l'Afrique Centrale*, (Paris: Lechevalier).

Steveaux, J.C., 2000, Climatic events during the Late Pleistocene and Holocene in the Upper Parana River: Correlation with NE Argentina and South-Central Brazil. *Quaternary International*, **72**, pp. 73–85.

Steveaux, J.C. and Souza, I.A., 2004, Floodplain construction in an anastomosed river. Quaternary International, **114**, pp. 55–65.

Stoops, G., 1967, Le profil d'altération au Bas-Congo (Kinshasa). *Pédologie*, **17(1)**, pp. 60–105.

Taylor, K.C., Lamorey, G.W., Doyle, G.A., Alley, R.B. and Grootes, P., 1993, The "flickering switch" of late Pleistocene climate change. *Nature*, **361**, pp. 432–436.

Thomas, M.F., 1998, Late Quaternary Landscape Instability in the Humid and Sub-Humid Tropics. In *Palaeohydrology and Environmental Change*, edited by Benito, G., Baker, V.R. and Gregory, K.J., (Chichester Wiley and Sons), pp. 247–258.

Thomas, M.F., 2000, Late Quaternary environmental changes and the alluvial record in humid tropical environments. *Quaternary International*, **72**, pp. 23–36.

Thomas, M.F., 2004, Landscape sensitivity to rapid environmental change—a Quaternary perspective with examples from tropical areas. *Catena*, **55**, pp. 107–124.

Thomas, M.F., 2008, Understanding the impacts of Late Quaternary climate change in the tropical and sub-tropical regions. *Geomorphology*, **101**, pp. 146–158.

Thomas, M.F. and Thorp, M.B., 1980, Some aspects of geomorphological interpretation of Quaternary alluvial sediments in Sierra Leone. *Zeitschrift für Geomorphologie, N.F.*, Suppl. Bd. **36**, pp. 140–161.

Thomas, M.F. and Thorp, M.B., 1995, Geomorphic response to rapid climatic and hydrologic change during the late Pleistocene and early Holocene in the humid and sub-humid tropics. *Quaternary Science Reviews*, **14**, pp. 193–207.

Thomas, M.F. and Thorp, M.B., 2003, Palaeohydrological reconstructions for tropical Africa since the Last Glacial Maximum - evidence and problems. In *Palaeohydrology: Understanding Global Change,* edited by Gregory, K.J. and Benito, G., (Chichester Wiley and Sons), pp. 167–192.

Thomas, M.F., Nott, J. and Price, D.M., 2001, Late Quaternary stream sedimentation in the humid tropics: A review with new data from NE Queensland, Australia. *Geomorphology*, **39**, pp. 53–68.

Thorp, M. and Thomas, M., 1992, The timing of alluvial sedimentation and flood-plain formation in the lowland humid tropics of Ghana, Sierra Leone and western Kalimantan (Indonesian Borneo). *Geomorphology*, **4**, pp. 409–422.

Toteu, S.F., Penaye, J. and Poudjom Djomani, Y.H., 2004, Geodynamic evolution of the Pan-African belt in central Africa with special reference to Cameroon. *Canadian Journal of Earth Sciences*, **41**, pp. 73–85.

U.S. Geological Survey, 2002, *Map showing Geology, Oil and Gas Fields, and Geologic Provinces of Africa*, version 2.0. 1:5,000,000.

van Zinderen Bakker, E.M. and Clark, J.D., 1962, Pleistocene climates and cultures in North-Eastern Angola. *Nature*, **196**, pp. 639–642.

Veatch, A.C., 1935, Evolution of the Congo Basin. *Geological Society of America*, **3**, pp. 1–183.

Vidal, L. and Arz, H., 2004, Oceanic climate variability at millennial time-scales: Models of climate connections. In *Past climate variability through Europe and Africa*, edited by Battarbee, R.W., Gasse, F. and Stickley, C.E., (Dordrecht: Springer), pp. 31–44.

Vincens, A., Schwartz, D., Bertaux, J., Elenga, H. and de Namur, C., 1998, Late Holocene climatic changes in western Equatorial Africa inferred from pollen lake Sinnda, Southern Congo. *Quaternary Research*, **50**, pp. 34–45.

Waegemans, G., 1953, Signification pédologique de la "stone-line". *Bull. agricole du Congo Belge et du Ruanda-Urundi*, **3(44)**, pp. 521–532.

White, F., 1983, The vegetation of Africa, a descriptive memoir to accompany the UNESCO/AETFAT/UNSO vegetation map of Africa. UNESCO, *Natural Resour. Res.*, **20**, pp. 1–356.

Weldeab, S., Schneider, R.R., Kölling, M. and Wefer, G., 2005, Holocene African droughts relate to eastern equatorial Atlantic cooling. *Geological Society of America*, **33(12)**, pp. 981–984.

Weldeab, S., Lea, D.W., Schneider, R.R. and Andersen, N., 2007, 155,000 years of West African monsoon ocean thermal evolution. *Science*, **316**, pp. 1303–1307.

Williams, M.A.J. and Faure, H. (Eds.), 1980, *The Sahara and The Nile: Quaternary Environments and Prehistoric Occupation in Northern Africa*. (Rotterdam: A.A. Balkema), pp. 1–607.

Woodward, J.C., Macklin, M.G., Krom, M.D. and Williams, M.A.J., 2007, The Nile: Evolution, Quaternary Environments and Material Fluxes. In *Large Rivers: Geomorphology and Management*, ed. A. Gupta, pp. 261–292. Chichester: John Wiley & Sons.

Zabel, M., Schneider, R., Wagner, T., Adegbie, A.T., De Vries, U. and Kolonic, S., 2001, Late Quaternary Climate Changes in Central Africa as inferred from Terrigenous Input in the Niger Fan. *Quaternary Research*, **56**, pp. 207–217.

Zeese, R., 1991, Fluviale Geomorphodynamik im Quartär Zentral- und Nordostnigerias. *Freiburger Geographische Hefte*, **33**, pp. 199–208.

Zeese, R., 1996, Oberflächenformen und Substrate in Zentral- und Nordostnigeria. Ein Beitrag zur Landschaftsgeschichte. *Berichte aus der Geowissenschaft*, Habil-Schrift Univ. Köln, (Aachen: Shaker Verlag), pp. 1–195.

CHAPTER 4

Lake level changes of Barombi Mbo (Cameroon) during the Late Quaternary: Compared catchment and crater lake records

Pierre Giresse
Centre de Formation et de Recherche sur les Environnements Méditerranéens, UMR 5110-CNRS, Université Perpignan Via-Domitia, France

Jean Maley
Département Paléoenvironnements et Paléoclimatologie, ISEM-CNRS, Université de Montpellier-2, Montpellier, France

Appolinaire Zogning
National Institute of Cartography, Ministry of Scientific Research and Innovation, Yaoundé, Cameroon

ABSTRACT: The deep water sediments of the crater-lake Barombi Mbo have been the object of previous studies permitting a palaeoenvironmental reconstruction going back to approximately 34,000 cal yr BP. The catchment area of the lake corresponds to a former caldera. The aim of the present study is to recognize the conditions of deposition and erosion of swampy and lacustrine sediments of the catchment area deposited in this catchment. The study also allowed us to push back the palaeoenvironmental history until approximately 46,000 cal yr BP. In the lower part of the slopes, we observe the change from a littoral, sometimes laminated lacustrine deposit, towards swampy sediments characterized by hydromorphic soils. The fern spores are always abundant, while the pollen are restricted to some Holocene and Pleistocene deposits where they allowed a palaeoenvironmental reconstruction which correlates well with that of the deep lake. Sections of the upper part of the slope show erosion surfaces indicating the Late Pleistocene passage of a swampy sedimentation towards alluvial and colluvial sedimentary deposition or towards lengthy emersion. This lowering of the lake level occurred in a step-wise manner controlled mainly by seismic activity. Although some short-term lowerings (ca. –6 m) of the lake level in particular during LGM and Younger Dryas were of climatic origin. They are attested by the setting of a swampy, Cyperaceae dominated environment on the lacustrine platform. These stepwise level falls establishes a basis of discussion to study the chronology of soil erosion observed on the slope of the crater above the lake. Pleistocene vivianite concretions, sometimes of centimetre-size, indicate conditions of long diagenesis in the catchment, according to the progress of emersion, the iron underwent fast and total oxidation leading to hardened ferric gravel. During wet Holocene periods and without ash layers, these concretions become rare and are dispersed in the sediment.

4.1 INTRODUCTION

The Quaternary sediments of Lake Barombi Mbo, a crater lake in the volcanic chain of Cameroon, have been the object of numerous multidisciplinary studies (Giresse *et al.*, 1991; Maley and Brenac, 1998). As such, this lake offers, together with Bosumtwi meteoritic impact lake (Talbot and Johannessen, 1992; Peck *et al.*, 2004) in Ghana, one of the rare palaeoenvironmental histories of West Africa back to more than 25,000 yrs BP.

A large part of the catchment corresponds to a former crater in which a second crater, filled by the lake, is located. During initial field studies on the lower slopes above the lake, we observed the presence of blue hydromorphic soils several metres above the current lake level. The soil is used for traditional clay supply for the potters of the nearby village (Clay Pit). After field survey, a campaign of soundings with a hand auger was carried out. The sediments retrieved has been weakly compacted and allowed sampling sometimes to more than 9 m in depth. The good recovering of sediments and their anoxic character allowed several sedimentological and mineralogical analyses to be carried out, as well as palynological analysis of the Holocene levels where pollen were preserved. The objectives of the study are double: (1) to examine the relations existing between the processes of erosion/sedimentation in the catchment and the deep-lake accumulation as much from the point of view of mechanical process as of diagenesis; (2) due to some more deeply buried lacustrine deposits, to push back the sedimentary history, currently limited to the study of the deposits of the nearby deep lake.

4.2 GENERAL SETTING

The Barombi Mbo is the largest lake (surface area 4.15 km^2) located on the active NE-SW Cameroon volcanic chain. It is inserted in the Upper Black Series of basaltic tuffs and lava flows which cover the granito-gneissic basement (Gèze, 1943; Dumort, 1968). The lake is situated in the recent easternmost crater of a succession of two overlapping maars, the presumed older one is in the West (Figure 1). They are entirely volcanic and show two similar series of basaltic tuff lapilli separated by a palaeosol (Gouhier *et al.*, 1974). Peridotite nodules and gneissic xenoliths are common. The low-angle stratification of the tuffs characterizes this structure as a tuff-ring. On the NE shore of the lake basaltic flow both anterior and contemporaneous to the explosion has been dated by six K/Ar measurements giving an age of ca. 1 Ma (Cornen *et al.*, 1992).

The walls of the maar rise about 100 m above the lake level. The lake has a bowl shaped morphology with a flat bottom and a generally narrowish littoral platform (Figure 2). The diameter of the lake is ca. 2 km, its altitude 301 m asl and its maximum depth 110 m. Nowadays, the lake level is stabilized by a natural spillway which has cut a sub-vertical gorge to the southeast. This spillover was reinforced ca. 40 years ago by a small concrete dam. The lake exhibits a thermocline oscillating between -30 m and -40 m, only the top portion contains sufficient oxygen levels to harbour vertebrate life. Diatoms are nearly absent, planktonic biomass is poor and composed essentially of cladocerans and copepods (Kling, 1987) enabling the growth of some endemic cyclid fishes (Green *et al.*, 1973).

The flat bottom of the oldest crater (8 km^2) is part of the catchment area of Barombi Mbo Lake. This western catchment is mainly drained by a small perennial stream called Toh Mbok which has built a steep delta cone prograding several hundred meters into the lake (Figure 2). The drainage basin is largely covered by a 2–3 m hydromorphic soil, including a bluish-grey gley horizon with rusty coloured pockets.

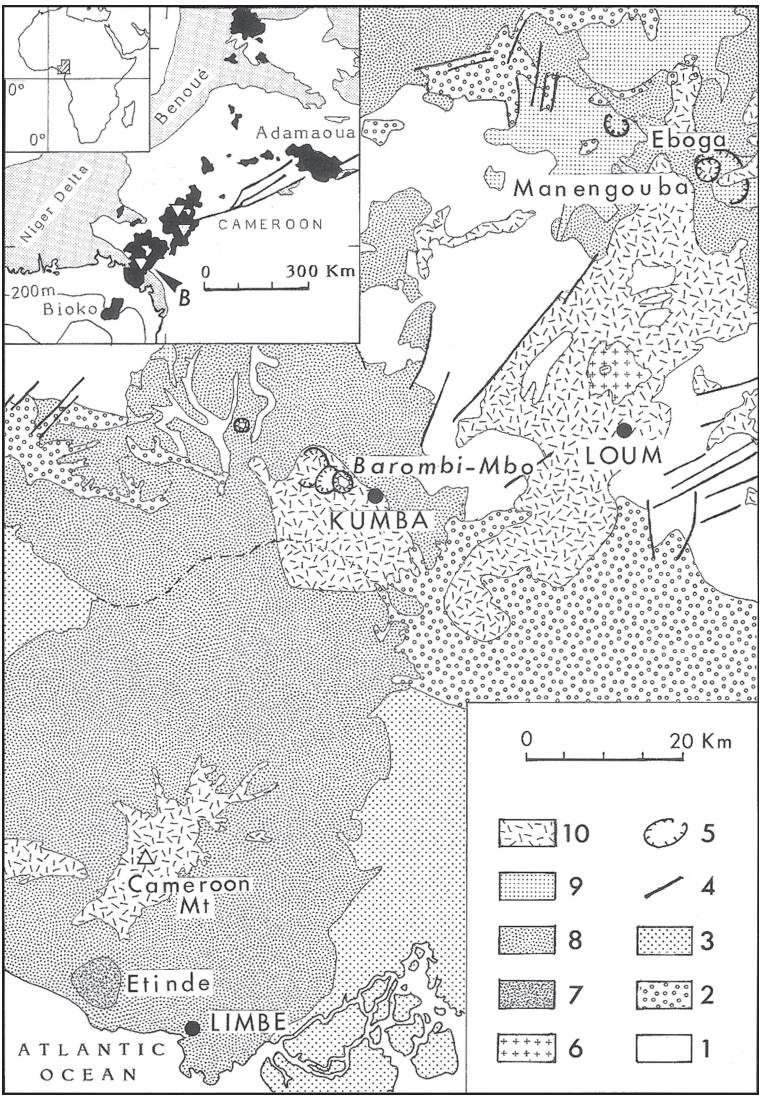

Figure 1. Geological map simplified from part of the 1:500,000 map of Dumort (1968). 1. Crystalline basement; 2. Cretaceous sediments; 3. Cenozoic s.l. sediments; 4. Fault; 5. Maar and caldeira; 6. Tertiary syenite of Mount Koupé; 7. Foidic lavas from Etinde; 8. Basalts of the « Lower Black Series »; 9. Trachytes; 10. Recent basalts of the « Upper Black Series ». Inset: Position of the Cameroon Line in Africa (top left). Attention: In black, volcanic ridge (Miocene to the Present), from West Cameroon to Adamaoua; stippled: Benue trench and Niger delta. Pointed triangles situate the approximate position of Lake Barombi Mbo (B) (after Cornen *et al.*, 1992).

However, owed to the amount of granito-gneissic pebbles in the streams, it seems likely that locally the pan-African crystalline basement is directly below the surface. Upstream, steep slopes have a thin cover of poorly developed soils or are denuded. The crystalline basement crops out in the outer rim of the drainage basin. This outer rim, from where the network of rivers descends, is a circumference which approximately follows the 360 m isobath, about 100 m above the lake level.

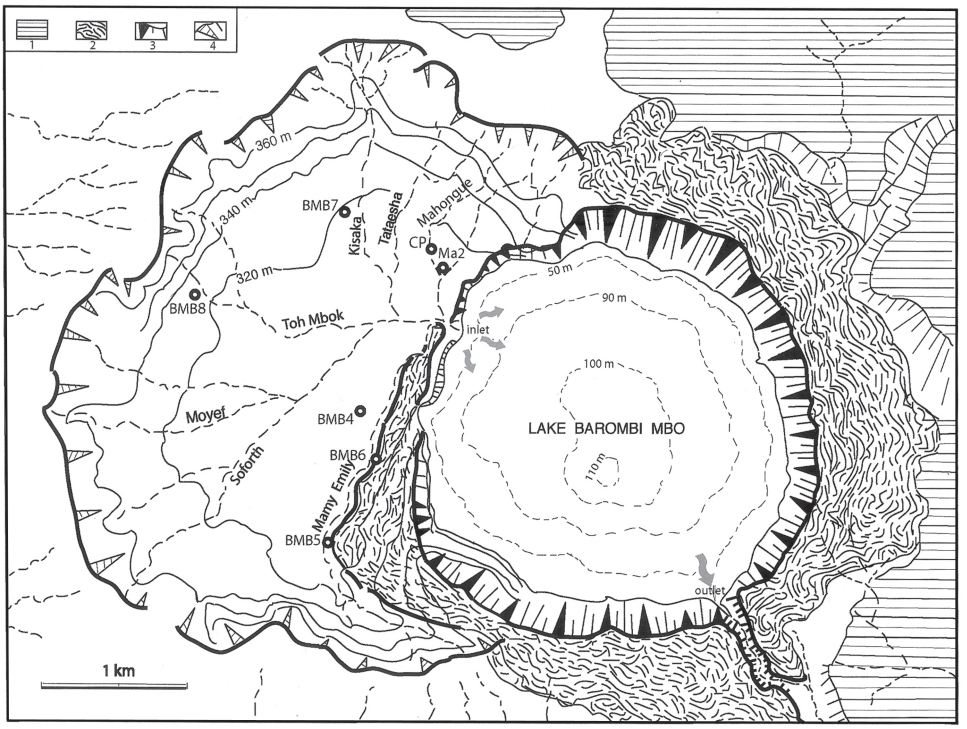

Figure 2. Rim position of the two boxed craters with simplified bathymetric map of Lake Barombi Mbo and simplified topographic map of its drainage basin. CP, Ma2, BMB7, BMB8, BMB4, BMB6 and BMB5 are sounding sites of the study. 1. Basaltic lavas; 2. Basaltic tuff lapilli; 3. Inner ring of the lake crater; 4. Outer ring of the drainage basin.

The lake is surrounded by lowland evergreen rain forest with patches of semi-deciduous type (Letouzey, 1985). Today, hillsides are covered by an evergreen dense forest interrupted by some small areas of farmland. The banks of the Toh Mbo pro-delta show, over approximately 10 m, a zonal succession composed of shrubs dominated by *Alchornea cordifolia*, then an area of ferns and, finally, a swamp composed of clumps of Cyperaceae.

4.3 QUATERNARY SEDIMENTARY PROCESSES OF THE DEEP LAKE (PREVIOUS RESULTS)

The previously presented data (Giresse *et al.*, 1991, 1994; Maley and Brenac, 1998) were mainly obtained from the 110 m depth BM6 core which is 24 m long. This represents only a fraction of the total accumulation of lacustrine deposits which may likely reach up to some 300 m. The entire sedimentary column is composed of millimetre- to centimetre-thick laminae, consisting of dark brown to green clay rich in organic material (5–10% organic carbon). Each lamina is composed of a lower micro-layer rich in quartz, feldspar, muscovite, pyroclasts, sponge spicules and woody plant fragments, and a more clayey upper micro-layer with yellow siderite crystals whose concentration determines the pigmentation of the deposit (from green to yellow).

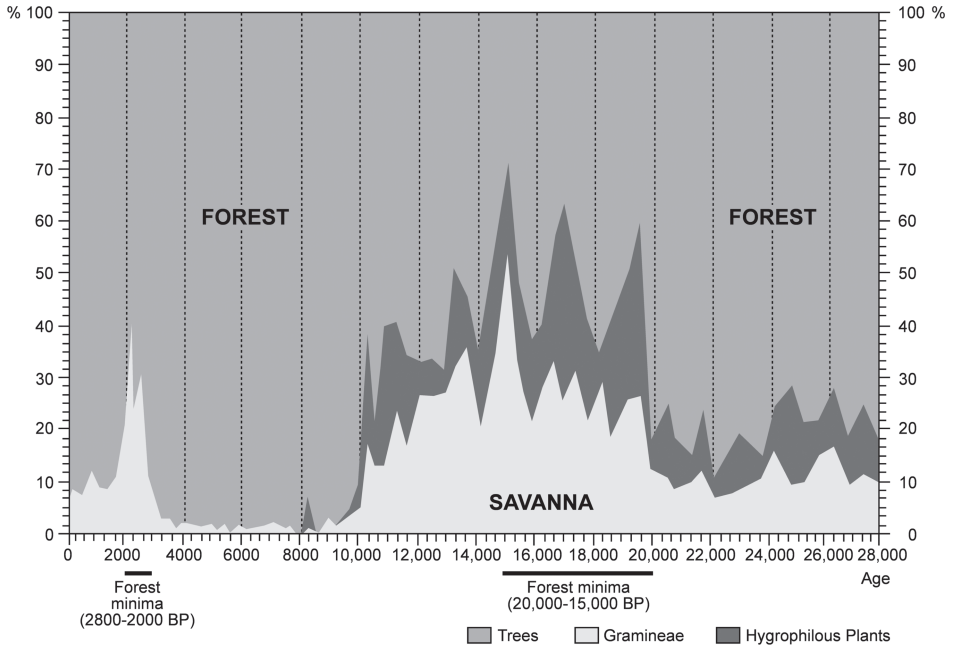

Figure 3. Synthetic pollen diagram of the deep water core BM6 taken in the centre of the Lake Barombi Mbo (Maley, 2002, 2004).

In the lower half of this core, between 23,000 and 11,000 cal yr BP, 21 black ash layers with millimetre to centimetre thicknesses have been observed. The particles are made of basanitoid pyroclasts and correspond to aerial fallout of alkaline (sodic) basaltic affinity, common in the area, but distinct from the mafic magmas which formed the maar. They are probably aerial ejecta related to phreatomagmatic episodes of the neighbouring strombolian volcanoes or even to other maars like that occupied by Lake Disoni, 15 km to the North–West (Cornen *et al.*, 1992). The upper half of the core (Holocene) does not present distinct ash layers: pyroclasts are rare and dispersed in the sediments. Such scarcity is indicative of a more discrete or more remote volcanic activity. These Holocene pyroclasts seem similar to volcanic rocks from the Manengouba massif, about 40–60 km ENE of Barombi Mbo.

Based on the main pollen results (Maley and Brenac, 1998), four palaeoenvironmental phases were recognized (Figure 3): (1) from ca. 28,000 to 22,000 cal yr BP, the dominant forest environment contained mountain components, (2) from 22,000 to 14,000 cal yr BP with a mosaic of forest and savanna, (3) from 14,000 to 2600 cal yr BP, the environment is forested with forest maximum between 8900 and 3200 cal yr BP, (4) a new dry phase between 2600 and 2000 cal yr BP with temporary openings of the forest before forest recovery during the last two millennia (Maley, 2002).

4.4 SAMPLES AND METHODS

Seven corings were carried out using a HELIX hand auger. These corings were distributed over the whole lake watershed (Figures 2 and 4) and reached a maximum

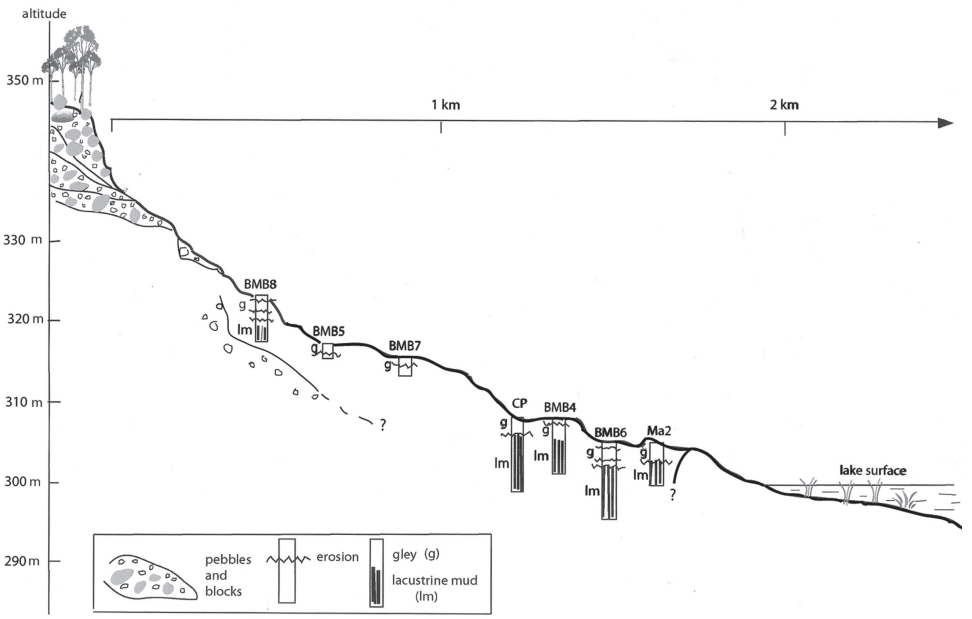

Figure 4. Cross-section of the drainage basin showing the location of the seven corings along the slope from the chaotic accumulation of Precambrian blocks down to Lake Barombi Mbo.

depth of 9.5 m; the limits of the penetration were being connected either to the depth of the groundwater table, or to ferruginous concretions at certain levels of iron nodules or siliceous gravel. Samples spaced out from 10 to 20 cm, sometimes less relating to the changes of sedimentary facies. After wet-sieving at 50 microns, the sand fraction was examined by stereomicroscope, and the clay fraction by X-ray diffraction (XRD) using cobalt Co Kα1 radiation. The shape and appearance of some grains were described using either a Hitachi Scanning Microscope (SEM) or, for chemical composition, using a fitted X-ray dispersive microprobe (Tracor). Whole-rock chemical analyses were undertaken by CRPG-CNRS, Nancy.

Several samples are siderite-rich, due to decarboniation by HCl 2 N for six hours before organic carbon dosage in the LECO. The efficiency of the elimination of the siderite was verified by X-ray diffraction.

An important part of the sediment corresponds to hydromorphic soils. The terms 'gley' and 'pseudogley' horizons were criticized because of their usage which can be different; according to Duchaufour (1977, 1997), we shall use the qualifiers of 'reductic' and 'redoxic' from to the pedological reference table (Nizier, 1992). Horizons with homogeneous distribution of Fe^{2+} are of reductic type and horizons with heterogeneous distribution of Fe^{2+} and Fe^{3+} are of redoxic type.

The samples were treated by standard palynological techniques with the addition of the Lüber method for the most organic rich sediments (Faegri and Iversen, 1975). These samples were taken at the same intervals as those of lithologic analysis (Tables 1 and 2). Given the relative poverty in pollen probably due to former alteration, only the Clay Pit core provided statistically acceptable pollen data with percentages based on a sum of at least 300 to 400 pollen grains and fern spores. For the Mahongue-2 core, the pollen analysis gave only counts related to the main vegetation formations (Table 3).

Table 1. List of the pollen and spore taxa.

Spores	Trees	Trees
Spore monolète	**Pioneer Forest**	**Evergreen Forest**
Spore trilète	*Aidia* (Rubiaceae)	*Bersama abyssinica* (Melianth.)
Pteris	*Alchornea* (Euphorbiaceae)	*Bridelia* (Euphorbiaceae)
Grasses	*Allophylus* (Sapindaceae)	Caesalpiniaceae
Gramineae	Combretaceae	*Canthium* (Rubiaceae)
Amaranthaceae	*Elaeis guineensis* (Arecaceae)	*Cissus* (Ampelidaceae)
Liliaceae	*Hymenocardia ulmoides* (Euphorb.)	*Cnestis* (Connaraceae)
Compositae	*Macaranga* (Euphorbiaceae)	*Dacryoides* (Burseraceae)
Hygrophilous	*Mallotus* (Euphorbiaceae)	*Drypetes* (Euphorbiaceae)
Cyperaceae	*Pentaclethra* (Mimosaceae)	*Entandophragma* (Meliaceae)
Nymphaea (Nymphaeaceae)	*Pycnanthus* (Myristicaceae)	*Klainedoxa* (Irvingiaceae)
Polygonum (Polygonaceae)	*Ricinus* (Euphorbiaceae)	*Lophira* (Ochnaceae)
Lemna (Lemnaceae)	*Sapium* (Euphorbiaceae)	*Martretia quadricornis* (Euphorbiaceae)
Pandanus (Pandanaceae)	*Sesbania* (Papilionaceae)	*Mitragyna* (Rubiaceae)
Raphia (Arecaceae)	*Tetrorchidium* (Euphorbiaceae)	*Psychotria* (Rubiaceae)
Myriophyllum	*Trema* (Ulmaceae)	Sapindaceae
Justicia (Acanthaceae)	*Zanthoxylum* (Rutaceae)	Sapotaceae
	Semi-Deciduous Forest	*Symphonia* (Clusiaceae)
	Bosqueia (Moraceae)	*Syzygium* (Myrtaceae)
	Ceiba pentandra (Bombacaceae)	*Uapaca* (Euphorbiaceae)
	Celtis (Ulmaceae)	
	Nesogordonia (Sterculiaceae)	
	Piptadeniastrum (Mimosaceae)	
	Sterculiaceae	

Table 2a. Pollen analysis results including all the pollen counting and the percentages (Mahongue-2 core).

Levels/Depth **Estimated Chronology**	05–25 Late Holocene	%	%	96–126 Mid Holocene	%	%
TOTAL (Pollen & Spores)	**306**	–		**428**	–	
SPORES	*180	*58,4		*105	*24,5	
Spore monolète	153	50,0		85	19,9	
Spore trilète	14	4,6		16	3,7	
Pteris	13	4,2		4	0,9	
TOTAL (Pollen-Spores)	**126**			**323**		
HERBS	10	*3,2	7,9	16	*3,8	5,0
Gramineae	6	2,0	4,8	11	2,6	3,4
Amaranthaceae	1	0,3	0,8	0		
Liliaceae	1	0,3	0,8	0		
Compositae (echin.)	2	0,7	1,6	5	1,2	1,5
HYGROPHILES	32	*10,4	25,4	48	*11,2	14,9
Cyperaceae	3	1,0	2,4	16	3,7	5,0
Nymphaea	0	0,0		0		
Polygonum	0	0,0		0		
Lemna	24	7,8	19,0	15	3,5	4,6
Pandanus	0			0		
Raphia	0			6	1,4	1,9
Myriophyllum Halo.	0			2	0,5	0,6
Justicia Acant.	5	1,6	4,0	9	2,1	2,8
TREES	84	*27,7	66,7	259	*66,4	80,2
PIONEERS	76	*25,2	60,3	177	*47,3	54,8
Aidia Rub.	0			3	0,7	0,9
Alchornea Euph.	33	10,8	26,2	55	12,9	17,0
Allophylus Sap.	0			2	0,5	0,6
Antidesma Euph.	0			0		
Bosqueia Mora.	0			0		
Cissampelos Menis.	0			0		
Combretaceae	4	1,3	3,2	7	1,6	2,2
Elaeis Palm.	28	9,2	22,2	30	7,0	9,3
Hymenocardia ulmoides Euph.	2	0,7	1,6	14	3,3	4,3
Macaranga Euph.	0			4	0,9	1,2
Mallotus Euph.	0			8	1,9	2,5
Malpighiaceae	0			1	0,2	0,3
Menispermaceae	0			1	0,2	0,3
Oldenlandia Rub.	1	0,3	0,8	0		
Pentaclethra Mimo.	0			25	5,8	7,7

(*Continued*)

Table 2a. *Continued.*

Levels/Depth **Estimated Chronology**	05–25 Late Holocene	%	%	96–126 Mid Holocene	%	%
Petersianthus Lecyth.	0			0		
Pycnanthus Myris.	5	1,6	4,0	15	3,5	4,6
Ricinus Euph.	0			2	0,5	0,5
Sapium Euph.	0			2	0,5	0,5
Sesbania Papil.	1	0,3	0,8	1	0,2	0,3
Spondianthus Euph.	0			1	0,2	0,3
Tetrorchidium Euph.	3	1,0	2,4	1	0,2	0,3
Trema Euph.	1	0,3	0,8	0		
Zanthoxylum Rut.	0			5	1,2	1,5
SEMI-DECIDUOUS	*0			30	*7	9,3
Ceiba pentandra Bomb.	0			8	1,9	2,5
Celtis Ulm.	0			1	0,2	0,3
Nesogordonia Sterc.	0			0		
Piptadeniastrum Mimo.	0			18	4,2	5,6
Sterculiaceae	0			3	0,7	0,9
EVERGREEN	8	*2,5	7,9	52	*12,1	16,1
Apocynaceae	0			1	0,2	0,3
Bersama abyssinica Melia.	0			2	0,5	0,5
Bridelia Euph.	0			18	4,2	5,6
Caesalpiniaceae	1	0,3	0,8	5	1,2	1,5
Canthium Rub.	0			2	0,5	0,5
Cissus Ampel.	0			4	0,9	1,2
Cnestis Conna.	0			0		
Dacryoides Burs.	0			0		
Drypetes Euph.	1	0,3	0,8	3	0,7	0,9
Entandophragma Mel.	0			0		
Ficus Mora.	0			1	0,2	0,3
Klainedoxa Irv.	0			1	0,2	0,3
Lophira Ochn.	0			2	0,5	0,5
Martretia quadricornis Euph.	0			2	0,5	0,5
Mitragyna Rub.	0			6	1,4	1,9
Psychotria Rub.	0			0		
Sapindaceae	0			3	0,7	0,9
Sapotaceae	0			0		
Symphonia Clus.	0			1	0,2	0,3
Syzygium Myrt.	0			0		
Uapaca Euph.	6	2,0	4,8	1	0,2	0,3

Table 2b. Pollen analysis results including all the pollen counting and the percentages (Clay pit core).

Levels/Depth **Estimated Chronology**	30–40 Late Holocene	%	95–120 Mid Holocene	%	134–164 Early Holocene	%	225–245 End Pleistocene	%
TOTAL (Pollen & Spores)	**62**	–	**86**	–	**83**	–	**142**	–
SPORES	*49	*79	*68	*79,1	*57	*68,7	*28	*19,7
Spore monolète	33	53,2	47	54,7	53	63,9	26	18,3
Spore trilète	16	25,8	21	24,4	4	4,8	0	
Pteris	0		0		0		2	1,4
TOTAL (Pollen-Spores)								
HERBS	*0		*0		*2	*2,4	*32	*22,5
Gramineae	0		0		2	2,4	30	21,1
Amaranthaceae	0		0		0		1	0,7
Liliaceae	0		0		0		0	
Compositae (Echin.)	0		0		0		1	0,7
HYGROPHILES			*7	*8,1	*9	*10,9	*62	*43,6
Cyperaceae	0		0		7	8,4	57	40,1
Nymphaea	0		0		1	1,2	0	
Polygonum	0		0		0		2	1,4
Lemna	0		0		0		2	1,4
Pandanus	0		7	8,1	1	1,3	0	
Raphia	0		0		0		0	
Myriophyllum Halo.	0		0		0		0	
Justicia Acant.	0		0		0		1	0,7
TREES	*13	*26,9	*11	*12,8	*15	*19,2	*20	*14
PIONEERS	*7	*11,2	*10	*11,6	*7	*9,1	*6	*4,2
Aidia Rub.	0		0		0		0	
Alchornea Euph.	2	3,2	2	2,3	1	1,3	3	2,1
Allophylus Sap.	0		0		0		0	
Antidesma Euph.	0		0		0		1	0,7
Bosqueia Mora.	3	4,8	0		0		0	
Cissampelos Menis.	0		0		0		1	0,7
Combretaceae	0		0		1	1,3	0	
Elaeis Palm.	0		0		0		0	
Hymenocardia ulmoides Euph.	0		0		0		0	
Macaranga Euph.	0		0		0		0	
Mallotus Euph.	0		8	9,3	2	2,6	1	0,7
Malpighiaceae	0		0		0		0	
Menispermaceae	0		0		0		0	
Oldenlandia Rub.	0		0		0		0	
Pentaclethra Mimo.	0		0		0		0	
Petersianthus Lecyth	0		0		1	1,3	0	

(*Continued*)

Table 2b. *Continued.*

Levels/Depth **Estimated Chronology**	30–40 Late Holocene	%	95–120 Mid Holocene	%	134–164 Early Holocene	%	225–245 End Pleistocene	%
Pycnanthus Myris.	1	1,6	0		0		0	
Ricinus Euph.	0		0		0		0	
Sapium Euph.	0		0		0		0	
Sesbania Papil.	0		0		0		0	
Spondianthus Euph.	0		0		0		0	
Tetrorchidium Euph.	0		0		0		0	
Trema Euph.	0		0		2	2,6	0	
Zanthoxylum Rut.	1	1,6	0		0		0	
SEMI-DECIDUOUS	*0		*0		*1	*1,3	*0	*0
Ceiba pentandra Bomb.	0		0		0		0	
Celtis Ulm.	0		0		0		0	
Nesogordonia Sterc.	0		0		1	1,3	0	
Piptadeniastrum Mimo.	0		0		0		0	
Sterculiaceae	0		0		0		0	
EVERGREEN	*6	*9,7	*1	*1,2	*7	*8,8	*14	*9,8
Apocynaceae	0		0		0		0	
Bersama abyssinica Melia.	0		0		0		0	
Bridelia Euph.	1	1,6	0		0		0	
Caesalpiniaceae	0		0		0		0	
Canthium Rub.	0		0		0		1	0,7
Cissus Ampel.	0		0		0		0	
Cnestis Conna.	0		0		3	3,6	0	
Dacryoides Burs.	0		0		0		1	0,7
Drypetes Euph.	0		0		0		0	
Entandophragma Melia.	0		0		0		3	2,1
Ficus Mora.	0		0		0		0	
Klainedoxa Irv.	0		0		1	1,3	0	
Lophira Ochn.	0		1	1,2	0		0	
Martretia quadricornis Euph.	0		0		0		1	0,7
Mitragyna Rub.	0		0		0		0	
Psychotria Rub.	0		0		0		2	1,4
Sapindaceae	0		0		0		0	
Sapotaceae	0		0		2	2,6	5	3,5
Symphonia Clus.	0		0		1	1,3	0	
Syzygium Myrt.	0		0		0		1	0,7
Uapaca Euph.	5	8,1	0		0		0	

Table 3. Synthetic pollen analysis results with the main percentages, classified following the grouping presented in Table 2.

	Mahongue 2		**Mahongue 2**		**Clay Pit**			
	Holocene		Holocene		Holocene			End Pleistocene
	Late	Mid	Late	Mid	Late	Mid	Early	
Core depth (m)	5–25	96–126	5–25	96–126	30–40	95–120	134–164	225–245
Basic Count (P + SP)	306	428			62	86	83	142
Spores (%)	58,8	24,5			79	79,1	68,7	19,7
Basic Count (P – SP)			126	323				
Herbs (total, %)	3,3	3,8	8	4,9	0	0	2,4	22,5
Graminae	2	2,6	4,8	3,4	0	0	2,4	21,1
Hygrophilous	10,5	11,2	25,4	14,9	0	8,1	10,9	43,6
Cyperaceae	1	3,7	2,4	5	0	0	8,4	40,1
Trees (total, %)	27,4	66,4	66,7	80,2	20,9	12,8	19,2	14
Pioneer	24,8	47,3	60,3	54,3	11,2	11,6	9,1	4,2
Elaeis guineensis	9,2	7	22,2	9,3	0	0	0	0
Semi-deciduous	0	7	0	9,3	0	0	1,3	0
Evergreen	2,6	12,1	6,4	15,5	9,7	1,2	8,8	9,8

Table 4. ^{14}C and calibrated ages for Clay Pit, Mahongue, BMB6 and BMB4 cores. Dates are from organic matter in bulk sediment samples. Calibrated ages are reported on the basis of the CalPal-2007 online version based on Weninger and Jöris (2008).

Core number	Depth core (cm)	Lab. no.	Conventional ^{14}C age (yr BP)	Calendar age (cal yr BP)	
				Mean	68% range cal BP
Clay Pit	335–348	Beta-74230	27,400 ± 450	32,127 ± 394	31,732–32,521
Clay Pit	790–805	Beta-74229	30,710 ± 1460	35,375 ± 1675	33,700–37,050
Clay Pit	885–901	Beta-74228	34,140 ± 1370	38,799 ± 1792	37,006–40,591
Mahongue	265–290	Beta-74231	20,740 ± 340	24,782 ± 521	24,261–25,303
Mahongue	382–407	Beta-74232	31,990 ± 2890	36,907 ± 3033	33,873–39,940
BMB6	360–370	Beta-099368	34,050 ± 1440	38,704 ± 1855	36,848–40,559
BMB6	924–959	Beta-099366	38,250 ± 950	42,820 ± 818	42,001–43,368
BMB4	546–504	Beta-?	42,060 ± 1310	45,762 ± 1463	44,299–47,225

The chronology has been determined from radiocarbon analyses on organic fraction after carbonate (siderite) dissolution (Beta Analytic, Miami). All ages are reported in the text in calibrated age. For comparison with previous studies, Table 4 includes the various equivalences according to CalPal-2007 (online version) which is described by Weninger and Jöris (2008).

4.5 OBSERVATIONS AND ANALYSES

The sites of the corings will be presented according to a globally downstream-upstream order, i.e., according to an increasing distance from the site of the pro-delta of the Toh Mbok River. Therefore, the sites of the lowest altitude will be considered first.

4.5.1 Clay Pit

The coring is situated on the right bank of the Mahongue River at an altitude close to 308 m asl spanning 9 m in depth. From 9 m to 2 m, we observe a clayey-sandy deposit with more sandy layers, towards 830 cm, 480 cm and 260 cm (Figures 5, 6). Independently of the grain size, the almost black pigmentation towards the base is associated with carbon organic contents close to 10%. The sediment is first slightly layered (millimetre-thick laminae) and passes around 8 m to a dark blue colour with dark nodules, then above 3.50 m to ultramarine to Prussian blue colour. Between 3.30 m and 3.10 m, there is again a blackish deposit associated with a 25% organic carbon content covered by a bluish sediment up to 2 m. Above 2 m, we observe a grey-blue deposit of gley type with numerous pipes and ochre spots which are locally hardened in ferruginous granules and nodules; the texture remains very sandy up to the surface which is represented by a humiferous horizon of the present soil. Siderite is present across the whole vertical line, but it is more abundant below 2 m and particularly in the most organic levels: 18.8% in 3.30 m (Figure 6). The vivianite is also quite ubiquitous in all blue and black levels; its nodules are more abundant in the clayey levels directly covered by sandy levels, in particular just above 8 m.

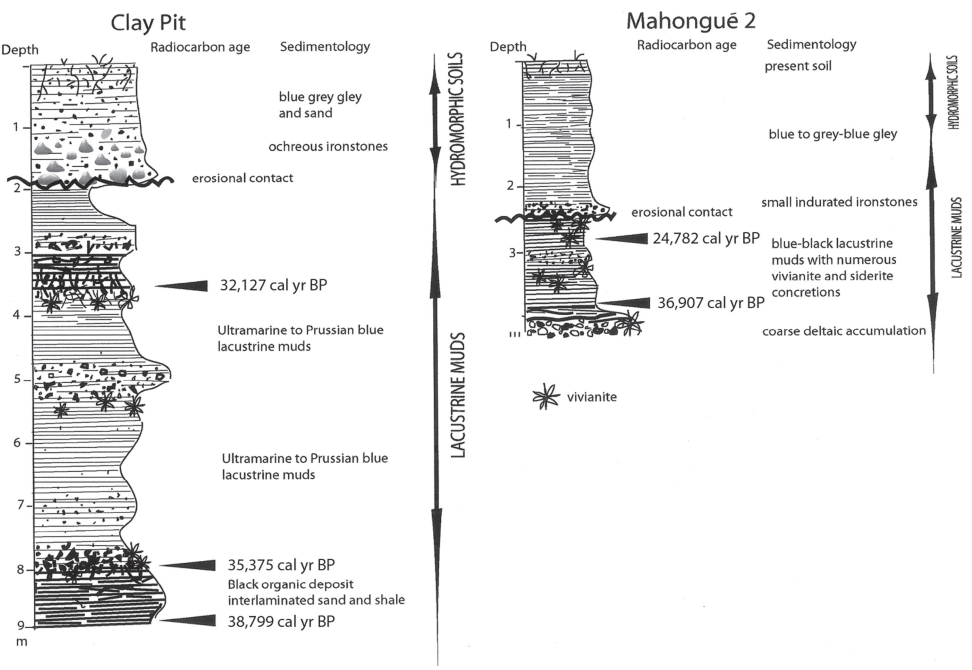

Figure 5. Simplified lithologic logs of Clay Pit (CP) and Mahongue (Ma2) cores showing the position of erosional contacts, neoformed aggregates and the ages from radiocarbon dating.

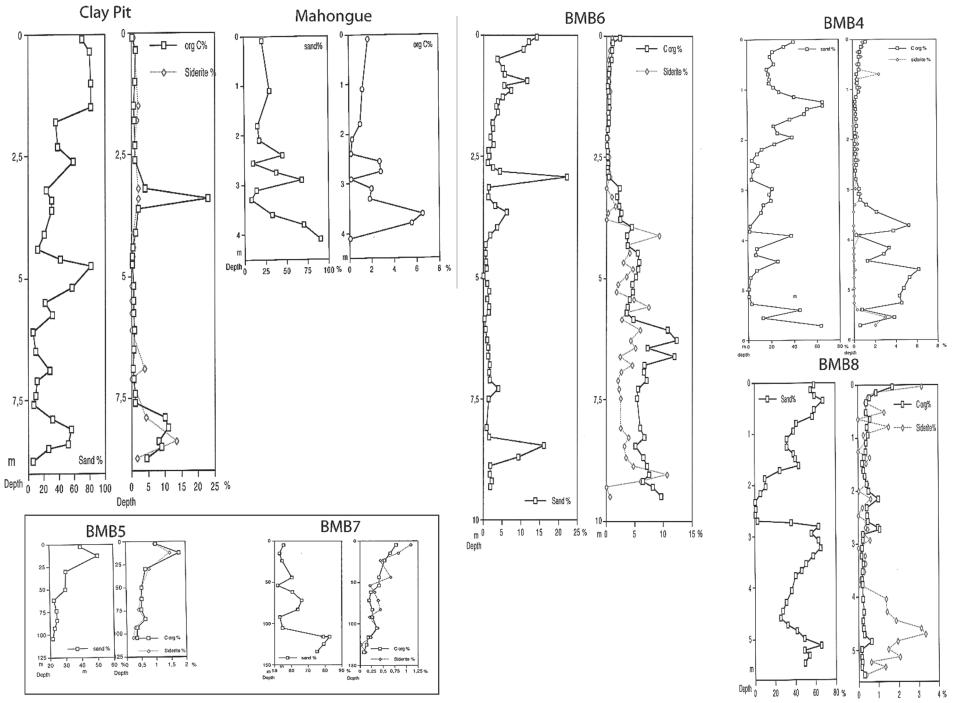

Figure 6. Vertical distribution of sand, organic carbon, siderite contents of the seven core sections (Clay Pit, Mahongue, BMB6, BMB4, BMB5, BMB7 and BMB8).

Under the microscope, the most poorly sorted sandy fraction consists of quartz, muscovite and feldspars, the latter decrease in the lower gley of the section. Gravels from sandstone, gneiss and sometimes basalt are observed in the sandy layer at 8 m depth. Volcanic glasses and magnetite granules are rather frequent, but also decrease towards the top of the section. The abundance of vegetal fibres and charcoal fragments in the upper two meters of the section has to be noted.

With the SEM, we observe an abundance of Silicospongiae spicules in the lower meter of the section (Figure 7f). Some bone fragments of fish are noted towards 8.50 m. In the blue levels of the accumulation, siderites appear in millimetre-large cauliflowers (Figures 7d, e). The rosettes of vivianite can reach a diameter of one centimetre where the iron phosphate is often more or less amorphous in the central part and crystallized in its radial outer part (Figures 7a, b, c).

15 palynological samples were prepared, but only 4 samples above 2.50 m depth (2.45–2.25 m, 1.64–1.34 m, 1.20–0.95 m, 0.4–0.3 m) stood out to exhibit some pollen, grains and spores, with a weak sum going from 62 to 142, so the calculated "percentages" gave just a global indication. The organic rest of the levels below 2.50 m are much altered and contain only monolet spores in a great number below 2.90 m, decreasing strongly or even disappearing particularly below 8 m. The 0.25–0.05 m level which is linked to the current humiferous soil contains only spores.

The uppermost three levels are relatively poor in pollen and widely dominated by the spores representing ca. 69 to 79%. The level 2.25–2.45 m is an exception with contents in spores not exceeding 20%. All the percentages of taxa were calculated by including spores. The level 2.45–2.25 m gives a very differing result from the three

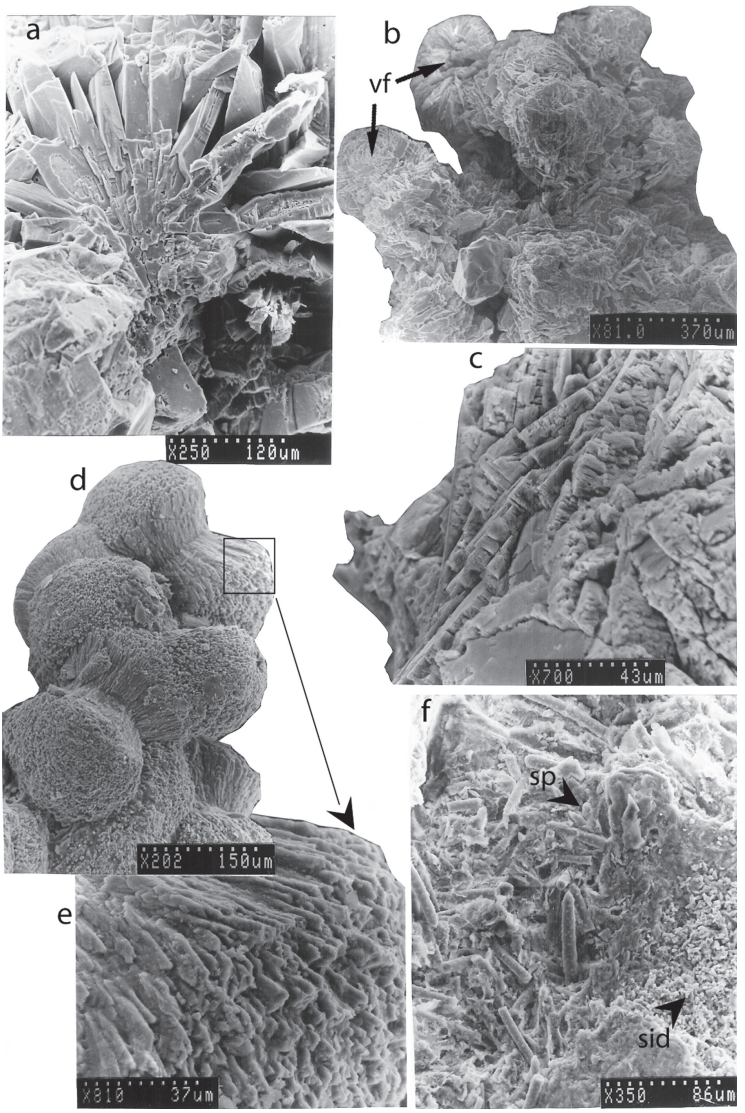

Figure 7. Scanning electron micrographs from Clay Pit core. **a.** 868–848 cm: stellate cluster of typically prismatic crystals of vivianite; **b.** 672–642 cm: radiating structures of blade-like shapes of vivianite around vegetal fibres (vf); **c.** 515–502 cm: surface of a vivianite nodule showing tabular masses of flattened crystals with lamellar twinning; **d., e.** 755–725 cm "grape-like" rounded forms of groups of siderite microcrystals, detail of apical end of microcrystals; **f.** 848–830 cm: transition from spicules-rich sponge (sp) microlamina to clay-rich microlamina containing microcrystals of siderite (sid).

overlying levels by the importance of herbaceous plants' pollen, approximately 22%, which corresponds almost exclusively to Gramineae reaching 21%. The hygrophilous plants decreases sharply in the overlying levels (10%, 8%) to disappear between 0.3 and 0.4 m.

The raised forest tree taxa are represented well enough in all the levels with ratio varying between 14 and 27%. This highest value was recorded in the top level of the

section (0.4–0.3 m). Especially pioneer forest taxa dominate (9 to 12%) in the three uppermost levels, except 2.45–2.25 m level containing a rather low content in forest pioneer trees' taxa (4%) and a relatively high content of the evergreen forest taxa (about 10%).

4.5.2 Mahongue 2 (Ma2)

The site close to the equally named river is located at an altitude of 305 m asl (Figure 4). The coring stopped at 4.10 m depth near the altitude of the present surface of Lake Barombi Mbo. The sedimentary column exhibits a dark blue to black colour in its lower half and clears up in the uppermost half (Figure 5). Between 4.00 and 3.80 m, we note a layered trend with more micaceous microbeds. The accumulation of organic carbon is greater in the dark beds inserted between the sandy layers in particular between 4.00 m and 3.50 m where the content reach 7%. It remains rather low in the upper 2.50 m where the content do not exceed 2% (Figure 6). Concretions of vivianite and siderite nodules increase below 2 m. Siderite is especially abundant in the first meter of the column (up to 6%) where it is more or less bound to the organic matter (Figure 10). Contrary to the nearby sounding at the Clay Pit, we observe no streaked facies of swampy gleys. Only the presence of ferruginous grains hardened around 2.30 m could indicate a fleeting tendency to the emersion, possibly accompanied by an erosive process.

Under the microscope, the sandy fractions consist of quartz, micas and feldspars associated with some volcanic glasses that are more abundant in the lower half of the column. Several gravels consisting of granite and sandstone are associated with the sandy deposits of the lower part of the section. Charcoals are restricted to the last meter, but we do not find vegetal fibres distinctive of the gley deposit of the Clay Pit, except in the superficial soil horizon.

In the SEM examination, the proximity of the basalt bedrock is attested by the presence of the remains of Silicospongiae tissues, in particular around 2.60–2.50 m (Figure 8a). The nodules of vivianite can reach a diameter of approximately one centimetre with the development of radial slates or needles (Figure 8b). In the black levels of the lower part of the section, the lacustrine organic matter contains *Botryococcus* and other *Cyanophyta* (around 2.30 m).

Palynological samples were systematically prepared but as in the case of the Clay Pit, only the highest levels of the section (1.26–0.96 m, 0.25–0.05 m) present a rather significant abundance in pollens associated to monolet spores (Table 2). Spores are still abundant in 2.90–2.65 and 2.40–2.25 m, but are very rare in 4.07–3.82 m, 3.45–3.20 m, and 3.00–2.90 m. Comments will refer to percentages excluding spores as in the case of the Clay Pit. The herbaceous plants are poorly represented in both studied levels, they reach respectively 3.8% in 1.26–0.96 m and 3.2% in 0.25–0.05 m. Hygrophilous plants of the swamp environment reach respectively 15% in 1.26–0.96 m and 25% in 0.25–0.05 m. Pollen assemblages show significant percentages of trees (e.g., 80% for the lowest level and 67% for the uppermost level). In both cases, the relatively wide taxonomic diversity must be underlined: 12 taxa for 0.25–0.05 m and 37 taxa for 1.26–0.96 m. Among arboreal taxa, the pioneer forest taxa are significantly dominant with 55% in 1.26–0.96 m and 60% in 0.25–0.05 m. This dominance of the pioneers can be explained by the extension of the swampy environment which characterizes the site, but also, especially for the uppermost level, by the progressive reconstruction of the forest setting. In the same level *Elaeis guineensis* occurs with a very high percentage of pollen reaching 22%. At 1.26–0.96 m, the development of the forest environment is well marked with approximately 15% of evergreen taxa and 9% of semi-deciduous taxa.

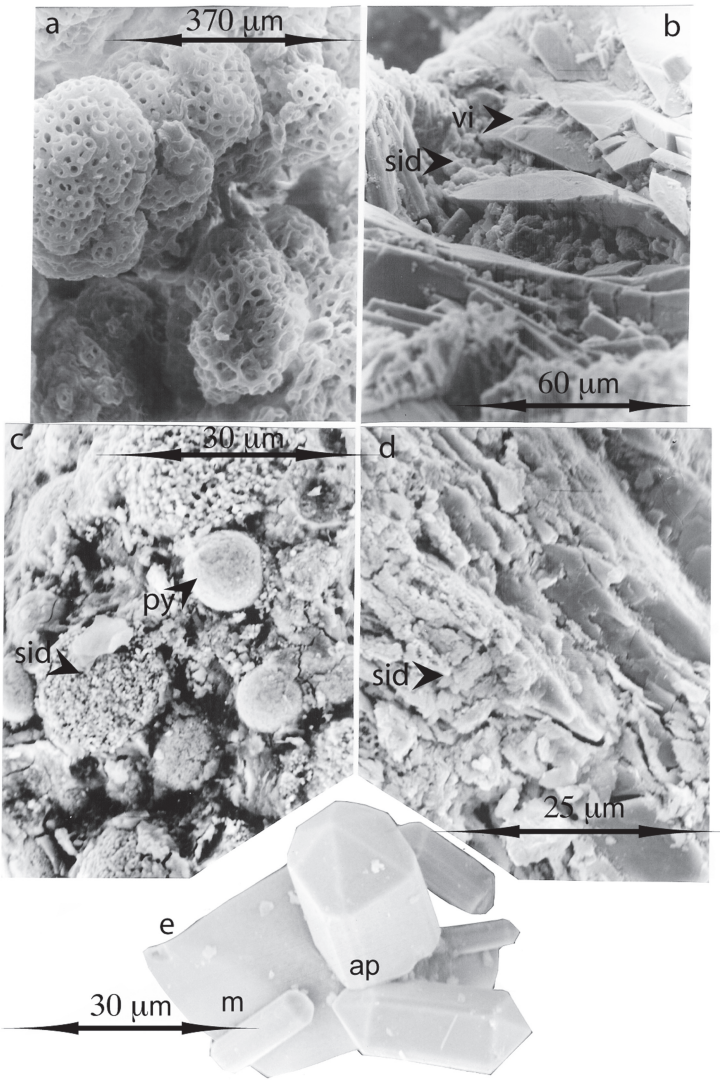

Figure 8. Scanning electron micrographs from Mahongue 2 (Ma2) and BMB6 cores. **a.** Ma2, 260–250 cm: Silicospongiae colonies included in siderite aggregates; **b.** Ma2, 240–225 cm: detail of the surface of a vivianite nodule, siderite microcrystals (sid) are included between vivianite blades (vi); **c.** BMB6, 458–442 cm: framboid pyrites (py) are associated with siderite aggregates (sid); **d.** BMB6, 389–370 cm: weathered facies, cleared siderite aggregate (sid) are bound to amorphous vivianite laths (vi); **e.** BMB6, 838–821 cm: hexagonal apatite sticks (ap) on octahedral magnetite (m).

4.5.3 BMB6

Taken at an altitude of 306 m asl (Figure 4), this 9.59 m long core shows, similar to the Clay Pit, the overlapping of a hydromorph redoxic deposit (gley) on a dark blue lacustrine deposit, but here the redoxic deposit has a substantial thickness of 3.70 m (Figure 9). The dark blue deposit contains few sand and organic clay including

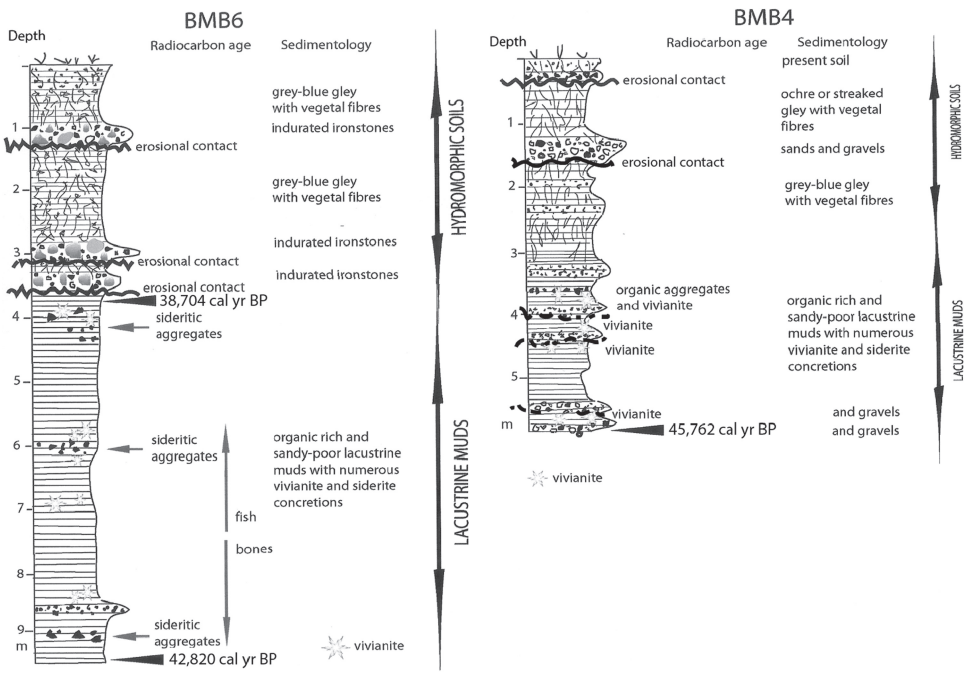

Figure 9. Simplified lithologic logs of BMB6 and BMB4 cores showing the position of erosional contacts, neoformed aggregates and the ages from radiocarbon dating.

recurrent concretions of vivianite and siderite. The gley above is light blue to grey with numerous spots and vertical cracks of ochre colour. It is affected by processes of hardening and concretion at three levels evolving finally in the formation of small ferruginous nodules. Upward, only some rare vivianite nodules are observed up to 1.90 m. The sand content is overall very low (2 to 3%) with some peaks from 10 to 20% which recur especially in the upper three metres (Figure 6). Contrarily, the organic carbon is more abundant in the clayey layers of the lowest three metres (6 to 12%). Then, it decreases in the two meters upward and remains lower than 1% in the gley levels. The rather abundant siderite in the lacustrine levels (4 to 10%) tends to disappear in the gley levels.

The microscopic analysis of sand reveals the dominating presence of white and unworn quartz linked to micas, feldspars, magnetite, pyroxene and volcanic glasses. The latter three tend to decrease in the gley deposits. Quartz grains present in gleys often show coatings with a metallic aspect associated by iron, manganese and titanium. Plant fibres are ubiquitously present mainly from 3.7 m up to the surface. The millimetre- to centimetre-long concretions of vivianite are abundant from the base to 4.0 m, but some are still observed up to 1.6 m. The spicules of Silicospongiae are especially connected to these concretions between 5.2 and 3.7 m, indicating also the proximity of the basaltic hard rock of the lake. Many fragments of fish skeleton (bones, teeth, scales) are regularly observed in the same interval.

The SEM revealed the presence of "cleared" siderite aggregates in several levels in particular at 3.6 m where they seem to be affected by possible emersions. The siderite can be inserted between the blades of other siderites during destructive processes

(no peak diffraction with the X-ray) (Figure 8d). Titanium-rich magnetite is very numerous, sometimes under an octahedral system, or associated with hexagonal forms doubtlessly allochthonous apatite (Figure 8e). At 4.50 m, young framboids of pyrite are observed, a totally unknown sulphide in the deep sediments of the nearby lake (Figure 8c).

4.5.4 BMB4

A 5.60 m depth coring was obtained on the right bank of the Mamy Emily River, which is located on the watershed between this river and the Soforth River (Figures 2 and 4). At an altitude of 305 m asl, this site is only 600 m away from the shore of Lake Barombi Mbo, from which it is isolated by a rim of basalt. A dark blue lacustrine facies is observed from the base to 2.85 m, a depth which coincides with the top of the phreatic level (Figure 9). The overlying redoxic facies begins with a grey-blue gley deposit including numerous spots with vertical elongation (former roots), then up to 1.20 m, the ochre and beige pigmentation becomes widespread. Nodule-like hardenings or concretions are observed around 0.30 m. The curve of sand content shows recurrent sandy segments which can exceed 60% (Figure 6). The sandier levels include some gravel and present graded bedding at their base. The high organic carbon contents are limited between the base and 3.40 m where they reach 4.6% in the inter-layered beds between the sandy peaks. In the upper three meters, they remain lower than 1%. Siderite is present on almost all the vertical line, but in a rather low concentration, only exceeding 2% towards 5.50 and 0.70 m (Figure 6).

Under the microscope, the sandy fraction is always poorly sorted and shows an association with minerals (quartz, muscovites, feldspars) and rocks of the Precambrian basement (sandstone and gneiss fragments) and with volcanic materials (glass, pyroxenes, magnetites, rare hornblendes, small basalt fragments) in unusual concentrations (up to 5% of the sandy fraction). In the gley layers, quartz with metallic black coatings is rather frequent and sometimes generating aggregates of grapestone type. Some show a ferromanganic structure with the remains of root sheathes being observed. Large vivianites concretions are often abundant below 3.00 m, but in the redoxic levels, some aggregates of dark blue colour are still observed.

In the SEM, the large radial vivianite crystallizations often show, even in the lacustrine levels, a partial destructive process: the core may be formed by amorphous crystallization or consists of goethite. In some redoxic levels, the siderite shows dissolution cavities or is transformed into goethite. With the microprobe, some black glasses present a composition close to that of chromium-rich spinel.

4.5.5 BMB5

The site is located at an altitude of 318 m asl close to the upstream part of the Mamy Emily River (Figures 2 and 4). The auger could not penetrate beyond 1.10 m because of adamant horizons of ferruginous nodules and plaques (Figure 10). Below the recent soil surface, the gley is grey to brown and very strongly oxidised. The brown and ochre nodules are especially observed between 0.96 and 0.80 m. The sand content regularly increases from the base to the top from 20 to 50% (Figure 6). The concentration in organic carbon which is only 0.3% in the gley, rises to 1.8% in the humiferous horizon (A) of the summit of the section. Siderite is not very abundant in these redoxic levels (0.2–0.4%). It rises up to 1.4% at the top of the section.

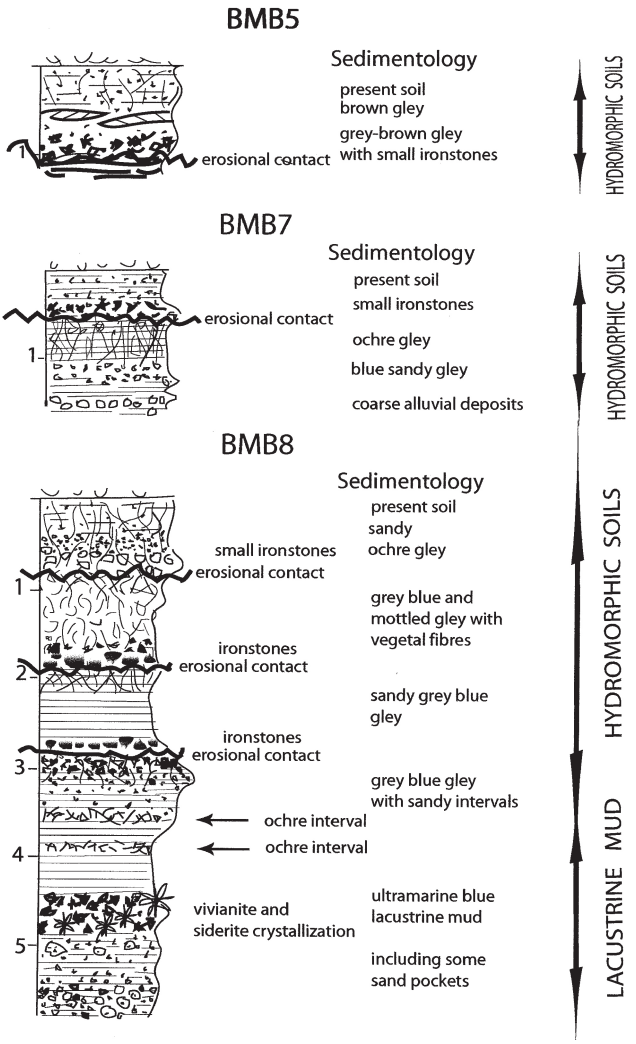

Figure 10. Simplified lithologic logs of BMB5, BMB7 and BMB8 cores showing the position of erosional contacts, neoformed aggregates.

4.5.6 BMB7

The site is at an altitude of 317 m asl on the hillside of the right bank of Kissaka River (Figures 2 and 4). The coring was not able to exceed 1.40 m in depth where it hits a 0.15 m thick rocky accumulation associated with a very compacted clayey matrix (Figure 10). These gravels are covered by a bluish sandy gley that quickly passes into the redoxic grey facies sometimes mottled with ochre dots. At 0.40 m, important ferruginous concretions give evidence of emersion conditions which remember those of BMB5. The current humiferous soil developed just above this level. The coarse deposit of the base corresponds to more than 82% of sandy fraction, and the gravels are composed of debris of the basement (sandstones, granites, gneiss). The sandy fraction decreases up to 55% near the surface. In this context of coarse sedimentation, organic carbon is very

low, increasing slightly upward and reaching 0.8% with increasing fine fraction. Also the siderite, very rare in bottom gravels, becomes abundant towards the top of the section (Figure 6).

Microscopic examination indicates the poor sorting of the coarse sand, which consists of white quartz and weakly dulled fragments of rock. Micas are still bound to the quartz grains. Further upward, particles are covered with ochre or metallic coatings. Vegetal fibres are abundant between 1.0 and 0.4 m depth. Volcanic glass is observed in low concentrations at all levels of the section, with exception of the bottom gravel; pyroxenes are associated to them in the upper 0.20 m.

4.5.7 BMB8

The core of 5.38 m was taken near the right bank of a small tributary of the Toh Mbok River at an altitude of 323 m asl which is the highest of the sites of this study (Figures 2 and 4). From the base to 3.80 m, we observe a rather sandy ultramarine blue deposit with numerous vivianite and siderite nodules, in particular between 4.90 and 4.60 m and above 3.80 m (Figure 10). This lacustrine deposit passes to a bluish grey gley which presents several recurrences of oxidised ochre layers. The presence of a high concentration of small gravels of ferric concretion is noted at 2.70 m, 1.80 m and 0.80 m. The sand and gravel contents are often high, reaching and even exceeding 60% (Figure 6). However, between 2.70 and 1.80 m, a very clayey episode interrupts this coarse accumulation. In connection with this large grain-size, the organic carbon is very low, generally less than 0.5% with the exception of the clayey layers and of the A horizon of the current soil. Siderite is rather abundant (up to 3%) in the lacustrine deposits between 5.38 m and 4.00 m, its contents are low and irregular in the redoxic levels of the gley (Figure 6). Microscopic examination reveals that the sandy fraction which associates quartzeous gravels, sand and silt with sometimes high muscovite content is always very badly sorted. This is characteristic concerning the abundance of polymineral grains (such as muscovite attached to quartz) which accompany fragments of sandstone, quartzite or gneiss. Quartz is white in the lacustrine levels whereas in the gley levels, some ochre quartz grains have one centimetre in diameter between 3.80 and 3.50 m and between 1.60 and 1.40 m. Some volcanic glass and pyroxenes are observed across the whole vertical line but with mainly low concentrations. Vegetal fibres and root remains are abundant from 1.50 m to the top.

Direct observations of the concretions of vivianite and siderite confirms, as in the other downstream sections, a greater abundance of these materials in the lacustrine levels, here in particular below 4.40 m. Close to 5.20 m the presence of large millimetre-long blades of well-preserved vivianite is to be noted. Both minerals are rare and degraded in the redoxic levels, their concretions disappear between 2.00 and 1.80 m.

With the SEM, in the redoxic levels the abundance of aggregates of quartz grains or ferruginous granules (facies grapestones) cemented by siderite oxidized in goethite and by kaolinite can be observed. Goethite epigenesis sometimes totally covers root remains.

Mineralogical and chemical analyses

The clayey phase is dominated by kaolinite associated with interlayered illite-smectite and a general vertical increase of kaolinite: in the Clay Pit, the ratio of kaolinite/interlayered illite-smectite is between 1.5 and 3 near the 4.40 m basis, then it is increasing between 6 and 10 in the upper redoxic levels, in BMB6, there is a rise of this ratio from the lacustrine deposits (1.5 to 3) towards the gleyey deposits (6 to 10), in BMB8, the ratio K/I-Sm varies between 5 and 8; in the lacustrine deposits below 4.50 m it is lower (2 to 5).

The whole-rock chemical analyses of the deep lacustrine sediment of Barombi-Mbo were realized to study the particularly favourable sedimentary environments in neo-formation of vivianite (Table 5). High contents in P_2O_5 rose in some levels from 0.6 to 1.97% (one value reaching 5.09%), particularly in the Pleistocene levels where small neo-formed vivianite crystals are more abundant than in Holocene ones (Giresse *et al.*, 1991). Sediments of Barombi present TiO_2 concentrations between 1.9 and 4.4%, those of Anloua have similar concentrations of TiO_2 between 3.5 and 5% (Oustrière, 1984).

Table 5. Chemical composition of Holocene and Pleistocene deep sediments of Lake Barombi-Mbo (<50 µm fraction).

Core depth (cm)	SiO_2	Al_2O_3	P_2O_5	Na_2O	K_2O	Fe_2O_3	TiO_2	MgO	CaO	MnO
Holocene										
20–30	42.7	25.1	0.95	0.27	1.26	20.2	4.05	1.15	0.17	0.47
120–130	40.5	25.6	0.87	0.10	0.57	22.03	4.05	1.04	0.08	0.44
220–230	39.9	24.9	0.87	0.13	0.56	26.18	3.31	0.99	0.08	0.20
310–320	40.35	24.96	1.12	0.12	0.58	19.83	4.16	1.10	0.08	0.40
410–420	44.01	28.09	1.06	0.10	0.66	18.39	4.41	1.10	0.65	0.31
510–520	41.65	25.82	1.03	0.21	0.59	22.02	4.13	1.2	0.42	0.11
560–570	38.58	24.34	1.09	0.11	0.57	18.40	3.80	1.01	0.02	0.53
650–670	46.14	28.86	0.93	0.13	0.66	15.52	4.36	1.2	0.13	0.31
850–860	44.34	27.82	1.04	0.09	0.52	18.88	3.80	1.07	0.17	0.50
940–950	44.95	26.26	1.42	0.13	0.69	18.26	3.81	1.15	0.14	0.39
Late Pleistocene										
1000–1010	43.49	27.34	1.10	0.09	0.60	17.52	3.94	1.08	0.13	0.58
1090–1100	45.10	28.36	1.07	0.09	0.53	16.38	3.31	0.98	0.14	0.64
1130–1140	42.04	25.2	1.14	0.14	0.59	22.71	3.95	1.01	0.09	0.36
1160–1170	50.13	17.26	1.38	0.30	0.70	20.7	2.98	1.50	0.30	0.82
1270–1280	50.95	18.17	1.24	0.36	0.73	20.54	3.17	1.68	0.42	0.78
1370–1380	51.68	19.94	0.59	0.33	0.94	16.69	3.15	1.83	0.38	0.27
1440–1450	46.10	20.04	1.33	0.37	0.70	20.47	3.83	1.77	0.66	1.58
1550–1560	39.29	20.42	1.1	0.22	0.73	27.35	3.72	1.34	0.29	1.13
1640–1650	39.40	12.48	1.21	0.27	0.62	41.37	1.91	1.24	0.55	2.78
1720–1730	49.72	17.81	1.05	0.41	0.71	21.05	3.10	1.57	0.56	1.25
1750–1760	47.24	15.51	1.08	0.31	0.55	25.21	2.81	1.47	0.62	1.48
1800–1810	43.78	15.90	1.16	0.31	0.67	26.12	2.84	1.52	0.46	0.90
1860–1870	29.64	11.89	1.89	0.19	0.53	43.01	1.96	1.15	0.40	3.0
1920–1930	51.88	20.48	1.42	0.31	0.84	23.88	3.56	1.61	0.03	0.67
2030–2040	31.70	12.66	1.80	0.21	0.45	40.38	2.28	1.17	0.48	7.27
2100–2110	46.36	17.48	1.16	0.78	0.90	24	2.98	1.95	1.39	1.87
2150–2160	40.93	16.66	0.97	0.83	0.91	19.39	3.84	1.84	0.40	0.97
2190–2200	45.82	24.3	1.70	0.24	0.73	21.61	3.29	1.44	0.30	0.85
2210–2220	46.48	19.64	1.96	0.25	0.76	22.85	3.31	1.56	0.16	0.51
2240–2220	48.41	20.58	1.66	0.24	0.78	20.65	3.44	1.66	0.24	0.36
2270–2280	51.20	23.13	0.97	0.35	0.94	21.90	3.64	1.75	0.38	0.47
2320–2330	43.68	18.76	1.97	0.27	0.75	21.76	3.32	1.51	0.30	0.70

4.6 AGES AND PALAEOENVIRONMENTAL INTERPRETATION

4.6.1 Clay Pit

Three radiocarbon ages were obtained: 38,799 cal yr BP at the basis (9 m), 35,375 cal yr BP at 8 m and 32,127 cal yr BP at 3,30 m. These dates enable the calculation of successive sedimentation rates of 29.2 cm/10^3 years, 14.5 cm/10^3 years and 10.3 cm/10^3 years (Figure 11). The slow-down of these rates may be connected to the proximity of the river. The recurrence of the sandy episodes gives evidence to the influence of the river's floods. However, this slow-down of the rate to one or several cut-and-fills which would have smoothed the top of the deposits, in particular around 1.80 m where a level of gley including strongly hardened ferruginous nodules, is present. The Holocene accumulation observed in the upper 1.20 m may correspond to a condensed series; the soil erosion also has to be suggested by the very coarse character of the deposits.

The pollen assemblage at 2.45–2.25 m indicates a widespread occurrence of herbaceous plants whereas the composition of forest taxa gives evidence of a higher representation of evergreen type than pioneer type species. Such characters are close to those of the LGM observed in the deep-water sediments of Lake Barombi-Mbo (Maley and Brenac, 1998). In coherence with the obtained ages and the palaeoenvironmental definition of the level 2.45–2.25 m, the important erosional contact which interrupts the lacustrine sedimentation at 2 m depth could correspond to the low level of the LGM and maybe also to that of the Younger Dryas without the possibility to separate both events. These palaeoclimatic processes were probably combined with

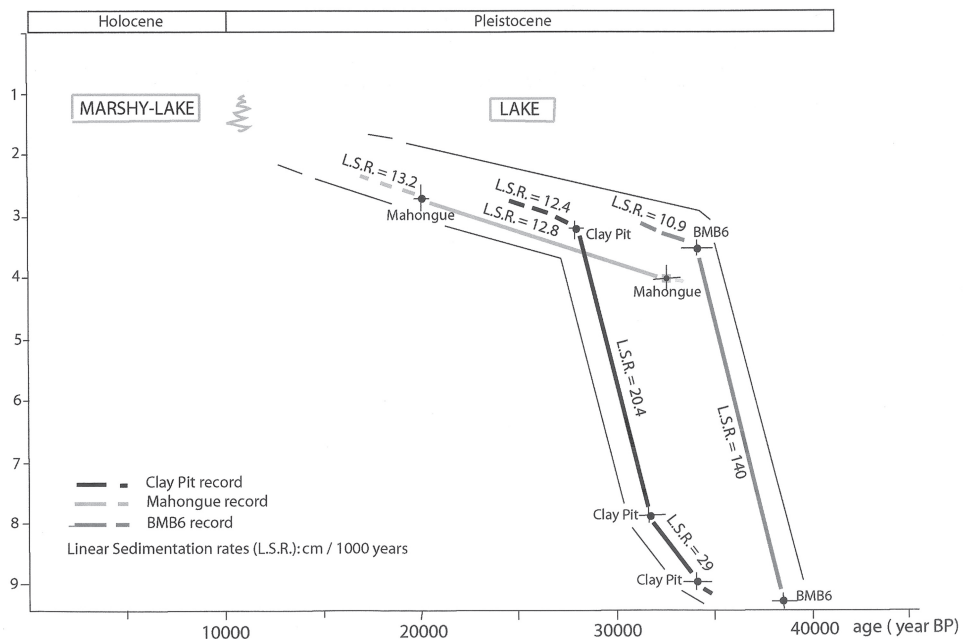

Figure 11. Continuous lines represent the age-depth function of Clay Pit, Mahongue and BMB6 cores with their corresponding linear sedimentation rates (LSR). A rough wrapping curve indicates the general decrease of linear sedimentation rates during the marshy-lake interval.

the progression of the outlet erosion (Figure 11). The three top levels, always considered to be related to the deep-water BM6 core, show compositional characteristics of the Early Holocene (1.64–1.34 m), the Mid-Holocene (1.20–0.95 m) and the Late Holocene (0.40–0.30 m) respectively. The upward succession is underlined by the presence of forest tree taxa, particularly of pioneer type, and also by the poverty in grasses and by the progressive decrease of swampy environment taxa. Pollen are absent in the deepest levels, therefore the abundance of spores between 8 and 6 m core depth need to be linked with the recurrence of soil erosion, particularly between 7.85 and 7.55 m.

4.6.2 Mahongue 2 (Ma2)

On the basis of two radiocarbon ages, 36,907 cal yr BP at the base (4.10 m) and 24,782 cal yr BP at 2.75 m, a remarkably constant sedimentation rate was calculated over the whole column: 11.13 cm/10^3 years between 36,907 and 24,782 cal yr BP and 11.09 cm/10^3 years after 24,783 cal yr BP (Figure 11). This site, at the lowest altitude of the study area, seems to have remained constantly immersed until quite recent times. The final emersion intervened without the swampy transition which is observed at the nearby Clay Pit. Between 4 and 2 m depth, the proxies that witness a lacustrine sedimentary environment are varied: tissues and Silicospongiae spicules, beginnings of beddings towards the base, extended aquatic diagenesis of the vivianite and the siderite and accumulations of very organic clayey muds incompatible with a swamp or river environment. In spite of the evidence of a first erosion episode around 2.30 m depth, we can envisage a nearly continuous lacustrine sedimentation, even if above this depth, the environment was credibly more littoral.

Considering the chronology of the deep water BM6 core taken in the centre of the lake (Maley and Brenac, 1998), ascribed 1.26–0.96 m and 0.25–0.05 m levels to the Mid and Late Holocene respectively. The Mid-Holocene is attested by the relative importance of forest tree pollen showing a rather wide diversity of taxa in which the evergreen and deciduous species are represented. Moreover the widely dominant forest environment is attested by the low contents in Gramineae pollens. The Late Holocene is characterized by the low herbaceous pollen contents. This parameter is an indication of sedimentation probably later than the major phase of landscape opening which ended by c. 2000 BP in the BM6 core of the deep lake. Forest tree taxa are abundant during this period as in the Late Holocene of the Clay Pit. The taxonomic diversity is relatively low and underlines a forest setting in reconstruction process. The large abundance of pollen of *Elaeis guineensis* could be correlated to that observed during the last thousand years of BM6 deposition.

In the context of palaeoenvironmental evolution, the erosional contact observed towards 2.30 m (just after 24,782 cal yr BP) may be related to the LGM main lake low level with possibly, as at the Clay Pit, another phase during the Younger Dryas event. This erosional contact is underlined by the abundance of spores in particular at the level of 2.40–2.25 m core depth.

4.6.3 BMB6

The base of the core of 9.60 m depth is dated to 42,820 cal yr BP, whereas the upper limit of the dark blue deposits at 3.70 m depth has an age of 31,704 cal yr BP. The sedimentation rate of the lacustrine blue deposits with 53 cm/10^3 years is high, and hence of the same order as at the deep lake (Giresse *et al.*, 1991). Later, the overlying swamp

deposits correspond to a global rate of sediment accumulation of 11.6 cm/10^3 years, which is closer to the value of the Clay Pit and Mahongue 2 (Figure 11). Our comments about the lacustrine deposits suggest a relatively deep-water sedimentation, attested by minor sandy fraction and, possibly by the unusual abundance of fish remains in these deposits. The presence of pyrite in the lake environment could be associated to the inheritance of allochthonous materials such as the tuff-ring breccia.

The swamps coming after the lacustrine environment favoured the weathering and erosion of the uppermost lacustrine deposits still containing some degraded vivianite nodules up to 1.90 m deep. Three ferruginous concretion-rich levels are identified close to 3.60, 3.05 and 1.00 m depths. Although no datings are available concerning the succession of the swampy deposits, it is suggested that both erosional contacts below 3 m depth are equivalent to both lake level declines during the LGM deduced from analogy with fluctuations of the lake level which is recognizable from from pollen content of Cyperaceae (Maley and Brenac, 1998; Maley, 2004). The one close to 1 m depth could correspond to the negative oscillation of the YD. The emersion trend was associated with erosional processes resulting in a globally rather low sediment accumulation rate.

4.6.4 BMB4

The site, slightly isolated from the lake, is near the channel of a river which flows on basalt and pyroclastic breccias along its right bank. The sediment shows strong recurrence of coarse alluvial layers (gravels, rock fragments) with an unusual proportion of materials in the sediment derived from the erosion of lavas and tuffs. From the geochemical point, the titanium credibly stemming from magnetite participates in the composition of the metallic coatings of the grains of the gley levels.

At the end of the Pleistocene, this site probably acted as a sort of small appendix of the main deep lake, even if it not contains coarse sediments representing the last 25,000 years. Only the basis of the section was object of radiocarbon dating: the age of 45,762 cal yr BP allows calculating an average sedimentation rate in the order of 11.5 cm/10^3 years. This average rate probably reflects fast lacustrine and then slower swampy sedimentation. A single level, suggesting both the emersion and the erosion, was characterized around 0.30 m depth that is close to the end of the sedimentary history. By analogy with the transition from the lacustrine environment towards the swampy environment observed in BMB6, the sandy levels present in the lower half of the section could correspond to the LGM and the very sandy level at 1.30 m to the YD. The similar transition from a lacustrine to a swampy sedimentation with the development of abundant vegetation may be explained only by marked lowering of the lake level.

4.6.5 BMB5

The insufficiency of the organic matter did not allow radiocarbon dating. The palaeogeographic interest of this little section is twofold. (1) The relative abundance of the sandy fraction testifies the strongly alluvial character of this accumulation which is similar to that observed at the downstream site of the same river (BMB6). (2) The exceptional oxidation and dehydration character of the levels between 1.10 and 0.80 m observed during the study express a prolonged emersion (final one) probably accompanied with distinct runoff.

4.6.6 BMB7

The contents in organic matter are too low to allow radiocarbon dating. The very pronounced alluvial character is explained by the proximity of Kandissa River. The coarse basal level is the most gravely encountered in this study. The polymineral character of certain gravels is a sign of the proximity of its source. The mixture of the basement minerals and the volcanic particles suggests erosion of peripheral volcanic tuffs. The strong accumulation of ferruginous concretions around 0.30 m depth indicates the final emersion that favoured the current soil development. It is likely that the top of the gley was more or less furrowed during the same period as observed at the top of BM4.

4.6.7 BMB8

This site is at the furthest upstream point of the watershed. In spite of an altitude of 323 m, i.e., more than 20 m above the present lake level, it is surprising to observe also the same succession from lacustrine deposits to swampy deposits. Unfortunately, the very low contents in organic matter do not favour any radiocarbon dating. The swampy deposits show a 3.80 m thick succession. Three accumulation layers containing hardened ferric pieces of gravel indicate an emersion tendency and probably the erosion of the nearby surface.

4.7 DISCUSSION

4.7.1 The distinctive facies of lake and swamp

In this study, the lower parts of the low-altitude sections show the presence of dark blue to black accumulations, generally of varied size and rich in organic matter. These sediments frequently contain Silicospongiae spicules and remains of tissues, more rarely fish remains. Sometimes micaceous varves are present which remember certain facies from the lacustrine platform off the mouth of Toh Mbok River. These characteristics define lacustrine conditions, probably rather littoral, whose lateral or vertical changes in grain-size are connected to the evolution of a deltaic landscape in decades-cycle floods (Giresse *et al.*, 1991). As in the Mamy Emily River valley, more sheltered depressions acted as lake appendices and facilitated more clayey and organic sedimentation. It has to be noted that, generally, the organic carbon contents are of the same order than those recorded in the deep-water deposits of the lake.

The upper parts of the low altitude sections and the major parts of the high altitude sections show grey-blue accumulations with ochre spots, implying heterogeneous distribution of iron and its redoxic character which corresponds to pseudo-gleys. They are hydromorphic soils affected by temporary surface water in contrast to gleys which are formed under permanent water-saturation (Duchaufour, 1977; Duchaufour, 1997). Such gleys of reductic type characterised by homogeneous distribution of the iron seem to be poorly represented in these accumulations because permanent water saturation was not achieved when the emersion intensified.

On the other hand, in some examples we observe black-grey deposits, rich in organic matter and including big nodules of partially weathered vivianite: such horizons could indicate either a stage from lacustrine environment to seasonal swampy environment or a hydromorphic pedogenetic top of the lacustrine sediment. Such cases

are presumed in BMB4 (3.00–2.80 m), in BM8 (4.40–4.00 m), in BM6 (3.50–3.20 m) and in the Clay Pit (2.20–1.90 m).

4.7.2 Filling and drainage of the catchment basin

The shape of the catchment basin, in particular the watershed near an altitude of 360 m, evokes the initial caldera suggested by the map of Dumort (1968). However, it seems much less deep than the second one presently occupied by the lake.

In several points of the stream thalweg, in particular Toh Mbok River, the granito-gneissic basement crops out. The outer rim of 360 m altitude also includes basement outcrops. The soundings carried out were able to penetrate just to 9 m deep and do not allow to evaluate the total thickness of the sedimentary filling of this basin which is assumed to be deeper in some depressions of the drainage axes. It seems to be a very uneven filling with more or less deep and dissected pockets, in particular after the emersion.

The volcanic and seismic activity in the surroundings of the lake is attested by the presence of projected pyroclasts recorded at the deep bottom of the lake of ca. 21,000 and 11,000 yr BP in age, particularly in the sector of Roumpi Hills of about 15 km away. One paroxysm period of this period of instability could be indicated at about 21,000 yr BP in the deep lake deposition in which a 1.5 m slab of deposits was vertically tilted. Such tilting can support the hypothesis of a sudden expulsion of gas trapped in the volcanic pipe breccia of the crater below (Cornen *et al.*, 1992). This instability led to a step by step destruction of the restraint of the outlet. Then, since the beginning Holocene, the volcanic activity seems to have disappeared in the north-eastern part of the Cameroon Line: the current morphostructure of the lake had to be more or less acquired.

The results obtained from pollen analysis on the deep water lacustrine BM6 core can be used for the palaeoenvironmental analysis of a part of both Clay Pit and Mahongue-2 cores, and, hence, enrich the discussion on the cores on the top of the slope where pollen were nearly absent (Table 3). The ratio of Cyperaceae pollen can be used to reconstruct the curve of the relative variations of the lake level (Figure 12). Two regression phases of the order of approximately 5–6 m were insightful for the Late Pleistocene (Maley and Brenac, 1998; Maley, 2004). The oldest correspond to the LGM and occured between c. 24,000 and 17,000 cal. yr BP with two minima around 22,000 cal yr BP and 20,000 cal yr BP. The second regression is linked to Younger Dryas event intervened between 13,000 cal. yr BP and 12,000 cal. yr BP. Then rapidly, a lake level rather close to the present level of the overflow was reached at the beginning Holocene around 10,000 cal. yr BP. The erosional effects damaged probably the rocky dam of the outlet during the last thousands years. Later when a marked phase of opening of the landscape intervened towards the end of the Holocene between 2800 and 2000 cal yr BP, the lake level deduced from the Cyperaceae pollen analysis remained stable. This phase of savanna extension may not be connected to a decline of the total annual rainfall, but more credibly to an accentuation of the seasonality (decrease of rainy months per year).

4.7.3 Comparison of sedimentation processes between Lake Barombi Mbo and its catchment

The palaeoenvironmental reconstruction of the lake goes back to 34,230 cal yr BP (favour the dating of "uplifted" deposits), while that of the catchment dates back to

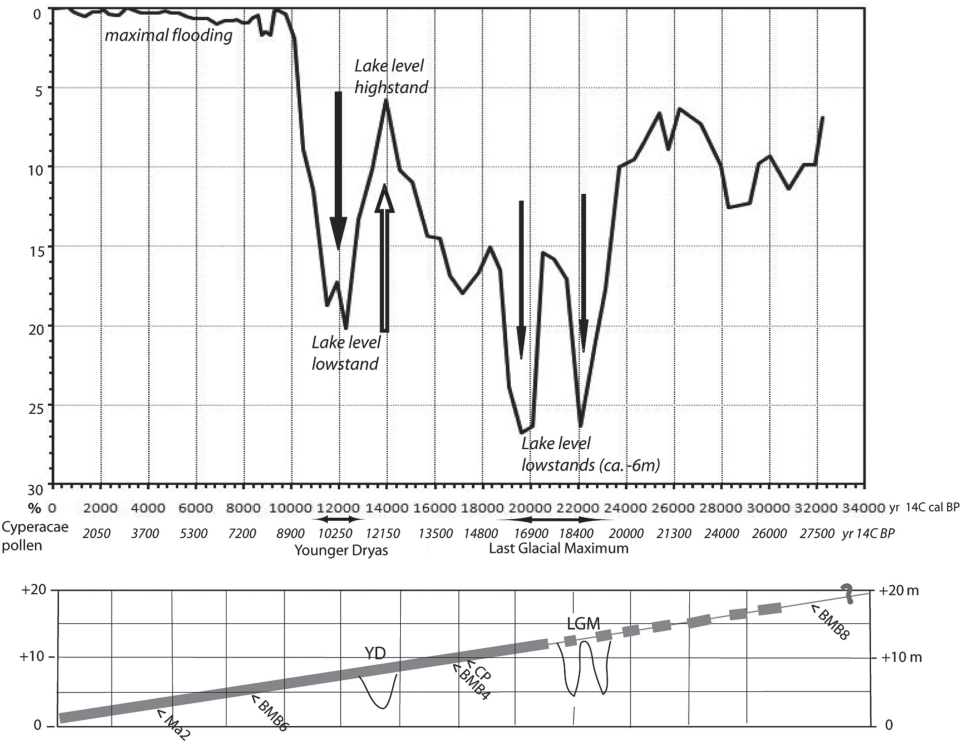

Figure 12. The relative variation of Cyperaceae pollen, aquatic plants, is a "proxy" of lacustrine level variations. Indeed, more the coastal platform, especially the deltaic one, was emerged when the lacustrine levels lowered, more Cyperacee could grow and spread on the platform (Maley and Brenac, 1998; Maley, 2004). The simplistic graph of bottom suggests the interference with the progressive lowering of the lake level controlled by the erosion of the outlet dam (grey curve) and the climatic lowstands (black curve) during Younger Dryas and Last Glacial Maximum.

45,762 cal yr BP. These two reconstructions thus overlap rather widely and enable a comparison of their sedimentary histories.

The calculated sedimentation rates in the deep lake core during the period 22,000 to 15,000 cal yr BP indicate their lowering (46–70 cm/10^3 yrs) due to less abundant precipitations and river flood (Giresse *et al.*, 1991). From around 15,000–12,300 cal yr BP and throughout the Holocene, there is a marked increase of the sedimentation rate (100–182 cm/10^3 yrs). In this study of the catchment, it was not possible to calculate the sedimentation rates during the Holocene. For the Clay Pit, figure 11 indicates after a phase of rather active sedimentation approximately between 45,800 and 34,000 cal yr BP, a slowing down of the accumulation rate (29 cm/10^3 yrs, 20.4 cm/10^3 yrs and 12 cm/10^3 yrs) which goes on until approximately 22,000 cal yr BP, remembering a similar phase recorded in the deep lake sediments between 22,000 and 15,000 cal yr BP. This chronology shows that for the comparable periods, the accumulation rates in the catchment are sharply lower than those of the deep lake and two to six times slower than the sedimentation at the end of the Pleistocene. This observation is not surprising because the slopes of the hillside were a place of transit and erosion as demonstrated in this study. The interest of this balance would rather be to propose storage at the catchment level which, according to sites, can achieve between the sixth and half of the flows as for the deep lake.

Taking into account the impossibility to date directly the Holocene or the last pre-Holocene deposits of the watershed, this comparison can bring some useful marks of stratigraphic correlation.

The continuous ash beds observed between 23,200 and 11,000 cal yr BP in the deep water deposits of the lake cannot be observed in the catchment where they were doubtlessly scattered by the river or delta dynamics. However, on the catchment sections glass fragments, plagioclases and magnetite are largely more abundant in the Pleistocene lacustrine deposits than in the Holocene swampy deposits. These materials, rich in ferro-magnesian particles to which the products from the tuff-ring erosion were added, constituted a raw material for the neo-formation of smectites abundant in the clays of the Pleistocene deposits of the lake. In the Holocene deposits, all these pyroclastic materials rarefy and the smectites of clays are spectacularly replaced by the neo-formed kaolinites, probably enhanced by climatic conditions implying hard hydrolysis. Finally, we may note the vertical increase of kaolinite similar to the trend in the nearby deep lake where the higher concentrations of kaolinite have been measured for the last ten millennia (Giresse *et al.*, 1991). Both, sedimentation in the catchment basin and in the lake, recorded simultaneously the changes in process.

The organic matter deposited in the deep lake is globally more abundant, but also more evolved during the Pleistocene than during the Holocene. The organic carbon exceeds 7% in the Pleistocene levels. Comparable values are observed in the catchment basin and remain around 5% in the Holocene levels. In the same lake deposits, the C/N ratio of the Pleistocene levels is higher than 15 with peaks up to 30 which correspond to occasional floods. Vectors of the transport of coarse plant debris are lower than 15 in the Holocene levels. This mature character of the coarse organic fragments was also observed in the Pleistocene deposits of the catchment where they were often used to hold the crystallizations of vivianite. Such an association has also been noted several times in the Miocene deposits of Anloua (Oustrière, 1984).

Cyperaceae pollen allow to bring to light several episodes of regressive movements of the lake level (Figure 12; Maley, 2004). These episodes intervened during the LGM and the Younger Dryas. They had an incidence on the erosion of slopes and seem to be well enough correlated to the chronology of major erosional contacts observed in the lacustrine or swampy deposits of the most downstream to hillside sites. The most upstream to hillside accumulations (e.g., BMB8) show lacustrine deposits covered by swampy ones, giving evidence of Late Pleistocene submergence of these hillsides up to 10 m height, possibly 20 m above the present lake level. It is thus possible to envisage independently from climate change a rather progressive regression induced by the dismantling of the dam during the last 25,000 years.

4.7.4 Vivianite and siderite and their process of formation

Both minerals present a paragenesis which has been recognized in rather numerous lacustrine environments (Burns, 1997; Deike *et al.*, 1997; Postma, 1981; Wersin *et al.*, 1991; Walker and Owen, 1999). This paragenesis has been observed especially in the microbeds of the late Pleistocene varves of the deep lake Barombi Mbo leading to a pigmentation of the deposit in yellow or in yellow green. In these varves, vivianite consists of nearly star- or rosettes-shaped grains of some hundred microns in diameter while siderite appears as "nebulas" of very small prisms of siderite of less than 5 µm long (Giresse *et al.*, 1991).

In the catchment sections, the siderite obviously shows very clear relations to the organic matter accumulation. This mineral is observed in the form of either relatively big cauliflowers which assemble beams of prisms sometimes surrounding plant

fragments, or more frequently, in much smaller crystals (2–5 μm) closely mixed with the phyllitic or organic material.

In the Late Pleistocene deposits of the catchment, the vivianite nodules, whether accompanied with siderite or not, can exceed one centimetre in diameter, a rather exceptional dimension on the scale of the Late Quaternary deposits. Several times, these nodules concentrations have developed in clayey levels just above the sandy beds: e.g., BMB4 (4.20–3.90 m), BMB8 (4.80 m), Mahongue 2 (2.50, 1.95 m) and the Clay Pit (7.90–7.50, 4.80 m). These conditions of neo-formation remember those of the Miocene sandy clays at the nearby Cameroonian site of Anloua, in Adamawa where "giant" vivianite crystals were discovered (Oustrière, 1984; Pillard, 1984). Such crystals of metric scale are especially observed at the base of black clays which overly sands rather rich in phosphorous minerals deriving from the leaching of nearby basalts.

While admitting a long diagenetic growth in Anloua, it is necessary to explain, that in Barombi and Anloua the kinetic growth is sharply higher than that generally measured in present natural environments. The lava of the maar is composed of olivine Fe_{82} phenocrysts and of titanomagnetite in a matrix of clinopyroxene microcrysts and abundant brownish glass without feldspar. With 40.31% SiO_2, 9.25% MgO, high levels of TiO_2 (3.65%) and P_2O_5 (1.1%), this mafic alkaline lava corresponds to a limburgite (Cornen *et al.*, 1992). These analyses are comparable with those obtained for peripheral basalts and basanites in the Miocene vivianites of Anloua where strong contents in TiO_2 (3 to 5%) and in P_2O_5 (0.5 to 1.6%) were recorded (Oustrière, 1984). The various layers of ashes deposited in the deep lake between 22,000 and 11,000 BP also contain quantities in P_2O_5 between 0.49 and 0.63% (Cornen *et al.*, 1992). The quantity of phosphorous in Pleistocene sediments of Lake Barombi Mbo is in the same order of value as that contained in basalts. This implies great trapping of P in the lacustrine basin, in particular in the more confined environments of the catchment basin depressions. These vivianite crystals tend to rarefy in the Holocene levels as soon as the ash layers had nearly disappeared and the climate was wetter.

We still need to explain the kinetics of growth resulting in a rather exceptional dimension of crystals. In the absence of a thermal factor, we can consider in both cases catalysis of growth of metallic phosphates exercised by the strong concentrations of titanium oxide (anatase, titano-magnetite). In Barombi lavas, TiO_2 contents are between 3.4 and 3.6%, those of the ash beds are included between 3.1 and 3.6% (Cornen *et al.*, 1992) and the quantity of phosphorous in Pleistocene sediments of Lake Barombi Mbo is in the same order of value as that contained in basalts. In Anloua, diagenesis remained in an almost permanent aqueous environment and secondary minerals arose from a colloidal phase of transition derived from the change of the vivianite.

4.8 CONCLUSION

In the lower part of the Barombi Mbo catchment, various sections show Late Pleistocene stage from lacustrine, probably rather littoral conditions, to the seasonal swampy environment. In the higher altitude sections, there are soils with temporary surface water, i.e., pseudo-gleys through all the section. The lacustrine deposits in the most upstream to hillside give evidence of Late Pleistocene submergence of these hillsides up to a height of 10 m, possibly 20 m.

The Holocene deposits were not able to be dated, but the palynological assemblages indicate palaeoenvironmental successions in coherence with pollen data from the deep water core in the lake. Several AMS ^{14}C datings allow tagging on the chronology of the Late Pleistocene approximately from ~46,000 to ~24,000 cal yr BP.

A balance of the deposits on hillsides allows calculating for each site a storage which varies between the sixth and the half of the contemporaneous accumulation at the bottom of the deep lake.

Gravelly or rocky deposits testify recurring paroxysms of erosion of the bank, they are underlined by strong oxidations of the deposit's top. The spores-rich erosional contact which interrupts the lacustrine sedimentation is considered, according to continuous palynological recordings which were obtained from the nearby deep lake. In particular, the palaeoclimatic variation of the lake level can be deduced from the vertical variation of Cyperaceae pollen. Two low lake levels correspond respectively to the LGM and also possibly to the Younger Dryas event. In the Clay Pit section, the important erosional contact at 2 m depth could correspond to the low level of the LGM and also possibly to that of the Younger Dryas. In Mahongue 2 section, the most significant erosional contact observed towards 2.30 m depth and just after 24,782 cal yr BP is connected with the main lake low level of the LGM.

These palaeoclimatic lake level changes were added to the tectonic "instability" which, step by step, contributed to damage the restraint of the outlet and resulted in an irregular fall in the lake level. However, the seismic instability and the volcanic activity seem to have decreased in intensity during the Holocene.

The big crystals of vivianite associated to siderite aggregates develop in particular in the clayey and organic microbeds of the varves of Late Pleistocene deposits of the catchment. This crystallization involves an upward flow of the phosphor from underlying sandy microbeds. The phosphore arises from the leaching of ash layers in the clayey microbeds in anoxic conditions favourable to its solubility and to its mobility. The concentrations in titanium oxides participate in the catalysis of the growth of vivianite crystals. But during Holocene, this process decreased as soon as the ash layers tend to disappear and the leaching to increase.

REFERENCES

Burns, S., 1997, Early diagenesis in Amazon fan sediments. In *Proceeding ODP, Scientific Results,* edited by Flood, R.D., Piper, D.J.W., Klaus, A. and Peterson, L.C., **155**, pp. 497–504.

CalPAL-2007 (online version), Danzeglocke, U., Jöris, O., Weninger, B., 2011, CalPal-2007 online version. http://www.calpal-online.de/.

Cornen, G., Bandet, Y., Giresse, P., and Maley, J., 1992, The nature and chronostratigraphy of Quaternary pyroclastic accumulations from Lake Barombi Mbo (West-Cameroon). *Journal of Volcanology and Geothermal Research*, **51**, pp. 357–374.

Deike, R.G. Granina, L., Callender E. and McGee, J.J., 1997, Formation of ferric iron crusts in Quaternary sediments of Lake Baikal, Russia, and implications for paleoclimate. *Marine Geology*, **139**, pp. 21–46.

Duchaufour, P., 1977, *Abrégé de pédologie.* Masson. Paris, p. 273.

Duchaufour, P., 1997, *Pédologie et classification.* Masson, Paris, p. 477.

Dumort, J.C., 1968, *Carte géologique et notice explicative, feuille Douala-Ouest.* Direction Mines et Géologie, Bureau Recherches Géologique et Minière, Paris, p. 69.

Faegri, K. and Iversen, J., 1975, *Text book of Modern Pollen Analysis*. 2nd Edition. Blackwell, Oxford, p. 295.

Gèze, B., 1943, Géographie physique et géologie du Cameroun occidental. *Mémoire Muséum National Histoire Naturelle*, Paris, **117**, p. 272.

Giresse, P., Maley, J., and Kelts, K., 1991, Sedimentation and paleoenvironment in crater lake Barombi Mbo, Cameroon, during the last 25,000 years. *Sedimentary Geology*, **71**, pp. 151–175.

Giresse, P., Maley, J. and Brenac, P., 1994, Late Quaternary palaeoenvironments in the Lake Barombi Mbo (West Cameroon) deduced from pollen and carbon isotopes of organic matter. *Palaeogeography, Palaeoclimatology, Palaeoecology*, **107**, pp. 65–78.

Gouhier, J., Nougier, J. and Nougier, D., 1974, Contribution à l'étude volcanique du Cameroun ("Ligne du Cameroun"—Adamaoua). *Annales Faculté Sciences,* Yaoundé, Cameroon, **17**, pp. 3–48.

Green, J., Corbet, S.A. and Betney, E., 1973, Ecological studies on crater lakes in West-Cameroon: the blood of endemic cichlids in Barombi Mbo in relation to stratification and their feed habits. *Journal Zoology*, **170**, pp. 299–308.

Kling, G.W., 1987, *Comparative Limnology of Lakes in Cameroon, West Africa.* PhD Thesis, Duke University, p. 482.

Letouzey, R., 1985, *Notice de la carte phytogéographique du Cameroun au 1/500.000.* Institut Carte Internationale Végétation, Toulouse and Institut Recherche Agronomique, Yaoundé, Cameroon.

Maley, J., 2002, A catastrophic destruction of African forests about 2,500 years ago still exerts a major influence on present vegetation. *Bulletin Institute Development Studies, Brighton University*, **33**, pp.13–30.

Maley, J., 2004, Les variations de la végétation et des paléoenvironnements du domaine forestier africain au cours du Quaternaire récent. In *Évolution de la végétation depuis deux millions d'années*, edited by Sémah A. and Renault-Miskowsky, J.L., France, Paris, pp. 143–178.

Maley, J. and Brenac, P., 1998, Vegetation dynamics, palaeoenvironments and climatic changes in the forests of western Cameroon during the last 28,000 years BP. *Review of Palaeobotany and Palynology*, **99**, pp. 157–187.

Nizier, F., 1992, Éléments pour l'établissement d'un référentiel pour les solums hydromorphes. In *Référentiel pédologique, principaux sols d'Europe*, edited by Institut National Recherches Agronomiques, pp. 193–207.

Oustrière, P., 1984, *Étude géologique et géochimique du bassin lacustre d'Anloua (Cameroun). Application à la compréhension de la genèse de la vivianite.* Doctoral Thesis, Orléans University, p. 344.

Peck, J.A., Green, R.R., Shanahan, T., King, J.W., Overpeck, J.T. and Scholz, C.H., 2004, A magnetic mineral record of Late Quaternary tropical climate variability from Lake Bosumtwi, Ghana. *Palaeogeography, Palaeoclimatogy, Palaeecology*, **215**, pp. 37–57.

Pillard, P., 1984, *Contribution à l'étude de l'altération de la vivianite: cas de la vivianite d'Anloua.* Doctoral Thesis, Orléans University, p. 270.

Postma, D., 1981, Formation of siderite and vivianite and the pore water composition of a recent bog sediment in Denmark. *Chemical Geology*, **31**, pp. 225–244.

Talbot, M.R. and Johannessen, T., 1992, A high resolution palaeoclimatic record for the last 27,500 years in tropical West Africa from the carbon and nitrogen isotopic composition of lacustrine organic matter. *Earth and Planetary Science Letters*, **220**, pp. 23–37.

Walker, D. and Owen, J.A.K., 1999, The characteristics and source of laminated mud at Lake Barrine, Northeast Australia. *Quaternary Science Review*, **18**, pp. 1597–1624.

Weninger, B. and Jöris, O., 2008, Towards an absolute chronology at the Middle to Upper Palaeolithic transition in Western Eurasia: A New Greenland Hulu timescale based on U/Th ages. *Journal of Human Evolution*, **55(5)**, pp. 772–782.

Wersin, P. Höhener, P., Giovanoli, R. and Stumm, W., 1991, Early diagenetic influences on iron transformation in a freshwater lake sediment. *Chemical Geology*, **90(3–4)**, pp. 233–252.

CHAPTER 5

Palaeoenvironmental observations on a Late Holocene debris-flow process in Lake Assom (Adamawa, Cameroon)

Pierre Giresse
Centre de Formation et de Recherche sur les Environnements Méditerranéens (CEFREM), UMR 5110-CNRS, Université de Perpignan Via-Domitia, Perpignan, France

Simon Ngos III
Department of Earth Sciences, University of Yaoundé I, Yaoundé, Cameroon

ABSTRACT: A debris-flow of some 70 cm-thick covered the bottom of the Lake Assom just before 1629 cal yrs BP. This exceptional event is considered within the framework of the palaeoenvironmental evolution of the lake basin and on a larger scale, within the evolution of the Adamawa plateau. Sedimentological, mineralogical and geochemical analyses are used to determine the source of the compacted clayey clasts which are packed in this debris-flow and then to cast new light on the mechanism of this sedimentary process. The dark and compacted muddy clasts show the same abundance of siderite and vivianite concretions as the hydromorphic soils (gleys) which are extensive on the western side of the lake. The gleyed soils, dating to between 2540 and 5229 cal yrs BP, correspond to prograding deltaic deposits of the Mandjara River while eastward the more sandy deposits attest to the close presence of the basement rock (granite and gneiss) and colluvial reworking. The deposition of the debris-flow occurred just before the flooding on the depression of the new Lake Assom and testifies to a growing seasonal and/or interannual irregularity of the precipitation. This event is compared to the frequent oscillations of the surface level of the crater lakes of the nearby region of Ngaoundéré. In Lake Tizong, a 78 cm-thick pyroclastic debris and allochtonous organic supply were, according to the authors, abruptly deposited, a process which we can, by analogy with Assom, also interpret as debris-flow. This deposit is bracketed by two radiocarbon dates (1490 and 2230 cal yrs BP). In spite of the rough coincidence of the dates of the events of Assom and Tizong, we cannot envisage contemporaneous events, but rather the recurrent influence of the same threshold conditions related to a critical phase of climatic transition.

5.1 INTRODUCTION AND PALAEOENVIRONMENTAL BACKGROUND

Palynological studies on other lacustrine sites situated in the forest block of South Cameroon clearly show evidence of periods of extension and removal of the dense forest during the last 10 millennia: Lake Barombi-Mbo near Kumba town (Giresse *et al.*, 1994; Maley, 1997; Maley and Brenac, 1998) and Lake Ossa near Edea town

(Reynaud-Farrera *et al.*, 1996; Wirrmann *et al.*, 2001). The main fluctuations can be summarized as follows.

- A major phase of forest extension between ~9500 and 2800 cal yrs BP.
- A phase of destruction of the primary forest between ~2800 and 2000 cal yrs BP, linked to a pronounced growth of the savannah in Lake Barombi-Mbo while in the Lake Ossa area, a rapid replacement of this primary forest by pioneer forest formations occurred.

Forest sites, notably from South-Cameroon and Congo (Maley, 1992; Schwartz, 1992; Giresse *et al.*, 1994; Maley, 1997; Maley and Brenac, 1998; Vincens *et al.*, 1999) experienced mesophile humid forest expansion until 3000 cal yrs BP, followed by landscape clearing, implying both a change in the regime and the quantity of precipitations. Estimates of the date of the return of humid forest vary between 2000 and 800 cal yrs BP.

The ECOFIT (Ecosystem of Tropical Forests, a program sponsored by IRAD, CIRAD and CNRS, France) paid particular attention to the possible extension of the forest at the Adamawa plateau during the Holocene. The transitional position of Lake Assom between the southern rainy forest region and the northern Sahelian savannah plain seems to be the key for a better understanding of this palaeoenvironmental evolution.

The palaeoenvironment of Lake Assom over the last 4500 years was previously analyzed on the basis of two sediment cores drilled in the centre of the lake and six vertical sections sampled with an earth auger on the swampy banks (Ngos III *et al.*, 2003). One of the most spectacular results concerned the discovery, around 1700 yr BP of a cataclysmic deposition of muddy clasts (debris-flow) reworked from the nearby swamps.

The aim of this study is two-fold:

- Re-examine the succession of the sedimentary palaeoenvironments of the lake by means of new sedimentological (especially sediment markers) and more detailed mineralogical or geochemical observations.
- Place this succession, particularly the deposition of the debris-flow, in the new context of the recent palaeogeographic data which has just been published on the Adamawa region.

In the nearby volcanic crater lakes (Mbalang and Tizong) of the Adamawa plateau, several palaeoenvironmental reconstructions on Holocene time scales were obtained in particular on the basis of pollen analyses (Vincens *et al.*, 2010) or diatoms (Nguetsop *et al.*, 2011; Nguetsop *et al.*, 2013) or sediment markers (Ngos III and Giresse 2012).

Finally, the chronological scale of the analysis is situated within the framework of a very recent debate in the journal Science about the hypothetical impact on the forest environment of the first populations of Bantu farmers (Bayon *et al.*, 2012; Maley *et al.*, 2012; Neumann *et al.*, 2012).

5.2 GENERAL SETTING

Lake Assom (6°38′N–12°59′E) lies in the southern part of the Adamawa plateau, located at 900 m altitude, some 45 km west of Tibati town (Figure 1). Its mean diameter is 1–1.2 km and its maximum depth is not more than 3–4 m with a 1 m rise during the rainy season. The Mandjara River is the only one draining into the lake, it falls rapidly from the high-lying plateau which peaks at 1200 m altitude and reaches the lake

Figure 1. Geographical situation of Lake Assom in Cameroon.

through the swampy and deltaic zone on the northwest margin. It is a seasonal river which, today, passes from the north to the south through a narrow thalweg some 500 m west of the lake. To the west, the extent of various swampy zones indicates a previously larger size of the lake (Figures 2a, b). When the lake level rises during the rainy season, this western swampy zone and the small Boussemi and Ngwana depressions are flooded giving an idea of the earlier dimensions of Lake Assom (Figures 2a, b). The sandy texture of the soil in the zone linking Lake Assom to small Boussemi and Ngwana lakes probably results from repeated floods of the Mandjara River. Sand beds and lenses, observed in some exposures, indicate their recent deposition.

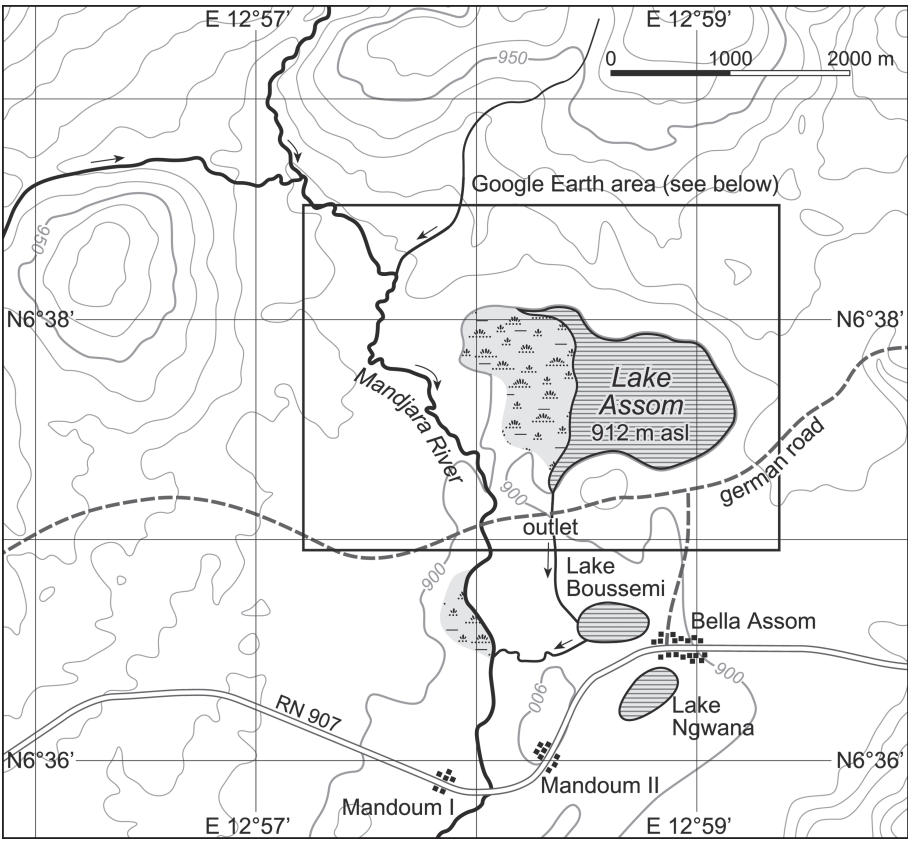

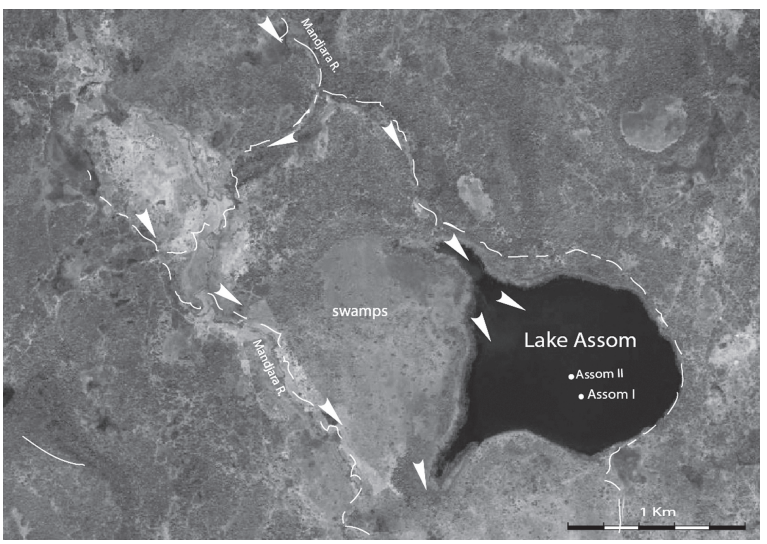

Figure 2a. Location of Lake Assom derived from the I.G.N. topographic map and **2b.** from Google Earth (Image: GeoEye 2012). Grey arrows indicate the direction of the current flow and sediment transport in the Mandjara River. The white broken line shows the extent of the former lake.

The climate of the region is a sub-type of the tropical climate, strongly influenced by altitude. It is intermediate between the bimodal wet equatorial climate and the dry unimodal climate to the north. Mean annual rainfall is about 1500 mm falling mainly during the rainy season (April–October) and correlated with a high monsoon flux. Conversely the dry season is a period during which the harmattan wind is very active from the North–East (Brabant, 1991).

The vegetation map of Cameroon by Letouzey (1968, 1985) indicates that Lake Assom lies in the Sudanese-Guinean woody savannah zone generally characterized by two main species: *Daniella olivieri* (Caesalpiniaceae) and *Lophira lanceolata* (Orchnaceae). This lake is located less than 50 km north of the most northerly patches of dense humid forest, thus providing a unique opportunity to examine the fluctuations of the northern limit of the forest domain of south Cameroon during the Holocene (Figure 3).

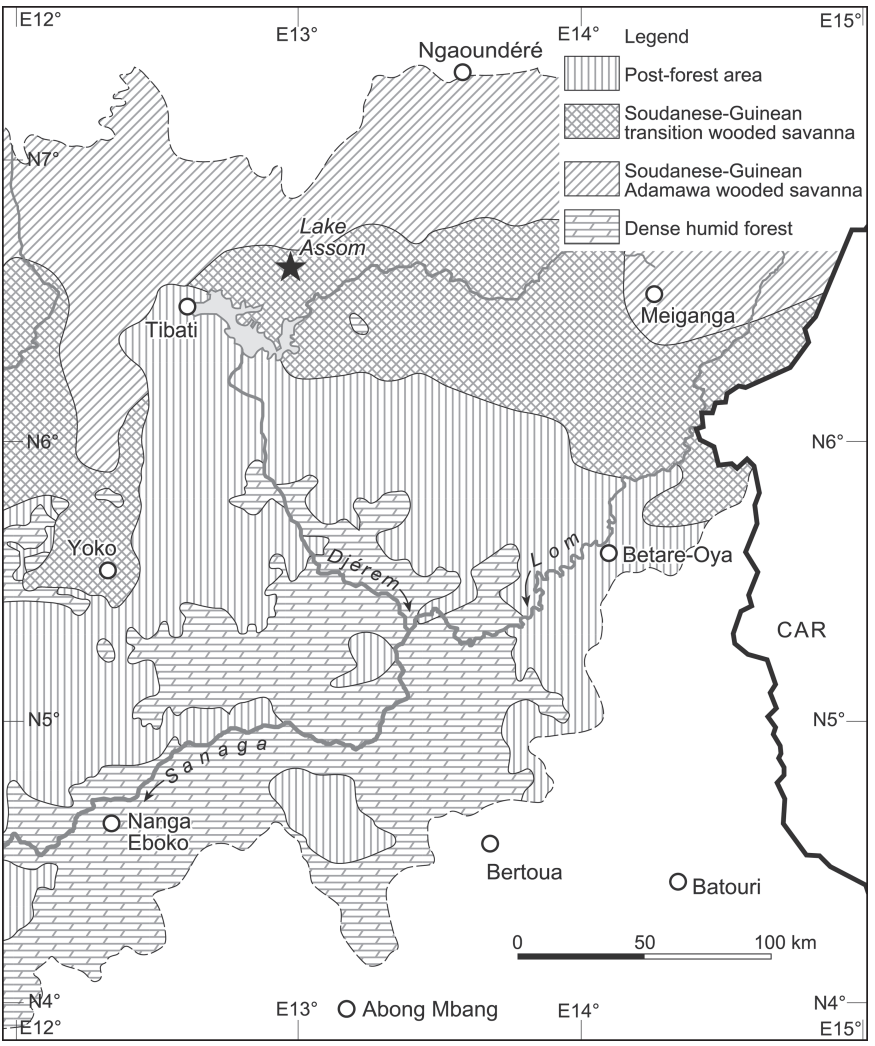

Figure 3. Extract of the phytogeographic map of the upper part of the Sanaga Basin according to Letouzey (1968).

The lake occupies a small flat zone on the southern side of the Adamawa horst which is composed of various transitional lithologies, from micaschists and gneisses to migmatites, and from migmatites to granites (Regnoult, 1989). These formations probably originate from the many Precambrian orogenic cycles (Bessoles and Trompette, 1980). More precisely, the basement below Lake Assom is composed of old syntectonic granites, some gneissic outcrops are found about 8 km north of the lake, upstream along the Mandjara River.

Delineation of the marginal environment of the lake indicated the annular-like relief created by outcrops of a hard iron duricrust on the eastern side (Ngos III *et al.*, 2003). Upstream/downstream degradation process of the lateritic crust supplies solution of ferrous iron, which is accumulated together with ferric iron in the phreatic sheet by percolation. This accumulation process induces saturation in the phreatic water table and precipitation as siderite (or vivianite) in the interstitial water of the hydromorphic soil. Generally near the banks, the vertical profiles are nearly similar: one metre-thick accumulation of a grey-beige (5/2 YR to 6/2 YR Munsell) gley overlies an ochre (7/6 to 7/8 YR) gley with red small mottles which makes the transition to the ferruginous nodules at the top of the degrading crust. The concentration of these nodules corresponds more or less to the top of the phreatic water table. It has been suggested that Lake Assom and its western swampy plain likely originate from karst-like dissolution processes that affected the lateritic unit and possibly the top of the underlying granites (Ngos III *et al.*, 2003).

5.3 SAMPLING AND METHODS

Two core sections were obtained in the central part of the lake, situated approximately 200 m apart (Figure 2b). The 2.5 m long Assom II core was drilled in a water depth of 3–4 m. The neighbouring Assom I core (2.2 m long) was taken in nearly the same water depth, but closer to the lake margin, further from the Mandjara River mouth.

Sampling was done every 10 cm with some modification when discontinuities were present. Samples were washed on a screen of 50 μm "mesh" size and the sand fraction was then scrutinised under a binocular microscope to identify the nature of the main sediment grains and sedimentary materials like vegetal remains, rock clasts, carbonised debris and diagenetic minerals like siderite and vivianite. A semi-quantitative evaluation was done and completed by some SEM observations associated to EDAX microprobe. XRD analyses were conducted on the bulk sediment and on the <50 μm fraction. In previous work (Ngos III *et al.*, 2003), total organic carbon was measured with a coulometer and total nitrogen was determined by the Kjeldahl method at the IRD Laboratory in Bondy, France.

Eight radiocarbon dates were obtained by conventional spectrometry (former Geochronology Laboratory of ORSTOM-Bondy and Radiocarbon Dating Centre of the University of Lyon I) and by AMS (Beta Analytic, Miami, USA). They were calibrated using the calibration curve CalPal2007_HULU proposed by Cologne Radiocarbon calibration & Paleoclimate Research Package Online CalPal (http://www.calpal-online.de—Copyright 2003–2007, CalPal Authors) (Table 1).

Since the two cores present comparable sedimentary successions, we decided to present the details of the thicker succession (Assom II) before proposing a correlation between both sections.

Table 1. Dating of organic matter in sediment cores Assom I and II.

Sediment core	Depth (m)	Lab codes	Material	Conventional ^{14}C ages (yrs BP)	Calibrated ^{14}C ages (cal yrs BP)	2-sigma calibrated ^{14}C ages range (cal yrs BP)
Assom II	0.35–0.40	Ly. 8952	Organic matter	670 ± 40	622 ± 44	577–666
	1.0–1.05	Ly. 8953	Organic matter	1710 ± 40	1629 ± 54	1574–1683
	1.55–1.60	Ly. 8954	Organic matter	2450 ± 75	2540 ± 130	2410–2670
	1.64–1.68	Beta-131686	Organic matter	3690 ± 40	4033 ± 55	3977–4088
	2.40–2.42	Beta-131687	Organic matter	2010 ± 40	1968 ± 46	1921–2014
Assom I	0.61–0.70	Ly. 8951	Organic matter	1315 ± 40	1244 ± 44	1197–1286
	1.0–1.05	Ly. 8955	Organic matter	4570 ± 210	5225 ± 266	4958–5491
	2.12–2.15	Beta-131685	Organic matter	2840 ± 40	2958 ± 60	2898–3018

5.4 BASIC STRATIGRAPHY OF ASSOM II CORE

The lowest 10 cm are composed of a dark-grey (5/1 YR Munsell) mud dated at 1968 cal yrs BP (2010 yrs BP) which probably indicates the top of a thicker muddy accumulation. From 2.4 to 1.7 m, compacted grey or bluish sands were observed, sometimes very coarse in texture as attested by high values of coarsest quartz grain-size (clasticity index) (Figure 4). The presence of a 40 cm-long vertical mottle of white sand indicates post-sedimentary mobilisation of iron. The fine fraction (<50 μm) is very sparse, with very low organic carbon contents (<1%), and the C/N ratio is lower than 10 suggesting a slow mineralization of the autochthonous organic matter under anaerobic conditions. Between 1.6 and 1 m depth, we observe various clay clasts and lenses, in the 1 cm to 10 cm diameter range, which are darker and have a harder consistency than the matrix mud. It seems that these clasts were deposited in two steps; the first, attested by a horizontal dark-coloured lens, was followed by deposition of a one centimetre-thick mud horizon before the main accumulation process. Two clasts have been dated at 4033 cal yrs BP (3690 yrs BP) and 2540 cal yrs BP (2450 yrs BP) respectively, thus corresponding to clasts reworked from older deposits. Above 1 m core depth, the water content increases and the upper part of the accumulation is composed of a dark grey, fluid mud with low sand content. According to the low C/N ratio ranging generally from 12 to 14, the organic matter is relatively well preserved and presumed to be of local origin, derived from bank and swamp vegetation (Figure 4). One exception (C/N~22) was noticed around 1.70 m depth, at the base of the dark clast accumulation, where an allochthonous origin could be considered. This last sedimentation began at 1629 cal yrs BP (1710 yrs BP) and an age of 622 cal yrs BP (670 yrs BP) was obtained at 0.40 m. It is capped by a 20 cm thick ochre-grey (5/2 YR) oxic horizon at the top. Throughout the unit the sedimentation was apparently uniform

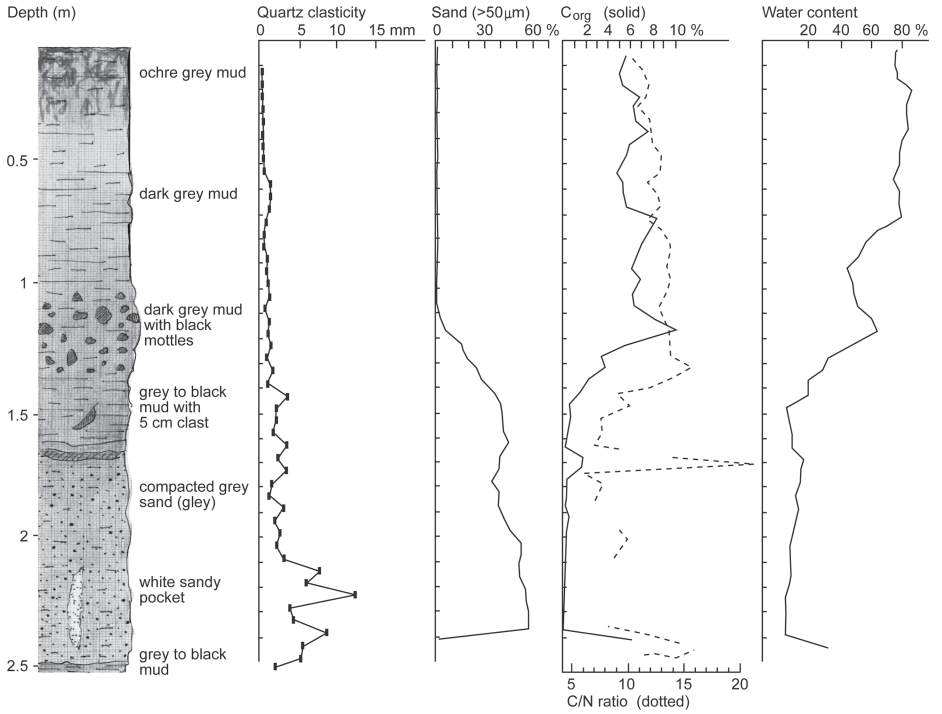

Figure 4. Assom II core. Lithological log and vertical distributions of the water and the sand (>50 µm) contents as well as the vertical distribution of the quartz grains clasticity index and the organic matter compounds; sand and organic matter lines are extracted from Ngos III *et al.* (2003).

apart from some faint laminae. Between 1.2 and 0.7 m, a significant concentration of carbonised wood debris occurs which could correspond to the mechanisms responsible for clay clast deposition or possibly to human occupation after approximately 1629 yrs cal BP. Some anthropic imprints (stones with grooves and/or cusps, grindstone) could attest a recent and even neolithic occupation (Oslisly, oral communication).

5.5 MICROSCOPIC AND XRD ANALYSES OF ASSOM II

Coarse lower sands are usually poorly sorted and contain some micaschists and gneiss rock fragments inherited from the nearby basement outcrops but also an abundant fine fraction content of up to 40–50%. At 1.8 and 2 m depths, tabular gibbsite crystals occur in cavities of some gneiss clast gravels (Figure 5a, b). Various hornblende grains and chlorite aggregates were also observed in these lower sands. The quartz grains are generally ochre (7/6, 7/7 YR) and subrounded and polished showing some aeolian abrasion marks. In the lowermost deposits of the section, the feldspar/quartz ratio ranges between 0.5 and 1, decreasing upward (Figure 6). The first siderite aggregates (Figure 7a, b, c), around 1.70 m, coincide with the first dark clay clasts and are frequently associated with tabular masses of vivianite crystals (Figure 5c, d). These two diagenetic minerals constitute a means by which to differentiate the dark compacted clast from the clearer and more fluid matrix mud. It should be noted that these two facies seem identical since they present the same contents in quartz, feldspars and in clayey minerals.

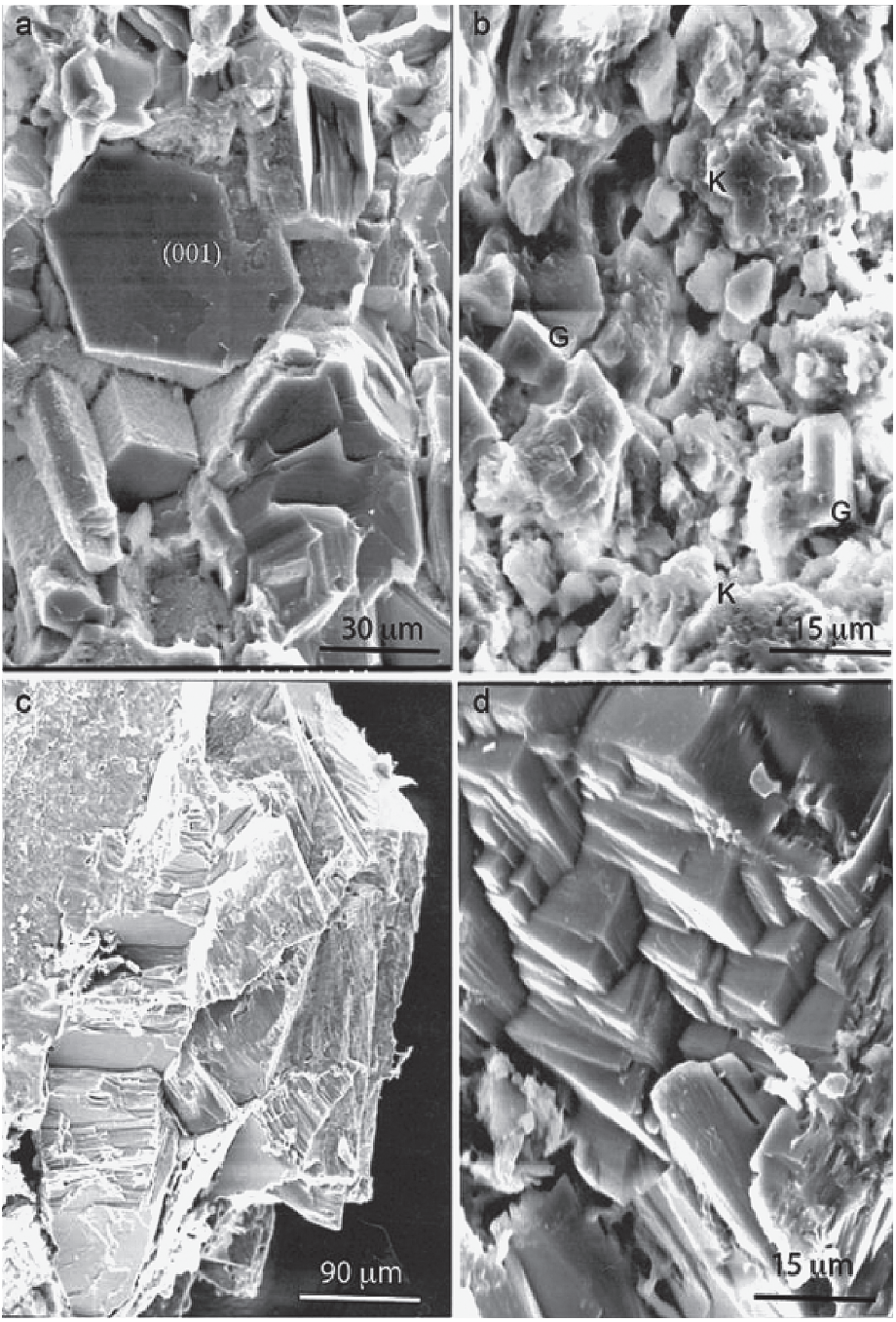

Figure 5a. Small tabular crystals of gibbsite with pseudo-hexagonal outline, twinning common on (001); it may also occur as prismatic crystals and in lamellar aggregates (190–200 cm); **b.** Gibbsite also occurs in cavities in igneous or aluminous metamorphic rocks associated with kaolinite aggregates from the alteration of plagioclase feldspars (190–200 cm); **c.** Prismatic crystals of vivianite with blade-shape or lamellar twinning on organic clayey matrix (50–55 cm); **d.** Tabular masses of several parallel vivianite crystals with well-developed edges, high magnification.

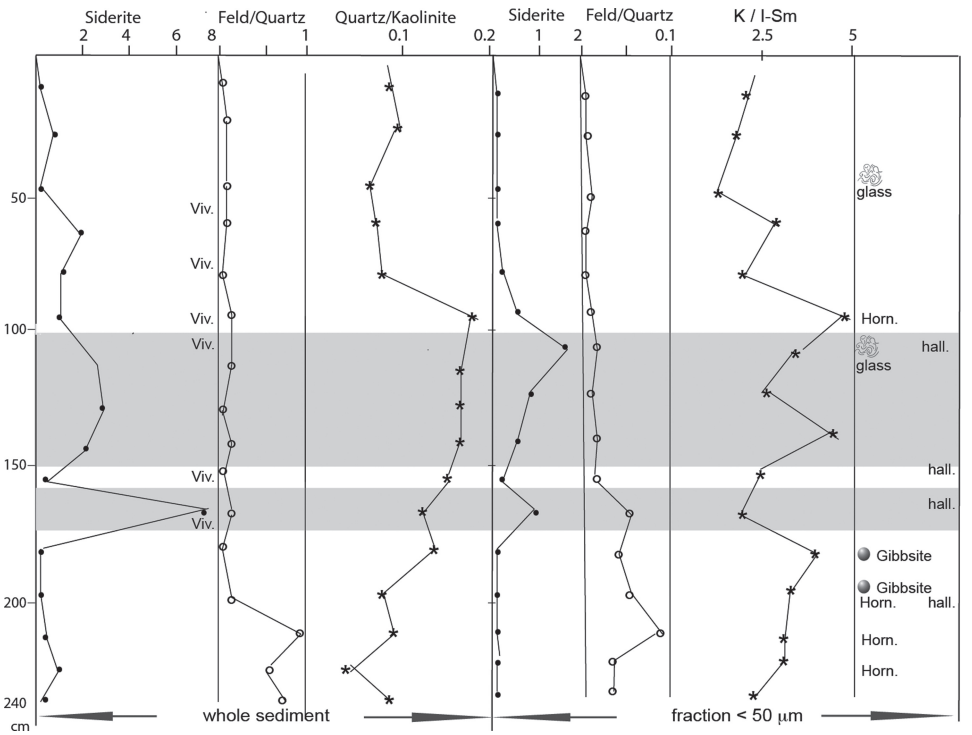

Figure 6. Assom II core. Mineralogical trends according to XRD and microscope examination.

Above 1 m depth, the mud is essentially composed of kaolinite and quartz-rich silts. The deposit is characterized both by very low sand content, low quartz clasticity, high water contents (up to 80%) and high organic carbon contents (5 to 7%). According to the very small size of sand or silt grains, the feldspar/quartz ratio decreases markedly both in the sand and the fine fraction (Figure 6). These muds are generally rich in fibres, plant seeds and fragments, some Chara gyrogonites are also observed. Siderite and vivianite growing on vegetal fibres are still observed in the sandy fractions as small concretions or very small isolated crystals (especially between 0.4 and 0.8 m).

The remote supply of volcanic dust is represented by the rare siliceous volcanic glass sherds at 120, 110, 45 cm depths (Figure 7d). Kaolinite is the dominant clay mineral throughout the section, with some illite, smectite and abundant I-Sm interlayered clay comprising the remainder of the clay assemblage. The presence of halloysite in various levels of the lower part of the section indicates irregular weathering (hydration) of the kaolinite. The vertical changes of the clay assemblages are insignificant and do not show any change of the sediment provenance (Figure 6).

5.6 COMPARISON WITH ASSOM I CORE

This second core presents approximately the same vertical succession as Assom II, so a detailed description is unnecessary. The first deposit of the section at 2.15 m depth is dated at 2958 cal yrs BP (2840 yrs BP). It is composed of grey bluish sand mainly between 50 and 400 μm. This sandy and argillaceous/clay-rich composition of this bed

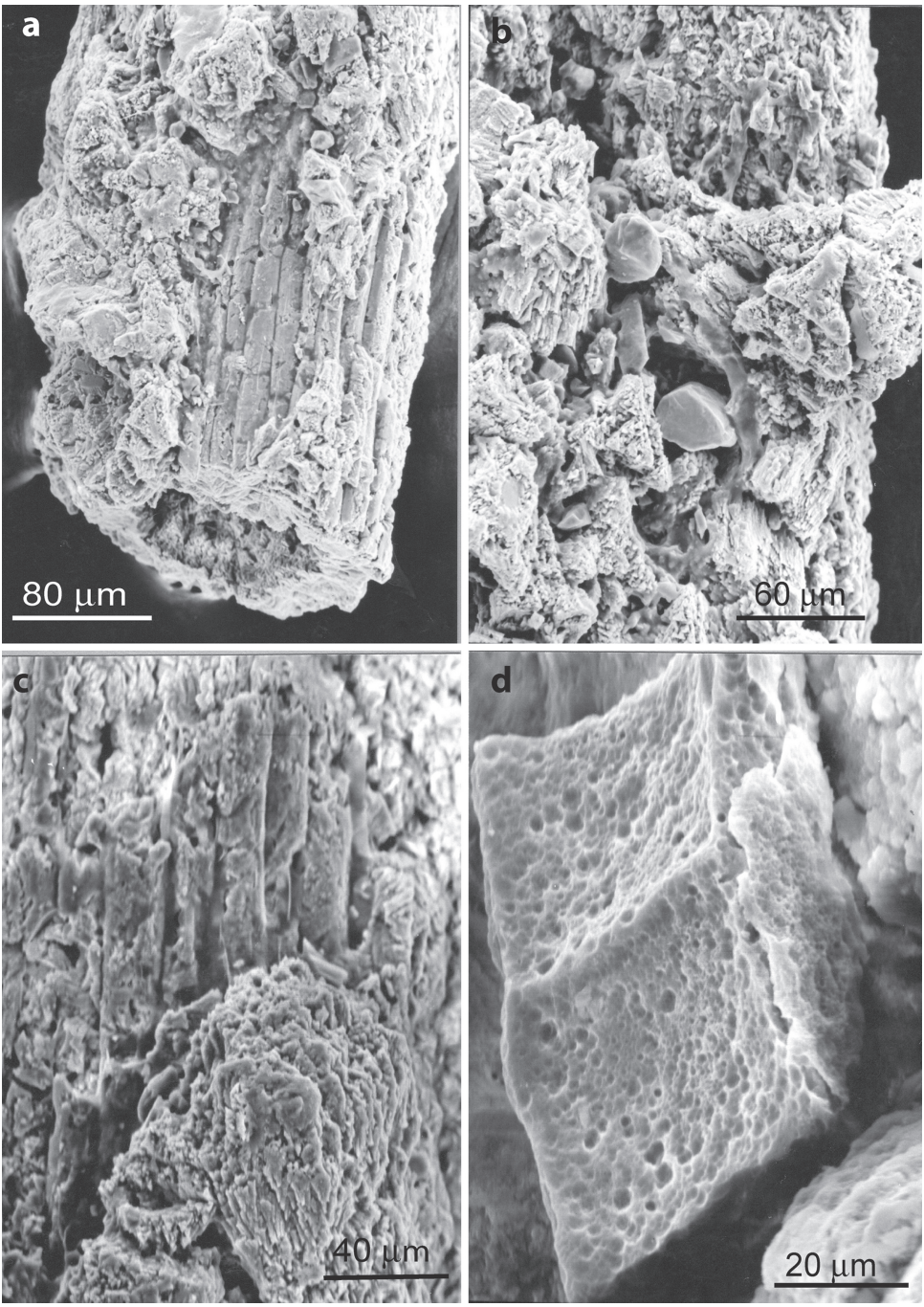

Figure 7a. Siderite growing on vegetal fibre (160–165 cm); **b.** Two successive formations of siderite-rich deposits, fine grains aggregates, then rhombohedral crystals (160–165 cm); **c.** High magnification of epigenic siderite aggregates on vegetal fibre (160–2165 cm); **d.** chip of vuggy volcanic glass (102–118 cm).

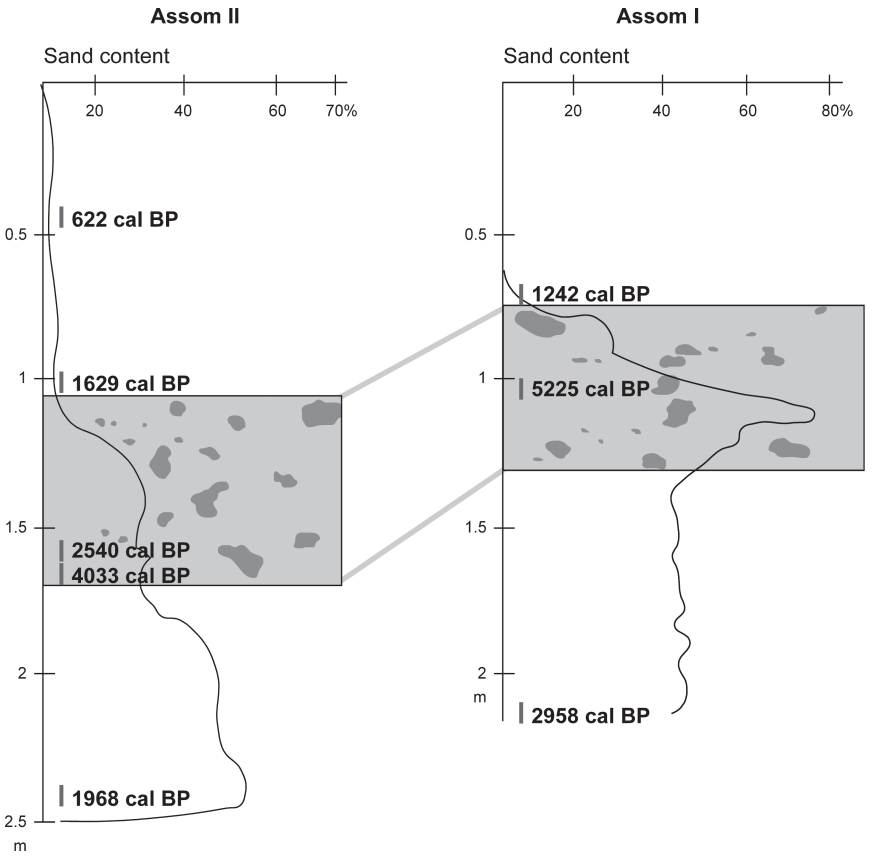

Figure 8. Comparison of lithological logs and ^{14}C chronologies from sediment of Assom II and Assom I.

remains constant up the profile to 1.30 m depth where the clast deposit appears. Root relics are observed all along this bed (Figure 8).

Consequently, the 1968 cal yrs BP dark mud of Assom II at 2.5 m depth was not deposited, due to probable pinching out from the slightly deeper centre of the lake toward the margin. This age indicates a plausibly lower sediment accumulation rate than that of Assom II. The interval with dark and clay clasts occurs from 1.30 m to 0.70 m depth, the highest transport energy is recorded near 1.05 m depth. A transported clay-chip clast has an age of 5225 cal yrs BP (4570 yrs BP). Finally, the dark grey and fluid upper mud is reduced to only 0.7 m thickness, with its base dated at 1242 cal yrs BP (1355 yrs BP) that confirms the lower sediment accumulation rate in this slightly more marginal site.

5.7 PALAEOENVIRONMENTAL INTERPRETATION

In previous work (Ngos III *et al.*, 2003), a pollen study done on various samples taken from Assom II core indicated that Gramineae pollen, the most characteristic savanna taxa, were very important constituents since c. 5225 cal yrs BP confirmed by the older mud clasts.

The first hypothesis of a general forest extension in the area for this period can therefore be rejected. It is thus necessary to interpret the sedimentary environments of the

Lake Assom site in a phyto-geographical context which remained relatively stable during the entire time interval represented by the cores, including the highest energy episodes.

The most significant aspect of the Assom II and I cores is related to the major event marked by the nearly cataclysmic deposition of a 60–70 cm thick, reworked clay-chip/clay-clast rich sedimentary unit.

This event must be contextualised by the chronology of the palaeoenvironmental history of Lake Assom and its surroundings. This history must be compared with that of the some other lakes on the Adamawa plateau region.

5.7.1 Initial low energy sedimentary environment

The oldest Holocene information on the sedimentation in the Assom lacustrine complex are supplied either indirectly through the dark and clayey, gleyed reworked mud clasts or directly from the deep, sandy gleyed basal sediment of both cores.

In the western swamp various grey (6/1 YR) or beige (5/2 YR) gleyed soils were recognized in the core sections described by previous work (Ngos III *et al.*, 2003). The one to two-metres thick gleyed sediment was characterized by its compacted consistency, its high clay and organic matter contents and its abundant siderite concretions. The same characteristics were observed in the reworked clasts from the accumulation nearby where they are dated between 5229 and 2540 cal yrs BP. These clayey materials represent a fine sediment accumulation facies of the Mandjara River deposited on a swampy prodelta which prograded into the western part of the depression. This sedimentation was nearing its end in the western deltaic plain by at least 1968 cal yrs BP after which the main lacustrine sedimentation was re-directed towards the eastern part of the depression (Figure 9).

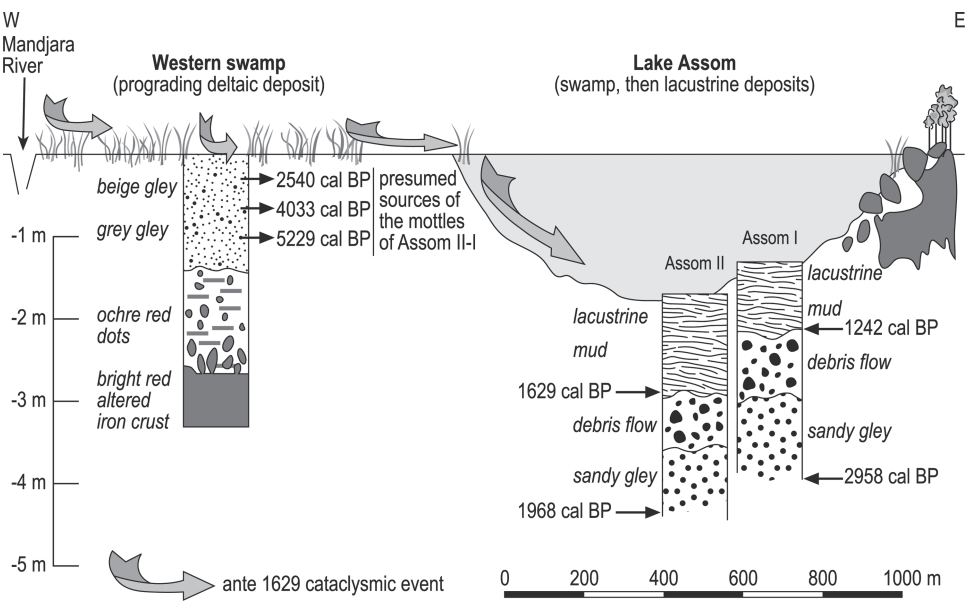

Figure 9. Schematic diagram showing the development of the 1629 cal. yrs BP debris-flow. The section of the western swamp represents a synthesis of the profiles studied in this zone by Ngos III *et al.* (2003). Three ages of the clayey clasts are indicated at the western swamp.

The easternmost and deepest zone of the depression, the present open water environment of Lake Assom originates from an episode of sedimentation in a swampy area covered by less than one meter of water. During this relatively dry phase precipitation was probably lower than today but the swamp emerged subaerially during several seasonal episodes. The eastern part of the wetland was distal to the main alluvial depocentre of the Mandjara River. Sedimentation in this area was mainly coarse, poorly sorted sediment, probably derived from short sheet wash. This colluvial material contains abundant minerals originating from the gneissic basement and associated soils. The gleyed sand displays characteristics that represent the anoxic conditions; strong compaction, mobility of the Fe_2+represented by bleached mottles, root relics, and reduced mineralization rate of the organic matter due to suppression of biologic activity (Vizier, 1992). The organic matter associated with the deposit at the base of the Assom I core was dated at 2958 cal yrs BP, comparable to the other ages of the pro-deltaic gleyed sediment in the western swamp.

The muddy sediment at the base of Assom II core, dated at 1968 cal yrs BP, represent the first inundation event in the deepest part of the lake, abruptly interrupting the sandy sedimentation. This event is not recorded in Assom I but its age may indicate an initial wetter episode.

5.7.2 The debris-flow

The 60–70 cm thick accumulation of clay clasts is recorded in both sections and is obviously connected to the same sudden sediment deposition process. In the case of Assom II record, it is possible that the accumulation developed in two very closely spaces events. After the alluvial deposition of thin dark clay layer a brief phase of mud deposition intervened just before the massive accumulation of clay clasts. In Assom I, evidence of a single depositional event is preserved. This distinct sediment deposition event, interpreted as a brief debris-flow event before 1629 cal yrs BP (Assom II) was probably associated with one or two catastrophic floods of the Mandjara River which drains nearby hillsides north of the Lake Assom basin.

Reworked clayey alluvium clasts deposited across the lake bed have variable range of ages (2540 cal yrs BP, 4033 cal yrs BP, 5225 cal yrs BP), but show similar textural characteristics of dark and consolidated mud, quite rich in large siderite and vivianite concretions which contrasts with the fluid mud matrix and from the overlying sediment. There are some allochthonous clasts (or extraclasts) that we can recognize due to their high-organic matter content to be reworked by the floods of the Mandjara River. Probably, they originate from the swampy depression less than 1 km east of the current lake Assom.

Debris-flows can be triggered by various different scenarios. In the case of the Lake Assom environment, a sudden flood after intense rainfall in the sparsely vegetated Mandjara River catchment, channelled over floodplain alluvium or semi-consolidated lacustrine, deposits could be scoured and redeposited in the basin as clay-clasts. The presumed hyper-concentrated flow can be highly erosive, especially after passing through a narrow channel some 500 m west of the lake. The river water soaks down into the debris, lubricates the material, adds weight, and triggers a debris-flow. This erosion can cut into thick deposits of saturated materials stacked high above the valley walls of the nearby channel. This erosion removes support from the base of the slope and can trigger a sudden flow of debris (Coleman, 1993; Pierson, 2005).

In this lacustrine deposition, flood deposits are characterized by sediment usually stratified-distinct laminae as in Assom II (1.65 m depth) or by beds with commonly cross-bedding exposures as in the western part of the depression.

In this humid environment, the high intensity, short duration storm rainfall would be the most likely trigger (Maley and Brenac, 1998).

5.7.3 After debris-flow event

After this gravity-induced event, the first low energy lacustrine episode is attested by the deposit of grey mud. This rise of the water depth occurred after 1629 cal yrs BP (2010 yrs BP) in the deeper central part of Lake Assom due to flooding associated with a period of high rainfall. This event is not represented in the Assom I site which is slightly elevated and closer to the lake margin. The first lacustrine deposits in Assom I appeared at 1242 cal yrs BP (1315 yrs BP) after which regular sedimentation continued under the influence of moderate floods, attested to by some vague laminites.

5.8 DISCUSSION

Preliminary palynological analyses done on some samples from the Assom II core indicate that Gramineae pollen which are very characteristic savanna taxa, have always been very abundant (Ngos III *et al*., 2003). This implies that the site has been a savanna-dominated area since ~5229 cal yrs BP. The reworked alluvium clasts confirm this assertion so any hypothesis of a general forest expansion for this period can therefore be rejected. These wet conditions are also identified in neighbouring areas at this time so the high energy event identified before 1629 cal yrs BP was probably associated with climate change, expressed by increased runoff and sudden inundation of the former large swamp basin. The contours of the lake depression and the presence of swamp relicts as small depressions imply a larger lake during the mid Holocene period than today.

From at least 2800 to 1800 cal yrs BP, the Lake Assom area was less humid than today. Lower and less regular precipitation resulted in the emergence of the elevated swampy banks. This trend can be correlated with the two low-stands observed at 2500 and 2200–2100 cal yrs BP in Lake Tizong, whereas in Lake Mbalang a continuous low-stand occurred between 2500 and 2100 cal BP (Nguetsop *et al*., 2011). Near the Atlantic coast, Lake Ossa was also very sensitive to the marked climatic change occurring between 2500–2100 cal yrs BP (Nguetsop *et al*., 2004).

Then, due to a sudden increase in precipitation, the greater part of the lake was flooded again and lacustrine sedimentation occurred since 1700 or 1300 cal yrs BP. However, the lacustrine domain has contracted over time, mainly due to the sedimentary infilling, possibly combined with a trend of decreasing precipitation. The current rainfall regime seems to be higher than that which occurred before 1800 cal yrs BP. The presence of intraclasts or mud clasts dated at 5225–2540 cal yrs BP is a key tool for the interpretation of the vegetal cover during the second half of the Holocene. The absence of forest signals indicates a more or less permanent, savanna woodland environment.

Research on the Holocene environments of Central Africa has highlighted large-scale evolutionary trends and processes with regional significance. The timing and magnitude of each event seems to vary from one site to another. The crater lakes of the Ngaoundéré region situated approximately 70 km NE of Lake Assom, allow close comparison with the Sudan-Guinean bush savanna phytogeographic zone.

The palynological study of Lake Mbalang indicates the presence of a semi-deciduous forest landscape from 7320 to 4200 cal yrs BP (Vincens *et al*., 2009). During the same period quartz-rich lamina, including black debris, are indicators of a wet period characterized by marked rainy seasons (Ngos III and Giresse, 2012). A phase of degradation of the vegetation cover was registered between 4200 and 2400 cal yrs BP. This last date corresponds to dry conditions and to the stabilization of the savanna, under low precipitation and high temperatures leading to a progressive disappearance of many lakes of the region. Holocene limnological conditions of Lake Mbalang and vegetation types were reconstructed from diatoms and sediment stable carbon isotope record $\delta^{13}C$ data that suggests more forested vegetation in the landscape before 3600 cal yrs BP (Nguetsop *et al*., 2011). The subsequent development of savanna appears as a result of strong seasonality and a well-marked dry season with more intense trade winds. Diatom data suggest a low lake level observed at 2400–2200 cal yrs BP with other low lake levels are observed 1800 and 1400 cal yrs BP. If we exclude the cataclysm of the debris-flow, this evolutionary trend essentially follows that of the Lake Assom.

Recently, another Late Holocene record based on diatom and stable carbon isotopes from nearby Lake Tizong indicates a greater precipitation minus evaporation ratio (P-E ratio) and accordingly a higher lake level from 4200 to 2800 cal yrs BP. From 2800 to 2500 cal yrs BP enriched C4 plant debris input indicates savannah patch development and changes in the rainfall distribution. Marked declines in lake level are registered at 2500, 2200–2100 and 1400–1000 cal yrs BP, the low-stand centred at 1300 cal yrs BP was probably the most significant (Nguetsop *et al*., 2011). The sedimentation of the Lake Tizong is disrupted enough by the gravity-induced accumulation of pyroclastic debris on the slopes and the bottom of the lake. However after 2500 cal yrs BP which corresponds to the beginning of savannah extension, the TOC declines from 15–20% to 10% in spite of in situ organic proliferation: a higher clarity of the lake waters could probably have favoured the significant development of Chlorophyceae filaments (Ngos III and Giresse, 2012). A radiocarbon hiatus was observed between 215 cm and 137 cm, represented by a 78 cm-thick layer of mixed pyroclastic debris and allochtonous organic matter deposited abruptly by a process which, by analogy with Lake Assom, can possibly also qualify as being a debris-flow. Five ^{14}C dates were older than expected and bracketed by two younger dates (1490 and 2230 cal yrs BP). It is difficult to compare the conditions of sedimentation in such a steep-sided crater lake subjected to intense fallout of volcanic ash with those of a swampy lake fed by a river, such as Lake Assom. However, the dates of both debris-flows occur within the same palaeoclimatic window. Even if both cataclysms were not simultaneous, they could however express the same response to the critical climatic transition where interannual variability and greater seasonal contrast were impacting on the distribution of precipitation. In Lake Kamalete (central Gabon), it was later between 1330 and 1220 yrs BP that gravity-induced flow layers of detrital material were transported during heavy rainfall (Ngomanda *et al*., 2007; Giresse *et al*., 2009).

This sedimentary palaeoenvironnements showed only modest indicators of human presence. In the sedimentary interval of Assom II coming after the deposit of the debris-flow, only some charcoals were observed. They disappear later and can indicate as well an erosion paroxysm as a significant Neolithic setting-up. In any case this possible human presence is not able to explain the important observed environmental changes interpreted as the consequence of natural climatic evolution of Central Africa (Bayon *et al*., 2012). Many archaeological, environmental (Neumann *et al*., 2012) and geochemical, sedimentological arguments (Maley *et al*., 2012) assert this conclusion. The recent and precise observations on the evolutionary history of several lakes of the nearby region of Ngaoundéré give evidence of significant changes of the level of these

lakes and their aquatic and the peripheral ground florae which cannot be determined by a human presence (Nguetsop *et al*., 2011).

5.9 CONCLUSIONS

By connecting the interpretation of reworked clasts, a picture of Lake Assom's history can be drawn covering approximately the last 5300 years. The presence of swamps relics and of palaeobanks as well as the study of some deposits give evidence of a lacustrine extent in the Mid-Holocene which was vaster than today.

Between 2800 and 1800 cal. yrs BP, the region experienced a decrease of precipitation which can also be observed simultaneously in several lakes nearby the Adamawa plateau. Then from 1700 cal. yrs BP (Assom II) to 1300 cal. yrs BP (Assom I), a part of the former lake was flooded again, but, hence, accompanied by sedimentary infilling that reduced the surface of the lake. Around c. 1630 cal. yrs BP, one or several simple or hyper-concentrated floods of Mandjara River induced swamp bottom erosion in the surroundings of the lake.

This can be considered as a paroxysmal and rare event, which occurs usually in an interval between restart and rise of precipitation in a region. The nearby Lake Tizong shows between 2230 cal. yrs BP and 1490 cal. yrs BP a debris-flow event comparable to that of Assom, but consisting of mixed pyroclastic fragments. Even if these two debris-flows, in 70 km of distance to each other, were probably not synchronous, they indicate the same climatic trend, whereas this episode is observed later (1330–1220 yrs BP) in central Gabon (Lake Kamalete). Finally, this study does not allow considering a significant impact of the first Bantu populations in the region.

ACKNOWLEDGMENTS

We would like to acknowledge Greg Botha who carefully read through this paper to improve its quality.

REFERENCES

Atlas du Cameroun, 1958, *IRCAM, Yaoundé*. p. 27 + 6 H.T. (5 books).

Bayon, G., Dennielou, B., Etoublleau, J., Ponzevera, E., Toucanne, S. and Bermell, S., 2012, Intensifying weathering and land use in Iron Age. *Science*, **335**, 1219.

Bessoles, B. and Trompette, R., 1980, *Géologie de l'Afrique: la chaîne panafricaine, zone mobile d'Afrique Centrale (partie sud) et zone mobile soudanaise*. (Orléans: Editions B.R.G.M), **92**, p. 396.

Brabant, P., 1991, *Les sols des forêts claires du Cameroun. Exemple d'étude d'un site représentatif en vue de la cartographie des sols et de l'évaluation des terres*, (Yaoundé: ORSTOM-MESIRES), 2 tomes, pp. 278–530.

Coleman, P.F., 1993, A new explanation for debris flow surge phenomena (abstract), *Eos Trans. AGU*, **74(16)**, Spring Meet. Suppl., p. 154.

Giresse, P., Mvoubou, M., Maley, J. and Ngomanda, A., 2009, Late-Holocene equatorial environments inferred from deposition processes, carbon isotopes of organic matter, and pollen in three shallow lakes of Gab,on, west-central Africa. *Journal of Paleolimnology*, **41(2)**, pp. 369–392.

Giresse P., Maley, J. and Brenac, P., 1994, Late Quaternary palaeoenvironments in the Lake Barombi-Mbo (Cameroon) deduced from pollen and carbon isotopes of organic matter. *Palaeogeography, Palaeoclimatolology, Palaeoecology*, **107**, pp. 65–78.

http://www.calpal-online.de, Copyright 2003–2007, CalPal Authors, *Cologne Radiocarbon calibration & Paleoclimate Research Package Online CalPal*.

Letouzey, R., 1968, *Étude de la carte phytogéographique du Cameroun au 1/500.000*, (Toulouse: Institut de la Carte Internationale de la Végétation and Yaoundé: Institut Recherches Agronomiques).

Letouzey, R., 1985, Notice phytogéographique du Cameroun. *Encyclopedia Bulletin*, **49**, p. 508.

Maley, J., 1997, Middle to Late Holocene changes in tropical Africa and other continents. Paleomonsoon and sea surface temperature variations. In *Proceedings of the NATO Advanced Research Workshop on Third Millennium BC Abrupt Climate Change and Old World Social Collapse, TurkeyThird*, edited by Dalfes, H.N, Kukla, G. and Weiss, H., (Berlin: Springer-Verlag), pp. 611–640.

Maley, J., 1992, Mise en évidence d'une péjoration climatique entre ca. 2500 et 2000 ans BP en Afrique tropicale humide. *Bulletin Société Géologique de France*, **163**, pp. 363–365.

Maley, J. and Brenac, P., 1998, Les variations de la végétation et des paléoenvironnements du sud Cameroun au cours des derniers millénaires. Etude de l'expansion du Palmier à huile. In *Géosciences au Cameroun*, edited by Bilong, P. and Vicat J.P., (Yaoundé: GEOCAM Yaoundé, Presses Universitaires Cameroun), pp. 85–97.

Maley, J., Giresse, P., Doumenge, C. and Favier, C., 2012, Comment on "Intensifying weathering and land use in Iron Age Central Africa". *Science*, **337**, 1040-d.

Neumann, K., Eggert, M.K.H., Oslisly, R., Clist, B., Denham, T., de Maret, P., Ozainne, S., Hildebrand, E., Bostoen, K., Salzmann, U., Schwartz, D., Eichhorn, B., Tchiengué, B. and Höhn, A., 2012, Comment on "Intensifying weathering and land use in Iron Age Central Africa". *Science*, **337**, 1040-d.

Ngomanda, A., Jolly, D., Bentaleb, I., Chepstow-Lusty, A., M'voubou, M., Maley, J., Fontugne, M., Oslisly, R. and Rabenkogo, N., 2007, Lowland forest response to hydrological changes during the last 1500 years in Gabon, Western equatorial Africa. *Quaternary Research*, **60**, pp. 411–425.

Ngos III, S., Giresse, P. and Maley, J., 2003, Palaeoenvironments of Lake Assom near Tibati (south Adamawa, Cameroon). What happened in Tibati around 1700 years BP? *Journal of African Earth Sciences*, **37**, pp. 35–45.

Ngos III, S. and Giresse, P., 2012, The Holocene sedimentary and pyroclastic accumulations of two crater lakes (Mbalang, Tizong) of the volcanic plateau of Adamawa (Cameroon): Palaeoenvironmental reconstruction. *The Holocene*, **22(1)**, pp. 31–42.

Nguetsop, V.F., Bentaleb, I., Favier, C., Martin, C., Bietrix, S., Giresse, P., Servant-Vildary, S. and Servant, M., 2011, Past environmental and climatic changes during the last 7200 cal yrs BP in Adamawa plateau (Northern Cameroun) based on fossil diatoms and sedimentary 13C isotopic records from Lake Mbalang. *Climate of the Past*, **7**, pp. 1371–1393.

Nguetsop, V.F., Bentaleb I., Favier, C, Bietrix, S., Martin, C., Servant-Vildary, S. and Servant, M., 2013, A late Holocene palaeoenvironmental record from Lake Tizong, northern Cameroon using diatom and carbon stable isotope analyses. *Quaternary Science Reviews*, **72**, pp. 49–62.

Nguetsop, V.F., Servant-Vildary, S. and Servant, M., 2004, Late Holocene climatic change in West Africa, a high-resolution diatom record from equatorial Cameroon. *Quaternary Science Reviews*, **23**, pp. 591–609.

Pierson, T.C., 2005, Distinguishing between debris flows and floods from field evidence in small watersheds. US Geological Survey, (Vancouver: US Department of the Interior), Fact sheet 2004-3142.

Regnoult, J.M., 1989, *Synthèse géologique du Cameroun*, (Yaoundé: Direction Mines et Energie), p. 119.

Reynaud-Farrera, L., Maley, J. and Wirrmann, D., 1996, Végétation et climat dans les forêts du sud-ouest Cameroun depuis 4770 ans BP, analyses polliniques des sédiments du lac Ossa. *Compte Rendus Académie des Sciences*, **2**, 322, pp. 749–755.

Schwartz, D., 1992, Assèchement climatique vers 3000 B.P. et expansion bantou en Afrique centrale atlantique: quelques réflexions. *Bulletin Société Géologique de France*, **163**, pp. 353–361.

Vincens, A., Buchet, G., Servant, M. and ECOFIT Mbalang collaborators, 2009, Vegetation response to the African Humid Period termination in central Cameroon (7°N)—New pollen insight from Lake Mbalang. *Climate of the Past*, **6**, pp. 281–294.

Vincens, A., Buchet, G., Servant, M., ECOFIT Mbalang collaborators, 2010, Vegetation response to the "African Humid Period" in Central Cameroon (7°N), a new pollen insight from lake Mbalang. *Climate of the Past. Discussions,* **5**, pp. 2577–2606.

Vincens, A., Schwartz, D., Elenga, H., Reynaud-Farrera, I., Alexandre, A., Bertaux, J., Mariotti, A., Martin, L., Meunier, J.-D., Nguetsop, F., Servant-Vildary, S., Servant, M. and Wirrmann, D., 1999, Forest response to climate changes in Atlantic Equatorial Africa during the last 4000 years BP and inheritance on the modern landscapes. *Journal of Biogeography*, **26**, pp. 879–885.

Vizier, J.F., 1992, Éléments pour l'établissement d'un référentiel pour les solums hydromorphes. Annexe 2. In *Référentiel pédologique des principaux sols d'Europe; techniques et pratiques*, (Institut National de la Recherche Agronomique INRA), pp. 193–207.

Wirrmann, D, Bertaux, J. and Kossoni, A., 2001. Late Holocene paleoclimatic changes in dated sediments from Lake Ossa (Southwest Cameroon-), *Quaternary Research*, **56**, pp. 275–287.

This page intentionally left blank

CHAPTER 6

Palaeoenvironmental characteristics of the Plio-Pleistocene Chiwondo and Chitimwe Beds (N-Malawi)

Tina Lüdecke

Institute of Geoscience, Johann Wolfgang Goethe University, Frankfurt, and Biodiversity and Climate Research Centre (BiK-F) & Senckenberg, Frankfurt am Main, Germany

Heinrich Thiemeyer

Centre for Interdisciplinary Research on Africa (ZIAF) and Institute of Physical Geography, Johann Wolfgang Goethe University, Frankfurt am Main, Germany

ABSTRACT: Field relationships and sediment characteristics of the Plio-Pleistocene Chiwondo and Chitimwe Beds in Northern Malawi are investigated with the attempt to draw conclusions about the palaeoenvironment in which hominid evolution took place. The objective is to gain information about palaeolake phases of water level transgressions or regressions and to narrow down the geochronological timespan. Widely distributed surface survey was performed to acquire a better understanding of the tectonic relationships and lateral variability of the different lithologies. Here, the descriptions of five exemplary profiles display characteristic features in terms of sediments and palaeosol remnants which indicate the dominance of large river systems and fluctuations of palaeolake levels during the last 4 Ma. The primary fluvial deposits reveal a high rate of pedogenic overprint indicated by abundant carbonate nodules; these erosion-resistant Bk-horizons are well preserved to the contrary to the carbonate depleted upper horizon of the palaeosols in this tectonically active region.

6.1 INTRODUCTION

Reconstruction of the palaeoenvironment in which faunal evolution occurred is a focus of ongoing research, with a strong emphasis on the early human history. Numerous studies, applying different methods, have documented the impact of long-term environmental change on the evolution of hominids with a regional focus on East African sites in Ethiopia, Kenya and Tanzania (e.g., Wesselman, 1985; Cerling and Hay, 1986; Cerling *et al*., 1988; Cerling, 1992; Plummer and Bishop, 1994; Sikes, 1994; Behrensmeyer *et al*., 1997; de Heinzelin *et al*., 1999; Sikes *et al*., 1999; Wynn, 2000; Levin *et al*., 2004 and 2011; Ségalen *et al*., 2007; Cerling *et al*., 2011; Magill *et al*., 2012a and 2012b; Feakins *et al*., 2013). Plio-Pleistocene sediments in the Karonga-Chilumba

area in northern Malawi are located in the south of the East African Rift System (EARS; see Figure 1) between the 'classical' eastern and southern African hominid localities. Therefore, the study area fills an important spatial gap for understanding the development of our early ancestors in a time during substantial junctures in human evolution. Field relationships, sediment characteristics and heavy minerals (HM) were

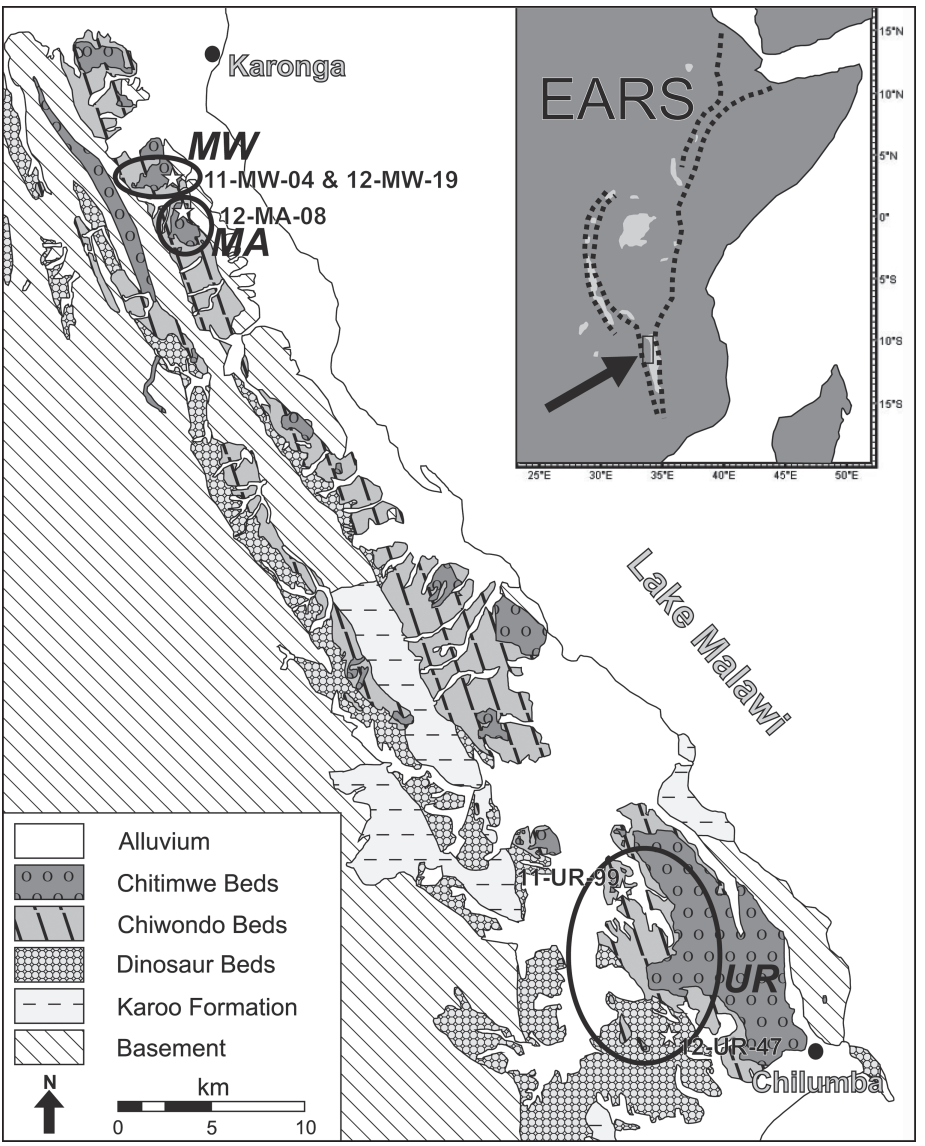

Figure 1. Inlet: East Africa with the East African Rift System, EARS (dotted lines) and rift lakes. Box indicates position of large map which shows the geology of the study area with circles around the three sampling localities (MW = Mwenirondo; MA = Malema; UR = Uraha) and logged profiles within (small stars).

analyzed to gain information about palaeoecological and palaeoclimatic conditions during deposition of the Chiwondo Beds.

During prior work, vertebrate and invertebrate fossils were recovered from the sediments, including two important hominid fossil finds, a maxillary fragment of *Paranthropus cf. boisei* (Kullmer *et al*., 1999) and a mandible of *Homo rudolfensis* (Schrenk *et al*., 1993 and 1995; Bromage *et al*., 1995b), as well as several cercopithecoid primate cranio-dental remains (Bromage and Schrenk, 1987; Frost and Kullmer, 2008; Kullmer *et al*., 2011).

6.1.1 Geologic and tectonic framework

The study area is located in the half-graben of the Malawi Rift zone, which is the southern part of the western branch of the EARS and extends over 900 km from the Rungwe Volcanic Province in the north (southern Tanzania) to the Urema Graben in the south (Mozambique). The examined sediments are exposed in the Karonga Basin in the northernmost part, which was formed by block faulting in response to ENE–WSW extension during the Late Miocene (Ebinger *et al*., 1993; Ring *et al*., 1992). It is, similar to other rift zones in the area, asymmetric and bordered by a steep westward dipping fault in the east and several sub-parallel eastward-dipping normal faults in the west (Ebinger *et al*., 1993; Ring and Betzler, 1995; Hamiel *et al*., 2012). Between the cities of Karonga and Chilumba Permo-Triassic, Jurassic, Cretaceous and the studied Plio-Pleistocene Chiwondo and Chitimwe Beds are exposed in two narrow northwest-southeast aligned stripes separated by Proterozoic metamorphic basement ridges parallel to the western shore of Lake Malawi (Betzler and Ring, 1995), ca. 70 km long (N to S) and 15 km wide (E to W). The focus is on two areas (Figure 1), both located in the eastern strip: i) the Malema and Mwenirondo region in the north, ca. 10 km south of Karonga, here the maxillary fragment "RC 911" of *Paranthropus cf. boisei* was recovered in 1996; and ii) the Uraha region, ca. 50 km southeast of Karonga where the mandible "UR 501" of *Homo rudolfensis* was discovered 1991.

The basement and Mesozoic shale- and sandstone-dominated Karoo Supergroup are covered by reddish and grayish sandstones, marls and clays of the Early Cretaceous Dinosaur Beds (Catuneanu *et al*., 2005; Schlüter, 2008). The Plio-Pleistocene sedimentary group overlies these sediments with a major angular unconformity which is locally pronounced; especially in the western sediment strip. The formation was first mentioned by Andrew and Bailey (1910) and the grayish sandstone and siltstones were named "Chiwondo" and "Chitimwe Beds" by Dixey (1927) who interpreted them as lake beds. The lacustrine origin was later confirmed by (Stephens, 1966; Charsley, 1972; Kaufulu, 1989; Betzler and Ring, 1995). The depositional facies of these sediments range from alluvial (braided and meandering system deposits, deltaic and fan sediments) to aeolian and lake (high and low energy) deposits (Betzler and Ring, 1995). The sediments are folded, tilted and colluvially translocated due to extreme tectonic uplift and extension in the Malawi Rift area (Ring and Betzler, 1995) which is still ongoing (Hamiel *et al*., 2012).

Betzler and Ring (1995) and Ring and Betzler (1995) described the tectonics, sedimentology and geology of the Plio-Pleistocene deposits. They divided the Chiwondo Beds into Units 1 to 4, followed by Unit 5, the Chitimwe Beds. The anthropologically important Unit 3 was subdivided into three zones based on faunal remains, mostly suid material (Bromage *et al*., 1995a; Kullmer, 2008).

After Betzler and Ring (1995) the braided stream deposits of the oldest Unit 1 are reddish coloured due to the partly reworking of the Dinosaur Beds which they

overlie with an angular unconformity. After a major calcimorphic palaeosol, lacustrine sediments of Unit 2 with high and low energy fan deposits and abundant calcimorphic palaeosol layers are present. The limestones comprehend pelecypods and gastropods, primary Bellamya freshwater snails. Separated by an angular unconformity, the sediments of Unit 3 are deposited in a mainly fluviatile environment, again interrupted by phases of pedogenesis. Due to biostratigraphic data of suid third molar fossils this unit can be differentiated into three zones (Kullmer, 2008). Zone 3A-1 and 3A-2 are made of meandering river deposits which accumulate lakeward in stream-mouth bars of deltas, whereas Subunit 3B is richer in stacked calcimorphic palaeosols than the older zones, some of them are ferruginous. Unit 4 follows after a major angular unconformity. Here aeolian sands and diatom-rich marls and limestones are exposed. Subunit 3B and Unit 4 are restricted to the southern part of the deposal area (Uraha region). Exposures of the up to 15 m thick reddish sands and conglomerates of the Chitimwe Beds (Unit 5) are variable through an overburden of colluvium and overly the Chiwondo Beds with an angular discordance (Betzler and Ring, 1995; Thompson *et al*., 2012). The grain size of the sub-angular to well-rounded particles ranges from fine sands to large cobbles, which are generally made out of basement or Karoo Supergroup materials. Lithic artifacts with limited indications of post-depositional transport are preserved in this unit (Thompson *et al*., 2012). The complete Plio-Pleistocene succession has a preserved maximal thickness of 100 m and represents a large-scale transgressive-regressive tectono-sedimentary cycle (Ring and Betzler, 1994). It is to note that due to erosion each of the units can reveal a direct contact to the basement, Karoo Supergroup or Dinosaur Beds.

6.1.2 Stratigraphy

Age determination of the exposed sediments is difficult to evaluate as volcanic layers for absolute dating are lacking in the area (Kaufulu and Stern, 1987; Betzler and Ring, 1994; Kullmer, 2008). Biostratigraphic correlation to well-dated fossil finds elsewhere in sub-Saharan Africa is possible. Here, the documentation of the structural density of enamel bands of suid molars are of importance (Kullmer 2008). However, vertebrate fossils are only found in Units 2 and 3. Suid material attributed to *Notochoerus jaegeri* was recovered in the south of the study area and suggests an age older than 4.0 Ma for Unit 2 (Kullmer, 2008). With the use of dental fossils of *Notochoerus euilu*s, *N. scotti, Metridiochoerus andrewsi* and *M. compactus* Bromage *et al.* (1995a) and Kullmer (2008) subdivided Unit 3 into three biozones with ages of 3.75 to 2.7 Ma, 2.7 to 1.8 Ma and 1.74 to 0.6 Ma respectively. The lack of fossils does not allow any biostratigraphical age for Units 1, 4 and 5 (Betzler and Ring, 1995). The maximum age of Unit 1 is restricted by the development of the Malawi Rift about 8.6 Ma ago (Ebinger *et al*., 1989; Ring *et al*., 1992). The age of the Chitimwe Beds could be assigned to the Middle and Late Pleistocene due to the presence of lithic artifacts (Clark *et al*., 1970). The sort and shape of the stone tools recovered classify the unit as Middle Stone Age (MSA; from ca. 0.285 to 0.030 Ma), based on east and central African data (Barham and Smart, 1996; Tryon *et al*., 2005; Thompson *et al*., 2012). An unpublished OSL-age of Chitimwe Bed sands near Karonga is reported, having a minimum age of 20 kyrs (S. Stokes, pers. comm. in Betzler and Ring, 1995). However, the Chitimwe Beds exhibit a broad horizontal and vertical variability in clast size. The strong red colour derives from intensive soil development resulting in Chromic Cambisols and Chromic Luvisols on the actual land surface. Soil depth ranges from 0.5 m up to 10 m in some places. The soils are decalcified, the calcic subsoil horizons developed mainly in the underlying Chiwondo sediments.

6.1.3 Palaeosols

Recently, palaeosols have been used to reconstruct palaeoenvironmental conditions of the classical hominid sites in East Africa (e.g., Wynn, 2000; Wynn and Retallack, 2001; Retallack *et al*., 2002; Wynn, 2004; Aronson *et al*., 2008; Levin *et al*., 2011). These studies enhanced the interpretation of environmental conditions of hominid habitation areas where well preserved palaeosols occur within the investigated sections. However, the excellent preservation conditions of the recognized palaeosols play a key role as they are an important prerequisite for proper interpretation.

The siliciclastic parent sediments of palaeosols within the Chiwondo Beds derived mostly from erosion of the hinterland consisting of Proterozoic metamorphic basement rocks and Permo-Triassic Karoo sediments that subsequently accumulated in the Malawi Rift. Due to alternating lake levels with transgression and regression of the shore line, fluvial sediments were partly reworked and sorted under deltaic and lacustrine conditions. Within this setting decalcified B horizons of terrestrial soils are rarely preserved. Moreover, although the Rungwe Volcanic Province, which had several magmatic pulses during the Plio-Pleistocene represented by tuffaceous sediments and lava flows (Delvaux *et al*., 1992; Ebinger *et al*., 1993; Fontijn *et al*., 2012), is located less than 150 km to the northwest of the study area, no volcanic ash covering older land surfaces (with palaeosols) has been detected in the entire area so far. Crossley (1982) describes a series of pyroclastic deposits overlying the basal lacustrine sediments of the Chiwondo Beds.

The calcimorphic palaeosols mentioned by Betzler and Ring (1995) show horizons with abundant carbonate nodules. They interpret these horizons as remnants of palaeosols which developed during phases of emersion and plant growth. Nonetheless, palaeosols of the Chiwondo and Chitimwe Beds have not been investigated in detail yet.

6.2 GOALS AND METHODS

Field relationships, sediment characteristics and heavy minerals (HM) were analyzed to gain information about palaeoecological and palaeoclimatic conditions during deposition of the Chiwondo Beds. With the attempt to narrow down the geochronological timespan of the Plio-Pleistocene units, datable material, namely volcanic tuffs, was searched for within the sediment sequence. Palaeosols were surveyed for the purpose of identifying marker horizons. Widely distributed surface survey was performed to gain a better understanding of the tectonic relationships and lateral variability of the different lithologies.

Reconnaissance field work comprised sediment and soil description of selected sections which were cut into prominently exposed slopes. Five exemplary profiles covering Unit 1, 2, 3A and 4 from three localities (Mwenirondo, Malema and Uraha; see Figure 1) are presented, which display characteristic features in terms of sediments and palaeosol remnants.

Description of sediment characteristics were done according to the standard of the German guidelines for soil and substrate description (Ad-hoc-AG Boden, 2005). For each section, stratification, texture, and soil horizon characteristics were recorded during field survey. Laboratory analyses comprised texture analysis following the German standard DIN ISO 11277 (2002). Determination of soil colour was performed using Munsell Soil Color Chart (2000).

For heavy mineral analyses fine sand (63–200 μm) was fractionized and treated with 5 N Na-dithionite to remove coatings of iron and manganese. Heavy minerals

were separated using Na-polytungstenate (d = 2.85 g/cm^3) and mounted with resin (refraction index n = 1.66) on microscope slides. Examination was done using a petrographic microscope; all samples were screened and the heavy mineral suites were recorded qualitatively. Here, a well-weathered saprolite 100 m west of profile 12-MW-58, 8 samples of a section in the Malema region examined by Sandrock (1999) in addition to 38 sediment-samples within profile 11-MW-04 were analysed.

6.3 PALAEOPEDOLOGICAL FIELD OBSERVATIONS

The Chiwondo Beds contain palaeosol horizons which can be described either as Bw-horizons, as oximorphic Cl-horizons or, more often, as Bk-horizons which are rich in carbonate nodules. In the whole sequence no complete palaeosol profile containing A, B and C horizons has been recognized.

The definition of the palaeosol horizons follows FAO (2006), despite the fact that pedofeatures may have changed in comparison with surface soils (Retallack, 1998). The defining properties of the palaeosol horizons in the area are colour, gleyzation, and carbonatization.

The Bw-horizons represent terrestrial palaeosols of Cambisol type. Their matrices generally have brown colour (10 YR to 7.5 YR) and do not contain carbonate unless infiltration from above has formed carbonate nodules subsequently. The parent material is composed of sand, most probably of alluvial or aeolian origin. Locally mottling of a fossil capillary fringe can be recognized.

Other remnants of palaeosols are represented by oximorphic horizons of Gleysols. These horizons developed close to a former surface from where atmospheric air could regularly enter the pore space. It seems that almost no post-burial alteration affected the horizons except later carbonate infiltration from above.

Large parts of the Chiwondo sediments show a light greenish to light greyish colour. This might be an effect of reduction and removal of oxides during times of groundwater influence, most probably directly after deposition of the respective strata. However, horizons with oxidation patterns, i.e. the upper part of Gleysols pointing to former surfaces, have been rarely observed.

Further palaeopedofeatures are Bk-horizons with abundant carbonate nodules. Superficial decalcified horizons as generally expected are absent. Thus, the main question is whether the concretionary carbonates represent genuine palaeosols. The parent material eroded from lime free sources (basement, Karoo Supergroup sediments) and consists of primarily non-calcareous sands and silts. A sedimentary reworking of concretions from elsewhere can be excluded in the dominantly fluvial setting, since their distribution in the respective strata is homogeneous and no placer-like deposits could be observed in the field.

All surface soils, even in the basement areas outside the rift, comprise Bk-horizons in the subsoil. Hence, calcium released by silicate weathering accumulates as carbonate crust in shallow depth and nodules form during pedogenesis. The shape of carbonate glaebules in the palaeosols ranges from diffuse patches of carbonate powder which may be early stages of nodules, to nodules up to 5 cm in diameter. The latter are generally massive with distinct outer boundaries indicating that finely distributed carbonate changed to the present form by subsequent leaching of calcareous phases from overlying soil horizons. Rarely concentric layers can be observed, which points towards a continuous growth (Retallack, 2011).

Tectonic activity resulted in a complex block pattern dissecting the sediments and correlation of the palaeosols with a small lateral extension is very challenging.

The observed palaeosols mentioned by Betzler and Ring (1995) are the most visible ones in the stratigraphy.

6.3.1 Mwenirondo

6.3.1.1 Field aspects

The Mwenirondo region is a flat, plateau area between the rivers of Masapa in the north and Ruasho in the south (Figure 1). Chitimwe deposits overlie the Chiwondo Beds with an unconformity. Due to a normal fault which is exposed on the eastern slope of the plateau, sediments of Unit 2 crop out on the northern slopes and Unit 3A on the southern ones.

6.3.1.2 Unit 2

The 13.2 m long profile 11-MA-58 (10°0.764′S, 33°53.916′E, 563 m asl), represents a typical sequence of Unit 2, on a steep cut bank of the Masapa river, which is water bearing only in the rainy season.

At the base of the section, saprolitic Precambrian basement gneiss is exposed. Its matrix is non-calcareous but contains detached carbonate-rich patches up to ~3 cm in diameter due to leaching from above.

A thick continuous sequence of Chiwondo Unit 2 sediments follows. The deposits are mainly coarse sand matrix supported fluvial conglomerates with fine to coarse pebbles and well-rounded cobbles (<15 cm). The conglomerates show a general fining up section and are successively enriched in pedogenic carbonate nodules towards the higher part of each layer, until a forming of massive caliche, followed by another conglomerate deposit. Four of those pedogenic cycles are present in the logged profile (Figure 2).

The heavy mineral analysis of the saprolite from approximately 100 m up the valley bottom revealed prevailing green amphibole with little garnet and zircon as accessorial minerals.

6.3.1.3 Unit 3A

The section representing a typical Unit 3A sequence in the Mwenirondo region consists of two separate profiles; 11-MW-04 (10°1.060′S, 33°55.242′E, 535 m asl) is located 155 m to the north of 12-MW-19 (10°0.980′S, 33°55.214′E, 560 m asl) along the southern slope of the plateau. Two step-like profiles with a combined thickness of 19 m were trenched in well exposed slopes and correlated them with a distinct lacustrine bed. The section represents a part of Unit 3A.

The succession consists mainly of fluvial silts and sands with pedogenic overprints (Figure 3). The variation of grain size and bedding structures indicates differences in sedimentation rates, whereas alternations of lacustrine lime represent transgression phases of the nearby palaeolake water level. Nearly the complete alternation comprehends abundant pedogenic carbonate nodules with sizes of 0.5 to 3 cm in diameter. Biogenic activity is reported by animal burrows which are refilled with calcareous silty clay; most seem to have a much younger age than the onset of the original pedogenesis in the sediments. The upper part of the section is calcareous whereas, for the most part, in the lower section the host-deposits around the nodules are non-calcareous.

In order to detect possible reworked volcanic material within the fluvial sediments of the Chiwondo beds heavy mineral analyses have been carried out. All 38 samples

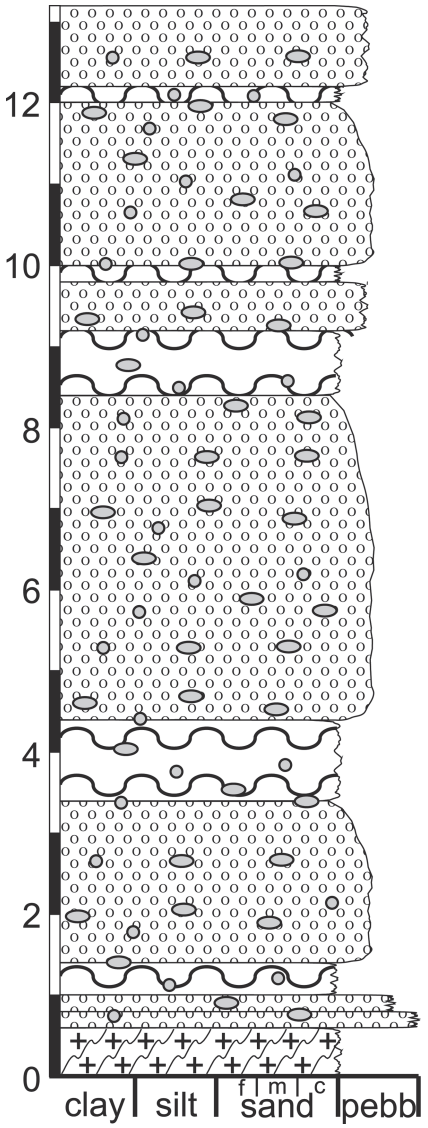

Figure 2. Stratigraphic column of profile 12-Ma-58 (10°0.764′S, 33°53.916′E), representing Unit 2 of the Chiwondo Beds in the Mwenirondo region with profile-meter, lithology and grain size. No inner structures are observed. For location see Figure 1, for legend Figure 7.

taken within Profile 11-MW-04 show a rather uniform composition. Despite some variations, garnet is always dominating, accompanied by epidote/zoisite, zircon, sphene, rutile, anatase, green amphibole, as well as tourmaline, kyanite and sillimanite as accessorial minerals. Definite volcanic components, which would represent the basaltic or trachytic character of the Rungwe tuffs, such as olivine, pyroxene, or brown amphibole, however, could not be recognized. Subrounded to rounded components dominate, and grains of euhedral shape are rare.

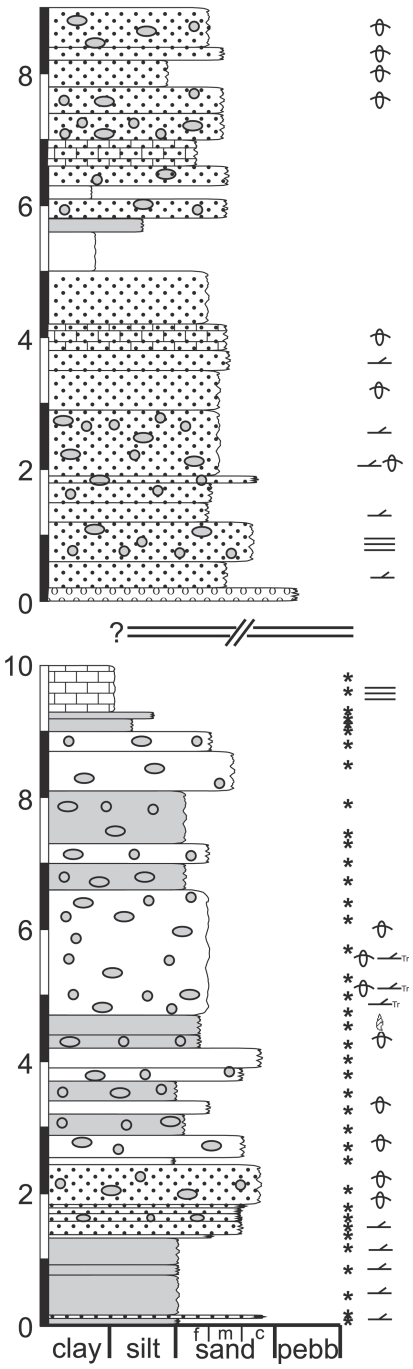

Figure 3. Stratigraphic column of profiles 11-MW-04 (10°1.060′S; 33°55.242′E) and 12-MW-19 (10°0.980′S, 33°55.214′E), representing Unit 3A of the Chiwondo Beds in the Mwenirondo region with profile-meter, lithology and grain-size, position of heavy mineral sample, structures and fossils. For location see Figure 1, for legend see Figure 7.

The weathering status of the heavy minerals differs within each sample. A considerable part of the stable group (zircon, rutile, and tourmaline) shows an advanced degree of corrosion. Also amphiboles are in an advanced stage of corrosion resulting in hacksaw terminations along their preferential crystallographic directions; however, intensive chemical weathering has not taken place.

6.3.2 Malema

6.3.2.1 Field aspects

The sedimentation circumstances of the Malema area south of the Ruasho River are similar to the Mwenirondo area; Chitimwe deposits form the cap sediments of a plateau area, whereas fluvial deposits of Unit 3A with pedogenic signatures are exposed along the slopes. A basement ridge crops out in the east, here Chiwondo or Chitimwe sediments overly the partly saprolitic gneiss with a major unconformity. The region experienced a large degree of tectonic activity which resulted in a complex block pattern; the correlation of palaeosols with a small lateral extension is therefore especially challenging. A bone-bed was excavated in the area; large terrestrial mammals, especially ungulates, dominate the fauna in this delta sequence along palaeolake Malawi (Sandrock, 1999; Sandrock *et al*., 1999). The occurrence of *Paranthropus cf. boisei* makes Malema the southernmost locality in East Africa yielding this early hominid taxon.

A screening of the heavy mineral assemblages of a 5 m long section close to a basement ridge (10°1.374′S, 33°55.815′E, 533 m asl; see profile S17 in Sandrock, 1999) revealed no volcanic material in the fine sand fraction. The spectra of 8 samples consist of garnet and green amphibole as the main constituents, accompanied by zircon, epidote, kyanite, sphene and rutile. The amount of green amphibole is higher than in other examined sediments.

6.3.2.2 Unit 3A

The 3.5 m long profile 12-MA-08 (10°1.323′S, 33°55.833′E, 538 m asl) is positioned on the northern wall of the archaeological excavation pit. The medium to coarse sands with fine (sub-)angular pebbles are part of Unit 3A (Figure 4). The upper 80 cm are made of Chitimwe fluvial sediments which are non-calcareous and have been subject to pedogenesis until today. The sharp transition to the Bk-horizon of a cut palaeosol within the Chiwondo Beds is marked by a colour-change from dark reddish-brown to beige, an abrupt calcification of the matrix and an appearance of pedogenic carbonate nodules. In the topmost 5 cm of the Chiwondo palaeosol the nodules have a rough surface which indicates modern etching of the fossil carbonate. The sediment is extremely rich in nodules, which are up to 3 cm in diameter and make up 50 to 70% of the palaeosol material; pebbles are often also coated with carbonate. It is not possible to distinguish different soil horizons.

6.3.3 Uraha

6.3.3.1 Field aspects

Due to the absence of Units 3B and 4 in the northern parts of the study area additional profiles were logged further south in the Uraha region, northwest of Chilumba (Figure 1). On the eastern slope of "Uraha Hill" Unit 1 and 2 are

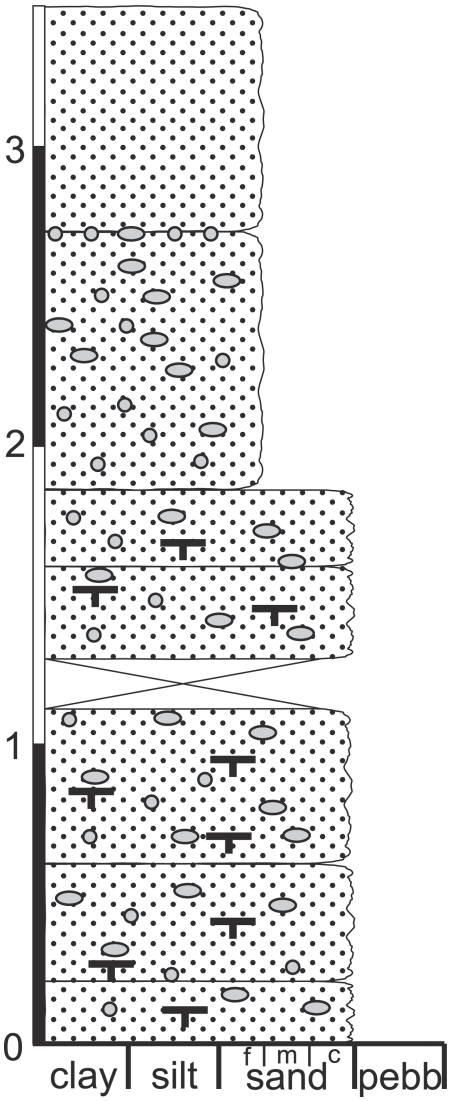

Figure 4. Stratigraphic column of profile 12-MA-08 (10°1.323′S, 33°55.833′E), representing Unit 3A of the Chiwondo Beds in the Malema region with profile-meter lithology and grain-size. No inner structures were observed. For location see Figure 1, for legend see Figure 7.

exposed, whereas Unit 4 is best exposed in an abandoned quarry almost 10 km further south.

In the region a mandible of *Homo rudolfensis* was recovered from a ferruginous palaeosol layer of Unit 3A (Bromage *et al*., 1995b).

6.3.3.2 Unit 1 and 2

Poor outcrop conditions on the steep slopes of Uraha Hill do not allow to produce continuous step-sections comparable to the northern parts. The profile 11-UR-99

(10°21.323′S, 34°8.483′E, 556 m asl) has a thickness of 24 m (Figure 5) and was surveyed by excavating holes every meter to log the lithology.

Unit 1 is exposed at the base, whereas the oncoids close to the top characterize Unit 2. The point of transition is most likely the onset of finer sediments at 10 m in the succession.

The fluvial Unit 1 deposits in the lower 10 m of the section range from fine to medium sands and inhabit pedogenic carbonate which is mainly represented in diffuse patches at the base of the section and becomes more and more consolidated to nodules towards the top. The matrix of these stream deposits is for the most parts non-calcareous and varies in colour from gray to reddish brown; latter is probably the result of reworking of the underlying red sands of the Dinosaur Beds (cf. Betzler and Ring, 1995).

The silt and clay deposits in the middle of the section display a general flooding of the area which describes the lower limit of Unit 2. For the most parts these calcareous sediments are also marked by pedogenesis which formed well consolidated nodules. Towards the top the lime content increases until a lacustrine limestone with abundant Bellamya gastropods is exposed. As a distinct feature of Unit 2 a layer of oncoids with Bellamya shells as nuclei formed is exposed laterally over a few kilometres in the Uraha region. The limestone in this upper part of the profile is interrupted by intercalations of sand deposits with carbonate nodules which indicate fluctuations of the water level of palaeolake Malawi during Unit 2.

6.3.3.3 Unit 4

In a valley ca. 8.5 km southeast of Uraha Hill Unit 4 overlies the Dinosaur Beds with a major unconformity. It is not possible to determine if Units 1 to 3 were eroded prior to the sedimentation of Unit 4 or never deposited at all in this area.

The 3.6 m long profile 12-UR-47 (10°25.215′S, 34°10.996′E, 572 m asl) is located along the slope of an isolated hill in the centre of the valley. White diatom-rich marls are interrupted by sand and conglomerates (Figure 6). Pedogenesis is strong in the sediments and the calcareous marls inhabit abundant nodules to the point of the forming of caliche. The fluvial deposits have also pedogenic carbonate nodules.

6.4 SYNTHESIS

The five profiles representing characteristic sections of the Chiwondo Bed consist primarily of fluvial sands with intercalations of silts and lacustrine limestones. Hence, during the last 4 Ma large river systems dominated the northern Malawi region. These probably braided and meandering streams eroded basement and Karoo Supergroup sediments and deposited silts, sands and conglomerates in a medium to high energy environment. Subrounded to rounded components dominate the heavy mineral fraction, which indicates reworking processes over long distances.

The limnic limestones with abundant pelecypods and gastropods (primary Bellamya), which built large portions of Unit 2, as well as the diatomite-rich silts in Unit 4 represent temporary transgressions of palaeolake Malawi. These rises in lake water can either be climatically induced, or present the influence of tectonic activity in the Malawi Rift, or, which is most likely, the result of both.

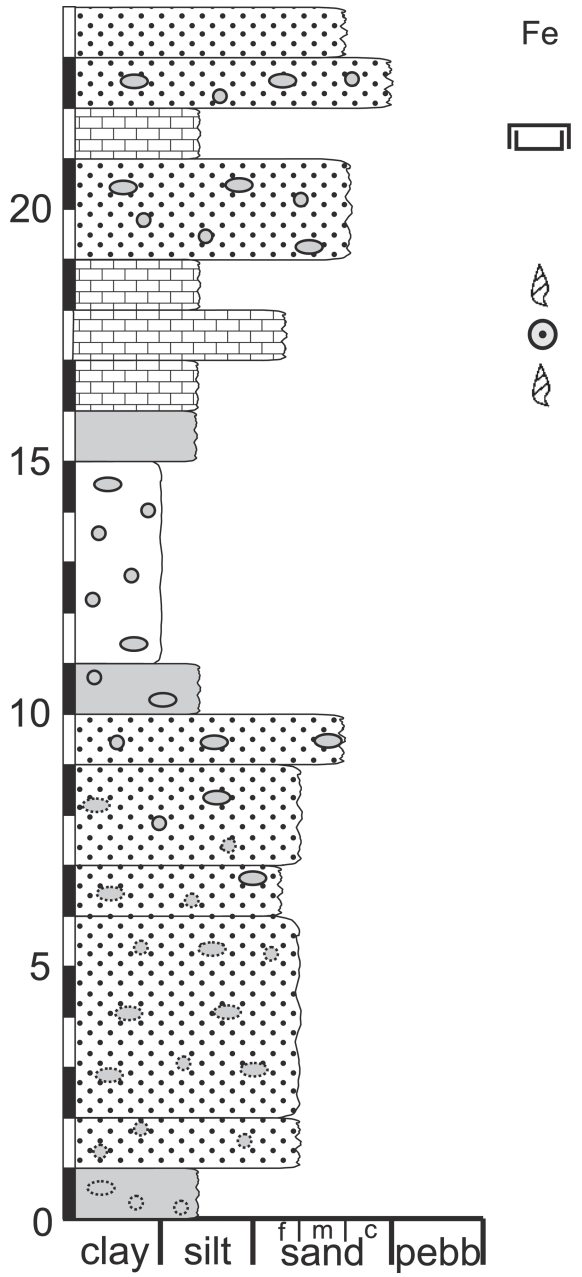

Figure 5. Stratigraphic column of profile 11-UR-99 (10°21.323′S, 34°8.483′E), representing Unit 1 and 2 of the Chiwondo Beds in the Uraha region with profile-meter, lithology and grain-size, structures and fossils. For location see Figure 1, for legend see Figure 7.

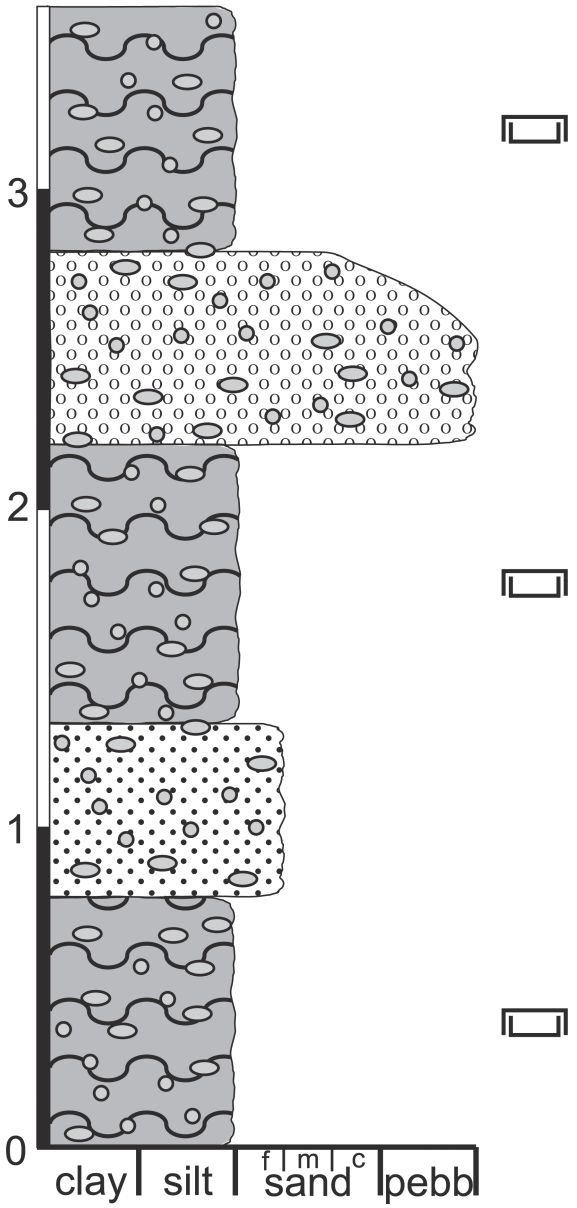

Figure 6. Stratigraphic column of profile 12-UR-47 (10°25.215′S, 34°10.996′E), representing Unit 4 of the Chiwondo Beds in the Uraha region with profile-meter, lithology and grain-size and fossils. For location see Figure 1, for legend see Figure 7.

Nearly all deposits comprehend abundant carbonate nodules, partly to the degree of forming caliche, which indicates a high rate of pedogenic overprint of the sediments. These erosion-resistant Bk-horizons are well preserved to the contrary to the carbonate depleted upper horizon of the palaeosols, which are seldom found in the region. This can be explained by morphodynamic processes such as erosion or

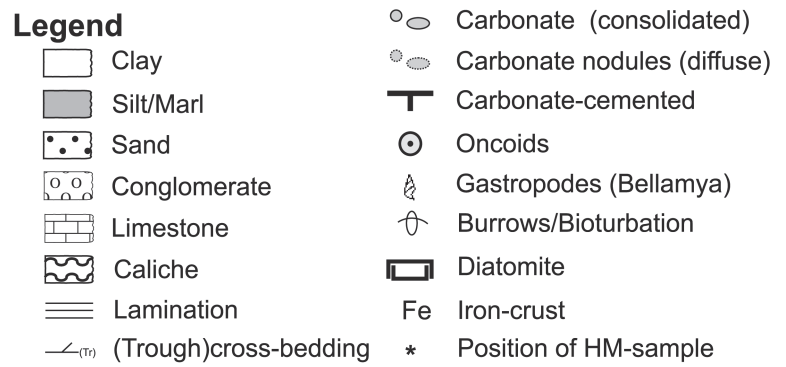

Figure 7. Key for lithology, structures, fossils and other sedimentary characteristics of the logged profiles displayed in Figures 2 to 6.

fluvial reworking of the loose sediment prior to the next sedimentation cycle. Carbonate nodules form in soils with a net water deficit, generally when precipitation is less than about 1000 mm/a (Jenny, 1980; Birkeland, 1984; Cerling and Quade, 1993), which seems to be the case during the whole timespan of deposition of the Plio-Pleistocene sediments. These circumstances are also given for the modern annual precipitation, which is actually less than 900 mm/a with a rainy season between November and April; subrecent nodules were found in cut banks of rivers. As described in chapter 3.2.2, pedogenic nodules close to the modern surface can have rough surfaces, which indicate recent etching of the fossil carbonate due to ongoing carbonate solution in the course of actual pedogenic processes. Further down in the soil profile this carbonate can form new coatings around fossil nodules or conglomeratic pebbles.

The stream deposits are composed of unconsolidated sediments, which are only occasionally cemented with carbonate. Post-sedimentary tectonic activity is difficult to evaluate, and a lateral continuation is often impossible to follow over a long distance. The latter is also hindered by the highly energetic fluvial environment, where sedimentation rates, but also erosion rates, are probably high in a cut-and-fill environment.

After extensive fieldwork and explicit searching for datable minerals, no volcanic layers were found. All heavy minerals samples analyzed for this study display an overall absence of volcanic minerals. As the Rungwe Volcanic Province, which had several magmatic eruptions during the Chiwondo Bed's deposition (Delvaux *et al.*, 1992), is located nearby one would expect tephra minerals as an evidence for the Rungwe volcanic ashes is mostly trachytic (Fontijn *et al.*, 2010). The lack of these could be explained due to the fact that the ashes were relocated from the palaeosurface in the highly erosive fluvial environment, or that they had never been deposited because of an opposite wind direction. The heavy mineral assemblages are dominated by the hinterland source areas and show only little variations; the content of green amphibole is higher in sections close to the basement source area. Grains of euhedral shape are rare. Besides the fact that they appear in all samples, even the sphene grains are generally well rounded, hence, it is unlikely that they sourced from tephra fallout.

There is no evidence on the timespan when palaeosols formed in the sediment sequence before they were covered by younger deposits. Hence, initial soil development in a fluvial environment under Plio-Pleistocene semi-arid conditions in an area of tectonic subsidence may have produced Calcisols with carbonate nodules in the first instance without adequate time to evolve decalcified B horizons.

Intensive in situ weathering of the Chiwondo Beds is unlikely since pH values are generally above pH 7. Thus, the heavy mineral associations throughout the investigated section represent only the input from the source areas into the Chiwondo Beds. The geochronology of the Pleistocene Chitimwe Beds is also still a matter of debate. The broad horizontal and vertical variability in clast size indicate a fluctuation in sedimentation and erosion rates, and topographic energy regime. Complex surficial processes triggered by droughts with dramatic lowering of lake level (c.f. Lyons *et al*., 2011; Scholz *et al*., 2011), faulting, tilting, and valley incision during the entire Pleistocene resulted in a highly variable spatial sediment pattern of this Unit 5. The brown to reddish colour of these sediments signifies the long time span of terrestrial soil development. The cover sediments of the plateau-like hills are generally made out of Chitimwe deposits which, in some places, eroded the underlying Chiwondo Beds, also supporting the high relief energy regime. Later, these old surfaces were cut by rivers which formed today's topography.

ACKNOWLEDGEMENTS

Tina Lüdecke acknowledges the support through the LOEWE funding program (Landes-Offensive zur Entwicklung Wissenschaftlich-ökonomischer Exzellenz) of Hesse's Ministry of Higher Education, Research and Arts. We thank Andreas Mulch, Friedemann Schrenk, Oliver Sandrock and Harrison Simfukwe for logistics and discussion. Two anonymous reviewers helped by additional comments to improve the manuscript.

REFERENCES

Ad-hoc-AG Boden, 2005, *Bodenkundliche Kartieranleitung*. 5th edition, Hannover, Germany, p. 438.

Andrew, A.R. and Bailey, T.E.G., 1910, The Geology of Nyasaland. *Quarterly Journal of the Geological Society*, **66**, pp. 189–237.

Aronson, J.L., Hailemichael, M. and Savin, S.M., 2008, Hominid environments at Hadar from paleosol studies in a framework of Ethiopian climate change. *Journal of Human Evolution*, **22**, pp. 532–550.

Barham, L.S. and Smart, P.L., 1996, An early date for the Middle Stone Age of central Zambia. *Journal of Human Evolution*, **30**, pp. 287–290.

Behrensmeyer, A.K., Todd, N.E., Potts, R. and McBrinn, G.E., 1997, Late Pliocene faunal turnover in the Turkana Basin, Kenya and Ethopia. *Science*, **278**, pp. 1589–1594.

Betzler, C. and Ring, U, 1995, Sedimentology of the Malawi Rift: Facies and stratigraphy of the Chiwondo Beds, northern Malawi. *Journal of Human Evolution*, **28**, pp. 23–35.

Birkeland, P.W., 1984, *Soils and Geomorphology*. Oxford University Press, New York, p. 432.

Bromage, T.G. and Schrenk, F., 1987, A cercopithecoid tooth from the Pliocene in Malawi. *Journal of Human Evolution*, **15**, pp. 497–500.

Bromage, T.G., Schrenk, F. and Juwayeyi, Y.M., 1995a, Paleogeography of the Malawi Rift: Age and Vertebrate Paleontology of the Chiwondo Beds, Northern Malawi. *Journal of Human Evolution*, **28**, pp. 37–57.

Bromage, T.G., Schrenk, F. and Zonneveld, F.W., 1995b, Paleoanthropology of the Malawi-Rift: An early hominid mandible from the Chiwondo Beds, northern Malawi. *Journal of Human Evolution*, **28**, pp. 71–108.

Catuneanu, O., Wopfner, H., Eriksson, P.G., Cairncross, B., Rubidge, B.S., Smith, R.M.H. and Hancox, P.J., 2005, The Karoo basins of south-central Africa. *Journal of African Earth Sciences*, **43**, pp. 211–253.

Cerling, T.E., 1992, Development of grassland and savannas in East Africa during the Neogene. *Palaeogeography, Palaeoclimatology, Palaeoecology*, **97**, pp. 241–247.

Cerling, T.E. and Hay, 1986, An isotopic study of paleosol carbonates from Olduvai Gorge. *Quaternary Research*, **25**, pp. 63–78.

Cerling, T.E. and Quade, J., 1993, Stable Carbon and Oxygen Isotopes in Soil Carbonates. *Geophysical Monograph*, **78**, pp. 217–231.

Cerling, T.E., Bowmann, J.R. and O'Neil, J.R., 1988, An isotopic study of a fluvial-lacustrine sequence: the Plio-Pleistocene Koobi Fora sequence, East Africa. *Palaeogeography, Palaeoclimatology, Palaeoecology*, **63**, pp. 335–356.

Cerling, T.E., Wynn, J.G., Andanje, S.A., Bird, M.I., Korir, D.K., Levin, N.E., Mace, W., Macharia, A.N., Quade, J. and Remien, C.H., 2011, Woody cover and hominin environments in the past 6 million years. *Nature*, **476**, pp. 51–56.

Charsley, T.J., 1972, The limestone resources of Malawi. *Geological Survey Department, Zomba, Memoir*, **6**, pp. 1–128.

Clark, J.D., Hayners, C.V., Mawby, J.E. and Gautier, A., 1970, Interim report on paleoantropological investigations in the Lake Malawi Rift, *Quaternaria*, **13**, pp. 305–354.

Crossley, R., 1982, Late Cenozoic stratigraphy of the Karonga area in the Malawi rift. *Palaeoecology of Africa*, **15**, pp. 139–144.

Delvaux, D., Levi, K., Kajara, R. and Sarota, J., 1992, Cenozoic paleostress and kinematic evolution of the Rukwa—North Malawi Rift Valley (East African Rift System). *Bulletin des Centres de Recherches Exploration-Production Elf Aquitaine*, **16**, pp. 383–406.

de Heinzelin, J., Clark, J.D., White, T., Hart, W., Renne, P., WoldeGabriel, G., Beyene, Y. and Vrba, E., 1999, Environment and Behavior of 2.5-Million-Year-Old Bouri Hominids. *Science*, **23**, pp. 625–629.

DIN ISO 11277, 2002, *Soil quality—Determination of particle size distribution in mineral soil material—Method by sieving and sedimentation*, Beuth, Berlin, p. 38.

Dixey, F., 1927, The Tertiary and Post-Tertiary Lacustrine Sediments of the Nyasan Rift-Valley. *Quarterly Journal of the Geological Society*, **83**, pp. 432–442.

Ebinger, C.J., Deino, A.L., Drake, R.E. and Tesna, A.L., 1989, Chronology of volcanism and rift basin propagation: Rungwe volcanic province, East Africa. *Journal of Geophysical Research*, **94**, pp. 15785–15803.

Ebinger, C.J., Deino, A.L., Tesha, A., Becker, T. and Ring, U., 1993, Tectonic controls on rift basin morphology: Evolution of the northern Malawi (Nyasa) rift. *Journal of Geophysical Research*, **98**, pp. 17821–17836.

Feakins, S.J., Levin, N.E., Liddy, H.M., Sieracki, A., Eglinton, T.I. and Bonnefille, R., 2013, Northeast African vegetation change over 12 m.y. *Geology*, **41**, pp. 295–298.

FAO (Food and Agriculture Organization of the United Nations), 2006, *Guidelines for soil description*. 4th edition, Rome, p. 97.

Fontijn, K., Ernst, G.G.J., Elburg, M.A., Williamson, D., Abdallah, E., Kwelwa, S., Mbede, E. and Jacobs, P., 2010, Holocene explosive eruptions in the Rungwe Volcanic Province, Tanzania. *Journal of Volcanology and Geothermal Research*, **196**, pp. 91–110.

Fontijn, K., Williamson, D., Mbede, E. and Ernst, G.G.J., 2012, The Rungwe Volcanic Province, Tanzania—A volcanological review. *Journal of African Earth Sciences*, **63**, pp. 12–31.

Frost, S.R. and Kullmer, O., 2008, Cercopithecidae from the Pliocene Chiwondo Beds, Malawi-Rift. *Geobios*, **41**, pp. 743–749.

Hamiel, Y., Baer, G., Kalindekafe, L., Dombola, K. and Chindandali, P., 2012, Seismic and aseismic slip evolution and deformation associated with the 2009–2010 northern

Malawi earthquake swarm, East African Rift. *Geophysical Journal International*, **191**, pp. 898–908.
Jenny, H., 1980, *The Soil Resource*. Springer, New York, p. 377.
Kaufulu, Z.M., 1989, Sedimentary conditions within a Plio-Pleistocene graben at Karonga, northern Malawi and their implications for the prehistoric record of the area. *Palaeoecology of Africa*, **20**, pp. 99–108.
Kaufulu, Z.M. and Stern, N., 1987, The first stone artifacts to be found in situ within the Plio-Pleistocene Chiwondo Beds in northern Malawi. *Journal of Human Evolution*, **16**, pp. 729–740.
Kullmer, O., 2008, The fossil Suidea from the Plio-Pleistocene Chiwondo Beds of Northern Malawi, Africa. *Journal of Vertebrate Paleontology*, **28**, pp. 208–216.
Kullmer, O., Sandrock, O., Abel, R., Schrenk, F., Bromage, T.G. and Juwayeyi, 1999, The first *Paranthropous* from the Malawi Rift. *Journal of Human Evolution*, **37**, pp. 121–127.
Kullmer, O., Sandrock, O., Kupczik, K., Frost, S.R., Volpato, V., Bromage, T.G. and Schrenk, F., 2011, New primate remains from Mwenirondo, Chiwondo Beds in northern Malawi. *Journal of Human Evolution*, **61**, pp. 617–623.
Levin, N.E., Quade, J., Simpson, S.W., Semaw, S. and Rogers, M., 2004, Isotopic evidence for Plio-Pleistocene environmental change at Gona, Ethiopia. *Earth and Planetary Science Letters*, **219**, 93–110.
Levin, N.E., Brown, F.H., Behrensmeyer, A.K., Bobe, R. and Cerling, T.E., 2011, Paleosol carbonates from the Omo Group: Isotopic records of local and regional environmental change in East Africa. *Palaeogeography, Palaeoclimatology, Palaeoecology*, **307**, pp. 75–89.
Lyons, R.P., Scholz, C.A., Buoniconti, M.R. and Martin, M.R., 2011, Late Quaternary stratigraphic analysis of the Lake Malawi Rift, East Africa: An integration of drill-core and seismic-reflection data. *Palaeogeography, Palaeoclimatology, Palaeoecology*, **303**, pp. 20–37.
Magill, C.R., Ashley, G.M. and Freemann, K.H., 2012a, Ecosystem variability and early human habitats in eastern Africa. *Proceedings of the National Academy of Science of the United States of America*, **110**, pp. 1167–1174.
Magill, C.R., Ashley, G.M. and Freemann, K.H., 2012b, Water, plants, and early human habitats in eastern Africa. *Proceedings of the National Academy of Science of the United States of America*, **110**, pp. 1175–1180.
Munsell Color Company, 2000, *Standard soil color charts*, Baltimore.
Plummer, T.W. and Bishop, L.C., 1994, Hominid Palaeoecology at Olduvai Gorge, Tanzania as indicated by antelope remains. *Journal of Human Evolution*, **27**, pp. 47–75.
Retallack, G.J., 1998, Adapting Soil Taxonomy for use with Paleosols. *Quaternary International*, **51/52**, pp. 55–60.
Retallack, G.I., 2011, *Soils of the past, 2nd edition*. Wiley-Blackwell, p. 512.
Retallack, G.J., Wynn, J.G., Benefit, B.R. and McCrossin, M.L., 2002, Paleosols and paleoenvironments of the middle Miocene, Maboko Formation, Kenya. *Journal of Human Evolution*, **42**, pp. 659–703.
Ring, U., Betzler, C. and Devaux, D., 1992, Normal vs. strike-slip faulting during rift development in East Africa: The Malawi Rift. *Geology*, **20**, pp. 1015–1018.
Ring, U. and Betzler, C., 1995, Geology of the Malawi Rift: kinematic and tectonosed-imentary background to the Chiwondo Beds, northern Malawi. *Journal of Human Evolution*, **28**, pp. 7–21.
Sandrock, O., 1999, *Taphonomy and Palaeoecology of the Malema Hominid Site, Northern Malawi*. PhD Thesis, University of Mainz, p. 277.

Sandrock, O., Dauphin, Y., Kullmer, O., Abel, E., Schrenk, F. and Denys, C., 1999, Malema: Preliminary taphonomic analysis of an African hominid locality. *Human Palaeontology*, **328**, pp. 133–139.

Schlüter, T., 2008, *Geological Atlas of Africa: With Notes on Stratigraphy, Tectonics, Economic Geology, Geohazards and Geosites of Each Country—2nd edition*. Springer, Berlin, pp. 1–308.

Scholz, C.A., Cohen, A.S., Johnson, T.C., King, J., Talbot, M.R. and Brown, E.T., 2011, Scientific drilling in the Great Rift Valley: The 2005 Lake Malawi Scientific Drilling Project—An overview of the past 145,000 years of climate variability in Southern Hemisphere East Africa. *Palaeogeography, Palaeoclimatology, Palaeoecology*, **303**, pp. 3–19.

Schrenk, F., Bromage, T.G., Betzler, C.G., Ring, U. and Juwayeyi, Y.M., 1993. Oldest *homo* and Pliocene biography of the Malawi Rift. *Nature*, **365**, pp. 833–836.

Schrenk, F., Bromage, T.G., Gorthner, A. and Sandrock, O., 1995, Palaeoecology of the Malawi Rift: Vertebrate and invertebrate faunal contexts of the Chiwondo Beds, northern Malawi. *Journal of Human Evolution*, **28**, pp. 59–70.

Ségalen, L., Lee-Thorp, J. and Cerling, T., 2007, Timing of C_4 grass expansion across sub-Saharan Africa. *Journal of Human Evolution*, **53**, pp. 549–559.

Sikes, N.E., 1994, Early hominid habitat preferences in East Africa: Paleosol carbon isotopic evidence. *Journal of Human Evolution*, **27**, pp. 25–45.

Sikes, N.E., Potts, R. and Behrensmeyer, A.K., 1999, Early Pleistocene habitat in Member 1 Olorgesailie based on paleosol stable isotopes. *Journal of Human Evolution*, **37**, pp. 721–746.

Stephens, E.A., 1966, Geological account of the Northwest coast of Lake Malawi between Karonga and Lion Point, Malawi. *American Anthropological Association*, Special Publication, **68**, pp. 50–58.

Thompson, J.C., Mackay, A., Wright, D.K., Welling, M., Greaves, A., Gomani-Chindebvu, E. and Simengwa, D., 2012, Renewed investigations into the Middle Stone Age of Northern Malawi. *Quaternary International*, **270**, pp. 129–139.

Tryon, C.A., McBrearty, S. and Texier, P.-J., 2005, Levallois lithic technology from the Kaphturin formation, Kenya: Acheulian origin and Middle Stone Age diversity. *African Archaeological Review*, **22**, pp. 199–229.

Wesselman, H.B., 1985, Fossil micromammals as indicators of climatic change about 2.4 Myr ago in the Omo Valley, Ethopia. *South African Journal of Science*, **81**, pp. 260–261.

Wynn, J.G., 2000, Paleosols, stable carbon isotopes, and paleoenvironmental interpretations of Kanapoi, Northern Kenya. *Journal of Human Evolution*, **39**, pp. 411–432.

Wynn, J.G., 2004, Influence of Plio-Pleistocene Aridification on Human Evolution: Evidence From Paleosols of the Turkana Basin, Kenya. *American Journal of Physical Anthropology*, **123**: pp. 106–118.

Wynn, J.G., and Retallack, G.J., 2001, Paleoenvironmental reconstruction of middle Miocene paleosols bearing *Kenyapithecus* and *Victoriapithecus*, Nyakach Formation, southwestern Kenya. *Journal of Human Evolution*, **40**, pp. 263–288.

This page intentionally left blank

CHAPTER 7

Why 'Younger Dryas'? Why not 'Antarctic Cold Reversal'? Eksteenfontein revisited

Klaus Heine
Phil. Fakultät I, Universität Regensburg, Regensburg, Germany

Uwe Rust (1940–2012)
Geographisches Institut, Ludwig-Maximilian-Universität, München, Germany

Alexandra Hilgers
Geographisches Institut, Universität zu Köln, Köln, Germany

ABSTRACT: The presence or the absence of the geographic extent and magnitude of the Younger Dryas (YD) event, a circum-North Atlantic cooling c. 12,800–11,700 years ago, in the Southern Hemisphere has been disputed for many decades. The Eksteenfontein pollen section in the winter-rain realm of the Northern Cape, South Africa, covers the late-glacial/Holocene transition and was assumed to represent the YD event. Some new AMS ^{14}C and OSL ages support the age of the Eksteenfontein site. However, the re-evaluation makes clear that the lower part of the section represents the Antarctic Cold Reversal (ACR, c. 14,700–12,700 ka BP) that preceded the YD event. The YD cannot be traced. These findings corroborate the absence of the YD in the Southern Hemisphere and support the conclusion that, in the past, late-glacial cooling phases of the Southern Hemisphere caused by the ACR were confused with the YD event.

7.1 INTRODUCTION AND MOTIVATION

During the transition from the last glacial maximum (LGM, c. 22,000 years ago) to the Holocene (since c. 11,600 years ago), ice-core records from Antarctica and Greenland indicate that rapid warming events happened first in the Southern Hemisphere (Blunier *et al*., 1997; White and Steig, 1998; Shi *et al*., 2000). These asynchronous temperature variations are recently confirmed by Stenni *et al*. (2011). Their chronology from Antarctica, based on methane synchronization, supports the hypothesis that the cooling of the Antarctic Cold Reversal (ACR, c. 14,700–12,700 ka BP) is synchronous with the Bølling-Allerød warming in the Northern Hemisphere 14,700 years ago. Conversely, the onset of the Younger Dryas (YD, c. 12,800–11,700 ka BP) cooling of the Northern Hemisphere is synchronous with the end of the ACR. Although it is clear since the 1990s that the cooling phases of the late-glacial/Holocene transition did not occur synchronously in both hemispheres, rapid late-glacial cooling oscillations were assigned to the Younger Dryas Phase and were used to confirm the synchrony of late-glacial cooling events in both hemispheres (Peteet, 1995). Thompson *et al*.

(1995), Clapperton *et al*. (1997), Heusser and Rabassa (1987), Lowell *et al*. (1995), amongst others, used ice cores and late-glacial moraines to postulate glacial advances of Younger Dryas age in the South American Andes and Denton and Hendy (1994) in the Alps of New Zealand. Heusser (1966; see also Heusser and Streeter, 1980) went into battle with Markgraf (1991) about the Younger Dryas oscillation in southern South America based on pollen records. Often these records were ambiguous (e.g., first critical reviews in Markgraf *et al*., 1992; J.T. Heine, 1993). In the southeastern Atlantic Ocean, Farmer *et al*. (2005) used Mg/Ca analyses of *Globigerina bulloides* and abundances of *Neogloboquadrina pachyderma* (left coiling) from Ocean Drilling Program (ODP) Leg 175 Hole 1084B in the Benguela coastal upwelling system to document lower sea surface temperatures during the Last Glacial Maximum (LGM), the Younger Dryas, the mid-Holocene, and the Little Ice Age. In southern Africa, Scott *et al*. (1995, 2012) used the Eksteenfontein record to characterize the Younger Dryas phase in South Africa's arid region.

While late-glacial climatic events have been resolved in much detail in the Northern Hemisphere, in Greenland and in Antarctica, terrestrial records of the late-glacial/early Holocene from arid and semi-arid southern Africa are scarce and show weak time resolution. In the tropics and subtropics, millennial-scale cooling and warming events were primarily reflected in altered patterns of precipitation (Peterson *et al*., 2000). In their synthesis of moisture and temperature trends during the late Quaternary based on pollen records from different regions in southern Africa, Scott *et al*. (2012) again refer to the Eksteenfontein site in the Richtersveld area (Figure 1). It is the only site in the arid southwestern African winter rainfall domain that might have been affected by late Quaternary spatial and temporal climate changes caused by shifts of the northern border of the winter-rains and the position and extension of the southern intertropical convergence zone (ITCZ). A study of shifts of the southwestern African biomes (e.g., Shi *et al*., 2001), the *Succulent Karoo*, *Nama Karoo* and *Namib*

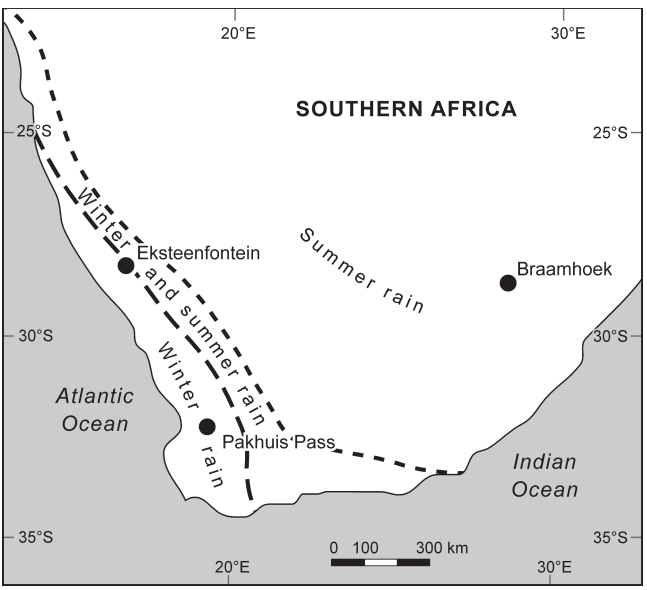

Figure 1. Locality map showing the Eksteenfontein site and other sequences discussed in the text.

Desert (Scott *et al*., 2012), permits a reconstruction of aspects of regional climate at that time. This is the reason why the Eksteenfontein record of Scott *et al*. (1995) is cited in many studies dealing with the Pleistocene/Holocene transition in southern Africa and the adjacent southeastern Atlantic Ocean (e.g., Dupont *et al*., 2004; Gasse, 2000; Gasse *et al*., 2008).

While Dupont *et al*. (2004), Gasse (2000) and Gasse *et al*. (2008) point to the possible influence of the ACR apart from the YD event (see also: Abell and Plug, 2000) and reflect on the difficulty that records based on terrestrial sediments indicate weak or ambiguous climate signals, Scott *et al*. (1995, 2012) did not mention the ACR at all, nor with respect to the Eksteenfontein site. Therefore, the Eksteenfontein record suggests a climate evolution connected to the YD chronozone and was used as such for correlating terrestrial and marine records from southern Africa. Yet, many terrestrial chronologies from southern Africa lack profound time control. Here we show that the Eksteenfontein record suggests a paleoclimatic interpretation that is characteristic for the late-glacial/Holocene transition in southern Africa and the Southern Hemisphere.

7.2 REGIONAL SETTINGS OF THE STUDY AREA AND SITE

The Eksteenfontein site is situated at 28°49′26,60″S and 17°14′46,04″E in about 630 m a.s.l. in a small valley at the western road exit of the Eksteenfontein village (Figure 2). The geology of the region (Martin, 1965; Frimmel, 2000) is dominated by the pre-Gondwanan violently folded and sheared rocks of the Gariep Belt within the

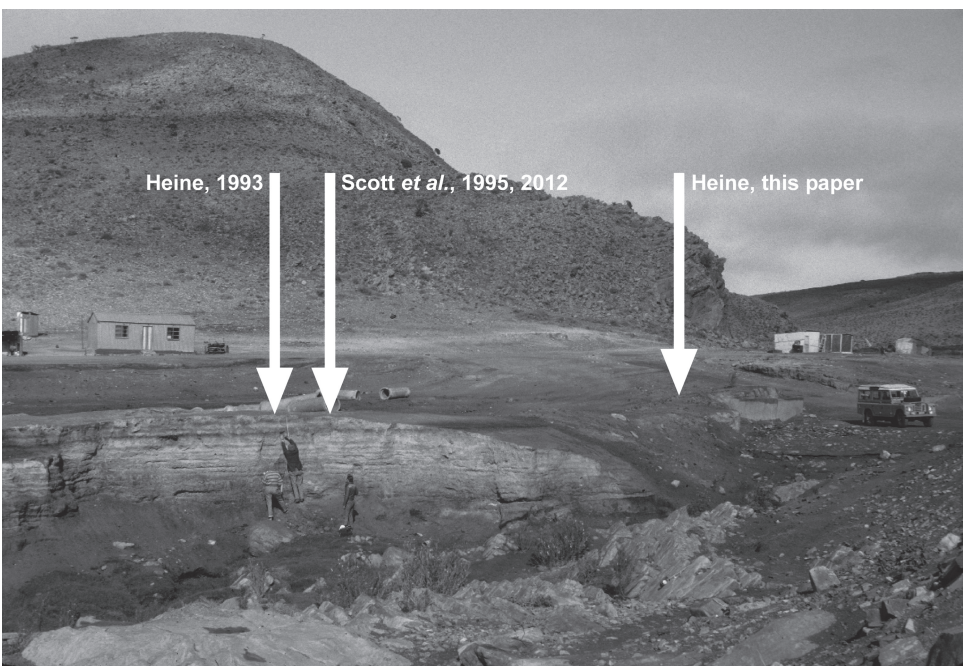

Figure 2. The Eksteenfontein sequence. The sections of Heine (1993) and Scott *et al*. (1995, 2012) are seen on the left side of this photo taken in 1981. Floods eroded these sections while the section of 2006 and 2009 was created by undercutting.

Neoproterozoic/early Paleozoic orogenic belts of southwestern Africa. Granite and gneiss intrusions are found beside quartzite, schist and dolomite. The dominant soils in the region are lithic and eutric leptosols. Colluvial sediments with calcrete formations form aprons at the base of the granite-gneiss hills. Middle Stone Age (MSA) artifacts were found in the stone pavement above the calcrete horizons (Heine, 1993). The small valley of the Eksteenfontein section runs from the West to the East cutting into the rocks and hillslope sediments. After a narrow part, the valley widens and spring water formed a sequence of sand and siliceous sinter in the valley (Figure 2). The sequence is about 3 m thick. The top layers were removed in the course of construction works.

The Eksteenfontein site is situated in the arid desert region of the Richtersveld of southwestern Africa. The region experiences a relatively mild desert climate where extremes are soothed by the proximity to the cold, upwelled waters of the Benguela Current. The climate is characterized by winter-rains (Waibel, 1922). Average annual precipitation is less than 50 mm with rain falling mainly between December and April (Mendelsohn *et al*., 2002). Total water deficit is about 2000 mm/year. Average annual temperatures are 16–18°C. Average minimum temperatures of the coldest month (July) are 6–8°C and average maximum temperatures of the warmest month (January) are about 30°C. The region belongs to the *Succulent Karoo Biome* (Cowling *et al*., 1999).

7.3 METHODS

Samples were gathered in 1981, 2006 and 2009 for grain size analyses, the determination of the $CaCO_3$ content, clay mineral analyses and ^{14}C and OSL dating. It turned out that the section of 1981 was subsequently spoiled by erosion so that in 2006 supplementary samples were taken further to the west (Figure 3). Between 2006 and 2009, again, flood water eroded parts of the section. By tracing several dark and light layers on pictures and field sketches from former years and by comparing them with the layers at the walls of the section it was possible to correlate the sections of the years 1981 not only with those of 2006 and 2009 but also with the section described by Scott *et al.* (1995).

The section of Heine (1993) is identical with the section analyzed by Scott *et al*. (1995, 2012) (Figure 4). In 2006 and 2009 we collected material for further AMS ^{14}C and OSL dating (Figure 5). The samples were taken from a part of the section that is about 40 m west of the section where Scott *et al*. (1995) collected the material for ^{14}C dating. Most of light and dark layers could be correlated with the 2006/2009 sections along the walls formed through bank caving and undercutting (Figures 2 and 3).

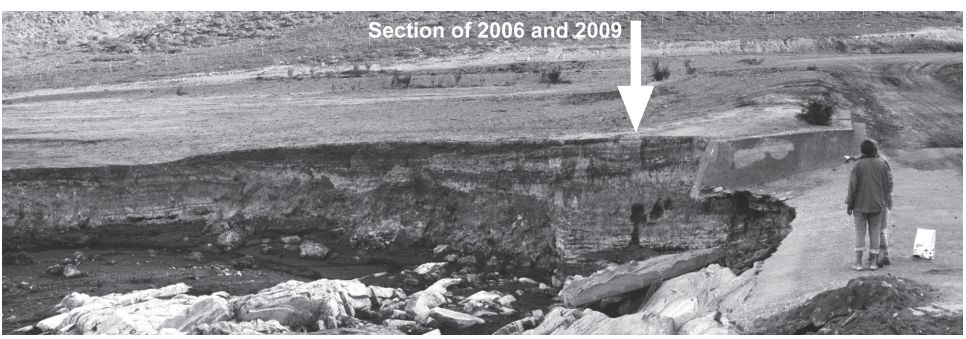

Figure 3. The section of 2006/2009.

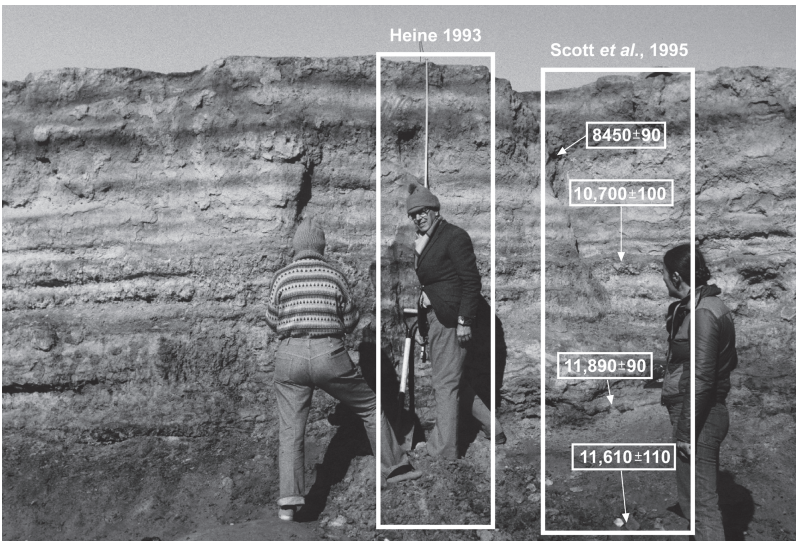

Figure 4. The section of Heine (1993) and Scott *et al.* (1995, 2012). The photo was taken in 1981. From left to right: J.A. Coetzee, E. van Zinderen Bakker and A. Heine.

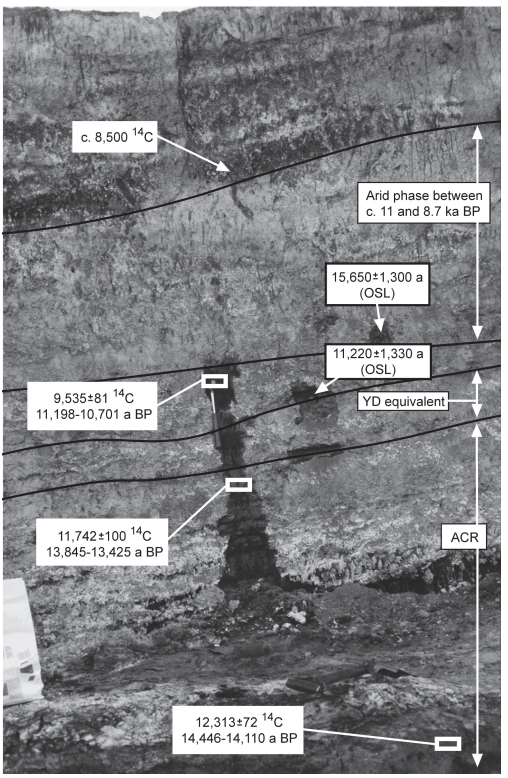

Figure 5. Details of the 2006/2009 section with sample sites for AMS ^{14}C and OSL dating. Hammer (30 cm) in the centre for scale.

AMS ^{14}C dating was performed by the *AMS-Labor Erlangen*. Calibration was attained by using the *IntCal04 Terrestrial Radiocarbon Age Calibration, 0–26 cal kyr BP* (Reimer *et al*., 2004). ^{14}C ages ($\pm 1\sigma$) are expressed in years before AD 1950 (e.g., 14,500 ^{14}C a BP), and AMS ^{14}C ages are given in calibrated years BP (e.g., 16,700 a BP). Optically Stimulated Luminescence (OSL) dating was done by A. Hilgers. The single-aliquot regenerative-dose protocol following in general the protocol described by Murray and Wintle (2000) was applied to two sediment samples. For equivalent dose determination quartz was extracted from the fine sand fraction. For optical stimulation the samples were exposed to blue light for 50s and held constantly at 125°C during illumination (SAR-BLSL) and the blue light stimulated luminescence of the quartz grains was measured in the UV wavelength range. A thermal pre-treatment of 220°C for 10s was chosen based on the results of the pre-heat plateau and dose recovery tests. About 30 aliquots were measured per sample, each containing on average 50 to 100 quartz grains.

7.4 RESULTS AND INTERPRETATION

The dominant lithology of the Eksteenfontein deposits is well-stratified thin layers. They consist of sand to silty sand and sandy silt (Figures 2, 3, 4 and 5). Grains > 2 mm Ø are rare. The colour (dry material, Munsell Soil Color Charts) varies from light grey (10 YR 7/1) to dark grey (organic sediment layers, 10 YR 4/1). Some small bands as well as reed casts and small patches show colours from yellowish brown to brownish yellow and yellow (10 YR 5/6, 10 YR 6/6 and 10 YR 7/6). The sediments do not contain $CaCO_3$, although calcrete formations cover the adjacent colluvial sediments on the lower slopes. Only traces of $CaCO_3$ were found in some layers. Mainly quartz grains with some micas compose the different layers. The quartz grains are angular documenting that they originate from the adjacent hill slopes and were not transported over larger distances in the valley. The layers vary with respect to the clay mineral content, percentage of rounded grains, aggregates of calcrete and silcrete remnants. In the eastern part of the sequence, the organic matter is mainly composed of dark grey to black humus mud with reed casts which are more or less vertical orientated. The thicker stems could be filled from above with fine sand, silt and clay. In the western part of the section the reed casts are almost absent and the yellowish colour is restricted to the lowermost layers where groundwater is present. The clay mineral spectrum of the Eksteenfontein sediments shows 35% illite, 40% smectite, 20% kaolinite, 5% mixed layers (14–14Å) and traces of chlorite, quartz, Fe oxides and feldspar. This clay mineral assemblage is characteristic for the region of the southern Namib Desert south of the Orange River (Heine and Völkel, 2010) and is found in slope colluvium and recent/subrecent stream-laid sediments of small local valleys.

The Eksteenfontein sequence was first radiocarbon dated by Scott *et al*. (1995). Four radiocarbon dates of dark organic sandy layers, which intercalate the lighter layers, suggests that the Eksteenfontein sequence covers the Pleistocene/Holocene transition between c. 8450 a BP and some time before 12,000 a BP (Figure 4). The bottom age of the sequence was chronologically anomalous and excluded, but based on extrapolation of the three upper radiocarbon dates, Scott *et al*. (1995, 2012) and Scott and Woodborne (2007) extrapolate an age between 14.5 and 15 ka (Table 1).

Our ^{14}C ages (Table 2, Figure 5) corroborate the ages mentioned by Scott *et al*. (1995). The ^{14}C ages are in good chronological order and the assumption of Scott *et al*. (1995) that their lowermost ^{14}C age was too young is substantiated by our results (sample Erl-13865). Based on the ^{14}C ages, there is no doubt that the Eksteenfontein

sequence comprises the Pleistocene/Holocene transition between c. 14,500 and, roughly, 7000 years. While the oldest sediments rest on the solid rock, the youngest layers are removed by caterpillars. Nevertheless, two OSL ages (Table 3, Figure 5) were obtained to make sure that the ^{14}C ages are reliable and not imprecise because of contamination of any kind. Heine (1993) reported some observations (Figure 6) that the Eksteenfontein sequence might have been covered by a calcrete horizon in the past. If this was the case, then the sedimentation of the underlying pollen bearing sequence should have started during the last ice age (Figure 6) because the calcrete layer was radiocarbon dated to 19,380 ± 330 ^{14}C years BP (Table 2; Heine, 1993).

Although the OSL ages are not in chronological order, they, at least, show that the Eksteenfontein sequence was deposited after c. 14,500 a BP (Table 3). Both OSL samples show comparatively broad distributions of the OSL ages or equivalent doses

Table 1. Radiocarbon dates of Eksteenfontein relating to the period c. 12,000 to 9,000 BP (Scott *et al.*, 1995).

Date (^{14}C age)	Lab. number	Material	Depth (cm) and/or zone
8450 ± 90	Pta-4826	organic sand	40–49
10,700 ± 100	Pta-5687	organic sand	130–138
11,890 ± 90	Pta-5684	organic sand	221–229
11,640 ± 110	Pta-4824	organic sand	±287–289

Table 2. Radiocarbon dates of Eksteenfontein.

^{14}C age	cal. age (1σ)	Lab. number	Material
9535 ± 81	9129–8994 BC 8927–8758 BC	Erl-10232	organic sand
11,742 ± 100	11,757–11,524 BC	Erl-10233	organic sand
12,313 ± 72	12,446–12,110 BC	Erl-13865	organic sand
19,380 ± 330		Hv 11641	calcrete

Table 3. OSL ages of Eksteenfontein sediments. Dose rate data, including uranium, thorium, and potassium concentrations, calculated dose rate during burial, equivalent dose values and resulting OSL ages. All uncertainties represent the 1σ confidence interval.

Lab. code	Sample	U (ppm)[a]	Th (ppm)[a]	K (%)[a]	Dose rate (Gy/ka)[b]	De (Gy)[c]	OSL age (ka)
C-L1991	06/V	2.00 ± 0.08	4.10 ± 0.37	1.63 ± 0.13	2.38 ± 0.14	37.3 ± 2.1	15.65 ± 1.30
C-L1992	06/VI	2.70 ± 0.11	4.00 ± 0.36	1.73 ± 0.14	2.62 ± 0.16	29.4 ± 3.0	11.22 ± 1.33

[a] The U, Th, and K concentrations were derived from ICP-MS analysis (Dr. H.-U. Kasper, Geology Department, University of Cologne).

[b] Dose rate to the samples was calculated using water contents in the range of 2 ± 1.5 to 5 ± 2.5 weight-%, and also includes the cosmic dose rate which was calculated following Prescott and Hutton (1988, 1994).

[c] The errors of the De values include the uncertainty of the beta source calibration of 5%. The average De value is based on the median of the measured aliquots (n = 28 for sample 06/V and 31 for sample 06/VI).

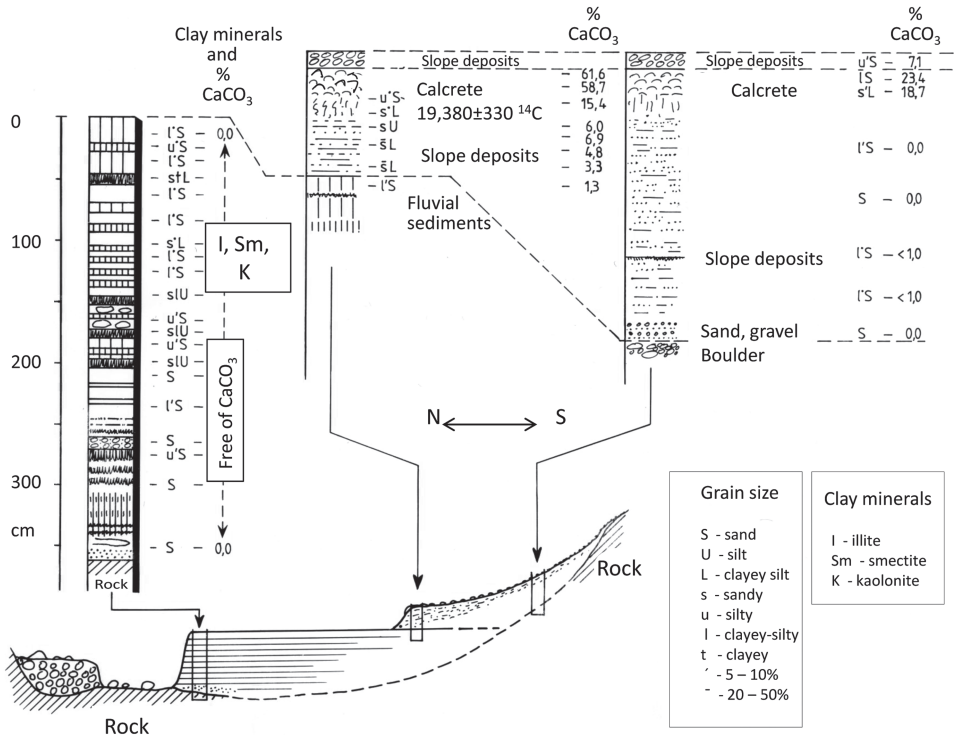

Figure 6. Stratigraphic correlation of the pollen section with slope deposits at Eksteenfontein (after Heine, 1993). The ^{14}C and OSL ages of the Eksteenfontein sequence do not allow the correlation of the hillslope calcrete section with the Eksteenfontein sequence.

(D_e), respectively, but without distinct outliers towards high values or positively skewed D_e distributions. These are often observed in OSL dating studies on fluvial deposits and hint towards poor resetting of the OSL signal prior to deposition and result in age overestimation. The observed relative standard deviation of 17% and 35% for samples 06/V and 06/VI, respectively, are most likely due to variable luminescence characteristics of the material. A dose recovery test carried out on 30 discs showed a similar broad distribution of the individual D_e values with a relative standard deviation of 22%. Partial bleaching, mixing of grains of different burial ages and hence doses, and microdosimetry effects all could cause a spread in D_e estimates. But these three factors are excluded in dose recovery tests, as the material used for OSL measurements is fully bleached and subsequently homogeneously irradiated under laboratory conditions. Finally, the data spread is considered to be caused by material inherent factors rather than poor bleaching. But it must be noted here, that further experiments using single grains ought to be carried out to further support this interpretation. The estimate of the average equivalent dose was based on the median, as this measure is considered to be most representative for the broad, but hardly skewed distributions. OSL-sample 06/VI roughly matches the ^{14}C ages, although the age of 11.22 ± 1.33 ka also may indicate incomplete bleaching. A single grain analyses test with only six grains per sample yielded slightly younger ages, 13.4 ka (06/V) and 10.3 ka (06/VI) with a deviation of only 18% and 14%, respectively. Many quartz grains of the dated layers are not well rounded by wind or water transport and originate from the weathered slope rocks in

the surrounding area. The ^{14}C and OSL ages of the Eksteenfontein sequence do not allow the correlation of the hillslope calcrete section with the Eksteenfontein sequence, as shown by Heine (1993, Figure 6). This correlation must be rejected.

Scott *et al*. (1995) presented preliminary palynological data of the Eksteenfontein sequence (Figure 7). The pollen diagram demonstrates that "a marked change [occurred] from assemblages of predominantly Cheno/Ams and different Asteraceae (including Stoebe-type) pollen in the late Pleistocene to assemblages totally dominated by succulent pollen of the Aizoaceae type in the Holocene. A tentative interpretation of this is that it suggests a change from cool and dry to warm and dry conditions around 10,700 BP [uncalibrated ^{14}C age]. A subtle, as yet unexplained, change in availability or seasonality of moisture is also suggested by the transition from shrubby to succulent vegetation. According to the available dates, it would seem that the Younger Dryas is represented in that part of the sequence immediately following this change. However, the pollen assemblage in this section is the same as in the overlying early Holocene assemblage of ca 8000 BP [uncalibrated ^{14}C age], suggesting that the Younger Dryas oscillation did not conspicuously affect the Richtersveld" (Scott *et al*., 1995:944).

According to cross-correlation of our sections with the section of Scott *et al*. (1995) (Figure 8) we conclude that the lower part of the section of Scott *et al*. (1995) represents the ACR while the upper part, starting at c. 160 cm depth (Figure 7), represents the YD and the early Holocene. The grain size analyses of the lower layers commonly show sand while the upper part contains sand with silt and clay (Figure 6). The changing grain sizes suggest changing erosion processes. Scott *et al*. (2012) assume an age of c. 15,200 a BP for the lowest sandy levels based on extrapolation. According to our ^{14}C ages the sedimentation of the lowermost organic sands started not earlier than c. 14,500 a BP. This is the beginning of the ACR. The end of the ACR is documented in the pollen section by changing conditions from a *Stoebe*/*Elytropappus* type to a succulent Aizoaceae type assemblage (Scott and Woodborne, 2007; Scott *et al*., 2012). It is noteworthy that the pollen spectra of the YD and the early Holocene do not differ very much. This observation makes Scott *et al*. (1995)

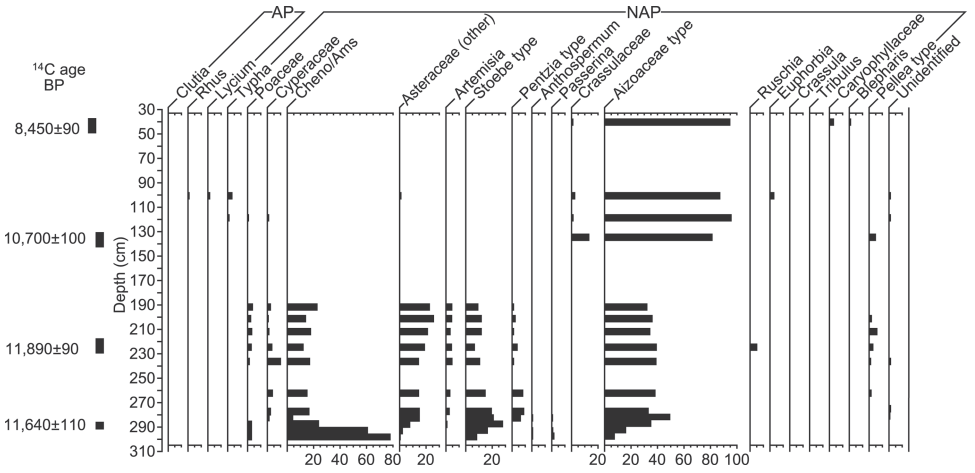

Figure 7. Palynological data of the Eksteenfontein sequence (after Scott *et al.*, 1995).

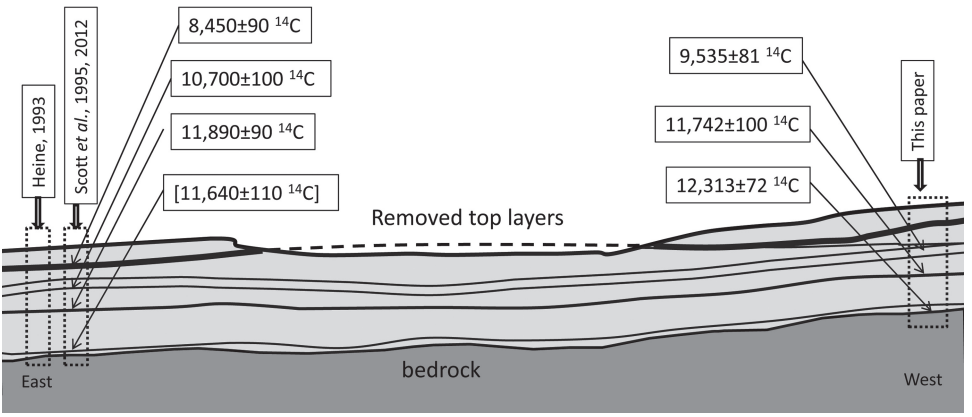

Figure 8. Cross-correlation of our sections with the section of Scott *et al.* (1995).

to conclude that the YD fluctuation "did not conspicuously affect the Richtersveld" (Scott *et al*., 1995:944). The most obvious environmental changes occurred around 12,700 a BP at the end of the ACR.

7.5 DISCUSSION AND REGIONAL PALAEOCLIMATIC IMPLICATIONS

In the late 1990s, there are still authors assuming synchronous interhemispheric climate changes (e.g., Bard *et al*., 1997; Steig *et al*., 1998). Kirst *et al*. (1999) tried to find a climatic phase in the marine cores off the southwestern African coast corresponding to the YD chronozone. Their chronostratigraphy was achieved by visual correlation with the normalized SPECMAP standard record (time scale), by correlation with a radiocarbon-dated core in the vicinity and by four AMS ^{14}C ages. Nevertheless, Heine (2002) concluded, "because of dating uncertainties, paleoclimate archives deposited in the southern African arid areas between c. 20 and 9 cal kyr BP can be neither cross-correlated, nor correlated with the well-known climatic fluctuations shown in ice cores. Only by referring to the marine sediment cores from the South Atlantic Ocean (see Shi *et al*., 2000) we can document increasing temperatures and precipitation [changes] since c. 17,500 cal kyr BP as well as an extremely arid phase between 14,400–12,500 cal kyr BP, which correlates with the ACR and stronger upwelling of the Benguela Current. A second arid phase occurred between 11,000 and 8900 cal kyr BP. For South Africa, isotope analyses of mollusk shells show two cooler climate phases during the Pleistocene/Holocene transition, with a temperature about 4°C cooler than during the early Holocene (Abell and Plug, 2000). According to ^{14}C ages the arid phases match the ACR and the early Holocene".

For the first time, Shi *et al*. (2000) presented strong evidence from a marine core that the start of the last deglacial warming (17,500 a BP) in southwestern Africa is obviously out of phase with the Bølling-Allerød warming in the Northern Hemisphere and the ACR is out of phase with the YD. More recently, Gasse *et al*. (2008) reconstructed climatic patterns in southern and equatorial Africa from 30,000 to 10,000 years ago from terrestrial and near-shore proxy data. Their review revealed a number of weaknesses and unresolved issues, particularly with regard to large uncertainties of chronologies. For the arid southwestern Africa "several records … suggest that the

19–10 ka interval has been more complex than the gradual transition from a cool-wet LGM to a warm mid-Holocene proposed by Chase and Meadows (2007), with several rapid wet/dry shifts. Too few high resolution records are available from the subtropical rainfall domain to draw definite conclusions about the region" (Gasse *et al*., 2008). Based on all available terrestrial and marine paleoclimate records, Gasse *et al*. (2008) argue that from c. 17.5 to c. 14.5 ka BP southwest African temperatures increased concomitant to Antarctic warming, but for the ACR the marine paleoclimate records show warming as well as cooling conditions and for the YD cooling and drying conditions (Figure 12 in Gasse *et al*., 2008). We suspect that the conclusion by Gasse *et al*. (2008) "that the 19–10 ka interval has been more complex than the gradual transition from a cool-wet LGM to a warm mid-Holocene proposed by Chase and Meadows (2007), with several rapid wet/dry shifts" is caused by weak age determinations of the marine sections. However, Gasse *et al*. (2008) could base their interpretation on only five marine cores off the Namib Desert and two terrestrial sequences, Eksteenfontein and Pakhuis Pass (32.04 S, 19.02 E, Scott and Woodborne, 2007). No supplementary records were available that present information about the Pleistocene/Holocene transition in some detail. Moreover, the time resolution is weak. For the Pakhuis Pass sequence in the winter-rain area about 400 km south of Eksteenfontein, Scott and Woodborne (2007) object that "warming and increasing moisture continued from 12 ka until ca 9.5 ka but the resolution of the sequence around this interval of the Pleistocene/Holocene transition is poor with only a suggestion of minor cooling at the end of the Younger Dryas ca 11 ka" (Scott and Woodborne, 2007). The Pakhuis section shows neither the ACR nor the YD event, but "the biggest contrast between the LGM and Holocene in the pollen sequence" (Scott and Woodborne, 2007) occurred around 13 ka BP. This is close to the end of the ACR.

Five marine cores off the southwestern African coast are mentioned by Gasse *et al*. (2008) that may help revealing the late-glacial/early Holocene climate. They are from North to South:

i. GeoB-1023–5 (17.16 S, 11.01 E), c. 1,500 km NW of Eksteenfontein
ii. MD96–2094 (20.00 S, 9.44 E), c. 1,250 km NW of Eksteenfontein
iii. GeoB 1711–4 (23.32 S, 12.38 E), c. 850 km NW of Eksteenfontein
iv. ODP 1084B (25.51 S, 13.03 E), c. 650 km NW of Eksteenfontein
v. MD96–2087 (25.60 S, 12.15 E), c. 600 km NW of Eksteenfontein

(i) **Core GeoB-1023–5** has provided a high time resolution (length of 938 cm, 112 samples, 7 AMS ^{14}C ages) varying between 45 and 350 years (Shi *et al*., 2000). Two dry phases have been inferred from the pollen and dinoflagellate cyst assemblages, at 14.3–12.6 ka and 11–8.9 ka, coincident with the ACR and the early Holocene period, respectively (Shi *et al*., 2000). Kim and Schneider (2002) present an alkenone-derived SST record of the core showing increasing temperatures from c. 21 ka BP to c. 14.5 ka BP, decreasing temperatures during the YD chron with a minimum around 12.5 ka BP, and, thereafter, increasing temperatures to the Holocene maximum c. 5 ka BP. The core GeoB-1023–5 was taken in front of the Cunene River mouth about 110 km off the coast. The dry phases are documented by the pollen record while the dinocyst assemblages are connected with phases of strong upwelling and a northward displacement of the Angola/Benguela Front (ABF). The arid phase, with increasing humidity between 11,000 and 8900 a BP, is represented in other paleoclimatic proxy data from southwestern Africa (e.g., Chase *et al*., 2009, 2010). The Younger Dryas event (c. 12,800–11,700 ka BP) is not visibly shown in the

pollen record, although the alkenone-derived sea surface temperatures of the Benguela waters have their minimum temperatures c. 12.5 ka BP, i.e., in the onset of the YD. Based on the findings of core GeoB-1023–5, Dupont *et al*. (2004, 321–322) conclude that coupling between cold Benguela Current SSTs and dry South African vegetation, apparently strong until 14,000 a BP, ceased to exist after 13,000 a BP and that 'the YD fluctuation … is clearly seen in the SSTs of the southeast Atlantic, but not very well expressed on the continent'. We assume that the interpretation of the pollen record by Shi *et al*. (2000) can be challenged (see also: Scott *et al*., 2004; Chase and Meadows, 2007). The Restionaceae pollen occurrence did not show a northward migration of the Cape vegetation to the Cunene region, but an influence of the Kalahari and/or East African mountains via the Angolan-Namibian highlands. Scott and Woodborne (2007) note, because of the absence of many fynbos pollen at the Pakhuis Pass, no marked northward intensification of Cape winter rain during the late Pleistocene. This is also recorded in hyrax dung from the Dâures Massif (Brandberg) in Namibia (Scott *et al*., 2004). To resolve these discrepancies, the discontinuous nature of the records, their low resolution and problematic chronologic control have to be improved to allow reliable correlations.

(ii) **At marine core MD96–2094** a "SW African humidity index" and a "SE trade wind index" have been obtained from grain-size distribution of the terrigenous fraction. The terrigenous fraction is "unmixed" into subpopulations which are interpreted as coarse eolian dust, fine eolian dust, and fluvial mud (Stuut *et al*., 2002, 2011; Stuut and Lamy, 2004). The authors suppose that the dust record in marine sediments indicates humid conditions during glacial times, but time resolution is poor and the results do not match the overall situation (Geyh and Heine, in press). Contrary to the terrestrial records that show arid glacials and interglacials with an increase in humidity/precipitation for the Namib Desert (e.g., Heine, 2002, Stone *et al*., 2010a, 2010b; Geyh and Heine, in press), Stuut *et al*. (2002, 2011) and Stuut and Lamy (2004) postulate aridity during interglacial phases and humidity during glacial phases. We doubt the results and recommend a critical reappraisal of all marine fine-grained mud and silt samples previously interpreted as having been continuously deposited since Schieber *et al*. (2007) and Macquaker and Bohacs (2007) indicate that many preconditions about the interpretation of fine-grained sediments are naïve. Deposition and burial of mud is dynamic and complex, "because of myriad processes—including grain-size changes due to aggregate growth and decay, presence of biofilms, reworking, and cement precipitation—that occur in mudstone to control their variability' (Macquaker and Bohacs, 2007).

(iii) **Alkenone-inferred SSTs** (Kirst *et al*., 1999) of marine core GeoB 1711-4 are cited by Gasse *et al*. (2008, Figure 6c). The data of Kirst *et al*. (1999) present evidence for the YD, yet time resolution is very poor so that, according to the AMS ^{14}C ages, the changes correlated with the YD easily can be ascribed to the ACR, too.

(iv) **Marine core ODP 1084B** reveal a temperature decrease, achieved by using the alkenone index, starting c. 14,200 a BP, i.e., contemporaneous to the ACR, but continued after 13,000 a BP. Minimum SSTs were reached during the YD (Kim *et al*., 2002; Farmer *et al*., 2005). Yet, the low time

resolution and problematic chronologic control make reliable correlations difficult.

(v) **Core MD96–2087** indicates cooling of SSTs and relatively wet conditions during the YD (Pichevin *et al*., 2005). The chronology suffers great uncertainties. The wind systems, on which the interpretation is based, have to be challenged. Pichevin *et al*. (2005) assume that the south-east trade winds transport aeolian material from inland southwestern Africa to the sea. No observations exist for dust transport with south-east trade winds (Eckardt *et al*., 2001; Eckardt and Kuring, 2005; Goudie and Middleton, 2006; Heine and Völkel, 2010). Dust movement in the Namib Desert/Benguela Current region is always associated with enhancement of the low-level easterly circulation over the interior (Eckardt *et al*., 2001) and is 'caused by the *Berg winds*, a warm, dry, off-plateau, partially katabatic phenomena' (Goudie and Middleton, 2006). The grain size variations, therefore, are no indicator of the strength of the trade winds. Furthermore, trade wind strength, upwelling intensity, a northward/southward shift of the ITCZ and vegetation changes have to be discussed with respect to the observed dust transport tracks and river discharge when marine cores are used as paleoclimatic archives and far reaching conclusions are drawn (Heine and Völkel, 2010). E.g., Dupont *et al*. (2004) conclude that after the ACR southeast Atlantic SSTs no longer influenced the vegetation development in the interior of southern Africa and that stronger trade winds during the ACR and the YD chronozone caused increased upwelling and a reduced influence of the Westerlies on the climate of southwestern Africa. Moreover, Gasse *et al*. (2008) suggest a different paleohydrologic interpretation of *Tribulus* pollen, indicating conflicting insights with respect to Dupont *et al*. (2004). Beside the trajectories of dust transport, the assumption that clusters of ^{14}C and luminescence ages stand for aridity must be challenged. Heine (1981) and Chase *et al*. (2007) present examples of increased windiness concurrent with increased humidity in the southwestern Kalahari and along the west coast, respectively. Rather than indicating phases of intensified aeolian activity, age frequency histograms from dunes describe a complex history of dunefield development (Chase *et al*., 2007; Chase, 2009; Thomas, 2013).

It is noteworthy that the remarkable fluctuations in temperature and precipitation between 15 and 11 ka BP that are found in the marine geoarchives off the Namib Desert coast, do not have any analogy on land (Heine, 2005, 2010; Chase and Meadows, 2007; Geyh and Heine, in press). For the Namaqualand succulent Karoo, Scott *et al*. (2012) take the Principal Components Analysis (PCA) to monitor taxa sensitive to moisture and temperature fluctuations. They use strong loadings on *Stoebe*/*Elytropappus* type pollen as a past temperature indicator and find cool temperatures c. 15.2 to 13.6 ka and warming by 12.5 ka. Several sites became drier between c. 13 and 11.5 ka, the YD interval. These sites include Wonderwerk Cave and Eksteenfontein from the western region. In the interior of southern Africa, Holmgren *et al*. (2003) used highly resolved $\delta^{18}O$ and $\delta^{13}C$ records of the Makapansgat Cave stalagmites to reconstruct the climate history since 23,000 a BP. The isotope records indicate dry, cool conditions at c. 23–21, 19.7–17.5 and during the ACR, c. 15–13.5 ka. Maximum cooling occurred at 17.5 ka, and a strong post-glacial warming took place after 13.5 ka. These results do not match with the alkenone-derived SST record from marine core GeoB-1023-5. Yet, we have to consider that the marine core is situated c. 1500 km to the north in

the tropical summer-rain region. Considering these limits, it is finally possible that all these apparently discrete events of cooling phases during the overall late Pleistocene warming trend, recognized between c. 14,500 and 11,000 a BP and derived from different marine cores off the southwestern African coast, correspond to the ACR.

7.6 SOUTHERN HEMISPHERE PALAEOCLIMATIC IMPLICATIONS AND CONCLUSION

Accurate constraint of both, the timing and magnitude of events, such as the ACR and the YD, is essential in order to test different hypotheses for the causes and extent of climate changes during the Pleistocene/Holocene transition (Bromley *et al*., 2011). The Eksteenfontein sequence started to accumulate at c. 15 ka BP. In southern Africa, many pollen sequences commenced growing between c. 15 and 11.5 ka BP (Meadows, 1988). This is impressively corroborated by the wetlands of the Braamhoek surroundings which are located in the summer rainfall region north of the border to Lesotho (28°14′S, 29°35′E). The pollen sequence shows the Pleistocene/Holocene transition in detail (Norström *et al*., 2009). The transition was relatively cool, while temperatures became warmer after 11–8 ka BP. Slightly wetter conditions started c. 14.3 ka BP and peaked between c. 13.7–12.8 and 10.5–9.5 ka BP (Norström *et al*., 2009). Apparently, the ACR caused a weak climatic break in the general warming after the LGM. This interruption was not only concentrated to the ACR phase between c. 14,700–12,700 ka BP, but got through to the YD phase without a pronounced climatic reversal limited to the YD chron.

From a global perspective, recently the ACR of the Southern Hemisphere is discovered not only in marine records of the Benguela region, but also in South America, New Zealand and Japan. Bromley *et al*. (2011) present ^{3}He surface exposure data for a glacier readvance or prolonged stillstand c. 13.9–11.9 ka BP in the southern Peruvian Andes (15°33′S, 72°93′W) far north of Antarctica. Glaciers in some regions of Patagonia also advanced during the ACR. Douglass *et al*. (2006) use ^{10}Be and ^{26} Al surface exposure ages of erratic boulders on moraines at Lago Buenos Aires, Argentina (71°W, 46°30′S) to date a late-glacial readvance at 14.4 ± 0.9 ka which is distinctively "Antarctic" in nature. It is contemporaneous with the ACR and precedes the YD chronozone (Douglass *et al*., 2006). Fogwill and Kubik (2005) report initial cosmogenic ^{10}Be results from a former ice limit in Torres del Paine indicating a stillstand or readvance of Patagonian ice culminating at 15–12 ka BP with a mean age of 13.2 ± 0.8 ka BP. McCulloch *et al*. (2005) present a revised glacial chronology for southernmost South America based on cosmogenic isotope analysis, ^{14}C assays, amino acid racemisation and tephrochronology. A glacier advance occurred 15,500–11,770 a BP during the ACR. The glacier retreated during the peak of the YD chronozone. These data tie in with the observation from the North Patagonian Icefield of Turner *et al*. (2005) who recognized a rapid glacier retreat at 16–15 ka BP, followed by a phase of glacier stability at 13.6–12.8 ka. The final stage of deglaciation occurred at c. 12.8 ka. All authors report from southern South America that no YD glacier advance could be recognized (Harrison and Glasser, 2011), an observation already published by Mercer (1976).

In the Alps of New Zealand, the Waiho Loop Moraine has been interpreted as evidence for YD cooling in southern New Zealand (Denton and Hendy, 1994), but recent dating and climatological studies have questioned this view. A detailed analysis of the sedimentology of the moraine suggests it was formed after a large landslide onto the Franz-Josef-glacier triggered a glacial surge, independent of climate forcing (Barrows *et al*., 2007; Santamaria Tovar *et al*., 2008). Putnam *et al*. (2010) report

^{10}Be ages of New Zealand moraines which show a regionally coherent expansion of glaciers on both sides of the Southern Alps 13,000 a BP and Hodgson and Sime (2010) confirm that "this glacier expansion coincides with a period of abrupt cooling in Antarctica between 14,540 and 12,760 years ago". Furthermore, a compilation of records of the late-glacial landscape and vegetation change reveals no significant reversals of the overall warming trend (McGlone, 1995). These observations corroborate the palynological records from southern Africa (Scott *et al*., 2012). In Australia, a speleothem from eastern Victoria was the only evidence for a cooling event approximately synchronous with the European YD; yet, a re-analysis challenged this hypothesis (Green *et al*., 2013).

Yoshida and Takeuti (2009) present robust palynological evidence that during the last termination (18–10 ka BP) the ACR event strongly affected the Pacific high pressure system while the YD event did not extend beyond the East Asian monsoon front. Their age-depth models are based on both, tephra ages and calibrated ^{14}C dates. Evidently, the East Asian monsoon front was an important geo-climatic boundary between ACR-like and YD-like deglacial climate changes (Yoshida and Takeuti, 2009). These data are corroborated by Sirocko (1996) and Sirocko *et al*. (2000) from the Arabian Sea where humid phases correlate with temperature maxima in Antarctica and show the influence of the Southern Hemisphere on the monsoon system, while secondary short fluctuations in precipitation can be correlated with climatic events recorded in Greenland ice cores (see also: Gasse, 2000; Heine, 2002).

The examples from South America, New Zealand and Japan reveal that the late-glacial climatic changes of the continents of the Southern Hemisphere were under the influence of the Antarctic realm and out of phase with those of the Northern Hemisphere. Unfortunately, contrasting the potential of using well-dated glacial chronologies from South America and New Zealand to reconstruct the late-glacial/Holocene climate changes, there are no such possibilities in southern Africa. Despite this limitation, a careful evaluation of the published data shows on the one hand no influence of the YD event, but on the other hand that the southern African Pleistocene/Holocene transition was controlled by the ACR. If the ACR strongly influenced the climate of southern South America and New Zealand and had a weak effect on the circum-Pacific regions (Chile, Peru, Japan), the South African climate may also have been affected by a hemispheric-scale climate change during the ACR. Moreover, changes of the westerly winds at a single site reflect shifts throughout the entire southern wind belt (Lamy *et al*., 2010). Changes in strength and position of the Southern Hemisphere westerly winds during the Pleistocene/Holocene transition, as reconstructed and modeled, suggest that the belt of westerly winds may move northwards during colder periods and thereby produced an atmospheric cooling that influenced the Southern Hemisphere around the globe (Hodgson and Sime, 2010). In the Southern Hemisphere, atmospheric heat transport is tied to the Southern Hemisphere westerly winds (McGlone *et al*., 2010).

By testing hypotheses on the timing and forcing of global climate changes, the assessment of the regional extent of the ACR and the YD is of fundamental interest. Our reflections clearly support the concept that major latitudinal shifts of the southern westerly wind belt were the cause of the last deglacial interhemispheric climatic asymmetry (De Deckker *et al*., 2012). In southern Africa and, in particular, in the African southwestern arid regions, late-glacial/early Holocene climatic changes can be assigned to the ACR and not to the YD chronozone of the Northern Hemisphere. By reconsidering (i) the facts which the terrestrial and marine geoarchives provide and (ii) the factors which drive climate change during the Pleistocene/Holocene transition in the region, it becomes evident that the weak time resolution of the geoarchives

led to errors in correlating climate changes with the ACR and/or the YD. Beyond doubt, the quality and time resolution of data from hyrax middens will revolutionize paleoenvironmental studies in southern Africa in the future (Chase *et al.*, 2009) and will clearly show that the YD event had no significant influence on the southern African climate.

ACKNOWLEDGEMENTS

Klaus Heine thanks the *Deutsche Forschungsgemeinschaft* (DFG, German Science Foundation) for continuous support of his research in southern Africa. This work was funded by the DFG Grant He 722/14-3 and by the *Japanese Ministry of Education, Science, Sports and Culture* (Project No. 13371013). The *AMS-Labor Erlangen* (A. Scharf) provided AMS ^{14}C data. We thank many colleagues and students for their discussions and very useful suggestions.

REFERENCES

Abell, P.I. and Plug, I., 2000, The Pleistocene/Holocene transition in South Africa: evidence for the Younger Dryas event. *Global and Planetary Change*, **26**, pp. 173–179.

Bard, E., Rostek, F. and Sonzogni, C., 1997, Interhemispheric synchrony of the last deglaciation inferred from alkenone palaeothermometry. *Nature*, **385**, pp. 707–710.

Barrows, T.T., Lehman, S.J., Fifield, L.K. and De Deckker, P., 2007, Absence of Cooling in New Zealand and the Adjacent Ocean During the Younger Dryas Chronozone, *Science*, **318**, pp. 86–89.

Blunier, T., Schwander, J., Stauffer, B., Stocker, T.F., Dällenbach, A., Indermühle, A., Tschumi, J., Chappelaz, J., Raynaud, D. and Barnola, J.-M., 1997, Timing of the Antarctic cold reversal and the atmospheric CO_2 increase with respect to the Younger Dryas event. *Geophysical Research Letters*, **24**, pp. 2683–2686.

Bromley, G.R.M., Hall, B.L., Schaffer, J.M., Winckler, G., Todd, C.E. and Rademaker, K.M., 2011, Glacier fluctuations in the southern Peruvian Andes during the late-glacial period, constrained with cosmogenic ^{3}He. *Journal of Quaternary Science*, **26**, pp. 37–43.

Chase, B.M., 2009, Evaluating the use of dune sediments as a proxy for palaeo-aridity: a southern African case study. *Earth Science Reviews*, **93**, pp. 31–45.

Chase, B.M. and Meadows, M.E., 2007, Late Quaternary dynamics of southern Africa's winter rainfall zone. *Earth Science Reviews*, **84**, pp. 103–138.

Chase, B.M., Thomas, D.S.G., Bateman, M.D. and Meadows, M.E., 2007, Late Quaternary dune development along the western margin of South Africa and its relationship to paleoclimatic changes inferred from the marine record. *PAGES News*, **15**, pp. 26–27.

Chase, B.M., Meadows, M.E., Scott, L., Thomas, D.S.G., Marais, M., Sealy J. and Reimer, P.J., 2009, A record of rapid Holocene climate change preserved in hyrax middens from southwestern Africa. *Geology*, **37**, pp. 703–706.

Chase, B.M., Meadows, M.E., Andrew S. Carr, A.S. and Reimer, P.J., 2010, Evidence for progressive Holocene aridification in southern Africa recorded in Namibian hyrax middens: Implications for African Monsoon dynamics and the "African Humid Period". *Quaternary Research*, **74**, pp. 36–45.

Clapperton, C.M., Hall, M., Mothes, P., Hole, M.J., Still, J.W. and Helmens, K.F., 1997, A Younger Dryas icecap in the Equatorial Andes. *Quaternary Research*, **47**, pp. 13–28.

Cowling, R.M., Esler, K.J. and Rundel, P.W., 1999, Namaqualand, South Africa—an overview of a unique winter-rainfall desert ecosystem. *Plant Ecology*, **142,** pp. 3–21.

De Deckker, P., Moros, M., Perner, K. and Jansen, E., 2012, Influence of the tropics and southern westerlies on glacial interhemispheric asymmetry. *Nature Geoscience*, **5**, pp. 266–269.

Denton, G.H. and Hendy, C.H., 1994, Younger Dryas age advance of Franz Josef Glacier in the Southern Alps of New Zealand. *Science*, **264**, pp. 1434–1437.

Douglass, D.C., Singer, B.S., Kaplan, M.R., Mickelson, D.M. and Caffee, M.W., 2006, Cosmogenic nuclide surface exposure dating of boulders on last-glacial and late-glacial moraines, Lago Buenos Aires, Argentina: Interpretive strategies and paleoclimate implications. *Quaternary Geochronology*, **1**, pp. 43–58.

Dupont, L., Kim, J.-H., Schneider, R.R. and Shi, N., 2004, Southwest African climate independent of Atlantic sea surface temperatures during the Younger Dryas. *Quaternary Research*, **61**, pp. 318–324.

Eckardt, F., Washington, R. and Wilkinson, M.J., 2001, The origin of dust on the West Coast of Southern Africa. *Palaeoecology of Africa*, **27**, pp. 207–219.

Eckardt, F.D. and Kuring, N., 2005, SeaWiFS identifies dust sources in the Namib Desert. *International Journal of Remote Sensing*, **26**, pp. 4159–4167.

Farmer, E.C., deMenocal, P.B. and Marchitto, T.M., 2005, Holocene and deglacial ocean temperature variability in the Benguela upwelling region: implications for low-latitude atmospheric circulation. *Palaeoceanography*, **20**. doi:10.1029/2004PA001049.

Fogwill, C.J. and Kubik, P.W., 2005, A glacial stage spanning the Antarctic Cold Reversal in Torres del Paine (51°S), Chile, based on preliminary cosmogenic exposure ages. *Geografisca Annaler*, **87A**, pp. 403–408.

Frimmel, H.E., 2000, The Pan-African Gariep Belt in southwestern Namibia and western South Africa. *Communications of the Geological Survey of Namibia (Special Issue Henno Martin Commemorative Volume)*, **12**, pp. 197–209.

Gasse, F., 2000, Hydrological changes in the African tropics since the Last Glacial Maximum. *Quaternary Science Reviews*, **19**, pp. 189–211.

Gasse, F., Chalié, F., Vincens, A., Williams, M.A.J. and Williamson, D., 2008, Climatic patterns in equatorial and southern Africa from 30,000 to 10,000 years ago reconstructed from terrestrial and near-shore proxy data. *Quaternary Science Reviews*, **27**, pp. 2316–2340.

Geyh, M.A. and Heine, K., accepted, Several distinct wet periods since 420 ka in the Namib Desert inferred from U-series speleothem dates. *Quaternary Research*.

Goudie, A.S. and Middleton, N.J., 2006, *Desert Dust in the Global System*, (Berlin—Heidelberg—New York: Springer).

Green, H., Woodhead, J., Hellstrom, J., Pickering, R. and Drysdale, R., 2013, Re-analysis of key evidence in the case for a hemispherically synchronous response to the Younger Dryas climatic event. *Journal of Quaternary Science*, **28**, pp. 8–12.

Harrison, S. and Glasser, N.F., 2011, The Pleistocene Glaciations of Chile. In *Quaternary Glaciations—Extent and Chronology. A Closer Look*, edited by Ehlers, J., Gibbard, P.L. and Hughes, P.D., (Amsterdam, Boston etc.: Elsevier), pp. 739–756.

Heine, J.T., 1993, A reevaluation of the evidence for a Younger Dryas climatic reversal in the tropical Andes. *Quaternary Science Reviews*, **12**, pp. 769–779.

Heine, K., 1981, Aride und pluviale Bedingungen während der letzten Kaltzeit in der Südwest-Kalahari (südliches Afrika). Ein Beitrag zur klimagenetischen Geomorphologie der Dünen, Pfannen und Täler. *Zeitschrift für Geomorphologie, N.F., Supplement-Band*, **38**, pp. 1–37.

Heine, K., 1993, Zum Alter jungquartärer Feuchtphasen im ariden und semiariden südwestlichen Afrika. *Würzburger Geographische Arbeiten*, 87, pp. 149–162.
Heine, K., 2002, Sahara and Namib/Kalahari during the late Quaternary—interhemispheric contrasts and comparisons. Zeitschrift für Geomorphologie, N.F., Suppl.-Bd. **126**, pp. 1–29.
Heine, K., 2005, Holocene Climate of Namibia: a Review based on Geoarchives. *African Study Monographs, Suppl.* (Kyoto), **30,** pp. 119–133.
Heine, K., 2010, Climate reconstructions based on fluvial deposits in hyper-arid desert environments: the Namib case. *Palaeoecology of Africa*, **30**, pp. 27–52.
Heine, K. and Völkel, J., 2010, Soil clay minerals in Namibia and their significance for the terrestrial and marine past global change research. *African Study Monographs (Kyoto), Suppl*., **40**, pp. 15–34.
Heusser, C.J., 1966, Polar hemispheric correlation: palynological evidence from Chili and the Pacific Northwest of America. In *World Climate from 8000 to 0 BP*, Proceedings International Symposium World Climate, edited by Swayer, J.S. (London, Royal Meteorological Society), pp. 124–142.
Heusser, C.J. and Streeter, S.S., 1980, A temperature and precipitation record of the past 16,000 years in southern Chile. *Science*, **210**, pp. 1345–1347.
Heusser, C.J. and Rabassa, J., 1987, Cold climate episode of Younger Dryas age in Tierra del Fuego. *Nature*, **328**, pp. 609–611.
Hodgson, D.A. and Sime, L.C., 2010, Southern westerlies and CO_2. *Nature Geoscience*, **3**, pp. 666–667.
Holmgren, K., Lee-Thorp, J.A., Cooper, G.R.J., Lundblad, K., Partridge, T.C., Scott, L., Sithaldeen, R., Talma, A.S. and Tyson, P.D., 2003, Persistent millennial-scale climatic variability over the past 25,000 years in Southern Africa. *Quaternary Science Reviews*, **22**, pp. 2311–2326.
Kim, J.-H. and Schneider, R.R., 2002, Low-latitude control of interhemispheric sea-surface temperature contrast in the tropical Atlantic over the past 21 kyears: the possible role of SE trade winds. *Climate Dynamics*, **21**, pp. 337–347.
Kim, J.-H., Schneider, R.R., Müller, P.J. and Wefer, G., 2002, Interhemispheric comparison of deglacial sea-surface temperature patterns in Atlantic eastern boundary currents. *Earth and Planetary Science Letters*, **194**, pp. 383–393.
Kirst, G.J., Schneider, R.R., Müller, P.J., von Storch, I. and Wefer, G., 1999. Late Quaternary temperature variability in the Benguela Current System derived from alkenones. *Quaternary Research*, **52**, pp. 92–103.
Lamy, F., Kilian, R., Arz, H.W., Francois, J.-P., Kaiser, J., Prange, M. and Steinke, T., 2010, Holocene changes in the position and intensity of the southern westerly wind belt. *Nature Geoscience*, **3**, pp. 695–699.
Lowell, T.V., Heusser, C.J., Andersen, B.G., Moreno, P.I., Hauser, A., Heusser, L.E., Schlüchter, C., Marchant, D.R. and Denton, G.H., 1995, Interhemispheric Correlation of Late Pleistocene Glacial Events. *Science*, **269**, pp. 1541–1549.
Macquaker, J.H.S. and Bohacs, K.M., 2007, On the Accumulation of Mud. *Science*, **318**, pp. 1734–1735.
Markgraf, V., 1991, Younger Dryas in southern South America? *Boreas*, **20**, pp. 63–69.
Markgraf, V., Dodson, J.R., Kershaw, A.P., McGlone, M.S. and Nicholls, N., 1992, Evolution of late Pleistocene and Holocene climates in the circum-South Pacific land areas. *Climate Dynamics*, **6**, pp. 193–211.
Martin, H., 1965, *The Precambrian Geology of South West Africa and Namaqualand*. Bulletin of the Precambrian Research Unit, University of Cape Town. p. 159.

McCulloch, R.D., Fogwill, C.J., Sugden, D.E., Bentley, M.J. and Kubik, P.W., 2005, Chronology of the last glaciation in central Strait of Magellan and Bahía Inútil, southernmost South America. *Geografisca Annaler*, **87A**, pp. 289–312.

McGlone, M.S., 1995, Lateglacial landscape and vegetation change and the Younger Dryas climatic oscillation in New Zealand. *Quaternary Science Reviews*, **14**, pp. 867–881.

McGlone, M.S., Turney, C.S.M., Wilmshurst, J.M., Renwick, J. and Pahnke, K., 2010, Divergent trends in land and ocean temperature in the Southern Ocean over the past 18,000 years. *Nature Geoscience*, **3**, pp. 622–626.

Meadows, M.E., 1988, Late Quaternary peat accumulation in southern Africa. *Catena*, **15**, pp. 459–472.

Mendelsohn, J., Jarvis, A., Roberts, C. and Robertson, T., 2002, *Atlas of Namibia. A Portrait of the Land and its People*, (Cape Town: David Philip Publishers).

Mercer, J.H., 1976, Glacial History of Southernmost South America. *Quaternary Research*, **6**, pp. 125–166.

Murray, A.S. & Wintle, A.G., 2000, Luminescence dating of quartz using an improved single-aliquot regenerative-dose protocol. *Radiation Measurements*, **32**, pp. 57–73.

Norström, E., Scott, L., Partridge, T.C., Risberg, J. and Holmgren, K., 2009, Reconstruction of environmental and climate changes at Braamhoek wetland, eastern escarpment South Africa, during the last 16,000 years with emphasis on the Pleistocene-Holocene transition. *Palaeogeography, Palaeoclimatology, Palaeoecology*, **271**, pp. 240–258.

Peteet, D., 1995, Preface, *Journal of Quaternary Science*, **14**, p. 811.

Peterson, L.C., Haug, H.G., Hughen, K.A. and Röhl, U., 2000, Rapid changes in the hydrological cycle of the tropical Atlantic during the last glacial. *Science*, **290**, pp. 1947–1951.

Pichevin, L., Cremer, M., Giraudeau, J. and Bertrand, P., 2005, A 190 kyr record of lithogenic grain-size on the Namibian slope: forcing a tight link between past wind-strength and coastal upwelling dynamics. *Marine Geology*, **218**, pp. 81–96.

Prescott, J.R. and Hutton, J.T., 1988, Cosmic ray and gamma ray dosimetry for TL and ESR. *Nuclear Tracks and Radiation Measurements*, **14**, pp. 223–227.

Prescott, J.R. and Hutton, J.T., 1994, Cosmic ray contributions to dose rates for Luminescence and ESR Dating: large depths and long-term variations. *Radiation Measurements*, **23(2/3)**, pp. 497–500.

Putnam, A.E., Denton, G.H., Schaefer, J.M., Barrell, D.J.A., Andersen, B.G., Finkel, R.C., Schwartz, R., Doughty, A.M., Kaplan, M.R. and Schlüchter, C., 2010, Glacier advance in southern middle-latitudes during the Antarctic Cold Reversal. *Nature Geoscience*, **3**, pp. 700–704.

Reimer, P.J., Baillie, M.G.L., Bard, E., Bayliss, A., Beck, J.W., Bertrand, C.J.H., Blackwell, P.G., Buck, C.E., Burr, G.S., Cutler, K.B., Damon, P.E., Edwards, R.L., Fairbanks, R.G., Friedrich, M., Guilderson, T.P., Hogg, A.G., Hughen, K.A., Kromer, B., McCormac, G., Manning, S., Ramsey, C.B., Reimer, R.W., Remmele, S., Southon, J.R., Stuiver, M., Talamo, S., Taylor, F.W., van der Plicht, J. and Weyhenmeyer, C.E. (2004): IntCal04 Terrestrial Radiocarbon Age Calibration, 0–26 cal kyr BP. *Radiocarbon* **46(3)**, pp. 1029–1058.

Santamaria Tovar, D., Shulmeister, J. and Davies, T.R., 2008, Evidence for a landslide origin of New Zealand's Waiho Loop moraine. *Nature Geoscience*, **8**, pp. 524–526.

Schieber, J., Southard, J. and Thaisen, K., 2007, Accretion of Mudstone Beds from Migrating Floccule Ripples. *Science*, **318**, pp. 1760–1763.

Scott, L., Steenkamp, M. and Beaumont, P.B., 1995, Palaeoenvironmental conditions in South Africa at the Pleistocene-Holocene transition. *Quaternary Science Reviews*, **14**, pp. 937–947.

Scott, L., Marais, E. and Brook, G.A., 2004, Fossil hyrax dung and evidence of Late Pleistocene and Holocene vegetation types in the Namib Desert. *Journal of Quaternary Science*, **19**, pp. 829–832.

Scott, L. and Woodborne, S., 2006, Pollen analysis and dating of Late Quaternary faecal deposits (hyraceum) in the Cederberg, western Cape, South Africa. *Review of Palaeobotany and Palynology*, **144(3–4)**, pp. 123–134.

Scott, L. and Woodborne, S., 2007, Vegetation history inferred from pollen in Late Quaternary faecal deposits (hyraceaum) in the Cape winter-rain region and its bearing on past climates in South Africa. *Quaternary Science Reviews*, **26**, pp. 941–953.

Scott, L., Neumann, F.H., Brook, G.A., Bousman, C.B., Norström, E. and Metwally, A.A., 2012, Terrestrial fossil-pollen evidence of climate change during the last 26 thousand years in Southern Africa. *Quaternary Science Reviews*, **32**, pp. 100–118.

Shi, N., Dupont, L.M., Beug, H.-J. and Schneider, R., 2000, Correlation between Vegetation in southwestern Africa and Oceanic Upwelling in the Past 21,000 Years. *Quaternary Research*, **54**, pp. 72–80.

Shi, N., Schneider, R., Beug, H.J. and Dupont, L.M., 2001, Southeast trade wind variations during the last 135 kyr: evidence from pollen spectra in eastern South Atlantic sediments. *Earth and Planetary Science Letters*, **187**, pp. 311–321.

Sirocko, F., 1996, The evolution of the monsoon climate over the Arabian Sea during the last 24,000 years. *Palaeoecology of Africa*, **24**, pp. 53–69.

Sirocko, F., Garbe-Schönberg, D. and Devey, C., 2000, Processes controlling trace element geochemistry of Arabian Sea sediments during the last 25,000 years. *Global and Planetary Change*, **26**, pp. 217–303.

Steig, E.J., Brook, E.J., White, J.W.C., Sucher, C.M., Bender, M.L., Lehman, S.J., Morse, D.L., Waddington, E.D. and Clow, G.D., 1998, Synchronous climate changes in Antarctica and the North Atlantic. *Science*, **282**, pp. 92–95.

Stenni, B., Buiron, D., Frezzotti, M., Albani, S., Barbante, C., Bard, E., Barnola, J.M., Baroni, M., Baumgartner, M., Bonazza, M., Capron, E., Castellano, E., Chappellaz, J., Delmonte, B., Falourd, S., Genoni, L., Iacumin, P., Jouzel, J., Kipfstuhl, S., Landais, A., Lemieux-Dudon, B., Maggi, V., Masson-Delmotte, V., Mazzola, C., Minster, B., Montagnat, M., Mulvaney, R., Narcisi, B., Oerter, H., Parrenin, F., Petit, J.R., Ritz, C., Scarchilli, C., Schilt, A., Schüpbach, S., Schwander, J., Selmo, E., Severi, M., Stocker, T.F. and Udisti, R., 2011, Expression of the bipolar see-saw in Antarctic climate records during the last deglaciation. *Nature Geoscience*, **4**, pp. 46–49.

Stone, A.E.C., Thomas, D.S.G. and Viles, H.A., 2010a, Late Quaternary palaeohydrological changes in the northern Namib Sand Sea: New chronologies using OSL dating of interdigitated aeolian and water-lain interdune deposits. *Palaeogeography, Palaeoclimatology, Palaeoecology*, **288**, pp. 35–53.

Stone, A.E.C., Viles, H.A., Thomas, L. and van Calsteren, P., 2010b, Quaternary tufa deposition in the Naukluft Mountains, Namibia. *Journal of Quaternary Science*, **25**, 1360–1372. DOI: 10.1002/jqs.1435 (IP/937/1106) GC

Stuut, J.B.W., Prins, M.A., Schneider, R.R., Weltje, G.J., Jansen, J.H.F. and Postma, G., 2002, A 300-kyr record of aridity and wind strength in southwestern Africa: inferences from grain-size distribution of sediments of Walvis Ridge, SE Atlantic. *Marine Geology*, **180**, pp. 221–233.

Stuut, J.B.W. and Lamy, F., 2004, Climate variability at the southern boundaries of the Namib (southwestern Africa) and Atacama (northern Chile) coastal deserts during the last 120,000 yr. *Quaternary Research*, **62**, pp. 301–309.

Stuut, J.B.W., Temmesfeld, F. and De Deckker, P., 2011, Late Quaternary aridity changes in the winter-rain areas on the Southern hemisphere: inferences from the marine sediment archive. *ADOM-MARUM Dust workshop 2011*, *Abstract, short presentations and posters*, p. 52.

Thomas, D.S.G., 2013, Reconstructing paleoenvironments and palaeoclimates in drylands: what can landform analysis contribute? Earth Surface Processes and Landforms, **38**, pp. 3–16.

Thompson, L.G., Mosley-Thompson, E., Davis, M.E., Lin, P.-N., Henderson, K.A., Cole-Dai, J., J. F. Bolzan, J.F. and Liu, K.-b., 1995, Late Glacial Stage and Holocene Tropical Ice Core Records from Huascaran, Peru. *Science*, **269**, pp. 46–50.

Turner, K.J., Fogwill, C.J., McCulloch, R.D. and Sugden, D.E., 2005, Deglaciation of the eastern flank of the North Patagonian Icefield and associated continental-scale lake diversions. *Geografisca Annaler*, **87A**, pp. 363–374.

Waibel, L., 1922, Winterregen in Deutsch-Südwest-Afrika. Eine Schilderung der klimatischen Beziehungen zwischen atlantischem Ozean und Binnenland. *Abhandlungen aus dem Gebiet der Auslandskunde, Hamburgische Universität*, **9**, pp. 1–112.

White, J.W.C. and Steig, E.J., 1998, Timing is everything in the game of the two hemispheres. *Nature*, **394**, pp. 717–718.

Yoshida, A. and Takeuti, S., 2009, Quantitative reconstruction of palaeoclimate from pollen profiles in northeastern Japan and the timing of a cold reversal event during the Last Termination. *Journal of Quaternary Science*, **24**, pp. 1006–1015.

This page intentionally left blank

CHAPTER 8

Historical and present-day landscape degradation in Anambra State (Nigeria): Impacts and remedial measures

Elizabeth I. Okoyeh
Department of Geological Sciences, Nnamdi Azikiwe University, Awka, Nigeria

Izuchukwu M. Akaegbobi
Department of Geology, University of Ibadan, Ibadan, Nigeria

Boniface C. Egboka
Department of Geological Sciences, Nnamdi Azikiwe University, Awka, Nigeria

ABSTRACT: The environment of Anambra State has been degraded with significant wide spread of gully erosion and mass wasting (e.g., landslides), also leading to water scarcity and loss of economic trees and herbs. The rate of gully erosion developed in the area has totally defaced the original geomorphological character of the formerly 'stable' undulating surface of Awka-Orlu upland. Sedimentation of rivers and lakes resulting in the loss of water resources is also linked to this environmental degradation. Today, in addition, also changes in climate associated with increased rainfall intensity within a short period and prolonged periods of dryness work in tandem with anthropogenic practices to reshape and degrade the entire landscape. High annual sediment removal estimated to reach around 10 tonnes/ha/year were attributed to the geology and change in climatic conditions. The latter are complimented by anthropogenic factors like bush burning, cultivation along hillslopes, deforestation and uncontrolled spontaneous urban development that equally has degraded the environment. This resulted in loss of soil nutrients and reduction of many economic and medicinal trees and herbs causing food insecurity and other negative economic implications. The slight acid nature of the groundwater resources with pH ranging from 5.6 to 6.5 undermine adopted control measures. Institution of research centres and adequate funding of research on environmental management with emphasis on adequate control measures is essential. Tree planting exercise to reclaim loss of vegetation and prevent further degradation of the environment is recommended while proper planning of urban development is essential for correct management of the environment for sustainable socioeconomic benefits.

8.1 INTRODUCTION

Historical and recent changes in the geomorphological and environmental setting of Anambra State by mass wasting (gully erosion and landslides) have generated negative

impacts affecting lives, properties and sustainable economic development. The major active gullies are rapidly widening approaching 'canyon' proportions. The gully system within the study area covers about 1100 km^2 (Egboka and Okpoko, 1984) and has recently expanded tremendously. The landscape dealt with is situated between 5°40' to 6°50'N and 6°35' to 7°10'E with an area extent in total of 4844 km^2 (Figure 1). This region is characterised by an undulating relief, typical for the Awka-Orlu upland. The north-south trending cuesta forms a marked scarp and steep slopes on the east and west respectively with major environmental problems concentrated along these hillslopes. Landscape degradation of Anambra State started as early in 1850 and first efforts to control geomorphic processes by the Brithish colonial office together with local inhabitants by constructing check dams and planting trees failed (Egboka and Okpoko, 1984). The major towns along the cuesta that are heavily affected by surface morphodynamics (sheet wash, gully erosion) include Agulu, Nanka, Ekwulobia, Uga, Umuchu, Alor, Oraukwu, Abagana, Umuoji, Obosi (Egboka and Okoro, 2007).

Development of the gullies has caused extensive damage to the environment. Earlier studies from Egboka and Okpoko (1984), Igbokwe *et al.* (2008) and Okoro *et al.* (2011b) attributed their genesis and growth mainly to geographic factors. Engineering and mechanical methods such as check dams and forestry measures (tree planting) employed to solve the problem were unsuccessful. However, research by Egboka and Nwankwo (1982) showed that the primary causes of gully erosion and its development over time lies in the hydrogeological and geotechnical properties of the complex aquifer system underlying the affected areas. The high hydrostatic pressure in the aquifer produces a reduction in the effective strength of the unconsolidated coarse sands on the walls of the gullies leading to intense erosion.

This is most pronounced during the rainy season. Water from the effluent seepages that feed streams at the bottom of the gully is slightly acid to slightly basic (Figure 2). It affects the colonial concrete check dams from 1850, originally set up to control gully erosion. The undulating geomorphic features of the area ensure a high surface and subsurface gradient, fast flow rates and groundwater recharge and discharge. Significant contributions have been made by Onuoha and Uma (2006), Onwuemesi and Egboka (1991), and Akudinobi and Egboka (1996) to establish the cause of environmental problems of gully erosion and landslide occurrence in Anambra State.

Erosion affects the nutrient content of the soils resulting in low crop productivity and in food insecurity. The essential elements for crop growth such as nitrogen, phosphorus and potassium that are usually present in proportion to the humus content of the soils are deteriorated by the environmental degradation; the greater the erosion rate, the less the humus content, and the lower the nitrogen content of the soil (Niu and Wang, 1992). In an eroded soil, the quantity of hydrolytic nitrogen is less than in a non-eroded one such is the case in most parts of Anambra State resulting in low crop yield and consequently in increased poverty of the population. The research presented here is aimed at the evaluation of the ecological problems of former and present-day environments of Southeastern Nigeria and possible remedial measures.

8.2 THE IMPACT OF PHYSIOGEOGRAPHY AND CLIMATE DYNAMICS

The physiogeographical setting of Southeastern Nigeria facilitates environmental hazards. The geomorphological frame conditions with a cuesta shaped topography underlain by the soft and friable Nanka Sands contribute to the development and increasing growth of erosion and landslide in the area. The climatic and physiographic features are major causes for gully origin. Also changing Holocene precipitation patterns in the

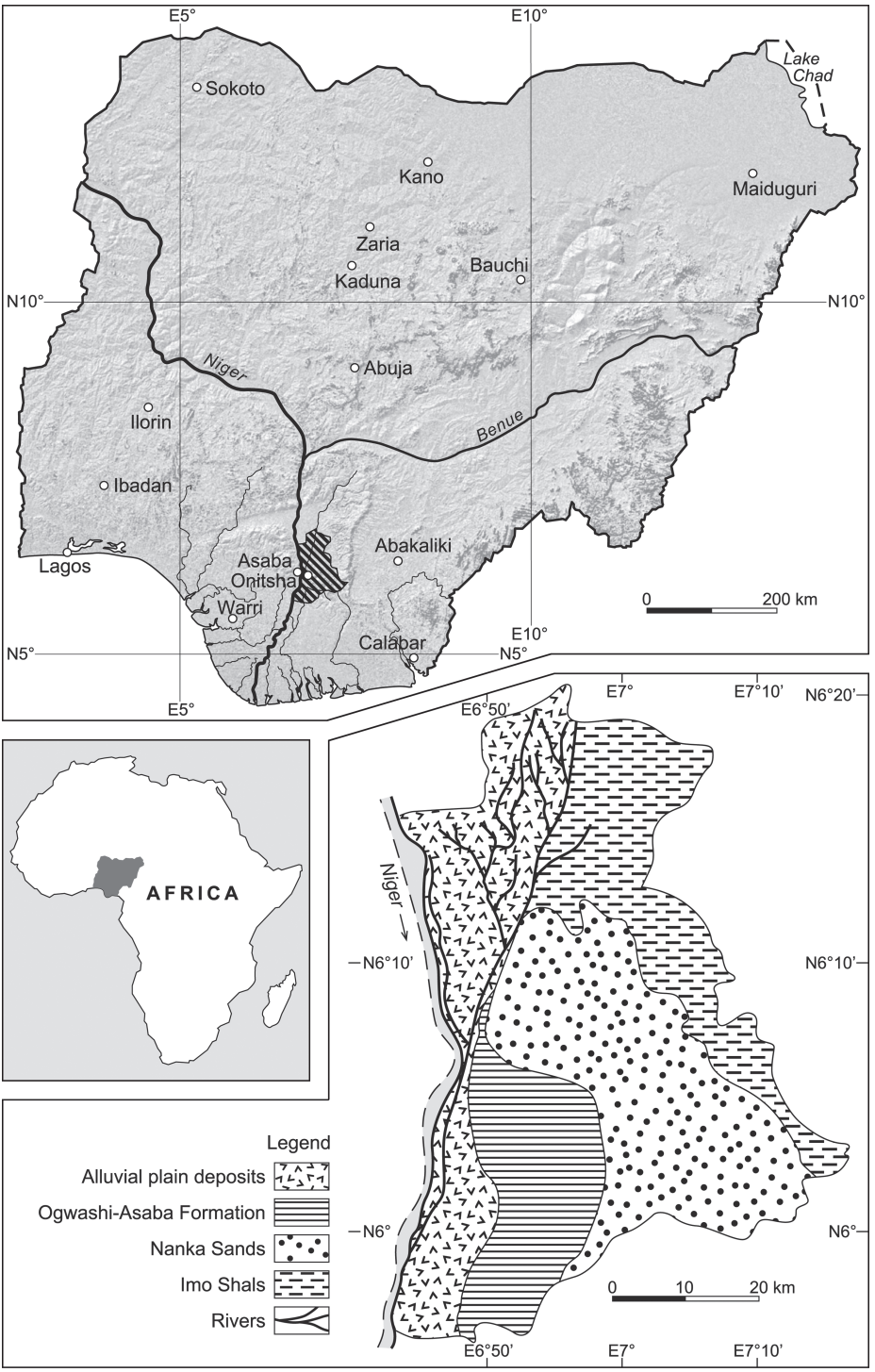

Figure 1. Location map of Anambra State within Nigeria and geological features of the study area.

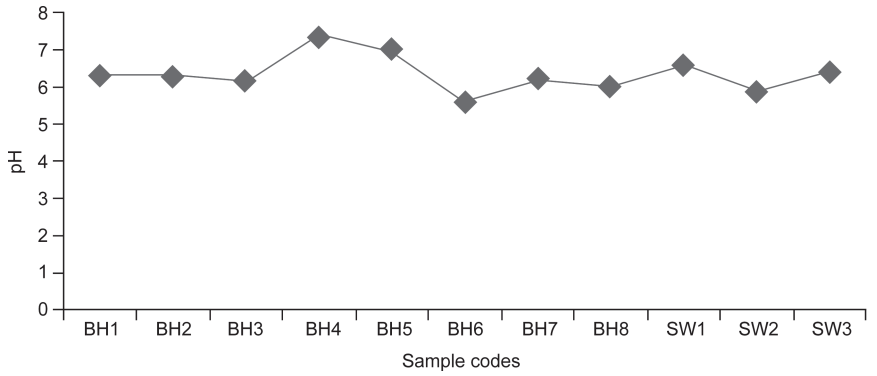

Figure 2. Characteristics from a collection of surface waters (pH) from sites with check dams.

mid-Atlantic region and their impact on the former environment are equally related to the effectiveness of today's geomorphodynamic processes (Cronin *et al.*, 2005; Willard *et al.*, 2005). The study area which used to be part of the formerly closed rainforest belt of equatorial West Africa has been strongly deforested exposing severe environmental degradation. The clearing of up to 80% of the forests during the late 19th century (Butler, 2005) increased surface erosion and downstream sedimentation fostering silting and decreased water clarity (Willard and Cronin, 2007). In addition reforestation of some agricultural land, increased fertilizer use and urbanization in the late 20th century lead to an exacerbating of water quality (Willard *et al.*, 2003).

The palaeoenvironmental frame conditions triggered gully formation within Anambra State which is gradually evolving into a savanna landscape as a result of human induced deforestation and encroachment of 'desert-like' landscape features. Changes in the on-set and cessation of rainfall attributed to climate change also affect vegetation cover and the spatial landscape elements developed in a palaeoenvironmental context. Today, two main climatic periods prevail in the study area: the dry season (October to March) and the rainy season (April to September). The dry season is characterized by marked aridity, lowering of surface waters and shallow groundwater levels. However, in total annual rainfall in the area is still around 2000 mm (Ogbukagu, 1976). The rainfall occurs as violent downpours accompanied by thunderstorms, heavy flooding, soil leaching and extensive sheet outwash facilitating groundwater recharge and fast flow velocities (Egboka and Okpoko, 1984).

8.3 GEOLOGICAL AND HYDROLOGICAL CHARACTERISTICS

The main geologic unit of the study area are the Nanka Sands (Eocene) which are overlain by Ogwashi-Asaba Formation (Oligocene) and underlain by Imo Shales (Palaeocene) (Figure 1). Lithologically the Nanka Sands consist of distinct units of sands, shale-siltstones and finely laminated shales. Sand subunits comprise uncemented, medium to coarse grained and pebbly quartz sand, with a thickness varying from 50 to 90 m (Nwajide and Hoque, 1979). Geomorphologically the Nanka Sands are associated with the North-South trending Awka-Umuchu-Orlu cuesta. The sandy units of the formation represent thick viable aquifers (Egboka and Nwankwo, 1982). The Imo Shales which resulted from the major Palaeocene transgression consists of blue to dark-grey shales, siltstones, mudstones containing sandstone lenses with the

Ebenebe Sandstone as the main sandy facies. The shale is highly fractured and fissile and lies east of the Nanka Sands (Figure 1).

The more elevated areas are capped by cohesionless medium to coarse sands and topped by lateritic crusts which are fairly porous and highly permeable. They are also described as part of the "acid sands of eastern Nigeria" (Egboka and Mbanugo, 1988). The lowlands are predominantly built up of fine to silty sands and clay that may be highly porous but aquitardly impermeable. This area is drained by numerous surface waters that indicate both surface and subsurface water divide.

8.4 HYDRO- AND GEOTECHNICAL CHARACTERISTICS

The study area consists of a series of aquifers, separated by aquitards that occur at depths between 15 to 120 m (Figure 3). These aquifer-aquitard units form a multi-aquifer system (Okoro *et al.*, 2011a). The calculated hydraulic gradient ranges from 0.0010 and 0.0178 m/m (Onwuemesi and Egboka 2006) and decreases away from the Awka-Orlu ridge towards the major surface water bodies on both flanks indicating principal groundwater flow direction. The hydraulic gradient (i) was obtained from Equation (1).

$$i = dh/dl \tag{1}$$

where dh = hydraulic head difference in (m), and dl = flow length difference in (m), $i = dh/dl$ (m/m), therefore, hydraulic gradient becomes unitless/dimensionless, but Onwuemesi and Egboka (2006) chose to leave it as (m/m).

Geogenic and anthropogenic activities have greatly influenced the geotechnical characteristics of the area thereby reshaping the palaeoenvironment.

A recent study by the National Geohazard Monitoring Center classified the gully and landslide prone areas into very active, active and 'dormant' states. Mapping of the gully sites distribution in the study area reveals that about 28% of the total landmass is moderately gullied, about 35% is mildly gullied while about 37% is severely gullied with depths ranging from 3 to 85 m (Figures 4 and 5).

While the fine grained sands of the Nanka Formation are highly aquiferous, the Imo Shale forms huge aquitard except the sandstone member. A considerable rise

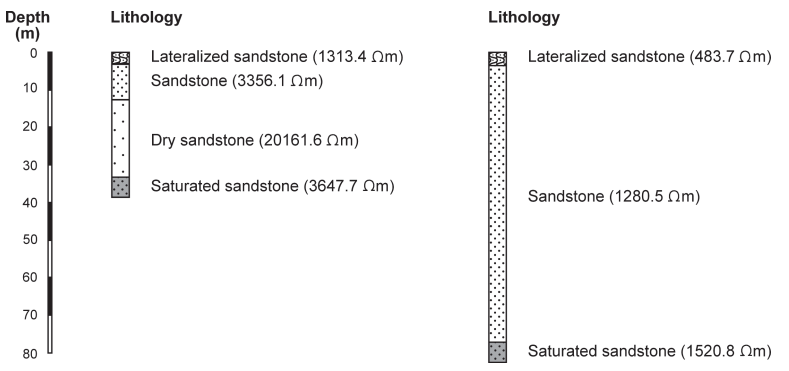

Figure 3. Depth of shallow aquifers and conductance of groundwaters in the study area.

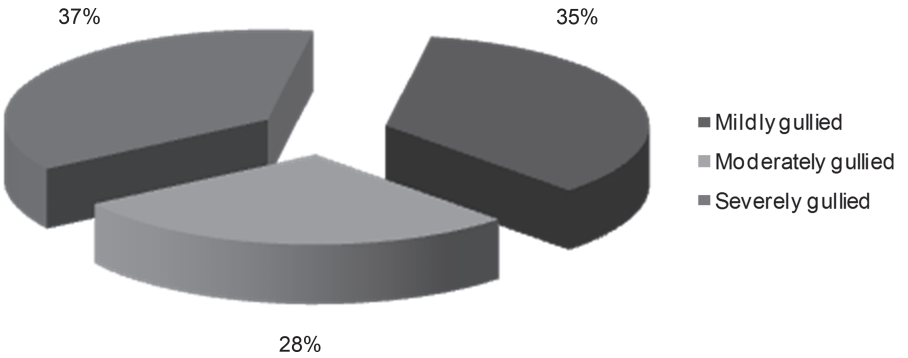

Figure 4. Gully distribution and impact on the landscape (three categories) in the study area.

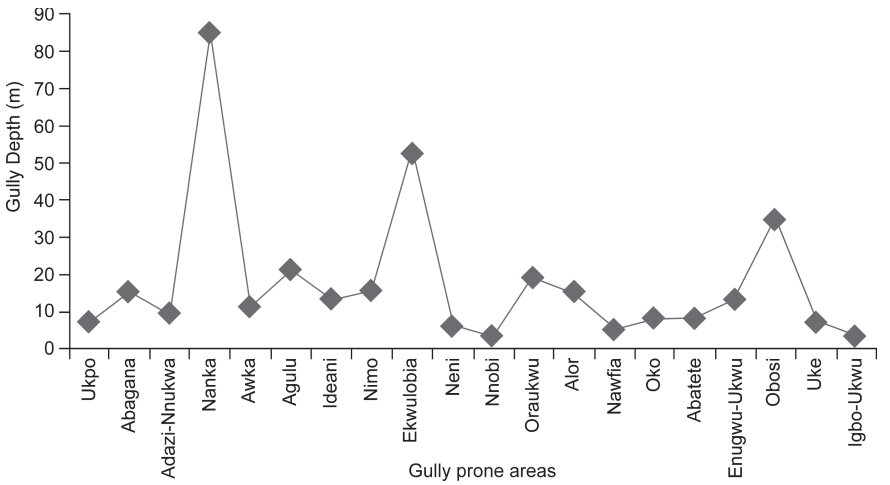

Figure 5. Depths of selected gullies compared to the original surface level in the affected areas.

in watertable occurs during the rainy season, despite the thick unsaturated zone of the predominant geologic formation. During the dry season, fall in watertable occurs as a result of hydraulic head decay. The rise in watertable increases the groundwater velocities, hence drastic gully erosion and landslide occur especially at the peak of groundwater recharge.

Gully erosion and mass wasting remain the predominant regional environmental and ecological problems in Anambra State (Egboka and Okpoko, 1984). They are promoted by heavy rain fall, floods and triggered by anthropogenic forces. These hydrogeoecological phenomenons follow palaeoenvironmental and neotectonic-morphodymamic pathways causing widescale land destruction (Egboka *et al.*, 1990) with direct and severe socioeconomic implications. The rate of gully erosion and landslide generally increase during the rainy season with annual soil loss estimated at 9.11 to10.03 tonnes/ha/year (Igbokwe *et al.*, 2008). High rainfall intensity and subsequent groundwater recharge results in high pore water pressure, effluent seepages and slope failures (Egboka and Okoro, 2007). The combination of sand and silt with low clay and organic matter content enhance moderate to high erodible conditions (Dhruba, 1997).

The plasticity index of soils from the affected and degraded areas ranges between 12 to 37% indicating high sand content with low cementing material providing condition favourable for soil erodibility (Okoro *et al.*, 2011a, 2011b).

Whereas the unconsolidated sand units of the Nanka Formation are easily eroded, the clay and shale layers are saturated and lubricated with groundwater to accelerate gullying. The inherent features of Nanka Sands favour the concentration of severe hydrogeoecological hazards of gully erosion and potential landslides in the areas predominantly covered by the formation.

8.5 SUGGESTED REMEDIAL MEASURES

Some of the basic factors that militate against solutions to environmental degradation in Anambra State include ignorance, lack of integrated professional approach by various stakeholders and lack of financial resources. The following suggestions when considered singly or jointly may go a long way in reclaiming the degraded environment:

- Improved gully erosion/landslides investigations and research.
- Appraisal of socioeconomic impacts of gully erosion and landslides.
- Inclusion of environmental education in school curriculum and creation of awareness.
- Sub-Catchment Multi technique/Integrated Approach on gully erosion control.
- Adequate funding for research, monitoring and maintenance control measures.
- International collaboration and linkages.

8.6 DISCUSSION AND CONCLUSION

Slopes of various steepness and stability significant in the Awka-Orlu upland play a major role in the more or less spontaneous gully development and growth. This is seasonally facilitated by heavy rain that occurs as torrential downpour exacerbating severe problems of environmental degradation. The gully erosion prone areas of Anambra State form part of the general deterioration of humid tropical ecosystems in Nigeria. The gully menace has attracted considerable concern since colonial era and extensive control programmes established to mitigate these environmental problems but have recorded minimal success.

The stratigraphic and structural features that exhibit regional trend aid and abate ecological dislocation of erosion and landslides.

The tectonically-disposed bedding plains and joint associated with palaeotectonic and neotectonic signatures undermine control measures thereby facilitating environmental degradation.

The activation media for these ecological problems are surface runoffs, soil water infiltration, groundwater recharge and discharge. The heavy precipitation during the rainy season enhances surface water and subsurface water inputs and flows, locally and regionally. The slopes, as exhibited by the escarpments (Nsukka-Okigwe and Awka-Orlu cuesta) the clayey or shaly beds enhance generation of floods and fast water flows.

Substantial evidence of degradation of the environment as hazards by erosion and landslide are also exacerbated by recent climate change (cf. Figure 6). During the peak periods of the rainy season, runoff increases, resulting in overland flow and gully erosion. Also rise in watertable resulting in increased pore water pressure which reduces effective stress of the soil leading to increased rate of erosion.

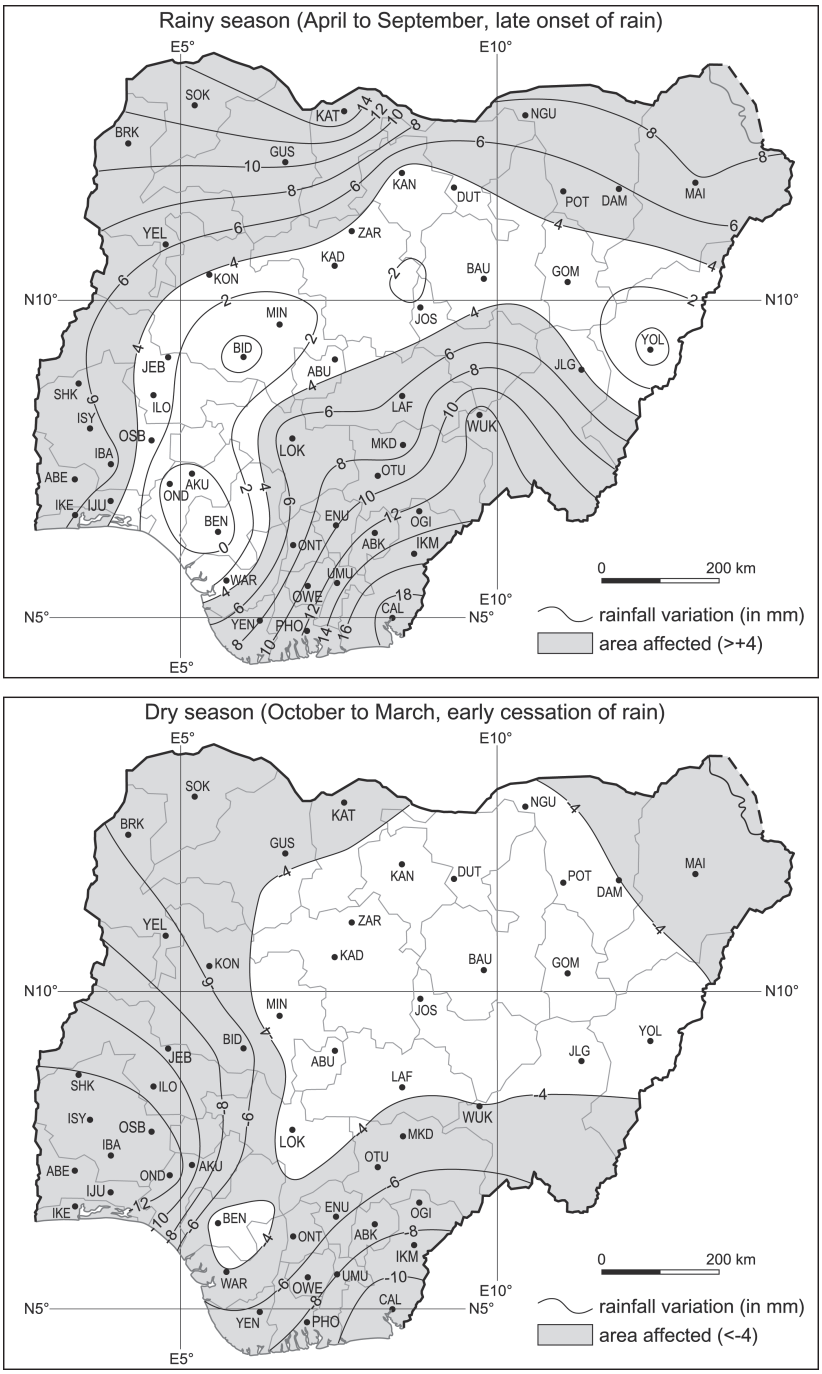

Figure 6. The effects of climate change in Nigeria: late onset during rainy season and early cessation during dry season (after Anuforom, 2009). Isolines represent observed rainfall variations in mm from the annual mean record. Shaded areas highlight areas that have more (top, >+4 mm) or less (bottom, <–4 mm) divergence from the annual mean precipitation (redrawn by P. Blank, Bielefeld).

Substantial environmental degradation in the area coincides with socioeconomic challenges like water scarcity, food insecurity and public health implications. The massive gullies and landslides that occur locally and regionally in parts of Anambra State in particular may be explained by the inherent hydrogeotechnical characteristics of the area. These features that may result in differential failures of roads, slopes, collapse of building, foundations and drainages facilitates conditions favourable for environmental degradation. Degradation associated with gully erosion and landslides has precipitated negative implications which disproportionally affected women and children. Measures of environmental degradation control have ranges of suitability. Integrated approach of control measures will be most appropriate for gully and landslide control. The surfacial outcrop exposures of the various geological formations and their structural features in terms of component shale, sandy members, and joints must be recognized appropriately during any socioeconomic relevant development project.

REFERENCES

Akudinobi, B.E.B. and Egboka, B.C.E., 1996, Aspects of Hydrogeological studies of the escarpment regions of Southeastern Nigeria. *Journal of the Nigeria Association of Hydrogeologist*, **7(1-2)**, pp. 10–27.

Anuforom, A.C., 2009, *Climate Change Impacts in Different Agro-Ecological Zones of West Africa.* Presentation at the International Workshop on Adaptation to Climate Change in West African Agriculture, Ouagadougou, Burkina Faso, held from April 27–30, 2009, www.wamis.org/agm/meetings/iwacc09/S3-Anuforom.pdf (2013-06-21).

Butler, R.A., 2005, *Nigeria has worst deforestation rate.* mongabay.com retrieved May 2007.

Cronin, T.M., Thunell, R., Dwyer, G.S., Saenger, C., Mann, M.E., Vann, C. and Seal II, R.R., 2005, Multiproxy evidence of Holocene climate variability from estuarine sediments, eastern North America. *Palaeoceanography*, **20**, PA4006, doi: 10.1029/2005PA001145, p. 21.

Dhruba, P.S., 1997, Assessment of soil erosion in the Nepalese Himalaya, a case study in Likhu Khola valley, *Middle Mountain Region Land Husbandry*, **2(1)**, (Oxford & IBH Publishing Co. Pvt.), pp. 59–80.

Egboka, B.C.E. and Mbanugo, E., 1988, Anthropogenically-caused road gullies in Anambra State, Nigeria. *India Journal of Earth Sciences*, **13(4)**, pp. 319–327.

Egboka, B.C.E. and Nwankwo, G.I., 1982, The Agulu-Nanka gully: An explanation for its origin. *Quarterly Journal of Engineers and Geologist*, **8**, pp. 54–61.

Egboka, B.C.E., Nwankwo, G.I. and Orajiaka, I.P., 1990, Implications of Palaeo- and Neo-tectonics in gully erosion-prone areas of Southeastern Nigeria. *Natural Hazards Journal Nertherlands*, **3(3)**, pp. 222–228.

Egboka, B.C.E. and Okoro, E.I., 2007, Implications of Massive Gully Erosion and Landslides at Agulu-Nanka/Alor-Oraukwu Complex, Anambra State Nigeria. In *Strategy and Implementation of Integrated Risk Management*, edited by Wang, S., Tang, G., Zhang, J., Song, W., Ammann, J. and Kux, C. Qunyan press China, pp. 426–430.

Egboka, B.C.E. and Okpoko, E.I., 1984, Gully erosion in the Agulu-Nanka Region of Anambra State, Nigeria. Challenges in African Hydrology and water resources, Proceedings of Harare Symposium, *IAHS Publication*, **144,** pp. 335–347.

Igbokwe, J.I., Akinyede, J.O.B., Dang, B.T., Alaga, T.M.N., Ono, M.N., Nnodu, V.C. and Anike, L.O., 2008, Mapping and Monitoring of the Impact of Gully Erosion in Southeastern Nigeria with Satellite Remote Sensing and Geographic Information

System, *The International Archives of the Photogrammetry, Remote Sensing and Spatial Information Sciences*, **XXXVII(B8)**, pp. 865–871.

Niu, C. and Wang, L., 1992, Erosion, Debris Flows and Environment in Mountain Regions. Proceedings of the Chengdu symposium, *IAHS Publication*, **209**, pp. 59–80.

Nwajide, S.C. and Hoque, M., 1979, Gully processes in Southeastern Nigeria. *The Nigeria Field Journal*, **44(2)**, pp. 64–74.

Ogbukagu, I.M., 1976, Soil erosion in the northern parts of Awka—Orlu uplands, Nigeria. *J. Min. and Geol.*, **13**, pp. 6–19.

Okoro, E.I., Akpan, A.E., Egboka, B.C.E. and Odoh, B.I., 2011a, Dimensional Analysis and Characterization of the Gully Systems in parts of Southeastern Nigeria, In *Water: Ecological Disasters and Sustainable Development (Monograph)*, edited by: Egboka, B.C.E. and Odoh, B.I., (Germany, UK, USA: LAP Lambert Academic Publishing), pp. 237–246.

Okoro, E.I., Egboka, B.C.E., Anike, O.L. and Enekwechi, E.K., 2011b, Evaluation of Groundwater potentials in parts of the escarpment areas of Southeastern, Nigeria. *Internatonal Journal of Geomatics and Geosciences*, **1(3)**, pp. 544–551.

Onuoha, K.M. and Uma, K.O., 2006, A Closer look at the Petroleum Potentials of the Anambra Basin: Input from Geophysics and Geohistory. In *Hydrocarbon Potentials of the Anambra Basin: Geology, Geochemistry and Geohistory Perspectives*, edited by Okogbue, C.O., (Nigeria: University of Nigeria), pp. 71–73.

Onwuemesi, A.G. and Egboka, B.C.E., 2006, 2-D Polynomial curve fitting techniques on watertable and hydraulic gradient estimations in parts of Anambra Basin, Southeastern, Nigeria. *Natural and Applied Sci. J.*, **7(1-2)**, pp. 6–13.

Onwuemesi, A.G. and Egboka, B.C.E., 1991, Implications of Hydrogeological investigations of Agulu-Nanka gully areas of Anambra State, Nigeria. *Journal of African Earth Sciences*, **13**, pp. 520–522.

Willard, D.A., Bernhardt, C.E., Korejwo, D.A. and Meyers, S.R., 2005, Impact of millennial-scale Holocene climate variability on eastern North American terrestrial ecosystems: pollen-based climatic reconstruction. *Global Planetary Change Letters* **47,** pp. 17–35.

Willard, D.A. and Cronin, T.M., 2007, Palaeoecology and ecosystem restoration: case studies from Chesapeake Bay and the Florida Everglades. *Front. Ecol. Environ*. **5(9)**, pp. 491–498.

Willard, D.A., Cronin, T.M. and Verardo, S., 2003, Late Holocene climate and ecosystem history from Chesapeake Bay sediment cores, USA. *The Holocene* **13**, pp. 201–214.

CHAPTER 9

Climate change analysis across rainfall-discharge variability in selected river catchments of Kenya and Central African Republic

Cyriaque-Rufin Nguimalet
Département de Géographie, Faculté des Lettres et Sciences Humaines, Université de Bangui, Bangui, République Centrafricaine

ABSTRACT: Climate change studies were carried out in Kenya and in Central African Republic (CAR) using precipitation and hydrological data to analyze inter-annual and spatio-temporal variability of rainfall-runoff relationships, their dynamics due to modes change occurrences and to climate extreme events. Statistics show observed hydro-climatic changes in the Lake Naivasha basin represented by the Malewa River at Morendat (Kenya) and in CAR evidenced by the Tomi River at Sibut, the Gribingui River at Kaga-Bandoro and the Fafa River at Bouca. At both sites rainfall and discharge data over the period from 1958 to 1995 were rendered to observe long series of past extreme events such as floodings, episodically low-groundwater levels and droughts occurring during several dry and wet phases of hydro-climatic fluctuations. The rainfall-discharge variability surprisingly induced an insignificant average rainfall decline of 3.23% for CAR river's catchments and of 1.7% for the Kenyan catchment respectively. In addition, a marked overall average hydrological deficit of –8% for the Malewa River (Kenya), –22% for the Fafa River and –39.49% for the Gribingui River (all CAR)—with the exception of the Tomi River at Sibut where an increase of +4% is recognizable. Hydrological deficit accentuation would probably raise in a non reconstitution of hydrological storage capacities due to droughts length and its relative intensities in each river basin. Similar tendencies are also observed on large rivers like the Oubangui at Bangui (CAR): its hydro-climatic record is extrapolated on CAR's catchments and equally adjusted to the Malewa River basin in Kenya.

9.1 INTRODUCTION

Research on climate change evidenced by comparative studies of different river catchments in Kenya and in the Central African Republic (CAR) consists to analyze the inter-annual and spatio-temporal variability of hydro-rainfall resources, their dynamics according to changes occurring in their modes and in terms of climatic extreme events. Climatic and extreme phenomena evolution (droughts, low-water levels, floods, violent storms) is a major concern in the younger past where aridification of climate was recognized since the 1970s (Olivry, 1987; Olivry *et al*., 1998; Laraque *et al*., 1998; Paturel *et al*., 1998; Servat *et al*., 1999; Ardoin-Bardin, 2004). Thus, short and long term hydrological periods and their variability would insinuate modifications in water 'behavior' according to different climatic types (Nguimalet, 2009). The periods of variability display rainfall and runoff and other hydrological data resources gathered.

They depend in particular on the feeding by rainfall on various catchments in selected study areas according to the influence of the regional climate. This paper states climate variability and change and its extension on rainfall-flow coupled with different river basins.

9.2 STUDIED CATCHMENTS

9.2.1 Presentation of selected river basins in Kenya and CAR

The selected catchments belong to East and Central Africa (Figure 1). In Kenya the Lake Naivasha basin, located in the central-west, covers a total area of 3300 km^2. Lake Naivasha is a freshwater lake that covers an area of about 145 km^2. It is located within the Rift Valley at 0°46′S and 36°21′E with an elevation of 1887 m asl; it is the highest of Kenya's Rift Valley lakes. Naivasha is fed by Malewa, Gilgil and Karati Rivers (Gathenya, 2007). The Malewa River is the biggest inlet of the lake. Its catchment is located between 0°08′ and 0°35′S as well as 36°17′ and 36°43′E. The Malewa basin covers 1700 km^2. Altitude varies from a minimum of 1880 m at Morendat to a maximum of 3906 m asl at the Aberdare Range (Figure 1).

The CAR catchments are located in the central-south and central-north part of the country between 5°30′ and 7°00′N as well as 18°00′ and 19°50′E. They are situated on the border of the Chad-Congo watershed (Fafa and Gribingui Rivers on the Chadian side and Tomi River on the Congolese side). The upper basins are located at an altitude of 735 m (Kaga Yagoua) and 725 m asl (Kaga Mbrés) along the watershed. Gribingui's source is at 550 m asl (Dékoa). Fafa and Tomi are rising at 690 m and 650 m asl respectively (Boulvert, 1987). Outlets of retention reservoirs in Kenya and Central Africa coincide with urban areas, except in the case of the town of Morendat (Kenya).

The geomorphology of the CAR basins correspond to planated surfaces over Precambrian basement regionally topped by a Cenozoic cover whose linear ridge delimits the catchments into the Chad-Chari basin to the north and the Congo basin to the south (Nguimalet, 2008). The geology of the three catchments is built up by Archean granites, amphibolites and meta-breccia of the Early Proterozoic. Sericitoschists, micaschists with garnets were formed around 2200 to 2000 Ma, granulitic gneiss and a migmatitic charnockitic complex around 630 Ma, and metamorphosed sandstone and migmatites around 600 Ma (Rolin, 1992). Additionally, some Archean granites, migmatites and metamorphosed sandstones are cropping out in the Gribingui and Tomi River basins.

The Kenyan Rift Valley is dominated by mountain chains in E and NNE strike direction (Aberdare Range) and plateaus derived from younger volcanic rocks that dominate the Lake Naivasha plain by a NNW–SSE oriented escarpment (about 200 m difference in altitude, Figure 1). These geomorphological features are strongly leading to rainfall variability in the basin. Additionally, the various rocks' hydrodynamism is influencing diversely not only the selected rivers' hydrology, but also the retention reservoirs which are indispensable to flow support during low-water levels.

Climate is different in each of the study sites. CAR's climate is wet tropical including five rainfall gradient types from south to north with 1600–800 mm/year: guinean-forest, sudano-oubanguian, sudano-guinean, sudano-sahalian and sahelian (Bouquet, 1984).

The studied river basins are located in the sudano-guinean subtype receiving an average annual rainfall of 1200–1400 mm (Nguimalet, 2009). Consequently, from South to North vegetation is composed by (i) semi-deciduous and dense forests and (ii) savanna types (Boulvert, 1986). Semi-deciduous forest comprises patches of dry dense forests which is degraded to savanna woodland between Dékoa, Kaga-Bandoro, Les Mbrés,

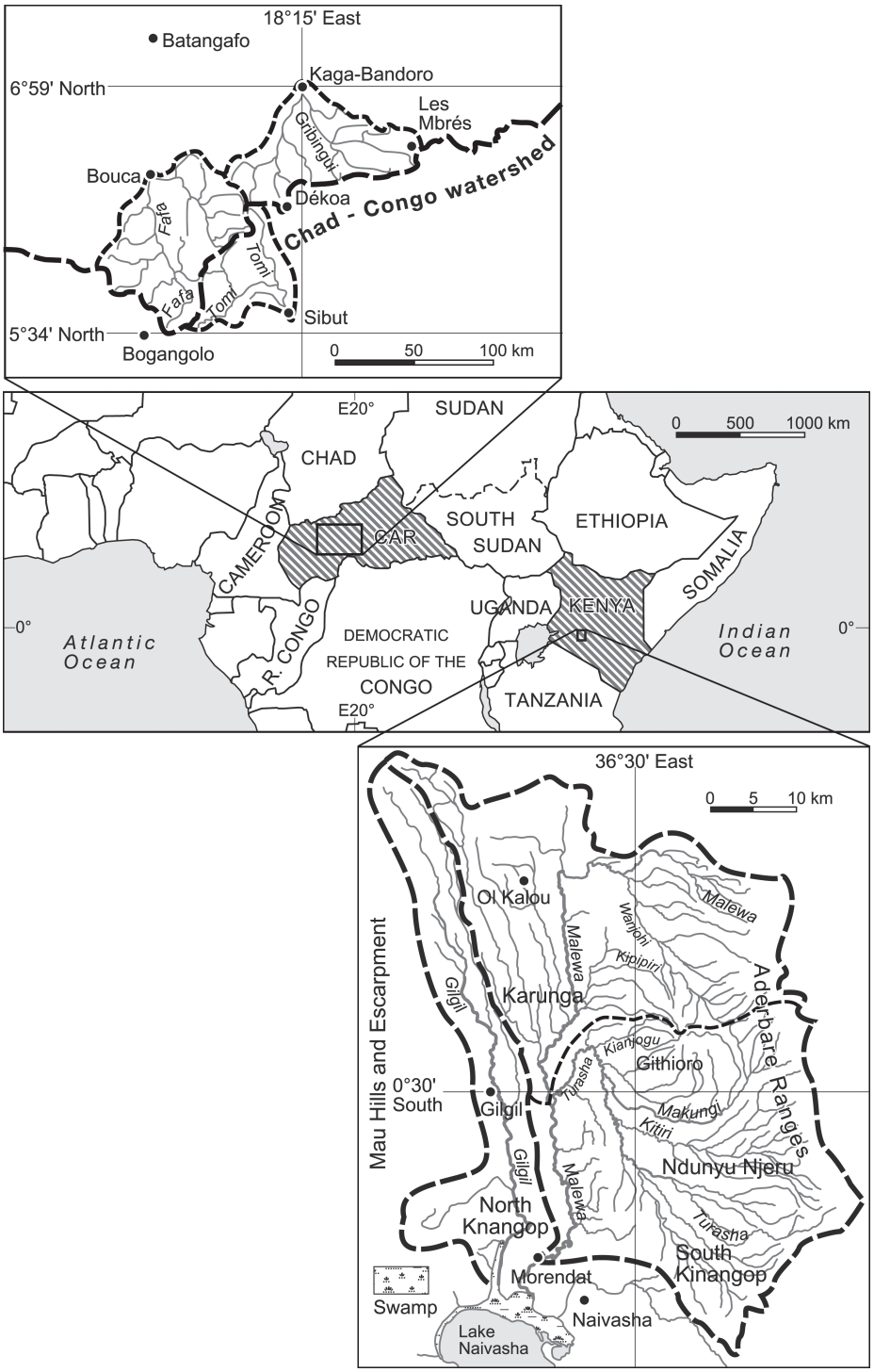

Figure 1. Location of selected river basins in Central African Republic (CAR) and Kenya.

Bogangolo and Bouca. The savannas are characterized by changes in grass types as well as tree size and density towards the North. Along the rivers gallery forest occurs.

Climate in Kenya's Rift Valley is influenced by both subequatorial Highlands (750–2000 mm/year) and the dry to semi-arid tropical belt (250–1000 mm/year, Primary Atlas, 2004). According to vegetation-climate interrelationships vegetation cover in Kenya and particularly in the Lake Naivasha basin changes significantly with increasing height in the Mount Kenya mountain area (Primary Atlas, 2004). Following this vegetation gradient, two main vegetation types can be distinguished: (i) short grass and scattered trees are found at low scale, and (ii) mountain forests with grassland developed at high altitudes. These cause changes in runoff modes depending on the relative water distribution in space and time.

9.2.2 State of the art and objectives

Climate change implications for water resources availability are noticeable today, mainly over fluvial regimes. Some earlier works from 1975–1995 (Sircoulon, 1976, 1985; Olivry, 1987, 1994; Nicholson, 1983; Nicholson *et al*., 1988) debate either on rainfall and runoff deficits, rainfall-runoff relationship (Mahé and Olivry, 1995; Boyer *et al*., 2006) or water resources assessment (Bricquet *et al*., 1997; Paturel *et al*., 2007). Olivry (1994) observed that rainfall decline becomes more marked in the 1980s when rainfall regime alterations affected areas in tropical Africa including Kenya and CAR. Conway *et al*. (2009) demonstrated that high levels of inter-annual variability exist in many African river basins. Flow decline is established mainly across tropical large rivers, particularly since the 1969–1970 interruption ('rupture') which occurred in West and Central Africa (Olivry *et al*., 1998). However, relationships between rainfall-runoff decline in Eastern and Southern Africa seems to be less substantially (Conway *et al*., 2009).

During the Holocene (and before) climatic dynamics and environmental deteriorations occurred several times, characterized by wet and dry periods such as revealed in many palaeoenvironmental studies in Africa (e.g., Roche, 1991; Schwartz, 1992; Maley, 2010; Thomas and Thorp, 1992; Thomas, 1994; Neumer *et al*., 2007; Runge, 2007). Empirical climate data became available onwards the late 19th century when rainfall and hydrometric gauging stations were implemented which allowed observing flows and climate evolution regionally and globally. Data interpretation led to a deepened knowledge on more recent climate dynamics in Africa (e.g., Olivry, 1987; Nicholson *et al*., 1988; Demarée, 1990; Olaniran, 1991; Mahé and Olivry, 1991; Servat *et al*., 1996, 1997a, b and c; Gautier *et al*., 1998; Olivry *et al*., 1998; Paturel *et al*., 1998; Conway *et al*., 2009). For evidencing climatic 'pejoration' and/or change, rainfall variability (Servat *et al*., 1997a and c; Paturel *et al*., 1998 and 2007; Kingumbi *et al*., 2000) and flow dynamics (Servat *et al*., 1997b; Laraque *et al*., 1997 and 1998; Orange *et al*., 1997; Olivry *et al*., 1998) were examined. These works identified climatic fluctuations in tropical Africa: wetter regimes towards the end of 1960s and since the 1970s a decline of rainfall. This persistent rainfall deficit, reaching 20–25% in Sahelian Africa (Paturel *et al*., 1998; Servat *et al*., 1999) induced a weakness or reduction of river discharge and an impact on water resources (Servat *et al*., 1997b; Laraque *et al*., 1997, 2001; Orange *et al*., 1997; Olivry *et al*., 1998; Kanohin *et al*., 2009). According to Paturel *et al*. (1998), in the arid and semi-arid zones of West and East Africa water resource precariousness is not recent, whereas drought affecting African tropical regions exposes some remarkable severity, persistence and extension simultaneously. Olivry (1994) and Olivry *et al*. (1998) evidenced that a certain durability of hydrological deficit since 1970s is due to cumulative effects of drought year's length, in particular

on intertropical African large rivers. Most certainly, drought cases are occurring in time and space, but the current drought appears like the most important, regarding duration and rainfall-runoff deficit.

In Central Africa runoff analysis of the Congo River identifies a certain hydro-climatic stability during the first half of the 20th century, but cyclic variations were observed in watercourses hydrology since 1960 (Orange *et al*., 1995; Wesselink *et al*., 1996; Orange *et al*., 1997; Laraque *et al*., 1997, 1998; Runge and Nguimalet, 2005). These authors showed that on the Congo basin scale the 20th century is marked by an ongoing 'drying out' recorded since the 1970s. Laraque *et al*. (1997, 1998) noted some weaker and fewer interruptions in rainfall (2–8%) than those of hydrological series (0 to more than 30%) on the Congo tributaries of the right bank (Oubangui at Bangui, Sangha at Ouesso, Likouala-aux-herbes at Botouali, Likouala-Mossaka at Makoua, Kouyou at Owando, Alima at Tchikapika, Nkéni at Gamboma, Léfini at Bwembé, Congo at Brazzaville). In CAR, Servat *et al*. (1999) estimated a 17% deficit since 1968 and 1969; Wesselink *et al*. (1996) reported 6% of rainfall deficit across Oubangui catchment. In addition, Runge and Nguimalet (2005) estimated that the extreme flows show slight trends of runoff declining of the Oubangui River at Bangui (1911–1999) which could be related to an aridification in the Sudano-guinean part of the basin. Flow regime seems to be characterized by a deficit before 1990 and an abundance afterwards, until 1999.

With reference to the Oubangui River Wesselink *et al*. (1996) indicate a succession of homogenous climatic periods in Central Africa since the beginning of the last century. According to them, current drought affecting this river affects also some of its tributaries (Lobaye, Kotto, Mbali, Mbomou). Laraque *et al*. (1998) attested more significant fluctuations over the Oubangui basin of 34% of Congo flow deficit at Brazzaville during the current drought, even though its basin does not represent the fifth of the total Congolese basin area. That shows how Oubangui yields support Congo flow regime. Unfortunately, only few studies were conducted on Oubangui's and also Chari's Central African tributaries and sub-tributaries. The Oubangui basin at Bangui, Mpoko at Bossélè-Bali (Gapia, 2007), Mbali at Boali (Bokonge Ntefo, 2008) and Pipi at Ouadda (Nguimalet *et al*., 2007; Nguimalet and Ndjendolé, 2008) have been studied showing how these hydrological fluctuations are influencing the whole basin. As for Chari's tributaries and sub-tributaries, hydro-climatic changes of Fafa at Bouca (Nguimalet, 2010a and b), Ouham at Bossangoa and at Batangafo were analyzed (Ardoin-Bardin, 2004; Azouka, 2011). The study of rainfall-runoff deficits in sub-basins will inform on the spatial heterogeneity, its impact at large basins' scale (Oubangui, Chari) and it is linked to regional basins in climate change context. In fact, the persistent climatic aridification impact on Tomi sub-basin at Sibut and two Chari's sub-basins, Fafa at Bouca (enlarging Ouham at Batangafo, Chari's principal tributary) (Boulvert, 1987), and Gribingui at Kaga-Bandoro (also joining River Chari) will be analyzed in details.

On decadal time scales western Sub-Saharan Africa exhibits drying out processes across the Sahel after early 1970s, meanwhile relative stability punctuated by extreme wet years in East Africa. The link between hydro-climatic fluctuations and extreme events were discussed by Conway (2002). According to Eriksen *et al*. (2008) Kenya is one of the most exposed East African countries to climate change impacts. Challenges are droughts, cyclones, local flooding, decline of lake levels, decrease and variation of river flow and others. Recent work on climate change and water resources in the Lake Naivasha basin was carried out on lake level variations between 1900 and 1997 (M'mbui, 1999), on climate variability and change impact on water resources (Lukman, 2003) or on lake level-flow-rainfall dependencies (Muthuwatta, 2004). The latter has used hydrological models for the better understanding of Lake Naivasha's hydrological dynamics.

Studies about small rivers or catchments with a surface less than 2000 km^2 are scarce (Fadika *et al*., 2008). Fadika *et al*. (2008) assessed hydrological variables in smallest catchments that are Tabou (810 km^2), Dodo (640 km^2) and Néro (1,210 km^2) in the west of Côte d'Ivoire. Results showed runoff decline varying from 33% (Tabou) to 45% (Dodo) mainly during 1980–1990 which is in contrast to the observed trends on large tropical rivers. Obviously, small African rivers record these changes lately. Smallest catchments are often steeper (0.0256 mm^{-1}, i.e. a topographic gradient of 256 m on 1000 m or 256‰ for the Malewa catchment at Morendat), causing sudden and fast increase in discharge. Also the relative narrowness of their channels prohibits easy collection of data representing the regimes oscillations based on runoffs (extreme and annual mean). Intra-seasonal or seasonal hydrological fluctuations and missing chronics of low-water level flow complicate the assessment of water deficits during the aridification period. Use of river water by farmers and agro-pastoralists is also frequent alongside Malewa River. The main interest of this work is the better understanding of Malewa's fluvial and hydrological dynamics since the beginning of the aridification phase during the 1970s.

9.3 METHODOLOGY

This study uses measured data on rainfall and discharge from Kenya in the Lake Naivasha basin (Nguimalet and Onyando, 2009; Nguimalet, 2010b) and from CAR for Tomi, Gribingui and Fafa catchments (Nguimalet, 2010a and b) to assess the impacts of climate fluctuations on small river catchments.

9.3.1 Data presentation

In Lake Naivasha basin (Malewa sub-basin), rainfall data (R) were recorded in four gauging stations (Kari Naivasha, Gilgil Kwetu, North Kinangop Forest Station and Geta Forest) from 1929–2003. The data have been made available by Water Resources Management Authorities (WRMA). Discharge data were collected in the respective sub-basins of Malewa at Gilgil (756.64 km^2) and at Morendat (1700 km^2) from 1931 to 1987.

In CAR, rainfall raw data were recorded at six gauging stations distributed over all catchments such as Bogangolo, Sibut, Dékoa, Bouca, Kaga-Bandoro and Les Mbrés (Figure 1) from 1904–1995. It has been made available for the study by the *Agence pour la Sécurité de la Navigation Aérienne en Afrique et Madagascar Service* (ASECNA) at Bangui and was supplemented by the *Institut de Recherche pour le Développement* (IRD) database.

Rainfall-runoff observation length has not been the same at the gauging stations. About In Kenya, observation periods of rainfall were 1959–2003 for Kari Naivasha, North Kinangop Forest Station and Geta Forest, and 1929–2003 for Gilgil Kwetu; in CAR records where available as follows: 1904–1989 at Kaga-Bandoro, 1931–1990 at Bouca, 1931–1995 at Sibut, 1952–1995 at Les Mbrés, 1954–1980 at Dékoa and 1954–1987 at Bogangolo. Data on rivers discharge were extracted from IRD's database and supplemented by those from CAR's Hydrological Yearbook (République Centrafricaine, 1985–1990; 1990–1991; 1991–1992; 1992–1993; 1993–1994; 1994–1995) and Callède *et al*. (2010). Data series were incomplete, particularly for Tomi River at Sibut between 1979–1985 and 1993–1995, Gribingui River at Kaga-Bandoro between 1977–1979 and 1981–1985s, and Fafa at Bouca Rivers between 1981–1983 and 1984–1985;

for Malewa River (Kenya), data were not recorded beyond 1985 (Malewa at Morendat) and in 1987 (Malewa at Gilgil). Missing data reduced observation cores for the R Irregularity coefficient calculation. Discharge data on Central African rivers generally covered the 1950–1995 period: Tomi at Sibut (1951–1995), Gribingui at Kaga-Bandoro (1951–1995) and Fafa at Bouca (1958–1995). The Oubangui River data set at Bangui covers the period from 1935–2000. Regional rivers which are influenced mainly by the Sudano-Guinean variety of wet tropical climate were used for comparing trends for both CAR rivers and Malewa River in Kenya.

9.3.2 Treatment and analysis

Rainfall and runoff data utilization was done over a common period 1958–1986 in order to compare observed trends in both study sites. The objective was to follow past extreme events' in terms of resources and risks (riverside or not) at Sibut, Kaga-Bandoro and Bouca (CAR) and Naivasha, Morendat, Gilgil and Olkalou (Kenya). Annual total rainfall, maximum and minimum daily mean of river discharge, and annual and monthly mean flows were used. To receive applicable data, gaps of a few months were filled by the averages framing method among the monthly totals or average. Available in calendar years in both sites, rainfall-discharge data were laid out according to the Hydrological year starting from April 1st to March 31st in CAR (Bruel, 1902; Nguimalet and Ndjendolé, 2008; Callède *et al*., 2010), and from March 1st to February 28th/29th in Kenya, precisely in Lake Naivasha basin. According to seasonal rainfall-runoff evolution, the Hydrological year for the Kenyan basin (i.e., Malewa River) was defined. Rainfall and average discharges were treated by statistical tests: rainfall and flow indices, R irregularity indices (Q_{max}/Q_{min}, Cosandey *et al*., 2003), seek for trends and ruptures in observation series, Hubert segmentation for establishing climate variability or change in each basin dataset (Nguimalet, 2009; Nguimalet and Onyando, 2009).

Rainfall indices defined by Lamb (1982, quoted from Paturel *et al*., 1998) was used:

$$(X_i - \overline{X})/S \tag{1}$$

where X_i: rainfall of year i; $\overline{X}$: inter-annual mean rainfall over reference period, and S: standard deviation of inter-annual rainfall over the reference period. This method allows deepening the first statement in sense that the index translates rainfall surplus or rainfall deficit for the considered year regarding the chosen reference period.

In addition, rainfall series were standardized by:

$$x' = (x - \text{average})/\text{standard deviation} \tag{2}$$

x' is an annual rainfall value; with x the annual rainfall value, one calculates the average rainfall and standard deviation from a year to another for each rainfall gauging station over common period (1958–1986) and it is averaged for the normalized index. That has been done for 3 gauging station covering each one of 3 CAR's basins and for 4 gauging stations for Malewa catchment in Kenya (Nguimalet, 2010).

Using Equation (3) the average Rainfall of year i for catchments (RBS) will be calculated:

$$\text{RBS}i = (a1 \cdot x(1, i) + a2 \cdot x(2, i) + a3 \cdot x(3, i) + \cdots) / (a1 + a2 + a3 + \cdots) \tag{3}$$

with $x(1, i)$: (normalized) rainfall of year i at station 1 and $a1$: the coefficient describing represented basin part of station 1, and so on for all gauging stations. The obtained final index was re-standardized and transformed into millimetre values, applying the standardization's opposite operation. Results of data gathered after 1986 were extrapolated for comparing rainfall evolution and runoff trend with gauging stations representing a long observation period, in order to assess climate variability or change effects on water resources (Sighomnou *et al*., 2007; Liénou *et al*., 2008).

Statistical segmentation of rainfall-runoff chronics allowed detecting occurred changes in rainfall and evolution of flow variables (Laraque *et al*., 1997; Gautier *et al*., 1998). The principle of the segmentation procedure is to "cut" the series in several segments so that the calculated average on any segment is significantly different from the neighbour segment average. This cutting led to identify one or more types of discontinuities in time series with alternating dry and wet periods (Hubert *et al*., 1998).

9.4 CLIMATE DYNAMICS AND EVIDENCE OF CHANGE IN THE STUDIED CATCHMENTS

Rainfall-runoff variables and parameters are archives of spatio-temporal events which were considered comparatively to exhibit climate deterioration in the four selected catchments. Witnesses for these hydro-climatic phenomena are floods, violent storms, droughts and severe low-water levels. Also wet and dry phases in the fluvial systems given by recorded rainfall and discharge data contribute to establish climate change.

9.4.1 Recorded rainfall trends per basin

9.4.1.1 Average rainfall and calculated indices in studied catchments

Inter-annual or annual evolution of average rainfall per catchment allows distinguishing two groups. The first group comprises Tomi and Malewa basins in which respective inter-annual mean rainfall (1419 mm and 982 mm) expose a null trend, having recorded neither a decline, nor a rainfall rise, although in certain years (1965–1966, 1972–1973, 1981–1983 and 1987–1988 for Tomi basin; 1958–1961, 1965–1966, 1969–1970, 1973–1974, 1984–1985 and 1993–1994 for Malewa at Morendat) the peaks were weak. The second group includes average rainfall from Gribingui at Kaga-Bandoro (1311 mm) and Fafa at Bouca (1399 mm) where rainfall declines noticeable, respectively $r = 0.35$ and $r = 0.26$. Also in the first group some dry phases were observed: 1958–1959s, 1965–1966s, 1972–1973, 1973–1974, 1984–1985 and 1987–1988.

If the calculated annual averages of rainfall per basin do not lead to clearly identifying rainfall surplus or deficit periods, the rainfall indices allow the identification (Figure 2). The rainfall anomalies indicate two tendencies: stationarity and decline. The stationarity relates to Tomi River at Sibut and Malewa River at Morendat basins' average rainfall, characterized by alternation of wet, dry and often short (3–4 years) sequences, which depicts quasi-null climate variability or change assumption (Figures 2a and b). The observed tendency shows a certain balance since 1958 until 1995. There is only one noteworthy tendency of the data of Malewa basin showing a long rainfall deficit from 1971–1977, whereas the deficit of 1984–1988 is rather "normal".

The Tomi and Malewa River basins succumbed a relative long dry phase before 1960, followed by a wetter episode from 1961 to 1971 (Figures 2a and b). Afterwards, short dry and wet episodes alternate confirming the specific absence of a clear rainfall trend in these fluvial systems. In Gribingui's basin, the rainfall index determines wet (1955–1969, 1975–1980) and dry (1970–1974, post-1981) periods (Figure 2d). Data of

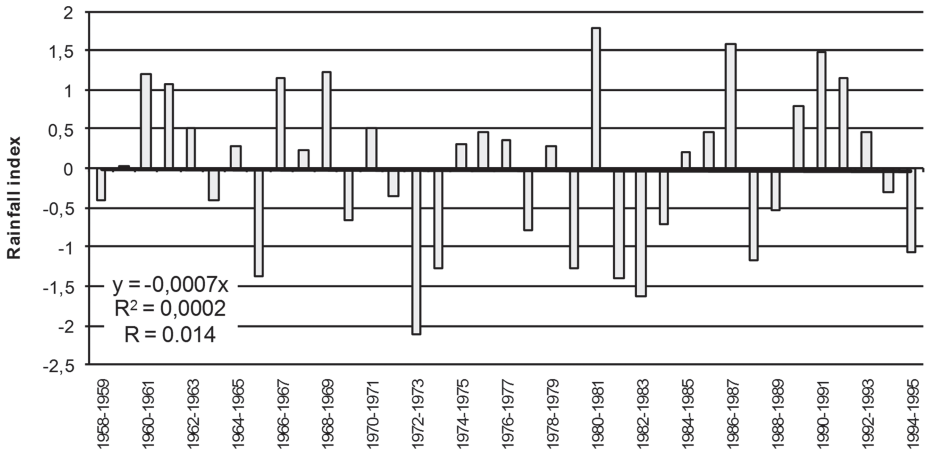

Figure 2a. River Tomi basin's Rainfall indexes, CAR.

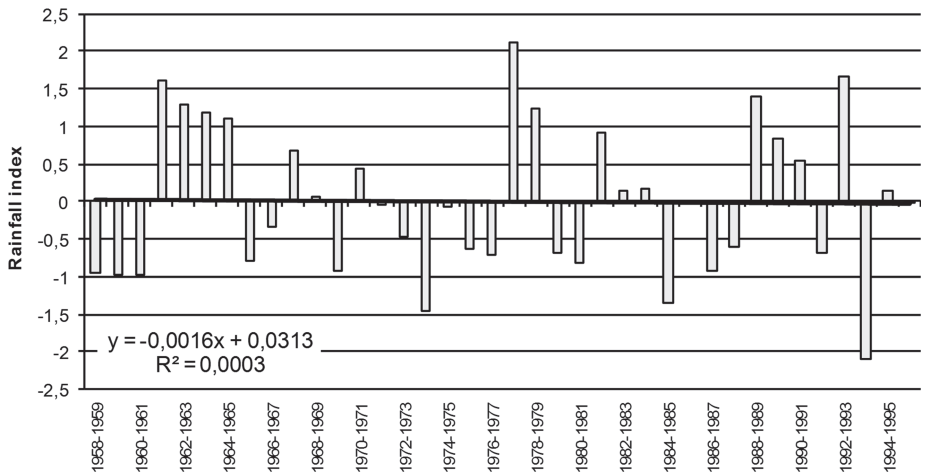

Figure 2b. River Malewa basin's Rainfall index, Kenya.

Fafa basin highlights long wet (1960–1969) and dry (1970–1980) periods and short wet (1981–1986) and drier (1953–1959, 1987–1990) periods (Figure 2c). These collected dry and wet alternated periods are the indicators of modification of climate type. The global trend shows variable and weak average rainfall decrease from one basin to another: 0.89% for Tomi basin, 1.7% for Malewa basin, 4.2% for Gribingui basin and 4.6% for Fafa basin.

9.4.1.2 Contribution of statistical segmentation in trends' rainfall analysis

At local scale, statistical segmentation allowed a better visualization of recorded wet or less wet and dry periods alternated per station in Kenya and CAR (Figures 3a and b). In spite of the obviousness of dry and wet periods, a synchronism can be admitted, even a regionalization of these climatic phenomena in both Eastern and Central Africa. These results show essential details for the understanding of climate modifications triggered by spatio-temporal rainfall variations in these African regions.

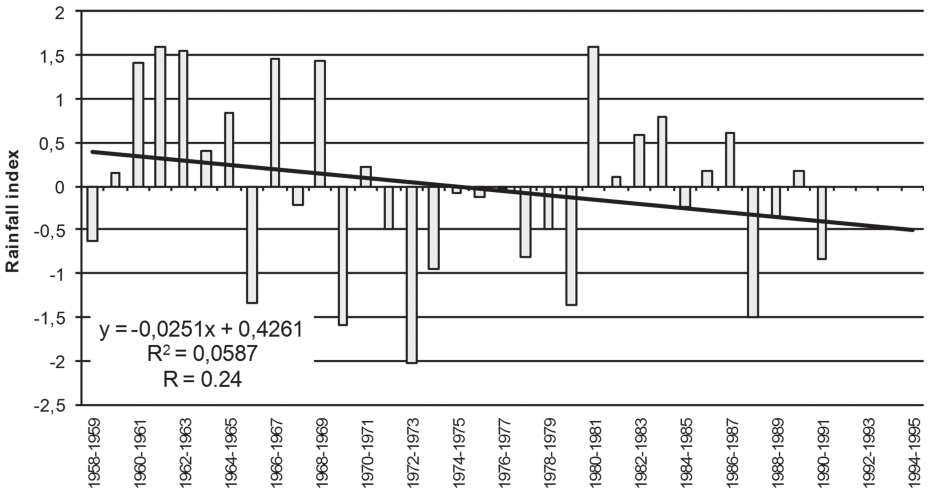

Figure 2c. River Fafa basin's Rainfall indexes, CAR.

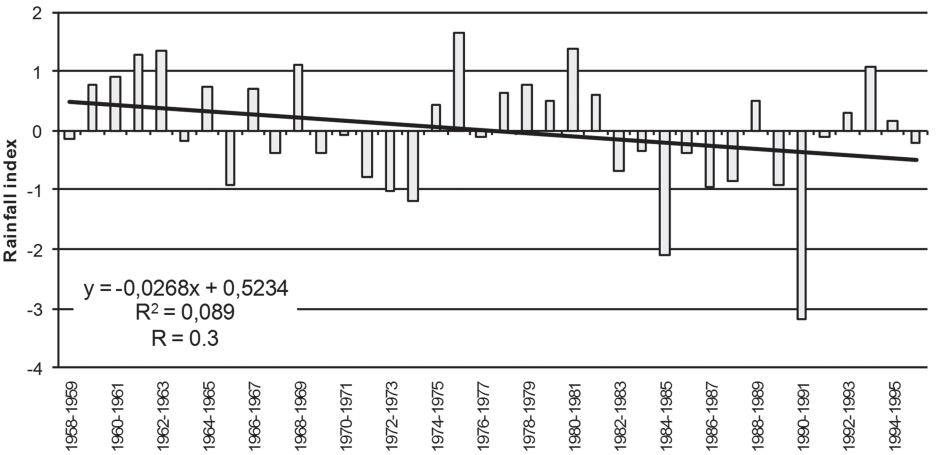

Figure 2d. River Gribingui basin's Rainfall index, CAR.

Beyond, calculated inter-annual indices of spatio-temporal variability show almost 2 to 3 ratio between maximum and minimum annual rainfall at four gauging stations in CAR (Bouca, Kaga-Bandoro, Les Mbrés and Sibut: Table 1) and from 1 to 1.5 at Kenyan stations (Table 2). At both sites, standard deviation trends can be read out from one rainfall gauging station to another. It indicates the relative acuity of rainfall modifications from one year to another and from one catchment to another. The gauging stations' coefficients of variation (CV) provide additional evidence to the range of this climatic phenomenon. However, the amplitude of rainfall variability is relatively important in Gribingui (1969–1974), Fafa (1969–1980) and Malewa (since 1972) basins, particularly on 1969–1970 interruption (Figure 2). Nevertheless, rainfall briefly increased in these basins in 1975–1980 at Gribingui, 1980–1986 at Fafa and 1988–1993 at Malewa, with data gaps since 1995 which excluded rainfall dynamics in this Sudano-Guinean area afterwards as compared to Malewa which is influenced by both highland and semi-arid climate.

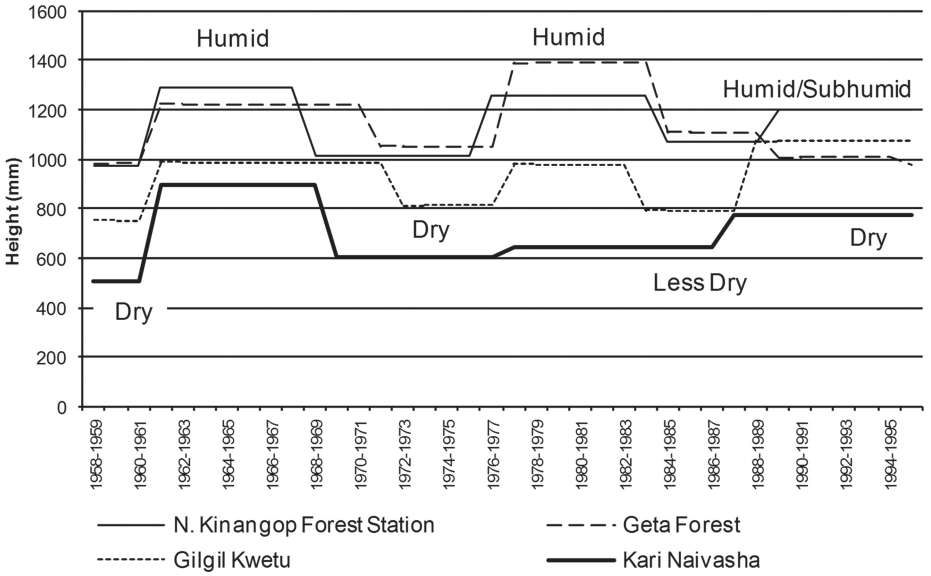

Figure 3a. Results of statistical segmentation at rainfall station scale in Malewa basin at Morendat, Kenya.

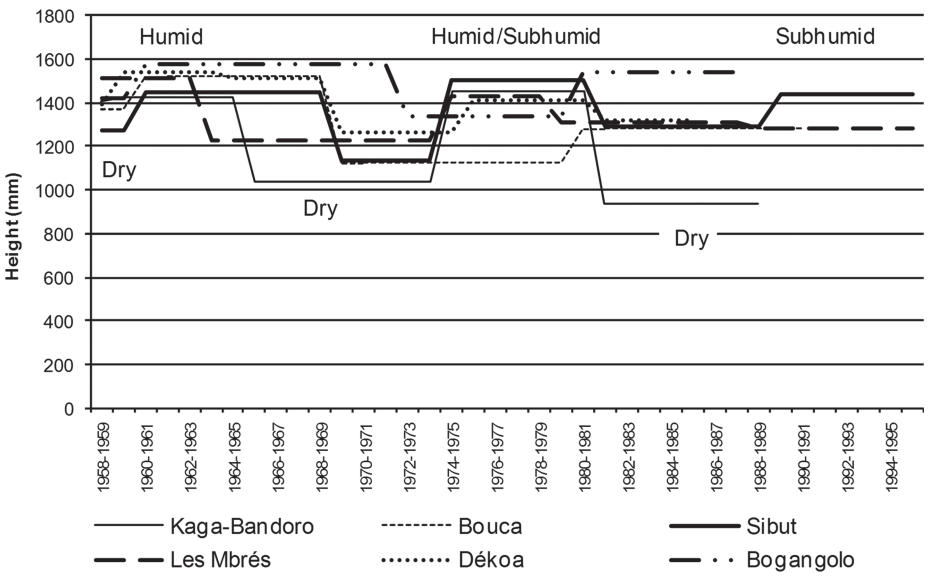

Figure 3b. Results of statistical segmentation at rainfall station scale in CAR catchments.

On annual or multiannual scale, important rainfall deficits are noted per basin. Common periods of drastic rainfall reduction are 1965–1966, 1972–1973, 1984–1985, 1987–1988 and 1993–1994 for Malewa basin, reaching values of 21–24.5%, 29.5–33.7%, 31.27–41.84%, 23.4–35.3% and 49.17% (Table 3).

Table 1. Inter-annual indices of spatio-temporal variability of rainfall in CAR basins.

Gauging stations	Inter-annual average (mm)	Standard deviation	CV (%)	Maximum/ Minimum (mm)	Report maxi/mini
Bogangolo (1954–1988)	1496.0	206.6	13.82	1825 (1984–1985) *1012* (1972–1973)	1.8
Bouca (1931–1991)	1356.8	245.56	18.1	2367.1 (1949–1950) *671.4* (1969–1970)	3.5
Dékoa (1954–1986)	1415.0	190.2	13.45	1860 (1966–1967 *1124* (1971–1972)	1.65
Kaga-Bandoro (1904–1989)	1290.9	217.9	16.88	1808.8 (1977–1978) *639.9* (1973–1974)	2.8
Les Mbrés (1952–1996)	1388.0	212.95	15.34	1862 (1975–1976) *947.2* (1973–1974)	1.96
Sibut (1931–1995)	1372.7	229.3	16.51	2095.1 (1934–1935) *852.5* (1973–1974)	2.46

Table 2. Inter-annual indices of spatio-temporal variability of rainfall in Malewa basin, Lake Naivasha catchment.

Gauging stations	Inter-annual average (mm)	Standard deviation	CV (%)	Maximum/ Minimum (mm)	Report maxi/mini
Kari Naivasha (1958–2004)	690	217.7	31.55	1206 (1967–1968) *309.8* (1993–1994)	3.89
Gilgil Kwetu (1958–2004)	1356.8	192.8	20.29	1350.1 (1964–1965) *581.7* (1965–1966)	2.32
Geta Forest (1958–2004)	1123.26	269.98	24.04	1728.25 (1978–1979 *589.85* (1993–1994)	2.93
North Kinangop Forest (1958–2004)	1142.89	229.8	19.9	1711 (1977–1978) *655* (2000–2001)	2.61

Table 3. Some spatio-temporal features of important annual rainfall deficits collected in the studied sites.

Periods	Tomi basin (%)	Gribingui basin (%)	Fafa basin (%)	Malewa basin (%)
1965–1966	21.1	24.5	23	17.25
1969–1970	–	–	24.3	21.14
1971–1972	–	22.5	–	–
1972–1973	31.8	26.9	32.41	10.19
1973–1974	–	25.24	–	34.19
1982–1983	22.5	–	–	–
1984–1985	–	41.84	–	31.27
1987–1988	–	34.15	23.63	–
1993–1994	–	–	–	49.17

1987–1988 was mostly severe in three Central African catchments and 1993–1994 for Malewa catchment. The spatio-temporal verifications of these events exhibit local or global variations for the same period or from one period to another per basin or group of basins. The persistence and duration of the current dry phase affects obviously the water resources and their use in the studied river systems. Orange *et al*. (1997) analyzed the lowering of Oubangui River's catchment groundwater table due to low rainfall, change in infiltration patterns and sustainability of river flows on a regional scale. Although, it is necessary for an overall outline to integrate piezometric tendencies into a water resources appraisal (Mahé, 2009).

9.4.2 Recorded hydrological trends per basin

9.4.2.1 Evolution of inter-annual and annual average discharge and flow indices from Tomi, Gribingui, Fafa and Malewa Rivers

In CAR inter-annual average discharge vary from 18.11 $m^3 s^{-1}$ (Tomi River), 21.25 $m^3 s^{-1}$ (Gribingui River) to 35.48 $m^3 s^{-1}$ (Fafa River). In the Kenyan Lake Naivasha basin, the values amount to 2.81 $m^3 s^{-1}$ and 6.1 $m^3 s^{-1}$ for Malewa River at Gilgil and Malewa at Morendat, respectively. The importance of water amount at each outlet is related to the catchment area. Particularly, the Fafa catchment has the highest inter-annual average discharge (35.48 $m^3 s^{-1}$) although its surface is not the largest of the studied basins (4380 km^2) compared to Gribingui catchment with a surface of 5680 km^2.

Annual average discharge fluctuates from year to year in each catchment, attesting a yearly variability of water flow per basin and maybe turbulent flow due to high river bed inclination of 24‰ for Tomi, 14‰ for Gribingui, 11‰ for Fafa (Nguimalet, 2010a) and 256‰ for Malewa at Morendat (Nguimalet and Onyando, 2009). The inclination influences significantly the seasonal chronology of flow. In addition, the rivers' flow indices led to understand their dynamics in the observed water deficit and surplus in periods 1958–1995 (Figure 4). Thus until 1970s, Gribingui's and Fafa benefited from effects due to wet periods (Figures 4b and c) though since then, their flow declined triggered by aridification. Tomi and Malewa River seem to have a similar

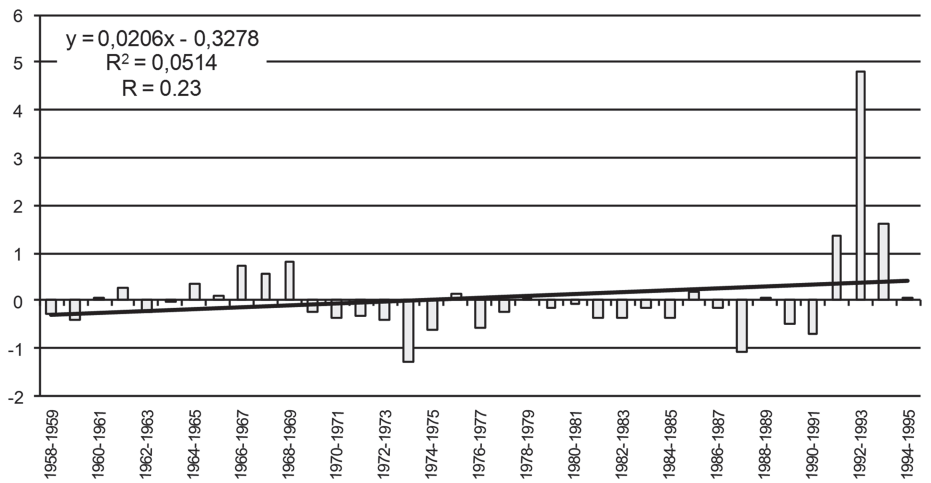

Figure 4a. Flow indices of Tomi River at Sibut, CAR.

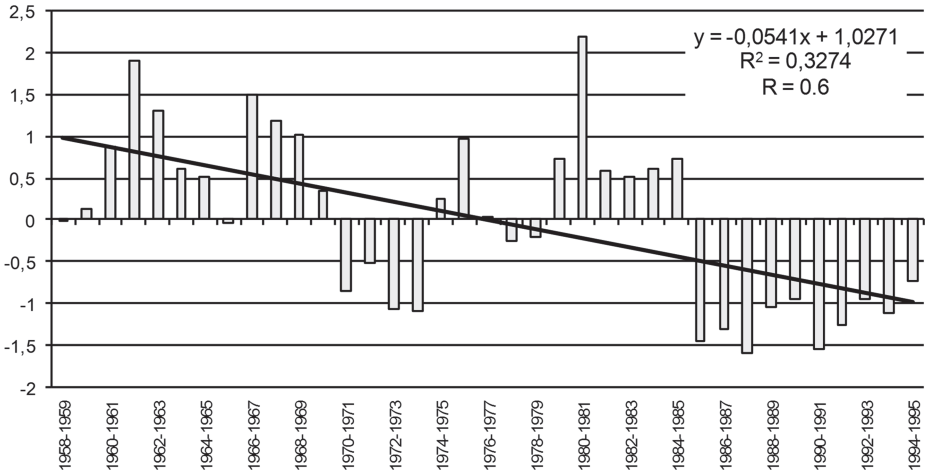

Figure 4b. Flow indices of Gribingui River at Kaga-Bandoro, CAR.

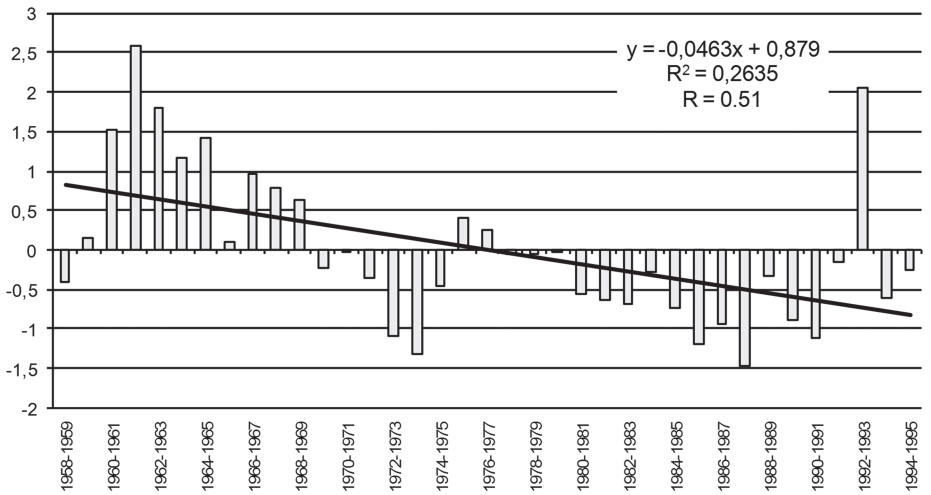

Figure 4c. Flow indices of Fafa River at Bouca, CAR.

dynamic with alternating wet and dry periods in 1967–1970 (Figures 4a and d). Since then, drought is visible in Tomi's and Malewa hydrological data until 1991, episodically interrupted by isolated wet years.

9.4.2.2 Trends from statistical segmentation

Fluctuations of flow modes appear simultaneously by periods with runoff abundance and discharge reduction (Figure 4). The 'harsh' flow rates of Malewa at Morendat, Tomi at Sibut or Fafa at Bouca, are probably linked to high inclination at their headwaters which would explain the fluctuations recorded on annual average discharge from 1958 to 1995. The data is insufficient to determine easily climate alteration tendencies over the basins. Therefore, statistical segmentation was used for detecting

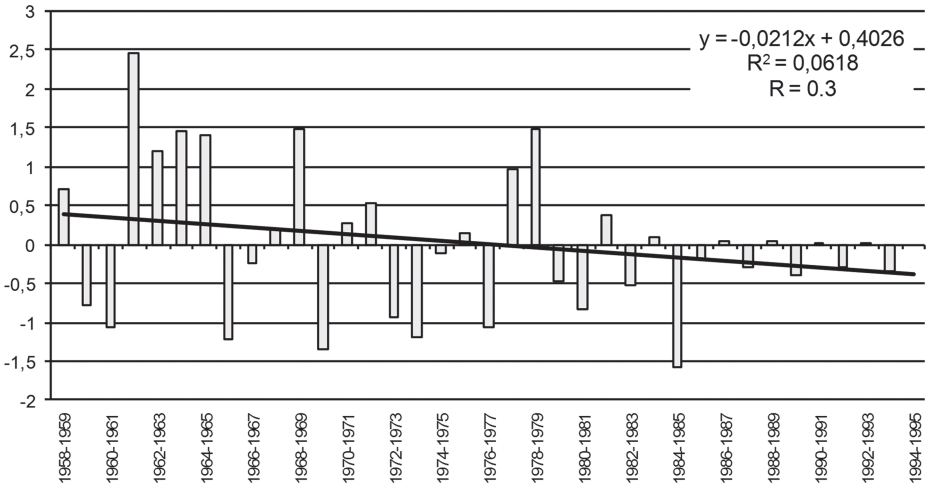

Figure 4d. Flow indices of Malewa River at Morendat, Kenya.

occurred changes along the watercourses (Figures 4a-d), because it allows visualizing dry (before 1955 for Malewa and 1950–1961 for Tomi, 1969/1970–1995 for Gribingui and Fafa), wet (1955–1968) and sub-wet (1969–1979) periods since 1950.

9.4.2.3 R Irregularity indices and changes evidenced in studied rivers' hydrology

Two tendencies show the R irregularity indices (Figures 5a-d). Firstly, the signal coefficients were weak or modest before 1970s (respectively varying R = 21 for Gribingui, R = 25 for Fafa, R = 66.72 for Tomi and R = 92 for Malewa); Tomi and Malewa have three to four times higher coefficients compared to Gribingui and Fafa ones. Secondly, in return there are more important coefficients calculated since 1970s until to date. These results exhibit the variation between annual extreme flows, translating the impact of climate modifications on the examined rivers, mainly on Tomi at Sibut and Fafa at Bouca coefficients (Figures 5a and c) in comparison to those from Gribingui at Kaga-Bandoro and Malewa at Morendat (Figures 5b and d). This impact could lead to a reduction of water availability probably everywhere in Africa, due to missing hydrological reserves for supporting low-water levels.

9.4.3 Rainfall-discharge dynamics within studied basins

Rainfall analysis showed an average rainfall reduction of 5% in both study sites over the considered period, varying from 0.89% for Tomi basin, 1.7% for Malewa basin, 4.2% for Gribingui's basin to 4.6% for Fafa basin. Flows recorded also a decline of their volumes in catchment outlets (Figures 6a-d). If Tomi at Sibut collected a 4% mean 'surplus' during 1970–1995 periods, due exclusively to 1992–1993 exceptional average discharge (66.12 $m^3 s^{-1}$), it has nevertheless experienced a 74% maximum annual hydrological deficit in 1973–1974. Gribingui at Kaga-Bandoro has a mean hydrological reduction of 39.49% in the same period with an observed 80% maximum in 1987–1988. The Fafa catchment described a 22% mean decline of its annual average discharge since 1970 even though the 75% maximum deficit has been recorded on 1987–1988. In Malewa at

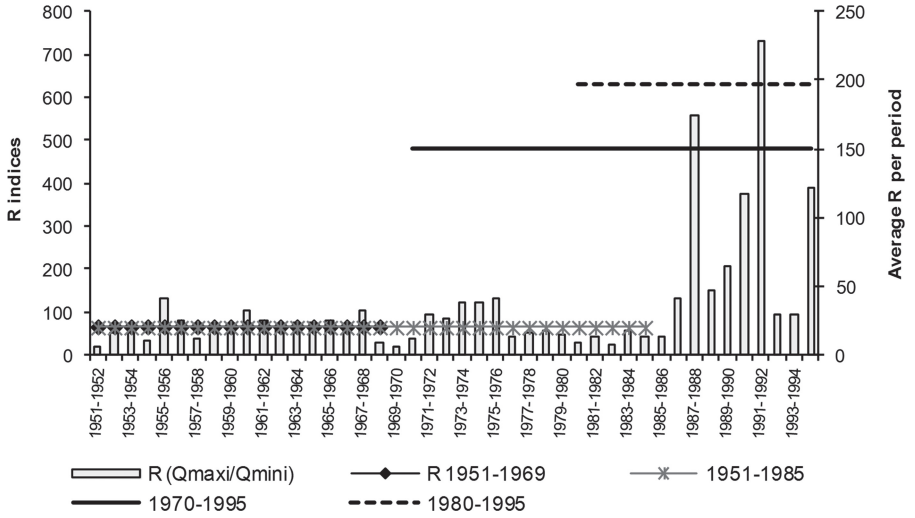

Figure 5a. Irregularity's R indices from Tomi River at Sibut, CAR.

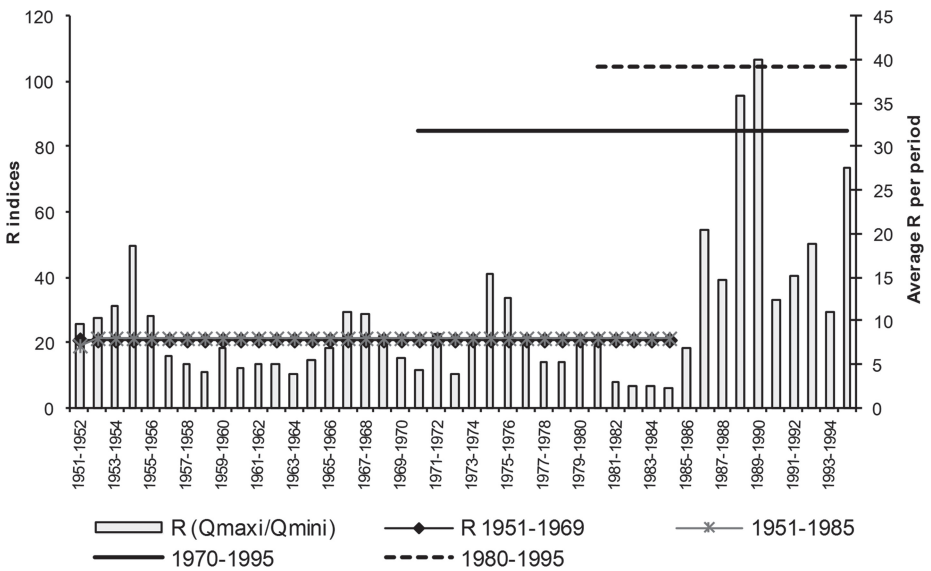

Figure 5b. Irregularity's R indices from Gribingui River at Kaga-Bandoro.

Morendat (Figure 6d), the hydrological reduction was about three to six times weaker than those of Gribingui (Figure 6b) and Fafa (Figure 6c) on 1970–1995, although the annual maximal deficit reached 75% in 1984–1985. This signal of hydrological reduction reached worse proportions from year to year and corroborates climatic aridification effects in Subtropical Africa since 1970, which yet persists.

In the declined rainfall-runoff context, the relation of rainfall-discharge is not uniformly operated in the CAR Sudano-guinean area: Tomi at Sibut presents the weakest

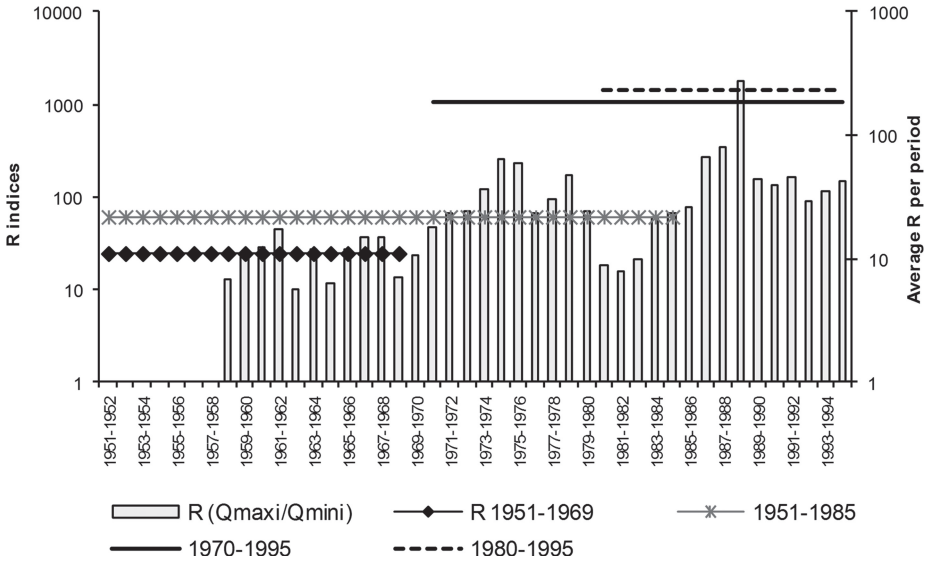

Figure 5c. Irregularity's R indices from Fafa at Bouca, CAR.

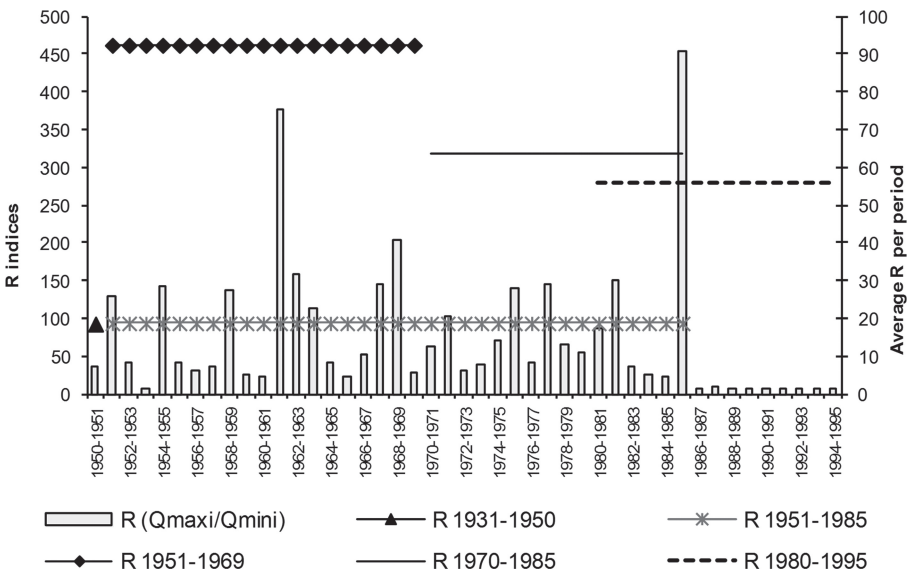

Figure 5d. Irregularity's R indices from Malewa at Morendat, Kenya.

relation ($r = 0.28$); Gribingui's at Kaga-Bandoro with $r = 0.78$ recorded more high relation followed by Fafa at Bouca (0.68). In return, in Kenya Malewa River at Morendat has a good rainfall-runoff relationship with $r = 0.85$ even if the hiatus between rainfall deficit and hydrological deficit in the whole catchment remains an enigma because reversely to weakest rainfall decline (average 3.23% in CAR and 1.7% in Kenya), the mean hydrological deficit is marked everywhere: –8% on Malewa, –22% on Fafa and

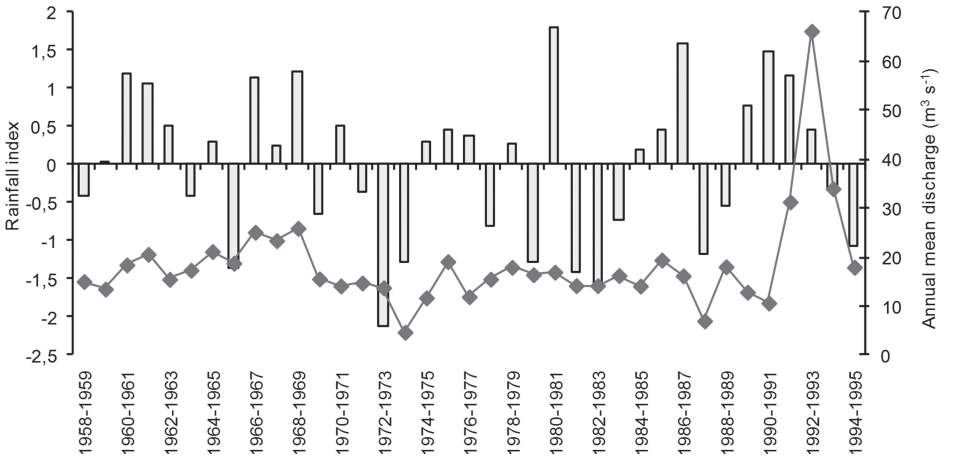

Figure 6a. Rainfall-runoff dynamics from Tomi at Sibut, CAR.

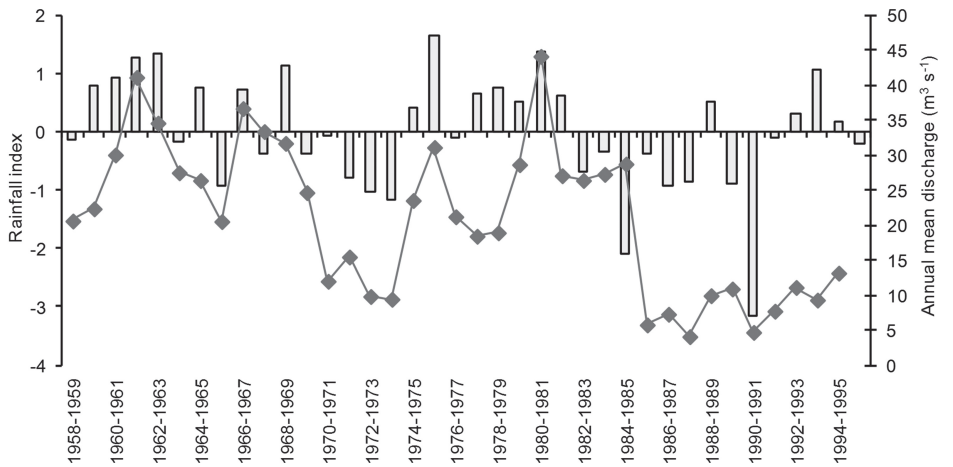

Figure 6b. Rainfall-runoff dynamics from Gribingui at Kaga-Bandoro, CAR.

–39.49% on Gribingui, excepted Tomi at Sibut (+4%). These results would indicate that rainfall-runoff variables are insufficient to explain hydrological degradation in four catchments. Nevertheless, the lowest annual average discharge corresponds to dry years or rainfall weakness and would suggest that runoff was spontaneous because it is linked to rainfall. In addition, annual rainfall weakness or spatio-temporal irregularity did not allow hydrological reserve reconstitution.

The conclusions of rainfall and discharge/runoff analysis establish noticeable modifications on recorded flow heights which deserve to link to climatic change or variability consequences. These tendencies are the same almost for Oubangui River at Bangui with varieties of wet tropical climate (Figure 7). 1935–1950 periods correspond once more to runoff stability of Oubangui River then a short drought intervenes for Oubangui and Tomi on 1951–1954, even though Gribingui's has surplus. Malewa at Morendat succumbed a decline from 1935 to 1954. Common wet period

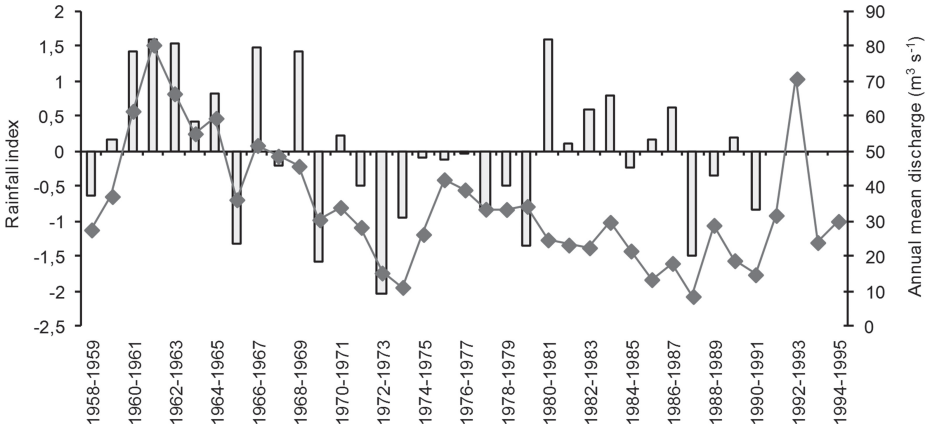

Figure 6c. Rainfall-runoff dynamics from Fafa at Bouca, CAR.

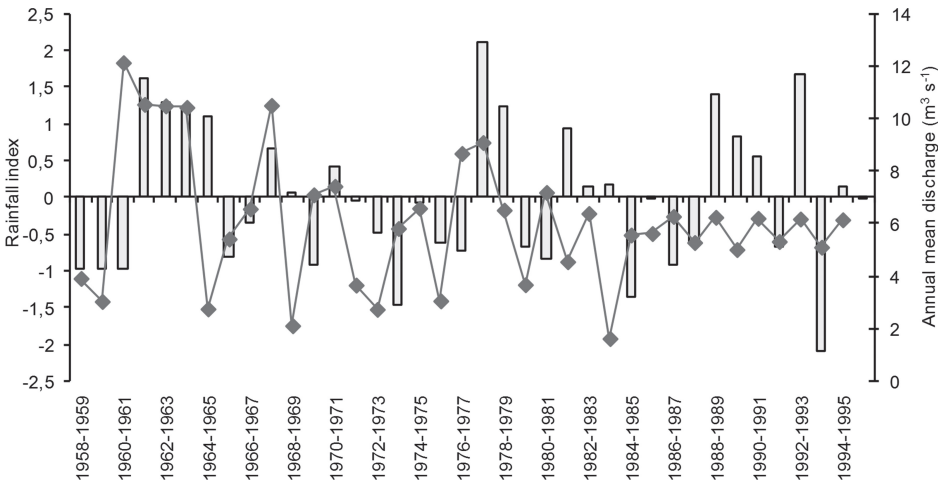

Figure 6d. Rainfall-runoff dynamics from Malewa at Morendat, Kenya.

to the studied rivers occured from 1955 to 1970, and drought ensues on 1971–1995 or 2000 for the Oubangui River. Nevertheless, some wetter episodes are noted within this dry period: 1975–1976, 1980–1981, 1988–1989 and 1992–1993, either for all rivers. The Malewa River discharge peak would possibly correspond to *El Niño* event on 1978–1979 which generated a high lake level of Lake Naivasha in this dry period. These outcomes would regionally testify the continental character of the hydro-climatic modifications combining Eastern, Central and Western Africa. This argument considers Fafa and Gribingui Rivers which flow to the North towards Chari River in the Sudano-guinean zone, but it recorded the same dynamics as Oubangui's and its tributary Tomi in the south, like Malewa River in the Kenyan Rift Valley. Nevertheless, a reduction of runoff is noted for Oubangui River on 1981–1990 decadal (Olivry, 1994; Olivry *et al*., 1998), afterwards short wet periods occurred between 1975 and 1980 and ongoing until today.

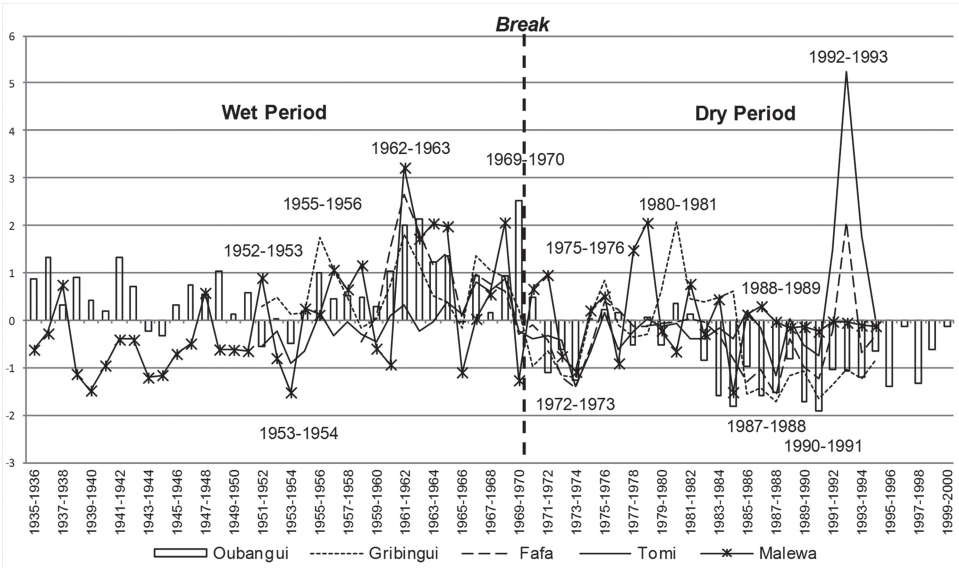

Figure 7. Compared hydrological variabilities' of the Oubangui River at Bangui (1935–2000) and the four studied rivers (y-axis shows Rainfall index).

9.5 CONCLUSION

This work reconstitutes observed hydro-climatic changes or variabilities, respectively, in Lake Naivasha basin, mainly that of Malewa catchment at Morendat (Kenya), Tomi at Sibut, Gribingui at Kaga-Bandoro and Fafa at Bouca (CAR). On the historical scale, the relative remote character of climate change (approximately 40 years) is examined in order to characterize past wet and dry phases having affected the basins. The rainfall and discharge data could channel a current and future management plan of next and perhaps more violent or intense events, such as observed droughts (1966, 1973, 1984, 1988, 1994, 2005–2008, 2009) or floods (1955, 1961, 1964, 1999, 2003) in the whole area.

Rainfall and runoff are the key variables of the conducted observation which can be connected to climate change impacts, local phenomena but global outcome with simultaneous processes in both countries and groups of studied basins. The impact on rainfall-runoff/discharge was recorded variously per basin and site. The data of the rainfall-hydrometric context which shows weakly rainfall compared to rivers' hydrology is declining with a chronic deficit since 1970. Besides, it describes a non-linearity of rainfall-runoff relationships. The accentuation of the hydrological deficit depicts a non-reconstitution of hydrological reserves due to droughts, its duration and relative intensities in each studied basin. The modifications of studied river flows of Oubangui River at Bangui displaying hydro-climatic phenomena of its basin extent can be extrapolated to the Kenyan Malewa basin, located in Eastern Africa which records the same drought. Thus, regional, even continental characters of hydro-climatic modifications are existent. Changes are characterized by alternating periods of drought and wetness or sub-wetness which triggers rainfall abundance and runoff/discharge, and rainfall reduction and severe low-water levels respectively, even water scarcity due to societal effects. In this direction, the reduction of water resources was proven in time relatively to climate modification for each catchment.

In addition, its implications for water availability were assessed throughout rainfall-runoff deficit analysis, seasons shortening or hydrological reduction, low-water levels' severity and hydrological phenomena width (droughts and floods). Beyond we noted that this hydro-climate variability characterize diversely extreme events per basin. In overall, 1958–1969 wet periods are furthermore marked by regular floods which effect demographic and human activities. In return, the current dry period (since 1970s up to date) is characterized by fewer floods with often catastrophic extent due to settlement and human activities increasing in studied basins, in particular along the rivers.

ACKNOWLEDGEMENTS

This work is a summary of my postdoctoral research in Egerton University, Kenya supported by 'Global Exchange SysTem for Analysis, Research and Training' (START) through African Climate Change Fellowship Programme (ACCFP), funded by IDRC (International Development Research Centre) and DFID (Department for International Development).

REFERENCES

Ardoin-Bardin, S., 2004, *Variabilité hydroclimatique et impacts sur les ressources en eau de grands bassins hydrographiques en zone soudano-sahélienne*. Thèse, Laboratoire des Sciences de la Terre et de l'Eau, Université Montpellier II, France, p. 437.

Azouka, J.B., 2011, *Variabilités de pluie et de débit dans le bassin-versant de l'Ouham à Batangafo (1950–1995)*. Mémoire Maîtrise, Géographie, Fac. Lettres et Sci. Hum., Université de Bangui (RCA), p. 99.

Bokonge Ntefo, G., 2008, *Fonctionnement hydrologique et gestion de l'hydrosystème Mbali à Boali*. Mémoire Maîtrise, Géographie, Fac. Lettres et Sci. Hum., Université de Bangui (RCA), p. 150.

Bruel, G., 1902, Note sur la météorologie du Haut-Chari. *Mémoires, Société Météorologique de France*, Avril 1902, p. 9.

Boulvert, Y., 1986, Carte phytogéographique de la République Centrafricaine à 1:1 000 000. *ORSTOM éd., Coll. Notice Explicative*, **104**, p. 131.

Boulvert, Y., 1987, Carte oro-hydrographique à 1: 1000000 de la République Centrafricaine (feuille ouest, feuille est). *ORSTOM, Coll. Notice Explicative*, **106**, p. 118.

Bouquet, C., 1984, Climat. In: *Atlas de la République Centrafricaine*, edited by Vennetier, P. and Laclavère, G., (Paris: Editions Jeune Afrique), pp. 13–17.

Boyer, J.F., Dieulin, C., Rouché, N., Crès, A., Servat, E., Paturel, J.E. and Mahé G., 2006, SIEREM: an environmental information system for water resources. In 5th FRIEND World Conference—Water Resource Variability: Processes, Analyses and Impacts, (La Havana, Cuba: IAHS Publ.) **308**, pp. 19–25.

Bricquet, J.P., Bamba, F., Mahé, G., Touré, M. and Olivry, J.-C., 1997, Evolution récente des ressources en eau de l'Afrique atlantique. *Revue des Sciences de l'eau*, **3**, pp. 321–337.

Callède, J., Boulvert, Y. and Thiébaux, J.P., 2010, Monographie du Bassin de l'Oubangui. *Éd. Orstom, Coll. Monographies Hydrologiques* (www.mpl.ird.fr/hydrologie/document/monogras/oubangui/index104.htm).

Conway, D., 2002, Extreme rainfall events and lake level changes in East Africa: recent events and historical precedents. In *The East African Great Lakes: Limnology,*

Palaeolimnology and Biodiversity, edited by Odada, E.O. and Olago, D.O., Advances in Global Change Research, **12**, (Dordrecht: Kluwer), pp. 63–92.

Conway, D., Persechino, A., Ardoin-Bardin, S., Hamandawana, H., Dieulin, C. and Mahé, G., 2009, Rainfall and water resources variability in sub-Saharan Africa during the 20th century. *Journal of Hydrometeorology*, **10(1)**, pp. 41–59.

Cosandey, C., Bigot, S., Dacharry, M., Gille, E., Laganier, R. and Salvador, P.-G., 2003, *Les eaux courantes. Géographie et environnement*. (Paris: Belin), p. 240.

Demarée, G., 1990, An indication of climatic change as seen from the rainfall data of a Mauritania station. *Theor. Appl. Climatol.* **42**, pp. 139–147.

Eriksen, S., O'Brien, K. and Rosentrater, L., 2008, Climate change in Eastern and Southern Africa: Impacts, vulnerability and adaptation. *GECHS Report*, **2**, p. 26.

Fadika, V., Goula Bi Tié, A., Kouassi, F.W., Doumouya, I., Koffi, K., Kagamate, B., Savane, I. and Srohorou, B., 2008, Variabilité interannuelle et saisonnière de l'écoulement de quatre cours d'eau de l'Ouest côtier de la Côte d'Ivoire (Tabo, Dodo, Néro et San Pédro) dans un contexte de baisse de la pluviométrie en Afrique de l'Ouest. *European Journal of Scientific Research*, **21(3)**, pp. 406–418.

Gapia, M., 2007, *Les méandres de la rivière Mpoko à l'Ouest de la ville de Bangui: dynamique des recoupements et impacts sur la gestion des bras-morts en lit majeur*. Mémoire Maîtrise, Géographie, Fac. Lettres et Sci. Hum., Université de Bangui (RCA), p. 111.

Gathenya, M.J., 2007, Feasibility Assessment for Naivasha—Malewa Payments for Watershed Services. Hydrological assessment. Consultancy Report, WWF/CARE PES Project, Naivasha, Kenya, p. 57.

Gautier, F., Lubès-Niel, H., Sabatier, R., Masson, J.M., Paturel, J.E. and Servat, E., 1998, Variabilité du régime pluviométrique de l'Afrique de l'Ouest non sahélienne entre 1950 et 1989. *Journ. Sci. Hydrol.,* **43(6)**, pp. 921–935.

Hubert, P., Servat, E., Paturel, J.E., Kouame, B., Bendjoudi, H., Carbonnel, J.P. and Lubès-Niel, H., 1998, La procédure de segmentation, dix ans après. In Proceedings of the Abidjan'98 Conference *Water Resources Variability in Africa during the XXth Century*, (Abidjan, Côte d'lvoire: IAHS Pub.) **252**, pp. 267–273.

Kanohin, F., Saley, M.B. and Savanné, I., 2009, Impacts de la variabilité climatique sur les ressources en eau et les activités humaines en zone tropicale humide: cas de la Région de Daoukro en Côte D'ivoire. *Europ. Journ. Sci. Res.*, **26(2)**, pp. 209–222.

Kingumbi, A., Bergaoui, Z., Bourges, J., Hubert, P. and Kallel, R., 2000, Etude de l'évolution des séries pluviométriques de la Tunisie Centrale. file:///C|/Apacheroot/htdocs/medweb/WEB- documents/kingumbi.htm (1 sur 8).

Laraque, A., Olivry, J.C., Orange, D. and Marieu, B., 1997, Variations spatio-temporelles des régimes pluviométriques et hydrologiques en Afrique Centrale du début du siècle à nos jours. In *FRIEND '97 Proceedings of the Postojna—Regional Hydrology: Concepts and Models for Sustainable Water Resource Management*, (Slovenia: IAHS Pub.), **246**, pp. 257–263.

Laraque, A., Orange, D., Maziezoula, B. and Olivry, J.C., 1998, Origine des variations des débits du Congo à Brazzaville durant le XXe siècle. In *Proceedings* of the Abidjan'98, *Water Resources Variability in Africa during* the *XXth Century*, (Abidjan, Côte d'Ivoire: IAHS Pub.), **252**, pp. 171–179.

Laraque, A., Mahé, G., Orange, D. and Marieu, B., 2001, Spatiotemporal variations in hydrological regimes within Central Africa during the twentieth century. *Journal of Hydrology*, **245(1–4)**, pp. 104–117.

Liénou, G., Mahé, G., Paturel, J.E., Servat, E., Sighomnou, D., Ecodeck, G.E., Dezetter, A. and Dieulin, C., 2008, Changements des régimes hydrologiques en

région équatoriale camerounaise: un impact du changement climatique en Afrique équatoriale? *Hydrological Sciences Journal*, **53(4)**, pp. 789–801.

Lukman, P.A., 2003, Regional impact of climate change and variability on water resources. Master Thesis, ITC, Netherlands, p. 89.

Mahé, G. and Olivry, J.C., 1991, Changements climatiques et variations des écoulements en Afrique occidentale et centrale du mensuel à l'interannuel. In: *Hydrology for the Water Management of Large River Basins*, edited by van de Ven, F.H.M., Gutknecht, D., Loucks, D.P. and Salewicz, K.A. (Vienna: IAHS Publ.), **201**, pp. 163–172.

Mahé, G. and Olivry, J.C., 1995, Variations des précipitations et des écoulements en Afrique de l'Ouest et Centrale de 1951 à 1989, *Sécheresse*, **1(6)**, pp. 109–117.

Mahé, G., 2009, Surface/groundwater relationships in two great river basins in West Africa, Niger and Volta. *Hydrological Sciences Journal*, **54(4)**, pp. 704–712.

Maley, J., 2010, Climate and palaeoenvironment evolution in north tropical Africa from the end of the Tertiary of the upper Quaternary. In: *African Palaeoenvironments and Geomorphic Landscape Evolution*, edited by Runge, *Palaeoecology of Africa*, **30**, pp. 227–278.

M'mbui, S.G., 1999, Study of long-term water balance of Lake Naivasha, Kenya. Master Thesis, ITC, Netherlands, p. 69.

Muthuwatta, P.L., 2004, Long term rainfall-runoff-lake level modeling of the Lake Naivasha basin, Kenya. Master Thesis, ITC, Netherlands, p. 89.

Neumer, M., Becker, E. and Runge, J., 2007, Palaeoenvironmental studies in the Ngotto Forest: alluvial sediments as indicators of recent and Holocene landscape evolution in the Central African Republic. In: *Dynamic of forest ecosystems in Central Africa during the Holocene, Past–Present–Future*, edited by Runge, J., *Palaeoecology of Africa*, **28**, pp. 121–137.

Nguimalet, C.-R., 2008. *Relief*. In *Atlas de la République Centrafricaine*, Tambashe, B.O., Ankogui-Mpoko, G.-F., Goulat, R., Macoumba, T. et Nguimalet, C.-R. (Coordinateurs), Editions Enfance et Paix, Kinshasa (R.D. Congo), pp. 19–22.

Nguimalet, C.-R., 2009, Hydropluviometric and climatic dynamics in the catchments of Tomi at Sibut, Gribingui at Kaga-Bandoro and Fafa at Bouca, Central African Republic. *4th Research Week and International Conference*, Egerton University, Njoro, Kenya, p. 9.

Nguimalet, C.-R., 2010a, Risings and floods from Rivers Tomi, Gribingui and Fafa in Centre and Centre-north of Central African Republic, Conference Proceedings of the third *International Disaster and Risk Conference IDRC* Davos *2010:* Extended Abstract Collection, Global Risk Forum GRF Davos, Davos, Switzerland, pp. 521–524.

Nguimalet, C.-R., 2010b, Climate change perceptions and local coping strategies of water management: comparison of Tomi, Gribingui and Fafa catchments (Central African Republic) and Lake Naivasha basin (Kenya). *Final Report*, *Postdoctoral Fellowship*, Egerton University of Kenya, p. 63.

Nguimalet, C.-R., 2010c, Drying-up of rivers: implications for rural livelihoods and community responses in Central and North-Central of Central African Republic. *Comm. Climate Change Adaptation in Africa (CCAA) Conference*, Egerton University, Njoro, Kenya, 2010, p. 5.

Nguimalet, C.-R., Ndjendolé, S. and Orange, D., 2007, Impact de la péjoration climatique sur la rivière Pipi à Ouadda, Haut bassin gréseux de la Kotto en République Centrafricaine. *XX*^{ème} *Colloque International de Climatologie*, *Climat, tourisme et environnement*, **20**, edited by Boubaker, H.B., Actes du colloque de Carthage, (Tunisie: CENAFFE), pp. 423–429.

Nguimalet, C.-R. and Ndjendolé, S., 2008, Les extrêmes hydrologiques: des indicateurs d'hydrodynamisme ou d'hydraulicité du plateau gréseux de Mouka-Ouadda sur la rivière Pipi à Ouadda (République Centrafricaine). *Zeitschrift für Geomorphologie*, **52 (1)**, pp. 125–141.

Nguimalet, C.-R. and Onyando, J.O., 2009, Preliminary results of climate change analysis and incidence in River Malewa Catchment, Lake Naivasha Basin, Kenya. *Comm. RUFORUM: 'Climate Change and Transboundary Animal Diseases Workshop'*, Entebbe, Uganda, p. 7.

Nicholson, S.E., 1983, Sub-Saharan rainfall in the years 1976–1980: evidence of continued drought. *Mon. Weath. Rev.*, **111**, pp. 1646–1654.

Nicholson, S.E., Kim, J. and Hoopingarner, J., 1988, *Atlas of African Rainfall and its Interannual Variability.* (Tallahassee, Florida, USA: Dept of Meteorol., Florida State Univ.).

Olaniran, O.J., 1991, Evidence of climatic change in Nigeria based on annual series of rainfall of different daily amounts, 1919–1985. *Climatic Change* **19,** pp. 319–341.

Olivry, J.C., 1987, Les conséquences durables de la sécheresse actuelle sur l'écoulement du fleuve Sénégal et l'hypersalinisation de la basse Casamance. In *Proceedings of Vancouver Symposium on The Influence of Climate Change and Climatic Variability on the Hydrologic Regime and Water Resources*, Vancouver, edited by Solomon, S.I., Beran, M. and Hogg, W., (Vancouver: IAHS Publ.), **168**, pp. 501–512.

Olivry, J.C., 1994, De l'évolution de la puissance des crues des grands cours d'eau intertropicaux d'Afrique depuis deux décennies. Actes des Journées Hydrologiques-Centenaire Maurice Pardé, Grenoble, *Dossiers Rev. Géogr. Alpine*, **12**, pp. 101–108.

Olivry, J.C., Mahé, G. and Bricquet, J.P., 1995, Les études du PEGI sur le bassin du Congo-Zaïre dans le contexte déficitaire des ressources en eau de l'Afrique humide. In *Actes du Colloque PEGI Grands Bassins Fluviaux Péri-Atlantiques: Congo, Niger, Amazone,* edited by Boulègue, J. and Olivry, J.C., Paris: INSU, CNRS, ORSTOM), pp. 3–12.

Olivry, J.C., Briquet, J.P. and Mahé, G., 1998, Variabilité de la puissance des crues des grands cours d'eau d'Afrique intertropicale et incidence de la baisse des écoulements de base au cours des deux dernières décennies. *Water Resources Variability in Africa during* the *XXth Century* (Proceedings of the Abidjan'98 Conference held at Abidjan, Côte d'Ivoire, November 1998). IAHS Publ. no. **252**, pp. 189–197.

Orange, D., Féizoure, C., Wesselink, A. and Callede, J., 1995, Variabilités hydrologiques de l'Oubangui à Bangui au cours du XX^{e} siècle. In *Proceedings Actes des Journées Scientifiques FRIEND-AOC*, Cotonou, Bénin), p. 20.

Orange, D., Wesselink, A., Mahe, G. and Feizoure, C., 1997, The effects of climate changes on river baseflow and aquifer storage in Central Africa. In *Proceedings of Rabat Symposium on Sustainability of Water Resources under Increasing Uncertainty*, (Rabat: IAHS Publ.) **240**, pp. 113–123.

Paturel, J.E., Servat, E., Delattre, M.O. and Lubès-Niel, H., 1998, Analyse de séries pluviométriques de longue durée en Afrique de l'Ouest et Centrale non sahélienne dans un contexte de variabilité climatique. *Journal des Sciences Hydrologiques,* **43(6),** pp. 937–946.

Paturel, J.E., Barrau, C., Mahé, G., Dezetter, A. and Servat E., 2007, Modelling the impact of climatic variability on water resources in West and Central Africa from a non-calibrated hydrological model. *Hydrological Sciences Journal*, **52(1)**, pp. 38–48.

Primary Atlas, 2004, Kenya. Revised Edition, The PHILIP'S-EAEP, p. 49.

République Centrafricaine, 1985–1990, Annales Hydrologique, Ministère des Transports et de l'Aviation civile, Direction de la Météorologie, Service de l'Hydrologie, Bangui, p. 226.

République Centrafricaine, 1990–1991, Annuaire Hydrologique, Ministère des Transports, des Travaux publiques, de l'Habitat et de l'Aménagement du Territoire, Direction de la Météorologie, Projet CAF/91/021, Bangui, p. 71.

République Centrafricaine, 1991–1992, Annuaire Hydrologique, Ministère des Transports, des Travaux publiques, de l'Habitat et de l'Aménagement du Territoire, Direction de la Météorologie, Projet CAF/91/021, Bangui, p. 65.

République Centrafricaine, 1992–1993, Annuaire Hydrologique, Ministère des Transports, des Travaux publiques, de l'Habitat et de l'Aménagement du Territoire, Direction de la Météorologie, Projet CAF/91/021, Bangui, p. 57.

République Centrafricaine, 1993–1994, Annuaire Hydrologique, Ministère des Transports, des Travaux publiques, de l'Habitat et de l'Aménagement du Territoire, Direction de la Météorologie, Projet CAF/91/021, Bangui, p. 63.

République Centrafricaine, 1994–1995, Annuaire Hydrologique, Ministère des Transports, des Travaux publiques, de l'Habitat et de l'Aménagement du Territoire, Direction de la Météorologie, Projet CAF/91/021, Bangui, p. 70.

Roche, E., 1991, Evolution des paléoenvironnements en Afrique centrale et orientale au Pléistocène supérieur et à l'Holocène. Influences climatiques et anthropiques. *Bulletin de la Société géographique de Liège*, **27**, pp. 187–208.

Rolin P., 1992, Nouvelles données tectoniques sur le socle précambrien de Centrafrique: implications géodynamiques. *C. R. Acad. Sci.*, Paris, **315**, sér. II a, pp. 467–470.

Runge, J., 2007, Des déserts et des forêts, histoire du paysage et du climat de l'Afrique Centrale au Quaternaire Supérieur/Of deserts and forests, Late Quaternary landscape and climate history of Central Africa. *Geo-Eco-Trop, 2007*, **31,** pp. 1–18.

Runge, J. and Nguimalet, C.-R., 2005, Physiogeographic features of the Oubangui catchment and environmental trends reflected in discharge and floods at Bangui 1911–1999, Central African Republic. *Geomorphology*, **70(3–4)**, pp. 311–324.

Schwartz, D., 1992, Assèchement climatique vers 3000 B.P. et expansion Bantu en Afrique Centrale atlantique: quelques réflexions. *Bull. Soc. Géol. France*, **163**, pp. 353–361.

Servat, E., Paturel, J.E. and Lubès, H., 1996, La sécheresse gagne l'Afrique tropicale. *La Recherche* **290,** pp. 24–25.

Servat, E., Paturel, J.E., Lubès-Niel, H., Kouamé, B. and Masson, J.M., 1997a, Variabilité des régimes pluviométriques en Afrique de l'Ouest et centrale non sahélienne. *Surface geoscences* (*hydrology-hydrogeology*), t. **324**, serie **II a**, pp. 835–838.

Servat, E., Paturel, J.E., Lubès-Niel, H., Kouamé, B., Travaglio, M. and Marieu, B., 1997b, De la diminution des écoulements en Afrique de l'Ouest et centrale. *Sciences de la terre et des planètes*, **325**, pp. 679–682.

Servat, E., Paturel, J.E., Lubès-Niel, H., Kouamé, B., Masson, J.M., Travaglio, M. and Marieu, B., 1999, De différents aspects de la variabilité de la pluviométrie en Afrique de l'Ouest et centrale on sahélienne. *Rev. Sci. Eau*, **12(2)**, pp. 363–387.

Sighomnou, D., Sigha, L., Liénou, G., Dezetter, A., Mahé, G., Servat, E., Paturel, J.E., Olivry, J.C., Tchoua, F. and Ekodeck, G.E., 2007, Impacts des fluctuations climatiques sur le régime des écoulements du fleuve Sanaga au Cameroun, prospectives pour le XXIème siècle. FRIEND International Seminar, *Technical Document in Hydrology*, **80**, pp. 173–182.

Sircoulon, J., 1976, Données hydropluviométriques sur la sécheresse de 1968 à 1973 en Centrafrique. multigr. Inédit. (Paris: ORSTOM), p. 23.

Sircoulon, J., 1985, La sécheresse en Afrique de l'Ouest. Comparaison des années "1982–1984" avec les années "1972–1973". *Cah. ORSTOM, sér. Hydrol.*, **21(4)**, pp. 75–86.

Thomas, M.F., 1994, *Geomorphology in the Tropics. A study of weathering and denudation in low latitudes*. Wiley and Sons, New York, Brisbane, Toronto. pp. 1–460.

Thomas, M.F. and Thorp, M.B., 1992, Landscape dynamics and surface deposits arising from late Quaternary fluctuations in the forest-savanna boundary. In *Nature and Dynamics of Forest-Savanna Boundaries*, edited by Furley, P.A., Proctor, J. and Ratter, J.A., pp. 213–253.

Wesselink, A., Orange, D., Feizoure, C. and Randriamiarisoa, 1996, Les régimes hydroclimatiques et hydrologiques d'un bassin-versant de type tropical humide: l'Oubangui (République Centrafricaine). In *L'Hydrologie Tropicale: géoscience et outil pour le développement*, edited by Chevallier, P. and Pouyaud, B., (IAHS), **238**, pp. 179–194.

Palaeoecology of Africa

International Yearbook of Landscape Evolution and Palaeoenvironments

ISSN: 0168-6208

Volume 1-12, 19, 21, 25 Out of Print

13. Palaeoecology of Africa and the Surrounding Islands
Editors: J.A. Coetzee & E.M. van Zinderen Bakker
1981, ISBN: 978-90-6191-203-3

14. Palaeoecology of Africa
Editors: J.A. Coetzee & E.M. van Zinderen Bakker
1982, ISBN: 978-90-6191-204-0

15. Palaeoecology of Africa
Editors: J.A. Coetzee, E.M. van Zinderen Bakker, J.C. Vogel, E.A. Voigt & T.C. Partridge
1982, ISBN: 978-90-6191-257-6

16. Palaeoecology of Africa
Editors: J.A. Coetzee & E.M. van Zinderen Bakker
1984, ISBN: 978-90-6191-510-2

17. Palaeoecology of Africa
Editors: J.A. Coetzee & E.M. van Zinderen Bakker
1986, ISBN: 978-90-6191-625-3

18. Palaeoecology of Africa
Editor: K. Heine
1987, ISBN: 978-90-6191-689-5

19. Palaeoecology of Africa – *Out of Print*
Editors: K. Heine & J.A. Coetzee
1988, ISBN: 978-90-6191-834-9

20. Palaeoecology of Africa
Editor: K. Heine
1989, ISBN: 978-90-6191-880-6

21. Palaeoecology of Africa – *Out of Print*
Editors: K. Heine & R.R. Maud
1990, ISBN: 978-90-6191-997-1

22. Palaeoecology of Africa
Editors: K. Heine, A. Ballouche & J. Maley
1991, ISBN: 978-90-5410-110-9

23. Palaeoecology of Africa and the Surrounding Islands
Editor: K. Heine
1993, ISBN: 978-90-5410-154-3

24. Palaeoecology of Africa
Editor: K. Heine
1996, ISBN: 978-90-5410-662-3

25. Palaeoecology of Africa – *Out of Print*
Editors: K. Heine, H. Faure & A. Singhvi
1999, ISBN: 978-90-5410-451-3

26. Palaeoecology of Africa and the Surrounding Islands
Editors: K. Heine, L. Scott, A. Cadman & R. Verhoeven
1999, ISBN: 978-90-5410-476-6

27. Palaeoecology of Africa and the Surrounding Islands: Proceedings of the 25th Inqua Conference, Durban, South Africa, 3-11 August 1999
Editors: K. Heine & J. Runge
2001, ISBN: 978-90-5809-350-9

28. Dynamics of Forest Ecosystems in Central Africa During the Holocene: Past – Present – Future
Editor: J. Runge
2007, ISBN: 978-0-415-42617-6

29. Holocene Palaeoenvironmental History of the Central Sahara
Editors: R. Baumhauer & J. Runge
2009, ISBN: 978-0-415-48256-1

30. African Palaeoenvironments and Geomorphic Landscape Evolution
Editor: J. Runge
2010, ISBN: 978-0-415-58789-1

31. Landscape Evolution, Neotectonics and Quaternary Environmental Change in Southern Cameroon
Editor: J. Runge
2012, ISBN: 978-0-415-67735-6

PALAEOECOLOGY OF AFRICA

International Yearbook of Landscape Evolution and Palaeoenvironments

32

Volume 32 of the internationally recognized and acclaimed yearbook series 'Palaeoecology of Africa' publishes nine new interdisciplinary scientific papers on former and recent landscape evolution and on past environments of the African continent (e.g. climate change, vegetation dynamics and growing impact of humans on ecosystems). These papers expand horizons and interconnections to various types and methodologies of research on environmental dynamics from the Pliocene up to the present. Review articles and regional case studies cover Nigeria, Cameroon, selected areas of the Congo basin, Kenya, Malawi, Namibia and South Africa. This volume also gives space to researchers from Africa to present their findings to a wider international audience.

Today, by growing awareness of the worldwide impact of global change, it has become obvious that aside from the northern and southern hemisphere Polar regions also the environmental setting in Africa was subject to considerable changes over time. Natural shifts in climate at least since the Pliocene have caused repeated and strong modification in the area dynamics of ecosystems located at lower latitudes. By a variety of so-called 'proxies' – researched and applied by the different authors from numerous disciplines – an attempt is made to reconstruct the evolution of landscapes over space and time. Besides such spatio-temporal oscillations in forested and savanna areas of Africa, this volume of 'Palaeoecology of Africa' also focuses on possible relationships between environmental change and human impact, as well as on the perception of this phenomenon of recent 'climate changes' by different stakeholders.

This book will be of interest to all concerned with low latitude ecosystem changes and their respective interpretation in the framework of natural climate and vegetation change evidenced by a variety of methods that allow us to read and learn from 'proxy data' archives. Archaeologists, palynologists, palaeobotanist, geographers, geologists and geomorphologists will find this edition equally useful for their work.

ISSN 0168-6208

ISBN 978-1-138-00116-9

CRC Press
Taylor & Francis Group
an **informa** business
www.crcpress.com

6000 Broken Sound Parkway, NW
Suite 300, Boca Raton, FL 33487
Schipholweg 107C
2316 XC Leiden, NL
2 Park Square, Milton Park
Abingdon, Oxon OX14 4RN, UK

an **informa** business